MATERIAL DESIGN OF BIODEGRADABLE CELL SCAFFOLDS FOR CONTROLLED RELEASE OF BONE MORPHOGENETIC PROTEIN-2 AND THE BONE REGENERATION POTENTIAL

YOSHITAKE TAKAHASHI

2007

CONTENTS

ABBREVIATIONS

ALP	Alkaline phosphate
bFGF	basic fibroblast growth factor
BM	Bone marrow
BMC	Bone mineral content
BMD	Bone mineral density
BMP	Bone morphogenetic protein
β-TCP	β-tricalcium phosphate
DDS	Drug delivery system
DDW	Double-distilled water
DEXA	Dual-energy X-ray absorptometry
DMEM	Dulbecco's modified Eagle's minimum essential medium
DNA	Deoxyribonucleic acid
EDTA	Ethylenediaminetetraacetic acid
EDX	Energy dispersive X-ray
ELISA	Enzyme-linked immunosorbent assay
FCS	Fetal calf serum
Gelatin-β-TCP	Gelatin incorporating β-TCP
HAp	Hydroxyapatite
HE	Hematoxylin and eosin
HGF	Hepatocyte growth factor
IBM	Insoluble bone matrix

IEP	Isoelectric point
LDH	Lactate dehydrogenase
μCT	micro-computed tomography
MSC	Mesenchymal stem cells
OP-1	Osteogenic protein-1
PBS	Phosphate buffered saline solution
PET	Poly(ethylene terephthalate)
pQCT	peripheral quantitative computed tomography
rhBMP	recombinant human bone morphogenetic protein
SDS	Sodium dodecyl sulfate
SEM	Scanning electron microscopy
SSC	Sodium citrate-buffered saline solution
TGF-β	Transforming growth factor-β
Tris	2-Amino-2-hydroxymethyl-1, 3-propanediol

GENERAL INTRODUCTION

Bone reconstruction is a clinically important procedure to treat bone defects and has been widely tried by different methods. Basically, bone has the inherent ability to spontaneously repair itself for the bone fracture of small size. However, such a self-repairing cannot always be expected for large-size defects that are caused by trauma, tumor resection, spinal arthodesis, and congenital abnormalities. This situation often happens clinically and the therapeutic demand has been being increased recently [1]. Autograft, which is considered to be a gold standard as bone substitutes, is applied to the defect site because it provides a suitable environment for cell attachment, proliferation, and differentiation for bone regeneration [2]. However, it has several disadvantages, such as the limited donor supply, potential complications with chronic pain at the donor sites [3, 4]. On the other hand, allograft is being performed clinically [2], but the rate of graft integration into the surrounding natural bone is lower than that of autograft. In addition, it is necessary for the allograft to consider a risk of disease transmission and postoperative complications due to the tissue rejection [4, 5]. Therefore, under these circumstances, as the substitute for the bone grafts, the biomaterials of metals and ceramics have been investigated and developed. Although the above problems may be cleared, they have other disadvantages, such as the lack of biodegradability under physiological conditions and the limited processability [6]. Especially, metals show poor integration property to the bone tissue at the implantation site compared with the autograft and allograft although they provide mechanical support [7]. Different from artificial biomaterials, one of the important advantages for the bone graft is to positively accelerate osteoconduction and osteoinduction. As one trial to tackle and improve the points to be resolved, bone tissue engineering has been attracted much attention as a new therapeutic technology [8-11]. The basic idea is to provide key cells the local environment suitable to promote their proliferation and differentiation for the induction of tissue regeneration.

Generally, there are three factors necessary for tissue engineering, such as cells, the scaffold for cell proliferation and differentiation, and growth factors. Without any treatments, a large-sized body

defect will be naturally occupied with the fibrous tissue. If this tissue occupation takes place, the defect will never be regenerated and repaired by the right tissue to be expected. For successful bone regeneration, it is indispensable to efficiently build up the regeneration environment by making use of various biomaterials or their combination with key cells and growth factors. It is well recognized that the extracellular matrix of natural scaffold provides not only a physical support for cells, but also plays an important role in the cell proliferation and differentiation or cell-mediated morphogenesis [11-15]. The scaffold of biomaterials has been designed and prepared for the local environment of tissue regeneration. The scaffolds should be biodegradable to disappear in the body accompanied with bone regeneration at the defect [12, 16, 17]. In addition, the degradation products should not be toxic and must be naturally excreted by metabolic pathways. So far, three-dimensional materials with a porous structure have been designed for the cell scaffold from glycolide-lactide copolymer non-woven fabrics, collagen sponges, calcium phosphate ceramics, and PEG-based hydrogels [2, 12, 18-21]. Among them, hydroxyapatite (HAp) and β-tricalcium phosphate (β-TCP) have been intensively investigated as the scaffold material for bone tissue engineering because it is well recognized that they are compatible to natural bone tissue and osteoconductive [2, 22-27]. However, HAp is not practically degraded under physiological conditions and remains inside the bone tissue regenerated. Therefore, as one trial to control the *in vivo* degradability, the HAp is combined with organic materials, such as collagen and glycolide-lactide copolymers [28-31]. The combination is effective in manipulating the degradation and mechanical properties for the HAp scaffolds. On the other hand, β-TCP is advantageous from the viewpoint of the biodegradability, although brittle compared with HAp [32, 33]. Several requirements should be considered in the design of three-dimensional scaffolds for bone tissue engineering. Firstly, the scaffold should have sufficient porosity for cell proliferation, differentiation, and ingrowth, resulting in promoted bone regeneration. Higher porosity more than 90 % is important for scaffolds [34, 35]. The pore size is one key factor for the scaffold design. It is reported that the pore size ranging 150-400 μm is preferable for the bone regeneration [36-38]. High interconnectivities between pores are also desirable for homogeneous cell seeding and distribution, oxygen or nutrient supply, and excretion of metabolic waste from the cell-scaffold

constructs [36]. It has been widely accepted that the cell-scaffold interaction is greatly influenced by their porous structure. In addition, the scaffold requires suitable surface properties because the cell behavior is greatly influenced by roughness, topography, wettability, charge, and chemical composition of scaffold surface [39, 40].

If the surrounding tissue of bone defect has a high potential toward regeneration, bone tissue will be newly formed in the scaffold implanted into the bone defect by seeded cells or cells infiltrating from the surrounding tissues. However, when the regeneration potential is very low, bone regeneration will not always be expected similarly. In this situation, it is one of the practically possible ways to utilize growth factors to accelerate the induction of bone regeneration. The recent research development of basic biology and medicine reveals that growth factors play an important role in the proliferation and differentiation of cells both *in vitro* and *in vivo* [41, 42]. However, only by the directed injection of growth factor in the solution form into the target site to be regenerated, we cannot always expect the growth factor-induced tissue regeneration. This is because the growth factor generally has a very short half-life in the body [43, 44], and is rapidly excreted from the site injected or deactivated by the attack of enzymes and antibodies. Consequently, the high dosage administration and repeated regimens are necessary for bone regeneration. However, they often cause adverse effects [45]. As one trial to efficiently enhance the *in vivo* biological efficacy of growth factor, it is practically possible to make use of the technology and methodology of drug delivery systems (DDS). For example, a growth factor is incorporated into a carrier matrix for the controlled release and applied to the site to be regenerated. It is likely that this release system efficiently enhances the local concentration of growth factor over a certain time period, resulting in promoted tissue regeneration.

Osteoinductive properties of bone morphogenetic protein (BMP) family have been attracted much attention in terms of bone regeneration because BMP has high potentials to stimulate the differentiation of MSC into osteogenic lineage. It is strong enough to induce bone formation even at ectopic sites, such as subcutis and muscle [45, 46]. There are at least 15 types of BMP currently reported, and some recombinant human BMPs (rhBMP) are available at large amounts by the recombinant DNA

technology [47, 48]. Among them, rhBMP-2 and rhBMP-7 (OP-1) have already been clinically applied to repair the critical-sized bone defect and accelerate fracture healing [49, 50]. On the other hand, several preclinical studies have revealed that BMP administrated in the solution form does not always induce the expected efficacy in bone regeneration. BMP at physiologically high doses is often required to achieve bone formation [51]. To tackle these problems, various biodegradable carriers, including collagen [52, 53], lactide-glycolide copolymers [54, 55], ß-tricalcium phosphate [56], and ethylene glycol-lactic acid copolymers [57], have been employed for the carrier matrices for BMP release. An osteogenic product composed of BMP-7 and collagen of the release carrier has been commercially available [58]. It is strongly indicated from these findings that the combination of BMP with the release material is absolutely needed to achieve the *in vivo* BMP-induced bone formation. However, little has been investigated on the ability of BMP for bone regeneration from the viewpoint of the *in vivo* release profile.

We have already prepared a hydrogel from gelatin with different biodegradabilities and succeeded in augmenting the biological effects of basic fibroblast growth factor (bFGF) [59, 60], transforming growth factor-ß1 (TGF-ß1) [61, 62], and hepatocyte growth factor (HGF) [63]. Gelatin was selected as the carrier material for growth factor release because it is commercially available with various physicochemical properties and has been extensively used for industrial, pharmaceutical, and medical purposes. The biosafety of gelatin has been proved through the long clinical use [64]. Another unique advantage is the electrical nature of gelatin which allows a growth factor with an electrical charge to physically immobilize into the gelatin-based hydrogel without its denaturation [65]. It is demonstrated that the time period of growth factor remaining in the hydrogel is good accordance with that of hydrogel remaining. Only when the hydrogel is enzymatically degraded to generate water-soluble gelatin fragments, the growth factor immobilized can be released from the hydrogel [65, 66]. The *in vivo* degradability of gelatin hydrogels depended on their water content which can be modified by changing the preparation conditions. Moreover, it should be noted that gelatin hydrogels can be formulated into different shapes, such as disks, tubes, sheets, and microspheres.

It is undoubtedly necessary for successful tissue regeneration to make use of cells constituting

tissue to be regenerated, such as mature, progenitor, precursor, and stem cells. Considering their proliferation and differentiation potentials, stem cells are practically promising. Among them, mesenchymal stem cells (MSC) have been extensively investigated for the therapeutic applications of regenerative medicine because they can be clinically isolated from the bone marrow of patients [67, 68]. It is well recognized that MSC have an inherent potential to differentiate into a variety of cell lineages, such as bone, cartilage, tendon, muscle, and fat cells [69, 70]. Osteogenic differentiation of MSC has been experimentally confirmed for the *in vitro* culture with ß-glycerophosphate, ascorbic acid, and dexamethazone. In addition, it is reported that MSC can be passaged *in vitro* over 30 population doublings *in vitro* and expanded in number by over 1 billion-fold without loss of the osteogenic potential [71]. Therefore, the MSC expanded *in vitro* up to large enough number are seeded into the scaffold, and the MSC-scaffold construct is applied to a bone defect for bone regeneration [72-75]. To prepare the MSC-scaffold construct with a good potential of bone regeneration, it is necessary to improve the cell seeding method which allows cells to distribute homogeneously inside the scaffold. The spatially uniform distribution of cells throughout the scaffold with a high density and good cellularity is essential for bone regeneration *in vitro* or *in vivo*. In spite of the practical significance, normally, cells are seeded into the scaffold by the conventional static seeding method, which often results in non-uniform distribution of seeded cells and poor cellularity [76, 77]. So far, some researches have focused on the cell seeding method to tackle the problems [78-81].

The objective of this thesis is to develop the cell scaffold which is applicable for the controlled release of BMP-2 as well as the three-dimensional culture of MSC aiming at bone regeneration. In Part I, biodegradable gelatin hydrogels incorporating BMP-2 with different water contents are prepared for the controlled release. The feasibility of ectopic bone formation and bone regeneration by the controlled release of BMP-2 from the hydrogel is investigated with various animal models. In addition, biodegradable scaffolds composed of gelatin and ß-TCP are designed to provide the material both the property of BMP-2 release and the culture substrate of cells. Part II is concerned with the combination of MSC with different scaffolds for the osteogenic differentiation and *in vivo* bone regeneration. The method

of cell seeding into the scaffold is also investigated in terms of distribution uniformity of cells, while the *in vitro* culture of MSC is performed to evaluate the effect of the scaffold type on the osteogenic differentiation.

Chapter 1 describes an investigation to design the material for the *in vivo* controlled release of BMP-2 from biodegradable gelatin hydrogels to enhance the activity of BMP-2 for bone formation. Gelatin hydrogels with different biodegradabilities were obtained by changing the concentration of gelatin and glutaraldehyde of chemical crosslinker used in hydrogel preparation. Following the subcutaneous implantation of various gelatin hydrogels incorporating BMP-2 into the back of mice, the time profile of BMP-2 release was examined to the influence on the BMP-2-induced ectopic bone formation.

Several research reports have demonstrated that BMP at physiologically high doses is required to achieve bone formation in non-human primates, which is in contrast to the case of other animals [51]. One of the possible reasons for this species-dependent dose issue is the immatured technology for the *in vivo* release of BMP. Chapters 2 and 3 deal with the orthotopic bone regeneration by the controlled release of BMP-2 at the bone defect of rabbits and monkeys, respectively. Chapter 2 describes the bone regeneration at a rabbit ulna defect by the controlled release of BMP-2 from the gelatin hydrogel. Hydrogels with three different biodegradabilities were prepared by changing the concentration of gelatin and glutaraldehyde in hydrogel preparation. The gelatin hydrogel incorporating BMP-2 was implanted into the ulna defect, while as a control, free BMP-2 was applied. Bone regeneration by the hydrogel incorporating BMP-2 at the defect was compared with that of free BMP-2. The effect of BMP-2 release profile on the bone regeneration was also evaluated.

Chapter 3 describes the bone regeneration by the controlled release of BMP-2 from the gelatin hydrogel for a skull bone defect of non-human primates and rabbits. The gelatin hydrogel incorporating BMP-2 with different biodegradabilities was implanted into both the skull defects. The effect of the hydrogel biodegradabilities and the BMP-2 dose on the BMP-2-induced bone regeneration was investigated, while the bone regeneration was compared with that of insoluble bone matrix (IBM) incorporating BMP-2 which is a gold standard material. The data obtained clearly indicated that the hydrogel of well-controlled

release system enabled BMP-2 to induce bone regeneration even at the bone defect of non-human primates at the doses as low as that of rabbits.

Gelatin hydrogel functions as the release carrier of BMP-2 to promote the ability for bone regeneration. If the gelatin hydrogel also has a pore structure, it is highly expected that the porous hydrogel functions as the scaffold for the attachment and proliferation of osteogenic cells, in addition to the carrier of BMP-2 release. For this purpose, it is necessary to improve the poor stiffness of gelatin hydrogel. In Chapter 4, the scaffolds of gelatin sponge incorporating ß-TCP granules are prepared to improve the mechanical problem. Gelatin scaffolds incorporating different contents of ß-TCP were fabricated by a simple forming method of gelatin solution in the presence of ß-TCP granules. Following incorporation of BMP-2 into the gelatin-ß-TCP scaffolds, the *in vivo* profiles of BMP-2 release and the osteoinduction activity were investigated in terms of the amount of ß-TCP incorporated.

PART II of this thesis is directed to evaluate the osteogenic differentiation of MSC cultured in various three-dimensional scaffolds and the property of MSC-scaffold construct to induce bone regeneration. The cell seeding method to achieve the uniform distribution of MSC inside the scaffold was optimized. The effect of the scaffold type on the osteogenic differentiation of MSC was investigated, while *in vivo* bone regeneration by the MSC-scaffold construct was evaluated. Chapter 5 focuses on the optimization of MSC seeding conditions for their uniform distribution inside the non-woven fabrics of scaffold. The initial attachment of MSC to the non-woven PET fabrics was evaluated in terms of the agitation speed, culture vessel shape, and volume of culture medium. The distribution pattern of cells seeded inside the fabrics was investigated and compared with that of the conventional static seeding method, while the cell damage during the seeding process was evaluated.

It is recognized that the physicochemical properties of scaffolds greatly affect the attachment, proliferation, and biological activity of cells, which consequently contributes to the process of tissue regeneration [14, 82, 83]. Among the scaffold properties, the surface morphology of scaffolds is one of the important factors contributing to the proliferation and differentiation of cells [39, 40]. Chapter 6 investigates the effect of the fiber diameter and porosity of non-woven fabrics on the osteogenic

differentiation of MSC. The non-woven PET fabric of non-biodegradability was used as a model scaffold because the biodegradability of scaffold often makes it complicated to evaluate the cell-scaffold interaction. After seeding MSC into the non-woven fabric of PET fibers with different diameters, their attachment, proliferation, and osteogenic differentiation were investigated. The effect of the fabrics porosity on the proliferation and differentiation of MSC was also evaluated.

Chapter 7 describes the osteogenic differentiation of MSC in the biodegradable sponge scaffolds composed of gelatin and ß-TCP. The sponge with a pore structure functions as the scaffold for three-dimensional culture of MSC, in addition to the release carrier of BMP-2. It is also expected that the mechanical property and osteoinductivity of scaffold are improved by the ß-TCP incorporation. Gelatin scaffolds incorporating different amounts of ß-TCP were fabricated by simple forming procedure of gelatin solution in the presence of ß-TCP granules. After seeding MSC into the gelatin-ß-TCP scaffold by the agitating method, the cell-seeded scaffolds were cultured by the static or stirring culture method. The attachment, morphology, proliferation, and osteogenic differentiation of MSC were compared between the scaffolds incorporating different amounts of ß-TCP. The effect of the culture method on the MSC behaviors was also investigated.

After the surgical resection of cancer, X-ray irradiation is often performed to prevent the recurrence and metastasis of cancer. This irradiation often induces osteoradionecrosis, resulting in decreasing or losing the natural potential of bone regeneration [84, 85]. Therefore, it is practically necessary to develop a technology to induce bone regeneration even at the tissue site of such unhealthy conditions. For this purpose, combination of MSC, the scaffold, and the controlled release system of growth factor is promising. Chapter 8 investigates the feasibility of gelatin-ß-TCP scaffolds in enhancing bone regeneration at a segmental ulna defect of rabbits X-ray irradiated. The gelatin-ß-TCP scaffold with or without the combination of MSC and/or BMP-2 was implanted into the ulna defect and the effect of the scaffold type on the bone regeneration at the defect was assessed in terms of the histological and pQCT examinations.

In summary, this thesis describes the feasibility of gelatin-based scaffolds in the controlled

release carrier of BMP-2 and the three-dimensional matrix of MSC for osteogenic differentiation. It is concluded that this material design of scaffold is promising to effectively induce bone regeneration based on tissue engineering.

REFERENCES

1. C. Laurencin, Y. Khan, and S. F. El-Amin, Bone graft substitutes, *Expert Rev. Med. Devices*, **3**, 49-57 (2006).
2. C. J. Damien and J. R. Parsons, Bone graft and bone graft substitutes: A review of current technology and applications, *J. Applied Biomaterials*, **2**, 187-208 (1991).
3. D. J. Prolo and J. J. Rodrigo, Contemporary bone graft physiology and surgery, **200**, 322-342 (1985).
4. E. M. Younger and M. W. Chapman, Morbidity at bone graft donor sites, *J. Orthop. Trauma*., **3**, 192-195 (1989).
5. B. E. Buck and T. I. Malinin, Bone transplantation and human immunodeficiency virus. An estimate of risk of acquired immunodeficiency syndrome (AIDS), *Clin. Orthop*., **240**, 129-136 (1989).
6. V. Maquet and R. Jerome, Design of macroporous biodegradable polymer scaffolds for cell transplantation, *Mater. Sci. Forum*, **205**, 15-42 (1997).
7. M. J. Yazemski, J. B. Oldham, L. Lu, and B. L. Currier, *Bone Engineering, 1st edition*, Em squared, Toronto (1994).
8. R. Langer and J. P. Vacanti, Tissue Engineering, *Science*, **260**, 920-926 (1993).
9. S. P. Bruder and B. S. Fox, Tissue Engineering of Bone, *Clin. Orthop. Rel. Res*., **367S**, S68-83 (1999).
10. B. D. Boyan, C. H. Lormann, J. Romero, and Z. Schwartz, Bone and cartilage tissue engineering, *Clin. Plast. Surg*. **26**, 629-645 (1999).
11. A, J. Salgado, O. P. Coutinho, and R. L. Reis, Bone Tissue Engineering: State of the Art and Future Trends, *Macromol. Biosci*., **4**, 743-765 (2004).
12. S. J. Peter, M. J. Miller, A. W. Yasko, M. J. Yaszemski, and A. G. Mikos, Polymer concepts in tissue engineering, *J. Biomed. Mater. Res*., **43**, 422-427 (1998).

13. U. A. Stock and J. P. Vacanti, Tissue engineering: current state and prospects, *Ann. Rev. Med*., **52**, 443-451 (2001).

14. X. Liu and P. X. Ma, Polymeric scaffolds for bone tissue engineering, *Ann. Biomed. Eng*., **32**, 477-486 (2004).

15. V. Oliver, N. Faucheux, and P. Hardouin, Biomaterial challenges and approaches to stem cell use in bone reconstructive surgery, *Drug Discovery Today*, **9**, 803-811 (2004).

16. J. E. Davies, J. M. Karp, and D. Baksh, Mesenchymal cell culture, *Methods in Tissue Engineering*, Academic Press, New York (2002).

17. K. Rezwan, Q. Z. Chen, J. J. Blaker, and R. Boccaccini, Biodegradable and bioactive polymer/inorganic composite scaffolds for bone tissue engineering, *Biomaterials*, **27**, 3413-3431 (2006).

18. K. J. L. Burg, S. Porter, and J. F. Kellam, Biomateral developments for bone tissue engineering, *Biomaterials*, **21**, 2347-2359 (2000).

19. L. L. Hench and J. M. Polak, Third-generation biomedical materials, *Science*, **295**, 1014-1017 (2002).

20. M. Geiger, R. H. Li, and W. Friess, Collagen sponges for bone regeneration with rhBMP-2, *Adv. Drug Deliv. Rev*., **55**, 1613-1629 (2003).

21. D. K. Han and J. A. Hubbel, Lactide-based poly(ethylene glycol) polymer networks for scaffolds in tissue engineering, *Macromolecules*, **29**, 5233-5235 (1996).

22. H. Ohgushi and A. I. Caplan, Stem cell technology and bioceramics: from cell to gene engineering, *J. Biomed. Mater. Res.*, **48**, 913-927 (1999).

23. S. P. Bruder and A. I. Caplan, Bone regeneration through cellular engineering, *Principle of Tissue Engineering 2nd ed.*, Academic Press, New York (2000).

24. M. Riminucci and P. Bianco, Building bone tissue: matrices and scaffolds in physiology and biotechnology, *Braz. J. Med. Biol. Res*., **36**, 1027-1036 (2003).

25. T. Kokubo, H. M. Kim, and M. Kawashita, Novel bioactive ceramics with different mechanical

properties, *Biomaterials*, **24**, 2161-2175 (2003).

26. H. Yoshikawa and A. Myoi, Bone tissue engineering with porous hydroxyapatite ceramics, *J. Artif. Organ*, **8**, 131-136 (2005).

27. A. El-Ghannam, Bone reconstruction: from bioceramics to tissue engineering, *Expert Rev. Med. Devices*, **2**, 87-101 (2005).

28. C. Du, F. Z. Cui, X. D. Zhu, and K. de Groot, Three-dimensional nano-HAp/collagen matrix loading with osteogenic cells in organ culture, *J. Biomed. Mater. Res*., **44**, 407-415 (1999).

29. C. V. Rodrigues, P. Serricella, A. B. Linhares, R. M. Guerdes, R. Borojevic, M. A. Rossi, M. E. Duarte, and M. Farima, Characterization of a bovine collagen-hydroxyapatite composite scaffold for bone tissue engineering, *Biomaterials*, **24**, 4987-4997 (2003).

30. C. T. Laurencian, M. A. Attawia, L. Q. Lu, M. D. Borden, H. H. Lu, W. J. Gorum, and J. R. Liebermen, Poly(lactide-co-glycolide)/hydroxyapatite delivery of BMP-2-producing cells: a regional gene therapy approach to bone regeneration, *Biomaterials*, **22**, 1271-1277 (2001).

31. H. H. K. Xu and J. C. G. Simon, Self-hardening calcium phosphate composite scaffold for tissue engineering, *J. Orthop. Res.*, **22**, 535-543 (2004).

32. H. U. Cameron, I. Macnab, and R. M. Pillar, Evaluation of a biodegradable ceramic, *J, Biomed. Mater. Res.*, **11**, 179-186 (1977).

33. P. J. Boyne, T. J. O'Leary, and C. F. Cox, Association reports, councils on dental materials, instruments, and equipment; research; therapeautics, hydroxyapatite, beta tricalcium phosphate, and autogenous and allogeneic bone for filling periodontal defects, alveolar ridge augumentation, pulp capping, *JADA*, **108**, 822-831 (1984).

34. J. P. Vacanti, M. A. Morse, W. M. Saltzman, A. J. Domb, A. Perezatayde, R. Langer, C. L. Mazzoni, and C. K. Breuer, Selective cell transplantation using bioabsorbable artificial polymers as matrices, *J. Pediatr. Surg*., **23**, 3-9 (1988).

35. P. X. Ma, R. Y. Zhang, G. Z. Xiao, and R. Franceschi, Engineering new bone tissue *in vitro* on highly porous poly(alpha-hydroxyl acid)/hydroxyapatite composite scaffolds, *J. Biomed Mater.*

Res., **54**, 284-293 (2001).

36. V. Karageorgiou and D. Caplan, Porosity of 3D biomaterial scaffolds and osteogenesis, *Biomaterials*, **26**, 5474-5491 (2005).

37. S. F. Hulbert, F. A. Young, R. S. Mathews, J. J. Klawitter, C. D. Talbert, and F. H. Stelling, Potential of ceramics materials as permanently implantable skeletal prostheses, *J. Biomed. Mater. Res.*, **4**, 433-456 (1970).

38. Y. Kuboki, Q. Jin, and H. Takita, Geometry of carriers controlling phenotypic expression in BMP-induced osteogenesis and chondrogenesis, *J. Bone Joint Surg. Am.*, **83A**, S105-115 (2001).

39. K. Anselme, Osteoblast adhesion on biomaterials, *Biomaterials*, **21**, 667-681 (2000).

40. B. D. Boyan, T. W. Hummert, D. D. Dean, and Z. Schwartz, Role of material surfaces in regulating bone and cartilage cell response, *Biomaterials*, **17**, 137-146 (1996).

41. J. Taipale and J. Keski-Oja, Growth factors in the extracellular matrix, *FASEB J.*, **11**, 51-59 (1997).

42. G. Ahrendt, D. E. Chickering, and J. P. Ranieri, Angiogenic growth factor: A review for tissue engineering, *Tissue Eng.*, **4**, 117-130 (1998).

43. M. C. Manning, K. Patel, and T. Borchardt, Stability of protein pharmaceuticals, *Pharm. Res.*, **6**, 902-918 (1989).

44. Y. J. Wang and A. Hanson, Parenteral formulations of proteins and peptides: stability and stabilizer, *J. Parenter. Sci. Technol.*, **Suppl. 42**, S2-26 (1988).

45. S. A. Gittens and H. Uludag, Growth factor delivery for bone tissue engineering, *J. Drug Targeting*, **9**, 407-429 (2001).

46. S. R. Winn, H. Uludag, and J. O. Hollinger, Sustained release emphasizing recombinant human bone morphogenetic protein-2, *Adv. Drug Deliv. Rev.*, **31**, 303-318 (1998).

47. J. M. Wozney, V. Rosen, A. J. Celeste, L. M. Mitsock. M. J. Whitters, R. W. Kriz, R. M. Hewick, and E. A. Wang, Novel regulators of bone formation; molecular clones and activities, *Science*, **242**, 1528-1534 (1988).

48. J. M. Wozney and V. Rosen, Bone morphogenetic protein and bone morphogenetic protein family in bone formation and repair, *Clin. Orthop.*, **346**, 26-37 (1998).

49. R. G. T. Geesink, N. H. M. Hoefnagels, S. K. Bulstra, Osteogenic activity of OP-1 morphogenetic protein (BMP-7) in a human fibular defect, *J. Bone Joint Surg. Br.*, **81-B**, 710-718 (1999).

50. J. R. Lieberman, A. Daluski, and T. A. Einhorn, The role of growth factors in the repair of bone: biology and clinical applications, *J. Bone Joint Surg. Am.*, **84-A**, 1032-1044 (2002).

51. A. Valentin-Opran, J. Wozney, C. Csimma, L. Lilly, and G. E. Riedel, Clinical evaluation of recombinamt human bone morphogenetic protein-2, *Clin. Orthop. Rel. Res.*, **395**, 110-120 (2002).

52. W. Friess, H. Uludag, S. Foskett, R. Biron, and C. Sargeant, Characterization of absorbable collagen sponges as rhBMP-2 carriers, *Int. J. Pharm.*, **187**, 91-99 (1999).

53. M. Geiger, R. H. Li, and W. Friess, Collagen sponges for bone regeneration with rhBMP-2, *Adv. Drug Deliv. Rev.*, **55**, 1613-1629 (2003).

54. B. D. Boyan, C. H. Lohmann, A. Somers, G. G. Niederauer, J. M. Wozney, D. D. Dean, D. L. Jr. Carnes, and Z. Schwartz, Potential of porous poly-D, L-lactide-co-glycolide particles as a carrier for recombinant human bone morphogenetic protein-2 during osteoinduction *in vivo*, *J. Biomed. Mater. Res.*, **46**, 51-59 (1999).

55. M. R. Urist, A. Lietze, and E. Dawson, ß-tricalcium phosphate delivery system for bone morphogenetic protein, *Clin. Orthop. Rel. Res.*, **187**, 277-280 (1984).

56. H. D. Zegzula, D. C. Buck, J. Brekke, J. M. Wozney, and J. O. Hollinger, Bone formation with use of rhBMP-2 (recombinant human bone morphogenetic protein-2), *J. Bone Joint Surg. Am.*, **79**, 1778-1783 (1997).

57. N. Saito, T. Okada, H. Horiuchi, N. Murakami, J. Takahashi, M. Nawata, H. Ota, K. Nozaki, K. Takaoka, A biodegradable polymer as a cytokine delivery system for inducing bone formation, *Nat. Biotech.*, **19**, 332-335 (2001).

58. H. Seeherman and J. M. Wozney, Delivery of bone morphogenetic proteins for orthopedic tissue

regeneration, *Cytokine & Growth factor Reviews*, **16**, 329-345 (2005).

59. Y. Tabata, S. Hijikata, and Y. Ikada, Enhanced vascularization and tissue granulation by basic fibroblast growth factor impregnated in gelatin hydrogels, *J. Control. Release*, **31**, 189-194 (1994).

60. Y. Tabata and Y. Ikada, Vascularization effect of basic fibroblast growth factor released from gelatin hydrogels with different biodegradabilities, *Biomaterials*, **20**, 2169-2175 (1999).

61. M. Yamamoto, Y. Tabata, L. Hong, S. Miyamoto, N. Hashimoto, and Y. Ikada, Bone regeneration by transforming growth factor ß1 released from a biodegradable hydrogel. *J. Control. Release*, **64**, 133-142 (2000).

62. L. Hong, Y. Tabata, S. Miyamoto, K. Yamada, I. Aoyama, M. Tamura, N. Hashimoto, and Y. Ikada, Promoted bone healing at a rabbit skull gap between autologous bone fragment and the surrounding intact bone with biodegradable microspheres containing transforming growth factor-ß1, *Tissue Eng*., **6**, 331-340 (2000).

63. M. Ozeki, T. Ishii, Y. Hirano, and Y. Tabata, Controlled release of hepatocyte growth factor from gelatin hydrogels based on hydrogel degradation, *J. Drug Target.*, **9**, 461-471 (2001).

64. D. Zekorn, Modified gelatin as plasma substitutes, *Bibl. Haematol.*, **33**, 30-60 (1969).

65. Y. Tabata and Y. Ikada, Protein release from gelatin matrices, *Adv. Drug Deliv. Rev.*, **31**, 287-301 (1998).

66. Y. Tabata, Tissue regeneration based on growth factor release, *Tissue Eng.*, **9**, S5-15 (2003).

67. A. I. Caplan, Mesenchymal stem cells, *J. Orthop. Res.*, **9**, 641-650 (1991).

68. S. E. Haynesworth, M. A. Bader, and A. I. Caplan, Cell surface antigens on human marrow-derived mesenchymal cells are detected by monoclonal antibodies, *Bone*, **13**, 69-80 (1992).

69. H. Nakahara, J. E. Dennis, S. P. Bruder, S. E. Heynesworth, D. P. Lennon, and A. I. Caplan, *In vitro* differentiation of bone and hypertrophic cartilage from periosteal-derived cells, *Exp. Cell Res.*, **195**, 492-503 (1991).

70. D. P. Lennon, S. E. Heynesworth, D. M. Arm, M. A. Baber, and A. I. Caplan, Dilution of human mesenchymal stem cells with dermal fibroblasts and the effects on *in vitro* and *in vivo* osteochondrogenesis, *Dev. Dyn.*, **219**, 50-62 (2000).

71. S. P. Bruder, N. Jaiswal, and S. E. Heynesworth, Growth kinetics, self-renewal and the osteogenic potential of purified human mesenchymal stems during extensive subcultivation and cryopreservation, *J. Cell. Biochem.*, **64**, 278-294 (1997).

72. H. Ohgushi, V. M. Goldberg, and A. I. Caplan, Repair of bone defects with bone marrow cells and porous ceramics. Experiments in rat, *Acta. Orthop. Scand.*, **60**, 334-339 (1989).

73. B. Johnstone, T. M. Hering, A. I. Caplan, V. M. Goldbelg, and J. U. Yoo, *in vitro* chondrogenesis of bone marrow-derived mesenchymal progenitor cells, *Exp. Cell Res.*, **238**, 265-272 (1998).

74. S. P. Bruder, A. A. Kurth, M. Shea, W. C. Hayes, N. Jaiswal, and S. Kadiyala, Bone regeneration by implantation of purified, culture expanded human mesenchymal stem cells, *J. Orthop. Res.*, **16**, 155-162 (1998).

75. H. Petite, V. Viateau, W. Bensaid, A. Meunier, C. de Pollak, M. Bourguignon, K. Oudina, L. Sedel, and G. Guillemin, Tissue engineered bone regeneration, *Nat. Biotechnol.*, 1**8**, 959-963 (2000).

76. L. E. Freed, J. C. Marquis, G. Vunjak-Novakovic. J. Emmanual, and R. Langer, Composition of cell-polymer cartilage implants, *Biotech. Bioeng.*, **43**, 605-614 (1994).

77. Y. L. Xiao, J. Riesle, and C. A. van Blitterwijk, Static and dynamic fibroblast seeding and cultivation in porous PEO/PBT scaffolds, *J. Mater. Sci. Mater. Med.*, **10**, 773-777 (1999).

78. G. Vunjak-Novakovic, B. Obradovic, I. Martin, P. M. Bursac, R. Ranger, and L. E. Freed, Dynamic cell seeding of polymer scaffolds for cartilage tissue engineering, *Biotech. Prog.*, **14**, 193-202 (1998).

79. M. Wiedmann-Al Ahmed, R. Gutwald, G. Lauer, U. Hubner, and R. Schmelzeisen, How to optimize seeding and culturing of human osteoblast-like cells on various biomaterials, *Biomaterials*, **23**, 3319-3328 (2002).

80. Y. Li, T. Ma, D. A. Kniss, L. C. Laski, and S. T. Yang, Effects of filtration seeding on cell density, spatial distribution, and proliferation in nonwoven fibrous matrices, *Biotechnol. Prog.*, **17**, 935-944 (2001).

81. L. E. Freed and Gordana Vumjak-Novakovic, Tissue Engineering Bioreactors, *Principles of Tissue Engineering 2nd ed.*, Academic Press, New York (2000).

82. P. K. Yarlagadda, M. Chandrasekharan, and J. Y. Shyan, Recent advances and cerrent developments in tissue sdaffolding, *Biomed. Mater. Eng.*, **15**, 159-177 (2005).

83. A. S. Mistry and A. G. Mikos, Tissue engineering strategies for bone regeneration, *Adv. Biochem. Eng. Biotechnol.*, **94**, 1-22 (2005).

84. I. Meyer, Infectious diseases of the jaws, *J. Oral Surg.*, **28**, 17-26 (1970).

85. R. E. Marx, Osteoradionecrosis: a new concept of its pathophysiology, *Oral Maxillofac. Surg.*, **41**, 283-288 (1983).

PART I

BONE REGENERATION BY CONTROLLED RELEASE OF BONE MORPHOGENETIC PROTEIN-2 FROM BIODEGRADABLE HYDROGEL SCAFFOLDS

Chapter 1

Ectopic bone formation by controlled release of BMP-2 from biodegradable hydrogels

INTRODUCTION

Osteoinductive proteins of bone morphogenetic protein (BMP) family have been attracted much attention in the field of bone reconstructive surgery because they show various biological activities to induce bone formation both orthotopically and ectopically in the body [1, 2]. The current recombinant DNA technologies have enabled recombinant human BMPs to produce the amount enough for the basic and applied researches [3]. Among them are recombinant human BMP-2 and BMP-7 (OP-1) of which the clinical trials have been started for local bone regeneration at the bone defect of size as large as impossible to naturally repair only by the self-healing ability of human body [4, 5]. However, the BMP administrated in the solution form does not always induce the expected efficacy in bone regeneration. This is mainly due to the *in vivo* short retention of BMP protein itself. Therefore, it is necessary to develop an administration carrier for the controlled release of biologically active BMPs over an extended time period.

Biodegradable carriers incorporating BMP have been placed in bone defects [1]. In this case the matrices serve as the carrier of the growth factors, and occasionally function also as the substrate for bone cell attachment. Numerous carriers were shown to be compatible with the osteoinductive activity of BMP [6]. Among them, collagen-based carriers are being used in a clinical setting. These choices have been based on a series of preclinical studies, which indicated a pharmacological induction of local bone formation by BMP. Uludag et al. have demonstrated from the pharmacokinetic study of BMP-2 with collagen sponge, demineralized bone matrix, polyglycolide, and calcium phosphates (hydroxyapatite, tricalcium phosphate) that the locally retained concentration of BMP well correlated with the osteoinductive potency; the higher the concentration of BMP at the site applied, the higher the

osteoinductive activity [7-12]. In spite of the significance of BMP localization in biological activity, little has been investigated on the relationship between the *in vivo* local retention of BMPs and osteoinductive potency, much less to positively change the BMP-2 retention by changing the release carrier.

Gelatin is biodegradable and has been extensively used for food, pharmaceutical, and medical purposes and its biosafety has been proven through their long practical applications [13]. The material advantages of gelatin are the easiness of chemical modification and the commercial availability of materials with different properties. We have prepared hydrogels of different biodegradable profiles from gelatin and succeeded in inducing the biological activities of basic fibroblast growth factor (bFGF) [14], transforming growth factor-β1 (TGF-β1) [15], and hepatocyte growth factor (HGF) [16] through their controlled release with the biodegradable hydrogel, although usage of the growth factors in the solution form was not effective.

The objective of this chapter is to prepare an *in vivo* release system of BMP-2 from biodegradable gelatin hydrogels for the enhancement of BMP-2 bone formation activity. Hydrogels with different biodegradabilities were obtained by changing the concentration of gelatin and glutaraldehyde used in hydrogel preparation. Following the subcutaneous implantation of various gelatin hydrogels incorporating BMP-2 into the back of mice, the time profile of BMP-2 retention was evaluated to compare it with the bone formation activity induced by the hydrogel.

EXPERIMENTAL

Radioiodination of BMP-2

Human recombinant BMP-2 (Yamanouchi Pharmaceutical Co., Japan) was radioiodinated according to the method of Greenwood et al. [17]. Briefly, 4 μl of $Na^{125}I$ was added to 40 μl of 3 mg/ml BMP-2 solution in 5 mM glutamic acid, 2.5 wt% glycine, 0.5 wt% sucrose, and 0.01 wt% Tween 80 (pH 4.5). Then, 0.2 mg/ml of chloramine-T in 0.5 M potassium phosphate-buffered solution (pH 7.5) containing 0.5 M sodium chloride (100 μl) was added to the solution mixture. After agitation at room

temperature for 2 min, 100 μl of phosphate-buffered saline solution (PBS, pH 7.5) containing 0.4 mg of sodium metabisulfate was added to the reaction solution to stop the radioiodination. The reaction mixture was passed through an anionic-exchange column to remove the uncoupled, free ^{125}I molecules from the ^{125}I-labeled BMP-2.

Preparation of gelatin and collagen hydrogels incorporating BMP-2

Hydrogels were prepared through the chemical crosslinking of aqueous gelatin solution with glutaraldehyde according to the method described previously [15]. Briefly, an aqueous glutaraldehyde solution of gelatin was cast into a polypropylene dish (138×138 mm^2, BIO-BIK) at various concentrations of glutaraldehyde and gelatin shown in Table 1-1, followed by the crosslinking reaction at 4 °C for 12 hr. The crosslinked hydrogel prepared was punched out to obtain the discs of 6 mm diameter. The hydrogel discs were stirred in 100 mM aqueous glycine solution at 37 °C for 1 hr to block the residual aldehyde groups of glutaraldehyde. Following washing three times with double-distilled water (DDW), the discs were freeze-dried and sterilized with ethylene oxide gas. The hydrogel weight was measured before and after complete drying at 70 ^{o}C under vacuum and the water content, the weight percentage of water in the wet hydrogel, was calculated from the weight values [18].

Table 1-1 Preparation of gelatin hydrogels with different water contents.

Concentration of gelatin (wt%)	Concentration of glutaraldehyde (wt%)	Water content (wt%)
5	0.83	93.8
3	0.65	96.9
3	0.16	97.8
3	0.09	99.1
3	0.06	99.7

A collagen sponge was kindly provided from Gunze Ltd. Japan [19]. For the sponge preparation, a collagen solution (0.3 wt % of type I atelocollagen, Cell matrix®; Nitta Gelatin Co. Ltd., Japan, pH 3.0) was stirred at 2,000 rpm for 1 hr at 4 ^{o}C to generate small bubbles and then freeze-dried. The resulting sponge of 3-mm thickness was thermally crosslinked under vacuum for 24 hr at 105 ^{o}C and additionally underwent chemical crosslinking in 0.2 vol% acetic acid solution of glutaraldehyde for 24 hr at 4 ^{o}C. Following DDW washing similarly, the sponge was freeze-dried and sterilized by ethylene oxide gas. The average pore size, pore volume fraction, and density of sponge prepared were measured by the method described elsewhere [20] and were 86 μm, 87 vol%, and 1.0×10^{-2} g/cm^3, respectively.

To prepare gelatin and collagen hydrogels incorporating BMP-2, 20 μl of aqueous solution containing BMP-2 (2.5×10^{-2}, 5.0×10^{-2}, and 2.5×10^{-1} μg/μl) or ^{125}I-labeled BMP-2 (1.2×10^{-1} μg/μl) was dropped onto the respective freeze-dried sample, followed by leaving them at 4 °C overnight. The BMP-2-incorporated gelatin and collagen hydrogels prepared were used without washing. Similarly, 20 μl of BMP-2-free PBS was impregnated into freeze-dried gelatin hydrogels to obtain BMP-2-free, empty hydrogels.

In vivo evaluation of controlled release of BMP-2 from gelatin hydrogels incorporating BMP-2

Table 1-2 summarized overall experimental design for *in vivo* evaluation of BMP-2 release. The ^{125}I-labeled BMP-2-incorporated gelatin and collagen hydrogels were implanted into the back subcutis of 6 week-age female ddY mice (Shimizu Laboratory Supply Inc., Japan) at the central position 15 mm away from their tail root. As a control, 100 μl of aqueous solution of ^{125}I-labeled BMP-2 (2.4×10^{-2} μg/μl) was subcutaneously injected into the mouse back. At different time intervals, the skin on the back of mice around the implanted or injected site of BMP-2 was cut into a strip of 3×5 cm^2 and the corresponding facia was thoroughly wiped off with a filter paper to absorb ^{125}I-labeled BMP-2. The radioactivity of gelatin and collagen hydrogels remaining, excised skin, and filter paper was measured on the gamma counter (ARC-301B, Aloka Co., Ltd., Japan) to assess the time profile of *in vivo* BMP-2 retention.

Table 1-2. The overall experiment design for *in vivo* evaluations of BMP-2 release and ectopic bone induction .

Group	*In vivo* BMP-2 release		Ectopic bone induction (ALP activity)		Ectopic bone induction (osteocalcin content)	
	Hydrogel	Solution	Hydrogel	Solution	Hydrogel	Solution
^{125}I-labeled BMP or BMP dose	2.4 μg/mouse	2.4 μg/mouse	0, 0.5, 1.0, and 5.0 μg/mouse	0, 0.5, 1.0, and 5.0 μg/mouse	0 and 5.0 μg/mouse	0 and 5.0 μg/mouse
Implantation site	Mouse back subcutis	Mouse back subcutis	Mouse back subcutis	Mouse back subcutis	Mouse back subcutis	Mouse back subcutis
Number of animals for a each point	3	3	6	6	6	6
Formulation	Water contents of 93.8, 96.9, 97.8, 99.1, 99.7 wt%	100 μl solution	Water contents of 93.8, 96.9, 97.8, 99.1, 99.7 wt%	100 μl solution	Water contents of 93.8, 96.9, 97.8, 99.1, 99.7 wt%	100 μl solution

The radioactivity was divided by the original radioactivity of gelatin and collagen hydrogels incorporating ^{125}I-labeled BMP-2 and aqueous solution of ^{125}I-labeled BMP-2 to calculate the percent remaining of BMP-2. All the radioactivities were compensated for the natural decay of ^{125}I. Experimental group was composed of 3 mice unless otherwise mentioned.

For evaluation of *in vivo* half-life period of BMP-2 in the solution or hydrogel-incorporating form, a biexponential model was used to obtain half-lives, $t_{1/2}$: $C(t)=Ae^{-mt}+Be^{-nt}$, where $C(t)$ = radioactivity at time t; A and B = constants; m and n = rate constants; and $t_{1/2}$ = 0.693/rate constant. In this model, BMP-2 release from hydrogels is assumed to be described by two distinct processes, each characterized by a $t_{1/2}$ that represents the average time required for 50 % of the dose to be released from the hydrogels [7].

In vivo degradation of gelatin hydrogels was examined by use of ^{125}I-labeled gelatin hydrogels. Briefly, gelatin hydrogels were radioiodinated by use of Bolton-Hunter reagent [18, 21]. The ^{125}I-labeled gelatin hydrogels were implanted in the back subcutis of mice (3 mice/experimental group). At different time intervals, the radioactivity of explanted hydrogels and the surrounding tissues was measured to evaluate the time profile of *in vivo* hydrogel degradation. The percentage of the remaining radioactivity was expressed as the radioactivity ratio of the remaining hydrogels to the original ^{125}I-labeled gelatin hydrogel.

Biochemical evaluation of BMP-2-induced ectopic bone formation

As shown in Table 1-2, gelatin hydrogels incorporating 0.5, 1.0, and 5.0 μg of BMP-2 and collagen hydrogels incorporating 1.0 and 5.0 μg of BMP-2 were implanted into the back subcutis of ddY mice (6 mice/experimental group), while 100 μl of aqueous BMP-2 solution at concentrations of 5×10^{-3}, 1×10^{-2}, and 5×10^{-2} μg/μl was injected subcutaneously into the mice back. The BMP-2-free, empty gelatin hydrogel and BMP-2-free PBS were used as controls. The skin tissue including the hydrogel-implanted or injected site was taken out for following biochemical assays 1, 2, and 4 weeks later.

The tissues obtained was freeze-dried and crushed. The crushed tissue (5 mg) was homogenized in 1 ml of mixed solution of 0.2 % Nonidet P-40, 10 mM Tris-HCl, and 1 mM $MgCl_2$ (pH 7.5). The

homogenate was centrifuged at 12,000 rpm and 4 ^{o}C for 15 min and the alkaline phosphatase (ALP) activity of supernatant obtained was determined by a *p*-nitro phenyl-phosphate method [22].

For the determination of osteocalcin content, the crushed tissue (5 mg) was decalcified with 40 % formic acid (1 ml) for 12 hr. During the decalcification process, the non-collagenous proteins of bone matrix were extracted. After desalting of the extracts with a gel filtration using Sephadex^{TM} G-25M column (PD-10, Amersham Pharmacia biotech AB, Sweden), the resulting solution was freeze-dried and subjected to an osteocalcin radioimmunoassay (mouse osteocalcin IRMA kit, Immutopics, Inc., USA) [22].

Histological evaluation of BMP-2-induced ectopic bone formation

The subcutaneous tissue including the BMP-2-incorporated or BMP-2-free gelatin hydrogel was embedded into Tissue-Tek (Sakura, Co., Ltd., Japan), followed by freezing in liquid nitrogen. After fixation with acetone, cryo-sections of the tissues (6 μm thickness) was stained for ALP by using sodium naphthol AS-BI phosphate and fast blue RR as a substrate and diazonium salt [23], while it was counter-stained with Mayer's hematoxylin solution.

Calcium deposition of the tissues was visualized by von Kossa staining according to the method described by Drury et al. [24]. Briefly, the paraffin-embedded tissues were sectioned and stained with silver nitrate, followed by washing with sodium thiosulphate and DDW. The sections prepared were histologically viewed on a light microscope (AX-80, Olympus, Japan).

Statistical analysis

All the values were shown as the mean value ± the standard deviation of the mean. The pairwise comparisons of individual group means were conducted based on the Tukey test. Values of $p < 0.05$ were considered statistically significant.

RESULTS

In vivo controlled release of BMP-2 from gelatin hydrogels

Figure 1-1 shows the *in vivo* decrement patterns of the remaining radioactivity at the implanted site of ^{125}I-labeled BMP-2-incorporated gelatin hydrogels with different water contents or at the injected site of ^{125}I-labeled BMP-2 solution. Irrespective of the hydrogel type, BMP-2 was retained in the mouse subcutis for longer time periods than free BMP-2 injected. The period of BMP-2 retention depended on the water content of hydrogels; the lower the water content of hydrogels, the longer the remaining period of BMP-2 radioactivity. No significant accumulation of radioactivity was detected in any organ during the experiment period, irrespective of the dosage form. Negligibly low radioactivity was detected in the thyroid gland for each experimental group, indicating no release of free radioactive iodine from ^{125}I-labeled BMP-2 (data not shown).

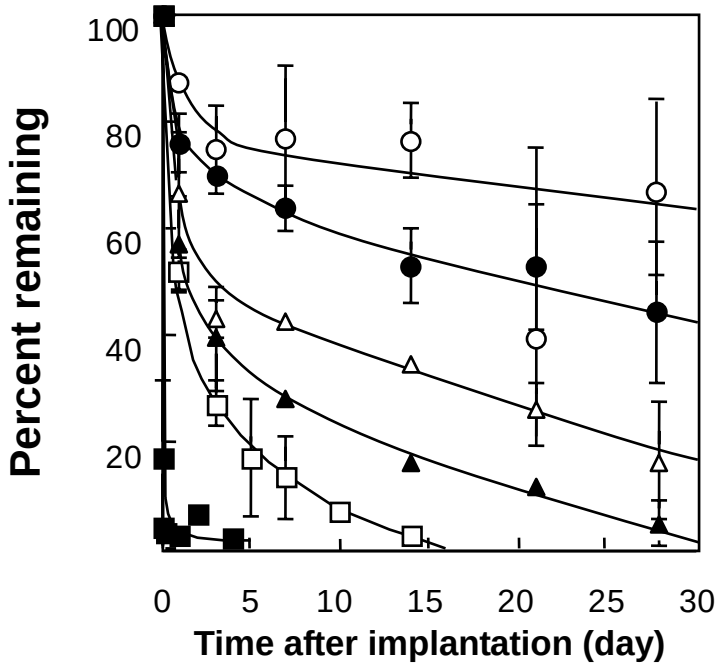

Figure 1-1. *In vivo* time profiles of the radioactivity remaining after the subcutaneous implantation of gelatin hydrogels incorporating ^{125}I-labeled BMP-2 into the back of mice. The hydrogel water contents are (○) 93.8, (●) 96.9 , (△) 97.8 , (▲) 99.1 , and (□) 99.7 wt%. The symbol (■) indicates the remaining radioactivity after injection of ^{125}I-labeled BMP-2 solution.

To study the relationship between the *in vivo* BMP-2 release and the gelatin hydrogel degradation, the time course of radioactivity remaining after subcutaneous implantation of ^{125}I-labeled gelatin hydrogels into the mouse back was determined. The remaining radioactivity percentage after implantation of the hydrogels incorporating ^{125}I-labeled BMP-2 was plotted against that of ^{125}I-labeled gelatin hydrogels in Figure 1-2. All the experimental data were normalized by the percent radioactivity remaining after one-day implantation. It is apparent that there was a linear correlation with the slope around 0.9 between the two remaining percentages.

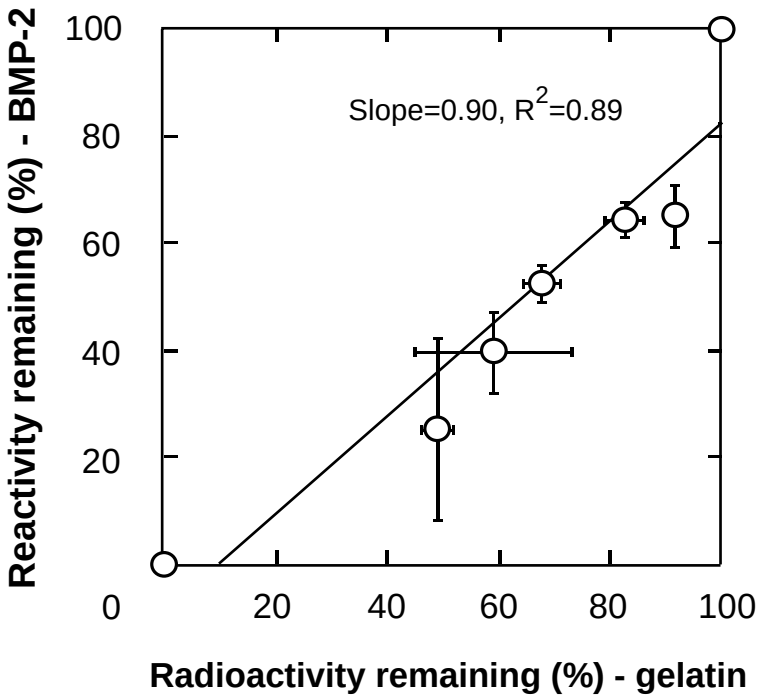

Figure 1-2. The remaining radioactivity of the gelatin hydrogel incorporating ^{125}I-labeled BMP-2 as a function of ^{125}I-labeled gelatin hydrogel after subcutaneous implantation into the mouse back.

Ectopic bone formation induced by gelatin and collagen hydrogels incorporating BMP-2

Figure 1-3 shows the ALP activity of subcutaneous tissues around the implanted site of gelatin hydrogels incorporating BMP-2 and injected site of free BMP-2 1, 2, and 4 weeks after implantation. It is apparent that the application of gelatin hydrogels incorporating 1 and 5 μg of BMP-2 enhanced the ALP activity of subcutaneous tissues to a significantly higher extent than that of free BMP-2.

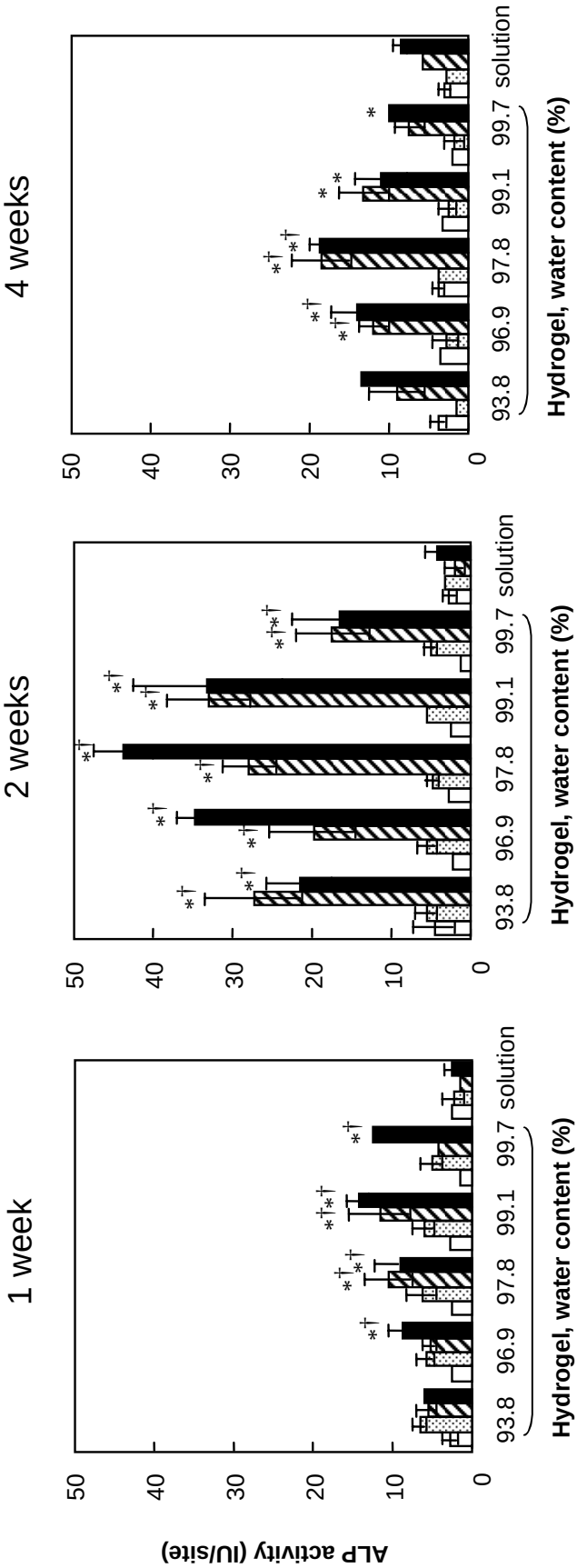

Figure 1-3. ALP activity of tissues around the implanted site of gelatin hydrogels incorporating BMP-2 and the injected site of BMP-2 solution 1, 2, and 4 weeks later. The BMP-2 doses are (□) 0, (▨) 0.5, (▨) 1, and (■) 5 μg. $^{*}p < 0.05$; significant against the ALP activity of the ALP activity of the control group receiving the injection of BMP-2-free PBS. $^{\dagger}p < 0.05$; significant against the activity of mice applied with BMP-2 solution at the corresponding BMP dose.

The tissue activity increased with time to attain a maximum level 2 weeks after implantation and thereafter decreased with time, irrespective of the hydrogel water content. No significant enhancement of ALP activity was observed for the gelatin hydrogel incorporating 0.5 μg of BMP-2. For gelatin hydrogels incorporating 5 μg of BMP-2 2 and 4 weeks after implantation, the hydrogel with a water content of 97.8 wt% showed the highest ALP activity, while other hydrogels with the higher or lower water content did lower ALP activities. BMP-2-free, empty gelatin hydrogels with any water content did not contribute to any increase in the tissue ALP activity.

Figure 1-4 shows the ALP activity of subcutaneous tissues 1, 2, and 4 weeks after implantation of collagen hydrogels incorporating 1 and 5 μg of BMP-2 together with the *in vivo* time profile of radioactivity remaining at the implanted site of ^{125}I-labeled BMP-2-incorporated collagen hydrogels. The tissue ALP activity was significantly lower for the collagen hydrogel incorporating BMP-2 than the gelatin hydrogel incorporating BMP-2 with a water content of 97.8 wt%, irrespective of the BMP-2 dose and implantation time. The period of BMP-2 retention by the gelatin hydrogels was longer than that of the collagen hydrogel.

Figure 1-5 shows the osteocalcin content of tissues around the implanted site of gelatin hydrogels incorporating BMP-2 and the injected site of free BMP-2 1, 2, and 4 weeks after implantation. The BMP-2-incorporated gelatin hydrogel with a water content of 97.8 wt% exhibited the highest osteocalcin content 2 and 4 weeks after the implantation. The osteocalcin content of tissue increased with implantation time although the dependence of hydrogel type on the osteocalcin level did not change. The BMP-2 free, empty hydrogels, BMP-2-free solution, and the solution containing 5 μg of BMP-2 were ineffective in increasing the osteocalcin content.

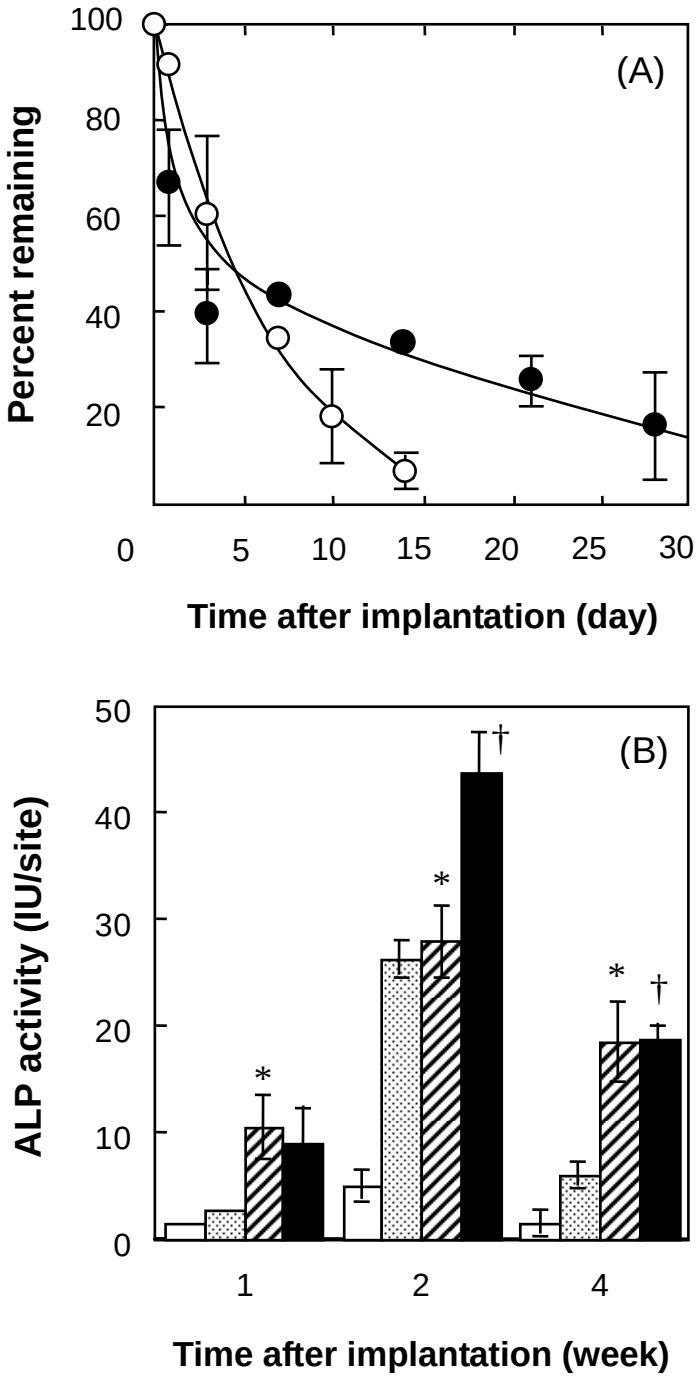

Figure 1-4. Comparison of BMP-2 retention profile and ALP activity between the gelatin and collagen hydrogels incorporating BMP-2. (A) *in vivo* decrement patterns of the remaining radioactivity at the implanted site of ^{125}I-labeled BMP-2-incorporated collagen hydrogel (○) and gelatin hydrogel with a water content of 97.8 wt% (●) and (B) the ALP activity of tissues 1, 2, and 4 weeks after implantation of collagen (□,⬚) and gelatin hydrogel (▨,■) incorporating 1 (□,▨) and 5 μg of BMP-2 (⬚,■). *$p < 0.05$; significant against the ALP activity of mice applied with collagen hydrogels incorporating BMP-2 at the corresponding BMP dose.

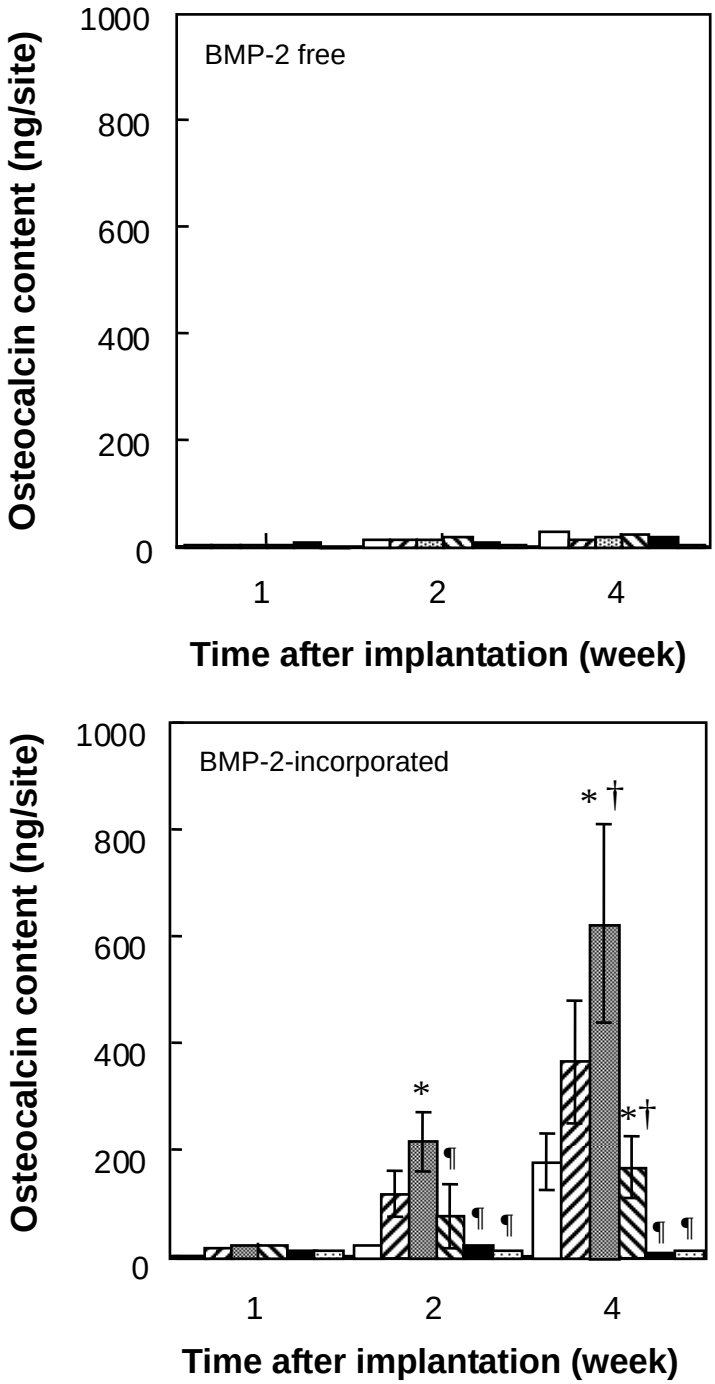

Figure 1-5. Osteocalcin contents of tissues around the implanted site of gelatin hydrogels incorporating BMP-2 (5 μg/site) and BMP-2-free, empty gelatin hydrogels 1, 2, and 4 weeks later. The hydrogel water contents are (□) 93.8, (▨) 96.9, (▩) 97.8, (▧) 99.1, and (■) 99.7 wt%. The symbol (⊡) indicates the osteocalcin content after subcutaneous injection of BMP-2-free PBS and BMP-2 solution (5 μg /100 μl/site). $^{*}p < 0.05$; significant against the osteocalcin content of mice applied with hydrogels incorporating BMP-2 (93.8 wt%). $^{\dagger}p < 0.05$; significant against the osteocalcin content of mice applied with hydrogels incorporating BMP-2 (96.9 wt%). $^{\P}p < 0.05$; significant against the osteocalcin content of mice applied with hydrogels incorporating BMP-2 (97.8 wt%).

Figure 1-6 shows the ALP and von Kossa-stained histology of subcutaneous tissues 2 and 4 weeks after the implantation of BMP-2-incorporated and empty gelatin hydrogels with a water content of 97.8 wt%. Apparently, ALP and calcium positive areas were seen around the BMP-2-incorporated gelatin hydrogel, in marked contrast to the empty gelatin hydrogel and well corresponded with the area of bone ectopically formed.

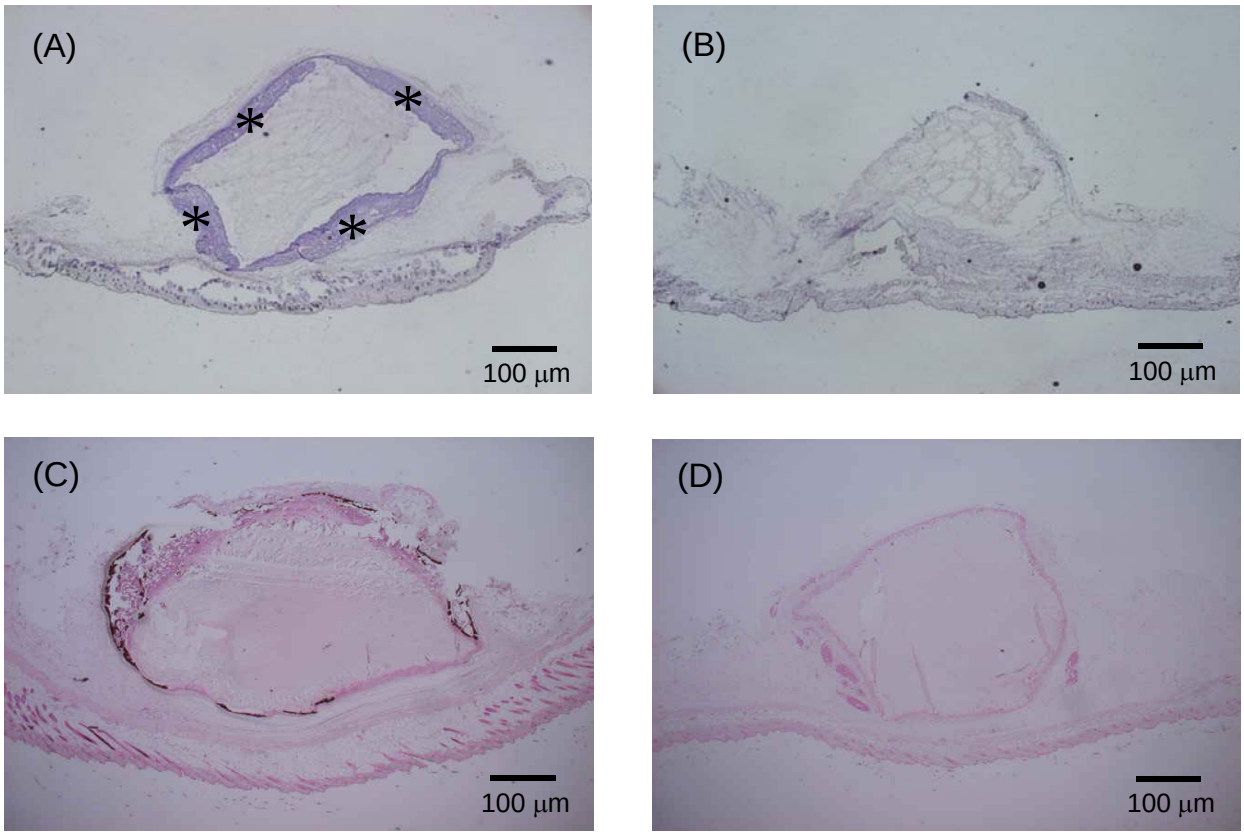

Figure 1- 6. ALP histochemistry (A, B) and von Kossa staining (C, D) of subcutaneous tissue around the implanted site of BMP-2 (5 μg)-incorporated (A, C) and BMP-2-free, empty gelatin hydrogels (B, D) with the water content of 97.8 wt% 2 and 4 weeks after implantation. Asterisks indicate the ALP-positive area. Original magnification: ×20.

DISCUSSION

The main objective of this chapter was to develop an *in vivo* release system of BMP-2 by biodegradable gelatin hydrogels which is expected to enhance the BMP-2 potential to induce bone formation. Gelatin hydrogels were effective in releasing BMP-2 *in vivo* and the *in vivo* release profile could be changed by altering the water content of BMP-2-incorporated hydrogels. This release system allowed BMP-2 to effectively induce the bone formation activity at the ectopic body site. As shown in Table 1-1, the water content of gelatin hydrogels can be easily modified by changing the concentration of gelatin and glutaraldehyde used for crosslinking reaction. The *in vivo* controlled release of BMP-2 was successfully achieved by changing the water content of hydrogels. The release period of BMP-2 became longer with a decrease in the water content of hydrogels. We have demonstrated that the *in vivo* biodegradability of gelatin hydrogels mainly depended on their water content [18]. Although the permeation rate was influenced by the water content of hydrogels, the interaction between the protein and gelatin molecules played a key role in determining the diffusion rate of protein through gelatin hydrogels. We have also demonstrated that bFGF molecules of positive charge were ionically immobilized in the hydrogels of gelatin with the opposite electric charge [25]. The immobilized bFGF was released from the hydrogel as a result of water solubilization of gelatin accompanied with *in vivo* hydrogel degradation, not by simple diffusion mechanism. When incorporated into the hydrogel prepared from gelatin of positive charge, the bFGF was rapidly diffused out from the hydrogel in the body, because of no ionic interaction between bFGF and gelatin molecules. When the time profile of *in vivo* hydrogel degradation was investigated and compared with that of BMP-2 retention, the two profiles were in good accordance to each other (Figure 1-2). This indicates that the BMP-2 release was governed by the biodegradation of carrier hydrogel. We do not think the controlled release of BMP-2 results from the simple diffusion throughout the hydrogel. As a result, in this hydrogel system, the BMP-2 release profile can be mainly controlled by regulating the degradation profile of hydrogels.

Although we did not examine the concentration of BMP-2 released at different skeletal locations

at present, previous researches revealed that there was no difference in the *in vivo* release of bFGF between the subcutis and muscle (unpublished data). Similar to BMP-2, bFGF is released from the hydrogel of gelatin based on hydrogel biodegradation and their release rate was changeable by use of hydrogels with different biodegradabilities. Taking the finding into consideration, it is possible that BMP-2 is released from the gelatin hydrogel at a similar release rate independent of skeletal locations.

In this study, the reason to select the ALP activity and content of a bone-specific extracellular matrix component, osteocalcin as the bone induction markers is that the significant increase of ALP activity followed by that of osteocalcin reflects well the biochemical step for bone formation. Yoshikawa et al. reported that the ALP activity in a hydroxyapatite disk seeded with fresh bone marrow cells began to increase 2 weeks after implantation and subsequently the osteocalcin began to appear 1 week later [26]. The similar time dependent of osteoinduction was observed for the gelatin hydrogels incorporating BMP-2 (Figures 1-3 and 1-5). This suggests that the BMP-2 released from the BMP-2-incorporated hydrogels stimulated the cells surrounding the hydrogels to differentiate into osteoblastic cells in the body, resulting in enhanced bone formation at the ectopic site.

As Wozney et al. reported, a carrier incorporating BMP allows osteoblast cells to induce the differentiation for bone formation at the ectopically implanted site. The BMP implanted activates a set of cellular events, including chemotaxis of uncommitted mesenchymal cells and possibly other target cells into the implanted site, and differentiation of these cells into mineral-depositing osteoblasts [27]. In addition, Thies et al. have reported that BMP-2 induced a high level of osteocalcin in bone marrow stromal cells in a dose-dependent manner [28]. Therefore, it is reasonable to think that a carrier allows BMP-2 to immobilize at the site of implantation or achieve the slow release, resulting in biological stimulation of cells surrounding the carrier to induce bone formation. However, when a sufficient amount of BMP is applied in the solution form, bone formation can be observed in the absence of the delivery system [29]. These phenomena suggest that a certain release period and dose of BMP-2 are possibly necessary for local enhancement of the bone induction activity. In this study, the maximum ectopic bone formation by the gelatin hydrogel incorporating BMP-2 with a water content of 97.8 wt%

Table 1-3. *In vivo* half-life period of BMP-2 in the hydrogel-incorporated or solution form.

Water contents (wt%)	Biexponential, $t_{1/2}$	
	Initial phase (day)	Secondary phase (day)
93.8	7.45	55.85
96.9	6.43	37.83
97.8	2.57	16.13
99.1	2.38	8.35
99.7	1.67	3.13
Solution	0.03	1.99

can be explained in terms of BMP-2 release. As shown in Table 1-3, the *in vivo* half-life period of BMP-2 in both the initial and secondary phases depended on the biodegradability of hydrogels studied. A similar rate of BMP-2 loss at the first phase was observed for the hydrogels with water contents of 97.8 and 99.1 wt%. However, the secondary loss kinetics showed that BMP-2 was lost more rapidly from the latter hydrogel than the former hydrogel. Taken together, it is possible that the hydrogel enabling a prolonged retention of BMP-2 increases the time period acting on the surrounding cells, leading to the enhanced bone induction. On the contrary, the hydrogels with water contents of 93.8 and 96.9 wt%, although they have longer half-lives, showed lower bone induction. This is probably due to the low level of the BMP-2 release. The concentration and exposure times of BMP-2 may play an important role in inducing the bone formation, but the optimal condition is not clear at present. It is possible that the hydrogel with a water content of 97.8 wt% enables BMP-2 to create the *in vivo* environment suitable to induce bone formation most effectively. To clarify the optimal condition, the cellular and biochemical studies are required to evaluate the effect of BMP-2 release kinetics on the proliferation and differentiation of osteoprogenitor cells in the body.

In clinical application, an absorbable collagen sponge, reconstituted from bovine tendon, and a collagen-based matrix, derived from demineralized bone matrix, have been used for the delivery of BMP-2 and BMP-7, respectively. A series of preclinical studies suggest that the carriers pharmacologically made

both the proteins stimulate local bone induction [6-12]. Since collagen is one of the materials having used for the carrier of BMP release, the collagen sponge was selected. This study also indicated that the collagen hydrogel showed the enhanced ALP activity of subcutaneous tissue around the implanted site, while it could achieve the *in vivo* BMP-2 release for 2 weeks (Figure 1-4). However, upon comparing the level of ALP activity, the gelatin hydrogel with a profile of BMP-2 release for 4 weeks was superior to the collagen hydrogel. Although there are several reasons to be considered for the enhanced ALP activity, the time period of BMP-2 release may be one of contributing keys to the gelatin superiority. It is also important to examine the influence of collagen biodegradability and gel formation on the *in vivo* release of BMP. However, in this study, the collagen sponge is a control matrix for BMP-2 release. Therefore, we selected a collagen sponge commercially available which has been mainly used as the release carrier of BMP-2. We can control the biodegradability of collagen sponges by changing the concentration of collagen and crosslinking agents [30]. This phenomenon may be also influenced by the nature of release carriers. Friess et al. have reported that the crosslinking of collagen sponges with formaldehyde reduced the binding of BMP-2 to the sponge, while the resistance of sponges to collagenase digestion correlated with their crosslinking extent [8-10].

The bone formation ectopically induced by the controlled release of BMP-2 from the gelatin hydrogel was found around the implanted hydrogels (Figure 1-6). The previous study reveals that it is difficult for cells to infiltrate into the interior of gelatin hydrogels [31]. Thus, it is likely that the osteoprogenitor cells recruited around the hydrogel are stimulated by BMP-2 released from the hydrogel efficiently enough to differentiate into bone-forming cells like osteoblasts, which consequently induces the bone formation thereat.

The mechanical properties of biomaterials for bone reconstruction are very important. However, it is practically difficult to give a high mechanical strength and modulus to a biomaterial which is degraded to disappear for a few months. One possible way to tackle this problem is to combine a biomaterial with high mechanical properties for mechanical support and a matrix of growth factor release to locally induce bone formation. The gelatin hydrogel has been investigated to evaluate the feasibility as the release

matrix to induce the BMP-2 activity for bone formation. When a high mechanical support is required, the bone plate, screw, and hydroxyapatite clinically used should be employed together with the release matrix. In conclusion, the *in vivo* profile of BMP controlled release by the gelatin hydrogel with an optimal degradability enables BMP-2 to efficiently induce bone formation.

REFERENCES

1. S. R. Winn, H. Uludag, and J. O. Hollinger, Sustained release emphasizing recombinant human bone morphogenetic protein-2, *Adv. Drug. Deliv. Rev.*, **31**, 303-318 (1998).
2. S. A. Gittens and H. Uludag, Growth factor delivery for bone tissue engineering, *J. Drug Target.*, **9**, 407-429 (2001).
3. J. M. Wozney, V. Rosen, A. J. Celeste, L. M. Mitsock, M. J. Whitters, R. W. Kriz, R. M. Hewick, and E. A. Wang, Novel regulators of bone formation: molecular clones and activities, *Science*, **242**, 1528-1534 (1988).
4. P. J. Boyne, R. E. Marx, M. Nevins, G. Triplett, E. Lazaro, L. C. Lilly, M. Alder, and P. Nummikoski, A feasibility study evaluating rhBMP-2/absorbable collagen sponge for maxillary sinus floor augmentation, *Int. J. Periodontics Restorative Dent.*, **17**, 11-25 (1997).
5. M. Laursen, K. Hoy, E. S. Hansen, J. Gelineck, F. B. Christensen, and C. E. Bunger, Recombinant bone morphogenetic protein-7 as an intracorporal bone growth stimulator in unstable thoracolumbar burst factures in humans: preliminary results, *Eur. Spine J.*, **8**, 485-490 (1999).
6. H. Uludag, Osteoinductive alternatives to bone grafts, *Curr. Opin. Orthop.*, **9**, 31-37 (1998).
7. H. Uludag, D. D'Augusta, R. Palmer, G. Timony, and J. Wozney, Characterization of rhBMP-2 pharmacokinetics implanted with biomaterial carriers in the rat ectopic model, *J. Biomed. Mater. Res.*, **46**, 193-202 (1999).
8. H. Uludag, W. Friess, D. Williams, T. Porter, G. Timony, D. D'Augusta, C. Blake, R. Palmer, B. Biron, and J. Wozney, rhBMP-2-collagen sponges as osteoinductive devices: effects of in vitro sponge characteristics and protein pI on *in vivo* rhBMP pharmacokinetics, *Ann. NY Acad. Sci.*, **875**, 369-378 (1999).
9 W. Friess, H. Uludag, S. Foskett, R. Biron, and C. Sargeant, Characterization of absorbable collagen sponges as rhBMP-2 carriers, *Int. J. Pharm.*, **187**, 91-99 (1999).

10. W. Friess, H. Uludag, S. Foskett, and R. Biron, Bone regeneration with recombinant human bone morphogenetic protein-2 (rhBMP-2) using absorbable collagen sponges (ACS): Influence of processing on ACS characteristics and formulation, *Pharm. Dev. Technol.*, **4**, 387-396 (1999).

11. H. Uludag, D. D'Augusta, J. Golden, J. Li, G. Timony, R. Riedel, and J. Wozney, Implantation of recombinant human bone morphogenetic proteins with biomaterial carriers: A correlation between protein pharmacokinetics and osteoinduction in the rat ectopic model, *J. Biomed. Mater. Res.*, **50**, 227-238 (2000).

12. H. Uludag, T. Gao, T. J. Porter, W. Friess, and J. M. Wozney, Delivery systems for BMPs: Factors contributing to protein retention at an application site, *J. Bone Joint Surg.*, **83-A**, S1 128-135 (2001).

13. D. Zekorn, Modified gelatin as plasma substitutes, *Bibl. Haematol.*, **33**, 30-60 (1969).

14. Y. Tabata, S. Hijikata, and Y. Ikada, Enhanced vascularization and tissue granulation by basic fibroblast growth factor impregnated in gelatin hydrogels, *J. Control. Rel.*, **31**, 189-199 (1994).

15. M. Yamamoto, Y. Tabata, L. Hong, S. Miyamoto, H. Kikuchi, and Y. Ikada, Bone regeneration by transforming growth factor β1 released from a biodegradable hydrogel, *J. Control. Rel.*, **64**, 133-142 (2000).

16. M. Ozeki, T. Ishii, Y. Hirano, and Y. Tabata, Controlled release of hepatocyte growth factor based on hydrogel biodegradation, *J. Drug Targ.*, **9**, 461-471 (2001).

17. F. C. Greenwood, W. M. Hunter, and T. C. Gglover, The preparation of ^{131}I-labeled human growth hormone of high specific radioactivity, *Biochem. J.*, **89**, 114-123 (1963).

18. Y. Tabata, A. Nagano, and Y. Ikada, Biodegadation of hydrogel carrier incorporating fibroblast growth factor, *Tissue Eng.*, **5**, 127-138 (1999).

19. T. Fujisato, T. Sajiki, Q. Liu, and Y. Ikada, Effect of basic fibroblast growth factor on cartilage regeneration in chondrocyte-seeded collagen sponge scaffold, *Biomaterials*, **17**, 155-162 (1996).

20. K. Matsuda, S. Suzuki, N. Isshiki, K. Yoshioka, T. Okada, and Y. Ikada, Influence of glycosaminoglycans on the collagen sponge component of a bilayer artificial skin, *Biomaterials*,

11, 351-360 (1990).

21. A. E. Bolton and W. M. Hunter, The labeling of proteins to high specific radioactivities by conjugation to a ^{125}I-containing acylating agent, *Biochem. J.*, **133**, 529-539 (1973).

22. D. Kobayashi, H. Takita, M. Mizuno, Y. Totsuka, and Y. Kuboki, Time-dependent expression of bone sialoprotein fragments in osteogenesisi induced by bone morphogenetic protein, *J. Biochem.*, **119**, 475-481 (1996).

23. L. S. Kaplow, Cytochemistry of leukocyte alkaline phosphatase: use of complex naphthol HS phosphates in azo dye coupling techniques, *Am. J. Clin. Pathol.*, **39**, 439-449 (1963).

24. R. A. B. Drury and E. Wallington, Demonstration of calcium salts. In: Carleton's Histological Techniques, 5th edition, Oxford: Oxford Univ. Press. pp 217-218 (1980).

25. M. D. Muniruzzaman, Y. Tabata, and Y. Ikada, Protein interaction with gelatin hydrogels for tissue engineering, *Mat. Sci. Forum*, **250**, 89-96 (1997).

26. T. Yoshikawa, H. Ohgushi, and S. Tamai, Immediate bone formation capability of prefabricated osteogenic hydroxyapatite, *J. Biomed. Mater. Res.*, **32**, 481-492 (1996).

27. J. M. Wozney and V. Rosen, Bone morphogenetic protein and bone morphogenetic protein gene family in bone formation and repair, *Clin. Orthop. Rel. Res.*, **346**, 26-37 (1998).

28. R. S. Thies, M. Bauduy, B. A. Ashton, L. Kurtzberg, J. M. Wozney, and V. Rosen, Recombinant human bone morphogenetic protein-2 induces osteoblastic differentiation in W-20-17 stromal cells, *Endocrinology*, **130**, 1318-1324 (1992).

29. J. M. Wozney, V. Rosen, M. Byrne, A. J. Celeste, I. Moutsatsos, and E. A. Wang, Growth factors influencing bone development, *J. Cell Sci. Suppl.*, **13**, 149-56 (1990).

30. Y. Tabata, M. Miyao, M. Ozeki, and Y. Ikada, Controlled release of vascular endothelial growth factor by use of collagen hydrogels, *J. Biomater. Sci. Polym. Ed.*, **11**, 915-30 (2000).

31. M. Yamamoto, K. Kato, and Y. Ikada, Effect of the structure of bone morphogenetic protein carriers on ectopic bone regeneration, *Tissue Eng.*, **2**, 315-326 (1996).

Chapter 2

Bone regeneration at an ulna defect of rabbits by controlled release of BMP-2 from biodegradable hydrogels

INTRODUCTION

Bone regeneration is an attractive research field of tissue engineering because of its highly clinical requirement. It is widely recognized that various osteogenic growth factors, such as bone morphogenetic protein (BMP), transforming growth factor-β1 (TGF-β1), and basic fibroblast growth factor (bFGF), regulate the proliferation and differentiation of osteogenic cells and enhance bone formation [1]. Thus, if one can accelerate bone regeneration using osteogenic growth factors in a suitable manner, this regeneration technology will provide a new clinical procedure to promote bone repair and be substituted for autogenous and allogenous bone grafts or biomaterial implants.

BMPs with a potential to promote bone formation *in vivo* have been used for regeneration repairing bone injuries and bone defects [2]. The current DNA technologies have enabled recombinant human BMPs to produce the amount large enough for the basic and applied researches. Among them, BMP-2 and BMP-7 (OP-1) have already been clinically applied to accelerate bone regeneration both in fracture healing and spinal fusion [3]. On the other hand, several preclinical experiments have demonstrated that the BMP administrated in the solution form does not always induce the expected efficacy in bone regeneration [4]. To tackle this problem, BMP has been combined with various biodegradable carriers, such as collagen [5, 6], β-tricalcium phosphate [7], lactide-glycolide copolymers [8, 9], ethylene glycol-lactic acid copolymer [10] for the controlled release. It is conceivable that these combinations were effective in enhancing the *in vivo* BMP retention to induce bone formation. However, little has been investigated on the ability of BMP for bone regeneration from the viewpoint of the *in vivo* release profile.

We have already prepared the hydrogels from gelatin with different biodegradabilities and

succeeded in inducing the biological activities of bFGF [11], TGF-β1 [12], and hepatocyte growth factor (HGF) [13] through their controlled release with the biodegradable hydrogel, although application with the growth factors in the solution form was not effective. In a previous chapter, we have also demonstrated that the *in vivo* profile of BMP-2 release could be changed only by altering the biodegradability of gelatin hydrogels and affected the enhancement of BMP-2-induced ectopic bone formation at the subcutis of mice [14]. However, when the gelatin hydrogels incorporating BMP-2 are applied to the critical-sized defect which will never be regenerated spontaneously, it is unclear whether new bone tissue is regenerated.

The objective of this chapter is to explore feasibility of the gelatin hydrogel as a controlled release carrier of BMP-2 in enhancement of bone regeneration at a segmental bone defect. Hydrogels with different biodegradabilities were prepared by changing the concentration of gelatin and glutaraldehyde in preparation. We examine the effect of the biodegradability of hydrogels on the promotion of bone regeneration at a rabbit model of ulna defect.

EXPERIMENTAL

Materials

A gelatin sample with an isoelectric point (IEP) of 9.0 and human recombinant bone morphogenetic protein-2 were kindly supplied from Nitta Gelatin Co. Osaka, Japan and Yamanouchi Pharmaceutical Co., Japan, respectively. Glutaraldehyde, glycine, and other chemicals were purchased from Wako Pure Chemical Industries Osaka, Japan and used without further purification.

Preparation of gelatin hydrogels incorporating BMP-2

Hydrogels were prepared through the chemical crosslinking of aqueous gelatin solution with glutaraldehyde according to the method described previously [14]. Briefly, an aqueous gelatin solution mixed with glutaraldehyde was cast into a polypropylene dish (138×138 mm^2, BIO-BIK) at various

concentrations of glutaraldehyde and gelatin (Table 2-1), followed by the crosslinking reaction at 4 °C for 12 hr. The crosslinked hydrogel prepared was cut into rod shape (20×5×5 mm^3). The hydrogel samples were stirred in 100 mM aqueous glycine solution at 37 °C for 1 hr to block the residual aldehyde groups of glutaraldehyde. Following washing three times with double-distilled water (DDW), the hydrogel samples were freeze-dried and sterilized with ethylene oxide gas. The hydrogel weight was measured before and after complete drying at 70 ^oC under vacuum and the water content, the weight percentage of water in the wet hydrogel, was calculated from the two weight values [14].

To prepare the gelatin hydrogel incorporating BMP-2, 100 μl of phosphate-buffered saline solution (PBS, pH 7.5) containing 17 μg of BMP-2 was dropped onto a freeze-dried gelatin hydrogel, followed by leaving overnight at 4 °C. Similarly, 100 μl of BMP-2-free PBS was dropped onto a freeze-dried hydrogel to obtain the BMP-2-free, empty hydrogel.

Table 2-1. Preparation of gelatin hydrogels with different water contents.

Concentration of gelatin (wt%)	Concentration of glutaraldehyde (wt%)	Water content (wt%)
5	0.83	93.8
3	0.16	97.8
3	0.06	99.7

Surgical procedure to prepare a segmental ulna defect of rabbits

In vivo bone regeneration experiment was performed by use of a segmental ulna bone defect model of skeletally mature New Zealand white rabbits (20-week age, male, 3.5 Kg, Shimizu Laboratory Supply Inc., Japan) according to the surgical procedure previously reported [6, 8, 9]. A 4 cm-length superomedial incision was made and the tissue overlying the diaphysis of the ulna was dissected. A segmental defect (20 mm) was prepared in the ulna of 24 rabbits with a surgical oscillating saw supplemented by copious sterile saline water irrigation. Our previous study demonstrated that the BMP-2

dose per volume (34 μg of BMP-2/cm^3 of hydrogel) was sufficient to induce bone formation at ectopic sites of mice [14]. Based on the volume of hydrogel implanted and the BMP-2 dose per volume, the amount of BMP-2 incorporated was calculated. The gelatin hydrogels incorporating 17 μg of BMP-2, empty gelatin hydrogels, and 100 μl of free BMP-2 solution (170 μg/ml) were placed in the defect as shown in Figure 2-1, while the empty defect was left without free BMP-2. Each experimental group was composed of 3 rabbits. Fixation of the ostectomized bone was unnecessary due to the fibro-osseous union between the ulna and radius located distal and proximal to the surgical site. The soft tissue was approximated with interrupted 4-0 Vicryl® (Ethicon Inc., Somerville, NJ) and the skin was closed with 3-0 silk sutures. After different time intervals, the radius-ulna complex containing the defect was taken out, fixed in 10 wt% neutral phosphate-buffered formalin solution for assessment of bone regeneration.

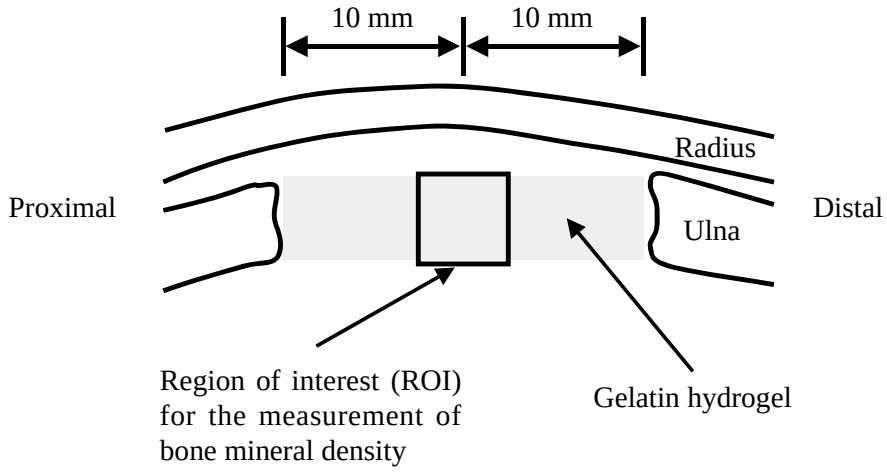

Figure 2-1. Schematic illustration of the gelatin hydrogel implantation into an ulna defect of rabbits and the region of interest for the DEXA measurement.

Assessment of bone regeneration

Bone regeneration at the bone defect was assessed by soft X-ray observation and dual energy X-ray absorptometry (DEXA) 2, 4, and 6 weeks after surgery. Histological examinations were carried out 6 weeks after application of the BMP-2-incoporated gelatin hydrogel with a water content of 97.8 wt%. Bone regeneration was radiographically examined by soft X-ray (Hitex-100, Hitachi, Japan) at 54 KVP and 2.5 mA for 20 sec. The bone mineral density (BMD) of each bone defect was measured at the 5×5 mm^2 region of interest (Figure 2-1) by using the DEXA with a bone mineral analyzer (DSC 600EX-III, Aloka Co., Ltd., Japan). This instrument was calibrated with a phantom of known mineral content according to the manufacture's instruction. Each scan was performed at a speed of 20 mm/sec and the scanning length was 1 mm.

Bone specimens were placed into 10 % neutral phosphate-buffered formalin solution, decalcified with 10 % formic acid, and processed for the paraffin embedding. Sections with a thickness of 3 μm were prepared and stained with hematoxylin and eosin (HE) to view by a light microscopy (AX-80T, Olympus, Tokyo, Japan).

Statistical Analysis

All the data were statically analyzed using Fisher's least significant difference test for multiple comparisons and statistical significance was accepted to be less than 0.05. The experimental results were expressed as the mean ± the standard deviation of the mean.

RESULTS

Soft X-ray examination at a segmental ulna defect of rabbits

Figure 2-2 shows soft X-ray photographs of ulna defects 6 weeks after application with gelatin hydrogels incorporating BMP-2. It is apparent that bone regeneration was detected radiographically in the

ulna bone defect (Figures 2-2A and 2-2E). On the other hand, no bone formation was radiographically observed at the bone defects applied with empty gelatin hydrogels (Figures 2-2B and 2-2F) and free BMP-2 (Figures 2-2C and 2-2G), and the appearance was similar to that of empty defect without free BMP-2 (Figures 2-2D and 2-2H).

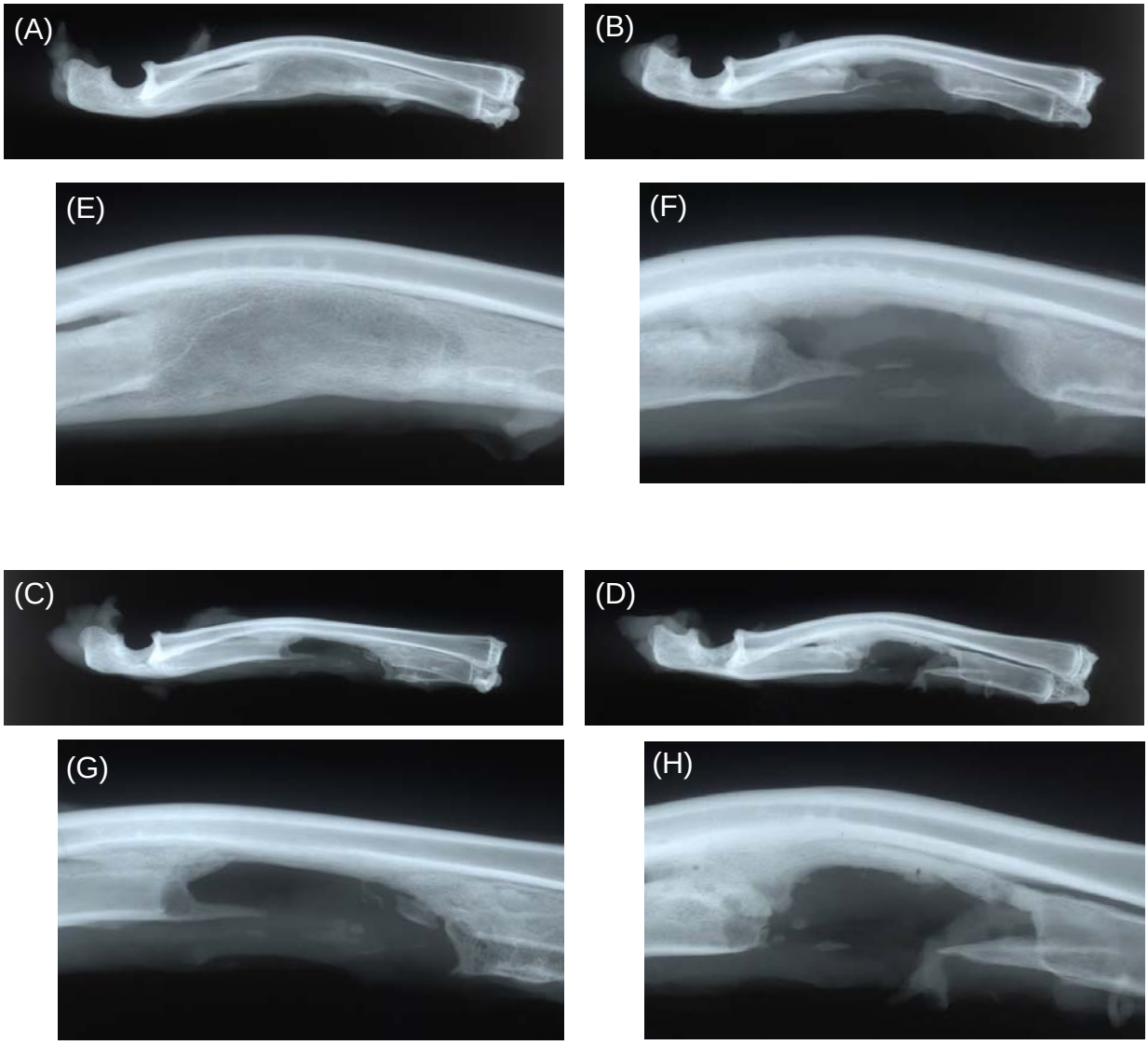

Figure 2-2. Radiographic appearance of ulna defects 6 weeks after application with a gelatin hydrogel incorporating BMP-2 (A and E), an empty gelatin hydrogel (B and F), and free BMP-2 (C and G) or an empty defect without free BMP-2 (D and H) at magnification ×1 (A-D) and 2 (E-H). The water content of hydrogels used was 97.8 wt% and the BMP-2 dose was 17 μg/site.

Histological evaluation of BMP-2-induced bone regeneration

Figure 2-3 shows histological sections of ulna defects 6 weeks after application with the gelatin hydrogel incorporating BMP-2. When applied with the gelatin hydrogel incorporating BMP-2, the bone defect was histologically occupied by bone tissue newly regenerated (Figure 2-3A). On the contrary, no bone regeneration was detected at the defect applied with the empty gelatin hydrogel (Figure 2-3B) or free BMP-2 (Figure 2-3C) and no application (Figure 2-3D), while remarkable ingrowth of soft connective tissue into the defect was observed.

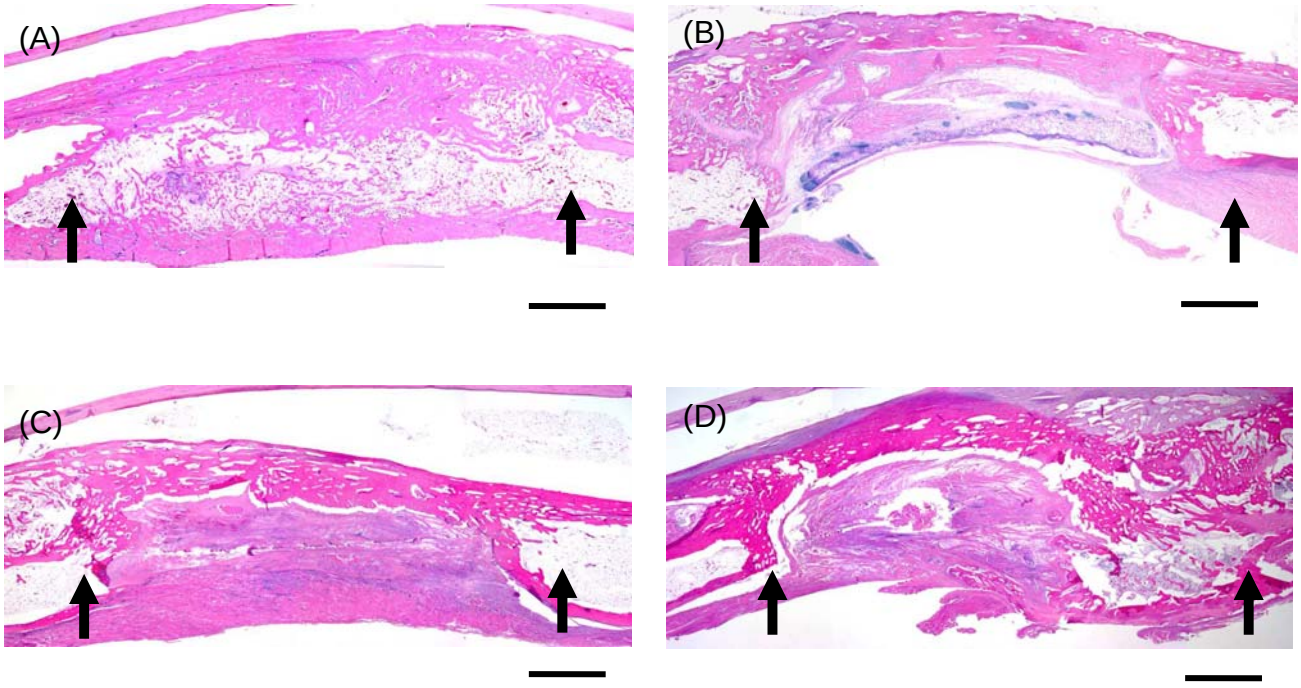

Figure 2-3. Histological sections of ulna defects 6 weeks after application with a gelatin hydrogel incorporating BMP-2 (A), an empty gelatin hydrogel (B), and free BMP-2 (C) or an empty defect without free BMP-2 (D). The water content of the hydrogels used was 97.8 wt% and the BMP-2 dose was 17 μg/site. Arrows indicate the edge of the defect. Every bar corresponds to 2 mm.

Evaluation of mineral deposition at a segmental defect of rabbits

Figure 2-4 shows the time profiles of BMD values at the ulna defect of rabbits after application with the gelatin hydrogel incorporating BMP-2. The BMD value at the bone defect applied with the gelatin hydrogel incorporating BMP-2 was significantly higher than that of the empty gelatin hydrogel, free BMP-2, and empty defect without free BMP-2 after 4 and 6 weeks of application.

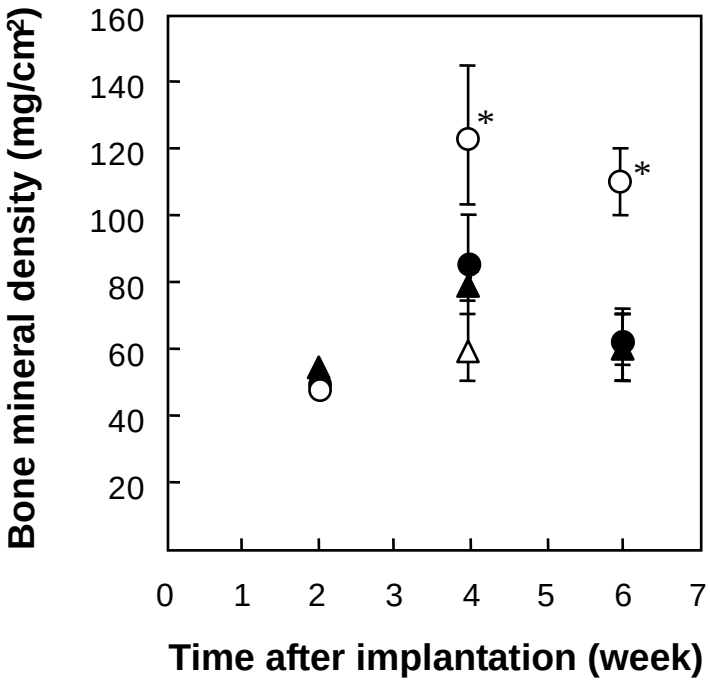

Figure 2-4. The time course of BMD at the ulna defect of rabbits after application with gelatin hydrogels incorporating BMP-2 (○), empty gelatin hydrogel (●), and free BMP-2 (△) or empty defect without free BMP-2 (▲). The water content of the hydrogels used was 97.8 wt% and the BMP-2 dose was 17 μg/site. *$p < 0.05$; significance against the BMD value of other groups at the corresponding time.

Effect of the water content of gelatin hydrogels incorporating BMP-2 on bone regeneration

Figure 2-5 shows soft X-ray photographs of bone defects 6 weeks after application with gelatin hydrogels incorporating BMP-2. Irrespective of the hydrogel type, bone regeneration at the defect was radiographically detected although the extent of radiopaque area for the hydrogel with a water content of 97.8 wt% (Figures 2-5B and 2-5F) was larger than that with the higher (Figures 2-5C and 2-5G) and lower (Figures 2-5A and 2-5E) water contents. On the other hand, no bone formation was radiographically observed at the bone defect applied with free BMP-2 (Figures 2-5D and 2-5H).

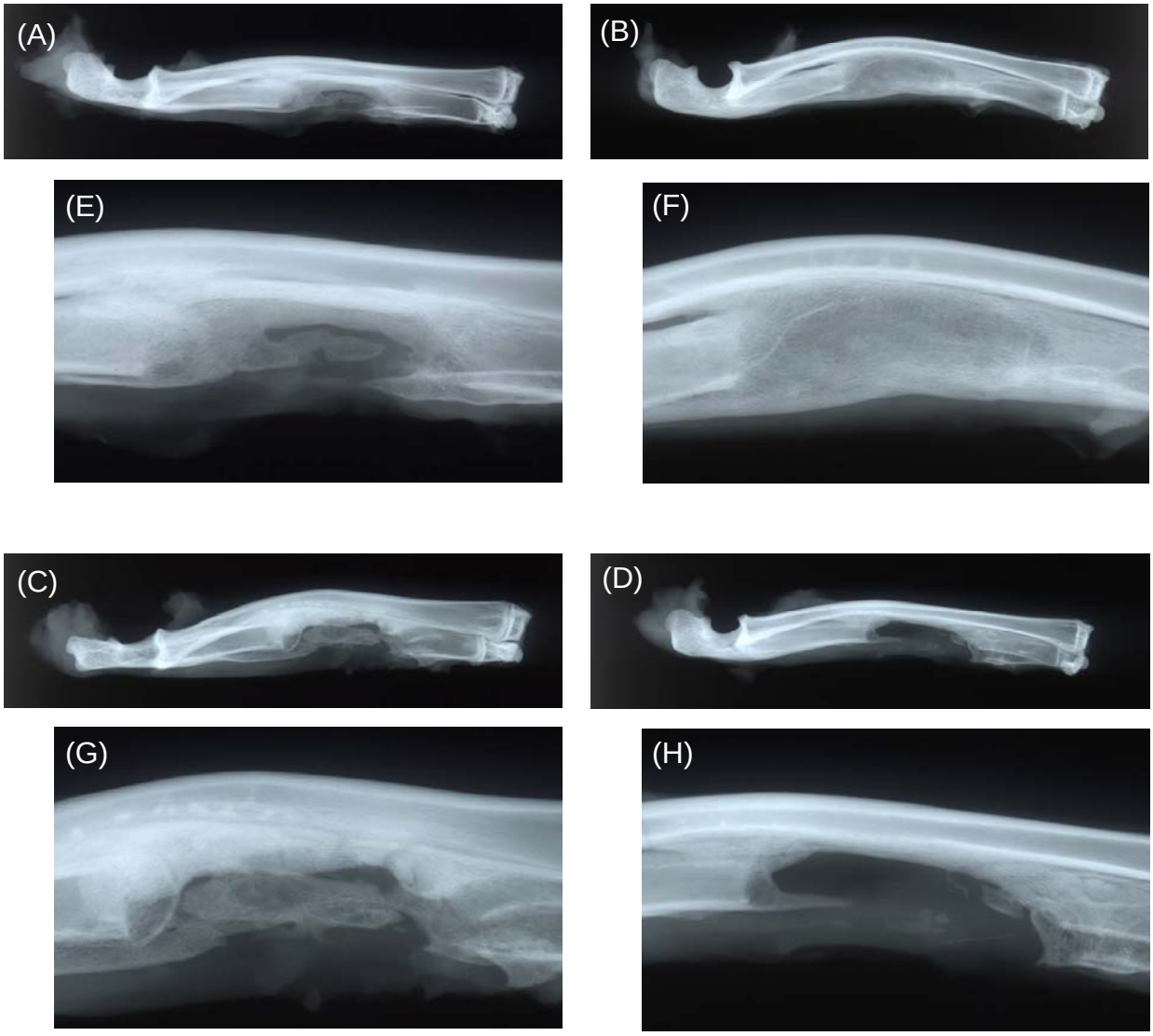

Figure 2-5. Radiographic appearance of ulna defects 6 weeks after application with gelatin hydrogels incorporating BMP-2 (A-C, E-G), and free BMP-2 (D and H) at magnification ×1 (A-D) and 2 (E-H). The water content of hydrogels used was 93.8 (A and E), 97.8 (B and F), and 99.7 wt% (C and G), respectively. The BMP-2 dose was 17 μg/site.

Figure 2-6 shows the BMD values at ulna defects 6 weeks after application with gelatin hydrogels incorporating BMP-2. It is clear that the gelatin hydrogel with a water content of 97.8 wt% (B) enhanced the BMD value at ulna defect to a significantly higher extent than both the hydrogels with water contents of 93.8 (A) and 99.7 wt% (C). Free BMP-2 did not enhance the BMD value at the bone defect.

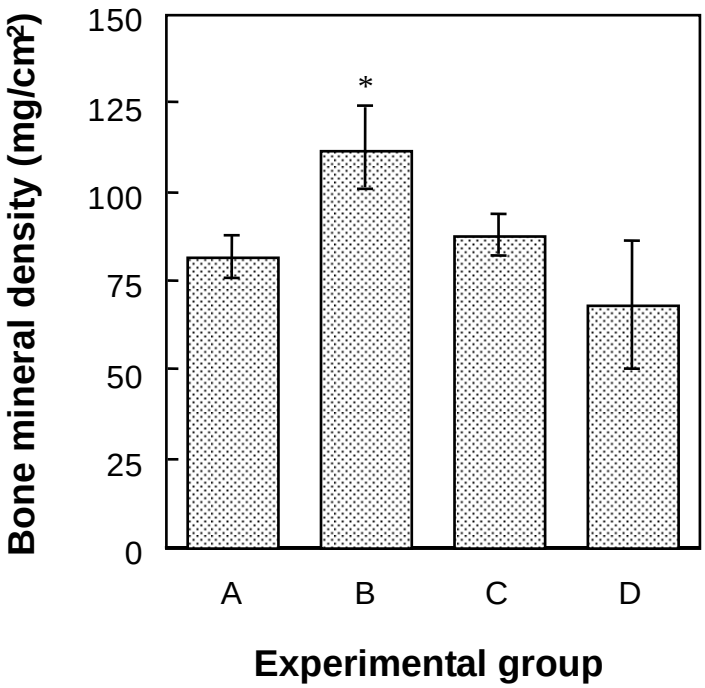

Figure 2-6. Influence of the water content of gelatin hydrogels on the BMD at the ulna defect of rabbits 6 weeks after application with gelatin hydrogels incorporating BMP-2 (A-C) and free BMP-2 (D). The water content of hydrogels used was 93.8 (A), 97.8 (B), and 99.7 wt% (C), respectively. The BMP-2 dose was 17 μg/site. *$p < 0.05$; significance against the BMD value of other groups.

DISCUSSION

This chapter demonstrates that the bone regeneration at the segmental bone defect of rabbit ulna induced by gelatin hydrogels incorporating BMP-2 was greatly influenced by the water content of hydrogels. The water content of hydrogels could be easily changed only by altering the concentration of gelatin and glutaraldehyde in crosslinking reaction (Table 2-1). Chapter 1 has demonstrated that gelatin hydrogels enabled BMP-2 to release at the implanted site for extended time periods and the *in vivo* release profile of BMP-2 was controllable by the water content of hydrogels [14]. The release period of BMP-2 became longer with a decrease in the water content of hydrogel carriers. When the *in vivo* time profile of hydrogel degradation was compared with that of BMP-2 retention, a good correlation between the two profiles was observed [14]. These findings suggest that the BMP-2 release is governed by the degradation

of the hydrogel carriers. Furthermore, our previous research revealed that significantly higher ectopic bone formation was induced by the BMP-2-incorporated gelatin hydrogel with a water content of 97.8 wt% than that with the lower or higher water contents. This phenomenon suggests that a certain release period of BMP-2 is possibly necessary for local enhancement of the bone induction activity.

In this chapter, we selected a rabbit model of 20-mm long ulna bone defects as a stable critical-sized defect according to the method of Hollinger et al. [6, 8, 9]. The 20-mm length ulna bone resection did not impair function for the experimental animal. Hollinger et al. reported that no bone formation was found both for the empty defect without free BMP-2 and the absorbable collagen carrier (Helistat®) without BMP-2 incorporation at the critical-sized (20-mm length) defect of rabbit ulna bone. Similarly to the Hollingers' study, no bone regeneration was detected for the empty defect without free BMP-2 (Figures 2-2H and 2-3D) from the viewpoint of the radiographic and histological observations. Free BMP-2 treatment did not induce bone regeneration at the defect (Figures 2-2G and 2-3C). The hydrogel itself had no ability for bone regeneration because the BMP-2 free, empty gelatin hydrogel showed similar appearance to that of empty defect without free BMP-2 (Figures 2-2F and 2-3B). These appearances strongly indicate that the size of the defect used to assess bone regeneration should be large enough to avoid spontaneous healing. The application of materials without any osteoinduction activity into the critical-sized defect results in the formation of fibrous connective tissue rather than bone (Figures 2-3B, 2-3C, and 2-3D).

The osteoinduction activity of BMP-2 released from gelatin hydrogels incorporating BMP-2 was evaluated in terms of bone regeneration at the ulna bone defect. The time course of BMD values at the critical-sized defect clearly shows that 4 and 6 weeks after application of gelatin hydrogels incorporating BMP-2 the BMD value was significantly higher than that of the empty gelatin hydrogel, free BMP-2, and no application. No enhancement of the BMD value was found for other experimental groups (Figure 2-4). Furthermore, Hollinger et al. reported that the collagen sponges incorporating BMP-2 promoted a significant increase in the percent of radiopacity from 2 to 4 weeks, but thereafter no difference with time was observed [6]. Indeed, their histological examinations revealed that numerous bony trabeculae were

observed at 4 weeks and the trabeculae were consolidating and cortices were reforming by 8 weeks after implantation. However, it is impossible to directly compare the present data with the Hollingers' ones because their dose of BMP-2 used is 35 μg which is larger than that used in our study. As shown in Figure 2-3A, cortices were observed 6 weeks after the application of the gelatin hydrogel incorporating BMP-2 even at the lower BMP-2 dose (17 μg) used. Taken together, it is apparent that the period to evaluate the osteoinduction activity should be long enough to fill the critical-sized defect with bone newly regenerated.

The activity of gelatin hydrogels incorporating BMP-2 to induce bone regeneration greatly depended on their water content as shown in Figures 2-5 and 2-6. It is likely that the fast-degraded hydrogel neither contributed to prolonged retention of BMP-2 nor to protect the defect from the ingrowth of fibrous tissue. When the rate of hydrogel degradation is too slow compared with that of bone regeneration at the ulna defect, the hydrogel remaining in the defect may physically impair bone regeneration, even though long-termed release of BMP-2 is achievable. Similar to this appearance, we have demonstrated that gelatin hydrogels with a slow degradability physically impaired bone regeneration induced by gelatin hydrogels incorporating TGF-β1 [12]. Interestingly, this dependency of the osteoinduction activity for gelatin hydrogels incorporating BMP-2 is highly correlated to that observed in our previous ectopic bone induction experiments, which revealed that the osteoinduction activity of the hydrogel with a water content of 97.8 wt% was significantly higher than that with the higher and lower water contents [14]. These findings indicate that a balance in the time profile between the BMP-2 retention and the bone formation is essential for the bone regeneration induced by gelatin hydrogels incorporating BMP-2.

Various doses of BMPs and delivery systems, such as collagen, bioceramics, lactide-glycolide copolymers, ethylene glycol-lactic acid copolymer, were employed to induce bone regeneration at a bone defect [4, 15]. Among them, a commercially available collagen sponge has been investigated as a promising carrier to reduce the BMP-2 dose, utilizing for delivering BMP-2 in the clinical application [3, 5]. Indeed our previous study also indicated that the collagen sponge incorporating BMP-2 showed the

enhanced osteoinduction activity at the subcutaneous tissue around the implanted site, while it could achieve the *in vivo* BMP-2 release for 2 weeks. However, upon comparing the level of osteoinduction activity, the gelatin hydrogel with the profile of BMP-2 release for 4 weeks was superior to the collagen sponge [14]. Although there are several reasons to be considered for the enhanced osteoinduction activity, the time period of BMP-2 release may be one of keys contributing to the gelatin superiority. On the other hand, Hollinger et al. compared the property as a carrier of BMP-2 release for bone regeneration between the collagen sponge and the poly (D, L-lactide) sponge. As the result, irrespective of the carrier type, the same dose of BMP-2 (35 μg) was required to promote nearly identical bone healing in a unilateral rabbit radius model [6]. Although it is impossible to directly compare the present data with the Hollingers' ones because of their larger BMP-2 dose used (35 μg), our hydrogel release system enables BMP-2 to enhance bone regeneration even at the lower dose (17 μg). The BMP-2 dose necessary to promote bone regeneration may be reduced by a good design of release profile of BMP-2.

Many preclinical studies reveal that BMP at physiologically high doses is required to achieve bone formation in non-human primates, which is different from the case of rodents [4]. One of the possible reasons for this species-dependent dose issue will be the immature technology to modify the *in vivo* retention of BMP. Considering the present results, we can say with fair certainty that the gelatin hydrogel is a promising carrier used to deliver BMP-2 and contributes to reduce the dose of BMP-2 suitable for successful bone regeneration and to diminish the side effects elicited by excessive administration of BMP-2 in the body.

REFERENCES

1. J. R. Lieberman, A. Daluiski, and T. A. Einhorn, The role of growth factors in the repair of bone. Biology and clinical applications, *J. Bone Joint Surg. Am.*, **84-A**, 1032-1044 (2002).
2. J. M. Wozney and V. Rosen, Bone morphogenetic protein and bone morphogenetic protein gene family in bone formation and repair, *Clin. Orthop. Relat. Res.*, **346**, 26-37 (1998).
3. M. A. Mont, P. S. Ragland, B. Biggins, G. Friedlaender, T. Patel, S. Cook, G. Etienne, A. Shimmin, R. Kildey, D. C. Rueger, and T. A. Einhorn, Use of bone morphogenetic proteins for musculoskeletal applications. An overview, *J. Bone Joint Surg. Am.*, **86-A Suppl 2**, 41-55 (2004).
4. S. A. Gittens and H. Uludag, Growth factor delivery for bone tissue engineering, *J. Drug Target.*, **9**, 407-429 (2001).
5. M. Geiger, R. H. Li, and W. Friess, Collagen sponges for bone regeneration with rhBMP-2, *Adv. Drug. Deliv. Rev.*, **55**, 1613-1629 (2003).
6. J. O. Hollinger, J. M. Schmitt, D. C. Buck, R. Shannon, S. P. Joh, H. D. Zegzula, and J. M. Wozney, Recombinant human bone morphogenetic protein-2 and collagen for bone regeneration, *J. Biomed. Mater. Res. (Appl. Biomater.)*, **43**, 356-364 (1998).
7. M. R. Urist, A. Lietze, and E. Dawson, β-tricalcium phosphate delivery system for bone morphogenetic protein, *Clin. Orthop. Relat. Res.*, **187**, 277-280 (1984).
8. H. D. Zegzula, D. C. Buck, J. Brekke, J. M. Wozney, and J. O. Hollinger, Bone formation with use of rhBMP-2 (recombinant human bone morphogenetic protein-2), *J. Bone Joint Surg. Am.*, **79**, 1778-1790 (1997).
9. D. L. Wheeler, D. L. Chamberland, J. M. Schmitt, D. C. Buck, J. H. Brekke, J. O. Hollinger, S. P. Joh, and K. W. Suh, Radiomorphometry and biomechanical assessment of recombinant human bone morphogenetic protein 2 and polymer in rabbit radius ostectomy model, *J. Biomed. Mater. Res. (Appl. Biomater.)*, **43**, 365-373 (1998).
10. N. Saito, T. Okada, H. Horiuchi, N. Murakami, J. Takahashi, M. Nawata, H. Ota, K. Nozaki, and K.

Takaoka, A biodegradable polymer as a cytokine delivery system for inducing bone formation, *Nat. Biotechnol.*, **19**, 332-335 (2001).

11. Y. Tabata, S. Hijikata, and Y. Ikada, Enhanced vascularization and tissue granulation by basic fibroblast growth factor impregnated in gelatin hydrogels, *J. Control Release*, **31**, 189-194 (1994)
12. M. Yamamoto, Y. Tabata, L. Hong, S. Miyamoto, N. Hashimoto, and Y. Ikada, Bone regeneration by transforming growth factor beta1 released from a biodegradable hydrogel, *J. Control Release,*. **64**, 133-142 (2000).
13. M. Ozeki, T. Ishii, Y. Hirano, and Y. Tabata, Controlled release of hepatocyte growth factor from gelatin hydrogels based on hydrogel degradation, *J. Drug Target.*, **9**, 461-471 (2001).
14. M. Yamamoto, Y. Takahashi, and Y. Tabata, Controlled release by biodegradable hydrogels enhances the ectopic bone formation of bone morphogenetic protein, *Biomaterials*, **24**, 4375-4383 (2003).
15. J. O. Hollinger, H. Uludag, and S. R. Winn, Sustained release emphasizing recombinant human bone morphogenetic protein-2, *Adv. Drug Deliv. Rev.*, **31**, 303-318 (1998).

Chapter 3

Bone regeneration at a skull defect in non-human primates by controlled release of BMP-2 from biodegradable hydrogels

INTRODUCTION

BMP has been expected as a therapeutic protein to induce regeneration repairing of bone injures and defects [1], since it has induced significant bone regeneration both orthotopically and ectopically in the body [2]. However, preclinical studies show that physiologically high doses of BMP are required to achieve bone formation for non-human primates, which is quite different from the case of rodents [3]. One of the possible reasons for this species-dependent dose issue is the immature technology to administer BMP *in vivo*. On the other hand, recombinant human BMP-2 and BMP-7 (OP-1) have already been applied for the regeneration therapy of human bone at the defect of size as large as impossible to naturally repair only by the self-healing ability [4]. However, efficient bone regeneration cannot be always expected due to the short half-life of BMP itself administrated in the body. Therefore, it is necessary to develop an administration carrier of BMP for the localized release at the site applied over the time period required. The drug delivery system (DDS), such as the controlled release technology will resolve the administration issue and additionally reduce the adverse effects caused by the high doses and repeated regimens.

BMP has been combined with various biodegradable carriers, such as collagen [5, 6], β-tricalcium phosphate [7], lactide-glycolide copolymers [8, 9] for the controlled release. However, little has been extensively investigated on the ability of BMP for bone regeneration from the viewpoint of the *in*

vivo profile of BMP release. In the previous chapters, we have designed biodegradable hydrogels of gelatin for the *in vivo* controlled release of BMP-2. The hydrogel system enabled BMP-2 to retain at the implanted site for extended time periods and consequently enhance the ability of bone induction in marked contrast to BMP-2 in the solution form [10]. The controlled release of BMP-2 induced bone regeneration at the defect of rabbit ulna, whereas the BMP-2 solution was ineffective [11].

The objective of this chapter is to evaluate feasibility of the gelatin hydrogel as a controlled release carrier of BMP-2 to enhance bone regeneration at a bone defect of monkey skulls. Hydrogels with different biodegradabilities were prepared by changing the concentration of gelatin and glutaraldehyde in hydrogel preparation. We examine the effect of the hydrogels biodegradability and the BMP dose on the promotion of bone regeneration comparing the regeneration effect with the insoluble bone matrix (IBM) incorporating BMP-2 of experimentally best choice [12, 13].

EXPERIMENTAL

Materials

A gelatin sample with an isoelectric point (IEP) of 9.0 and human recombinant bone morphogenetic protein-2 were kindly supplied from Nitta Gelatin Co. Osaka, Japan and Yamanouchi Pharmaceutical Co., Japan, respectively. Insoluble bone matrix [12] (IBM, particle size: 320-620 μm) was kindly supplied from Emeritus Professor Yoshinori Kuboki, Department of Oral Health Science, Graduate School of Dental Medicine, Hokkaido University. Glutaraldehyde, glycine, and other chemicals were purchased from Wako Pure Chemical Industries Osaka, Japan and used without further purification.

Preparation of gelatin hydrogels and IBM incorporating BMP-2

Hydrogels were prepared through the chemical crosslinking of aqueous gelatin solution with glutaraldehyde according to the method described previously [10]. Briefly, an aqueous gelatin solution mixed with glutaraldehyde was cast into polypropylene dish (138×138 mm^2, BIO-BIK) at various concentrations of glutaraldehyde and gelatin (Table 3-1), followed by the crosslinking reaction at 4 °C for 12 hr. The crosslinked hydrogel prepared was punched out to obtain the disks of 6 mm in diameter for the following *in vivo* experiment. The hydrogel discs obtained were stirred in 100 mM aqueous glycine solution at 37 °C for 1 hr to block the residual aldehyde groups of glutaraldehyde. Following washing three times with double-distilled water (DDW), the hydrogel discs were freeze-dried and sterilized with ethylene oxide gas. The hydrogel weight was measured before and after complete drying at 70 °C under vacuum and the water content, that is the weight percentage of water in the wet hydrogel to the hydrogel, was calculated from the two weights.

Table 3-1. Preparation of gelatin hydrogels with different water contents.

Concentration of gelatin (wt%)	Concentration of glutaraldehyde (wt%)	Water content (wt%)
5	0.83	93.8
3	0.16	97.8
3	0.06	99.7

To prepare the gelatin hydrogel incorporating BMP-2 for the *in vivo* experiment, 20 μl of phosphate-buffered saline solution (PBS, pH 7.5) containing various amounts of BMP-2 (5, 20, and 200 μg) was dropped onto a freeze-dried gelatin hydrogel disc, followed by leaving overnight at 4 °C.

Similarly, 20 μl of PBS containing 5 μg of BMP-2 was dropped onto IBM, followed by leaving overnight at 4 °C. As controls of these samples, BMP-2-free, empty gelatin hydrogel and IBM were obtained by dropping 20 μl of BMP-2-free PBS onto a freeze-dried gelatin hydrogel and IBM, respectively.

Surgical procedure to prepare a skull defect of monkeys

The skull defect model of monkeys was prepared according to the method described previously [14]. All the procedures were carried out under the institutional guidelines on animal experimentation. After the intramuscular injection of xylazine hydrochlorode (1.17 mg/kg body weight), the monkeys (Macaca fascicularis, male, 4 – 6 kg, 4 – 5 years) were further anesthetized by the intramuscular injection of ketamine hydrochloride (2.3 mg/kg body weight). In addition, local analgesia was induced by subcutaneous administration of 1 % lidocaine solution into the subcutis of the right temple (10 ml/head). The scalp and underlying temporal muscle were cut and the temporoparietal region of monkey skulls was exposed. After incision of the pericranium, five defects (each 6 mm in diameter) in each monkey's parietal bone were prepared using a microdrill without injuring the underlying dura mater with the aid of a surgical microscope, while the distance between the neighbering defects was 6 mm. The defects were tried to prepare at the same anatomical site, defined by the temporal and occipital crests and the temporoparietal suture. A preliminary experiment revealed that a 6 mm skull defect was not naturally closed even after 6 months without any applications. In addition, it is practically difficult to prepare five defects with a larger diameter at the monkey parietal bone. Taken together, the defect diameter was selected to be 6 mm in this study. As shown in Table 3-2, the gelatin hydrogel discs of 6 mm in diameter incorporating BMP-2 (5 μg/site) with various water contents (93.8 and 99.7 wt%), the gelatin hydrogel incorporating BMP-2 (5, 50, 200 μg/site) with a water content of 97.8 wt%, and IBM incorporating BMP-2 (5 μg/site) were applied to the skull bone defects prepared. As controls, the BMP-2-free empty gelatin

Table 3-2. The overall experiment design for *in vivo* evaluation of the skull bone regeneration in monkeys and rabbits.

Animal species	Experiment	Application	BMP-2 dose	Evaluation	Implantation period	Number of animals
Monkey	Skull bone regeneration in several scaffolds	PBS solution	0 μg/site	X-ray measurement Histological evaluation Bone mineral density measurement	12 weeks	6
		Empty gelatin hydrogel [1)]	0 μg/site			
		Gelatin hydrogels [2)] incorporated BMP-2	5 μg/site			
		IBM	5 μg/site			
	Influence of the BMP-2-dose on the skull bone regeneration	Free BMP-2	200 μg/site	Bone mineral density measurement		
		Gelatin hydrogel [1)] incorporated BMP-2	0, 5, 50, 200 μg/site			
Rabbit	Skull bone regeneration in several scaffolds	PBS solution	0 μg/site	Bone mineral density measurement	8 weeks	11
		Free BMP-2	5 μg/site			
		Empty gelatin hydrogel	0 μg/site			
		Gelatin hydrogels [2)] incorporated BMP-2	5 μg/site			
		IBM	5 μg/site			

1) Water content : 97.8 wt%
2) Water content : 93.8, 97.8, and 99.7 wt%

hydrogel, 20 μl of free BMP-2 solution (200 μg/site), and PBS solution were applied to the skull bone defect. After treatment, the pericranium and skin were carefully sutured with a 4-0 nylon monofilament to secure the stability of the samples. For each experimental group, 3 different defects were randomly selected from 3 different monkeys.

The X-ray measurement of skull bones was performed at 100 V and 10 mA for 2.75 sec. under anesthetized conditions 1, 2, 3, 4, 6, 8, 10, and 12 weeks after application. At 12 weeks postoperatively, all the animals were killed by overdose administration of anesthetic agents. The skull bone including the five defects was removed and used for all evaluations including soft X-ray, and Dual Energy X-ray (DEXA), and histological observations. No extraordinary behavior or body weight loss was observed for all the monkeys over the time period of 12 weeks.

Surgical procedure to prepare a skull defect of rabbits

In vivo bone regeneration was also evaluated for the bone defect of rabbit skulls according to the surgical procedure previously reported [15]. All the procedures were carried out under the institutional guidelines of Kyoto University on animal experimentation. Similarly to the monkey model, the head skin of rabbit (New Zealand white, male, 3.5 kg) was cut to expose the skull bone under anesthetization, and after pericranium incision, bilateral skull defects of 6 mm in diameter were carefully prepared by a microdrill with the aid of an operating microscope not so as to injure the underlying dura mater. As shown in Table 3-2, the gelatin hydrogel incorporating BMP-2 (5 μg/site) was applied to the skull defect, while the BMP-2-free empty gelatin hydrogel and 20 μl of free BMP-2 solution (5 μg/site) were employed as controls. Then, the pericranium and skin were carefully sutured with a 4-0 nylon monofilament. For each experimental group, 3 different defects of 3 different rabbits were used being selected either the right or left defect randomly. At 8 weeks postoperatively, the skull bone was removed

together with the defect and fixed with 10 vol% aqueous neutral formalin solution for histological observation.

Assessment of bone regeneration

Bone regeneration at the skull defect was assessed by soft X-ray, DEXA, and histological examinations. The bone defect was radiographically observed by soft X-ray (Hitex-100, Hitachi, Japan) at 54 kVP and 2.5 mA for 20 sec. The bone mineral density (BMD) of each bone defect was measured at the 5×5 mm^2 region of interest by using DEXA with a bone mineral analyzer (DSC 600EX-III, Aloka Co., Tokyo, Japan). This instrument was calibrated with a phantom of known mineral content according to the manufacture's instruction. Each scan was performed at a speed of 20 mm/sec and scanning length was 1 mm. Similarly, the BMD value of the intact bone surrounded with the defects was measured as a control.

Bone specimens were placed into 10 % neutral phosphate-buffered formalin solution, decalcified with 10 % formic acid, and processed for the paraffin embedding. The 3 sections, 3 μm thick from the center of bone specimens were prepared and stained with hematoxylin and eosin (HE) to view by light microscopy (AX-80T, Olympus, Tokyo, Japan).

Statistical Analysis

All the data were statistically analyzed using Fisher's least significant difference test for multiple comparisons and statistical significance was accepted to be less than 0.05. The experimental results were expressed as the mean ± the standard deviation of the mean.

RESULTS

Soft X-ray examination at a skull defect of monkeys

Figure 3-1 shows the soft radiographs of monkey skull defects 12 weeks after application of different gelatin hydrogels and the IBM incorporating BMP-2. Bone regeneration was detected for the gelatin hydrogel with a water content of 97.8 wt% incorporating BMP-2, regardless of BMP-2 concentrations (Figures 3-1C, 1F, and 1G). On the other hand, little bone formation was radiographically observed at the bone defect applied with PBS solution (Figure 3-1A), gelatin hydrogels with water contents of 93.8 and 99.7 wt% (Figures 3-1B and 1D) incorporating BMP-2, empty gelatin hydrogel (Figure 1E), and the IBM incorporating BMP-2 (Figure 1H).

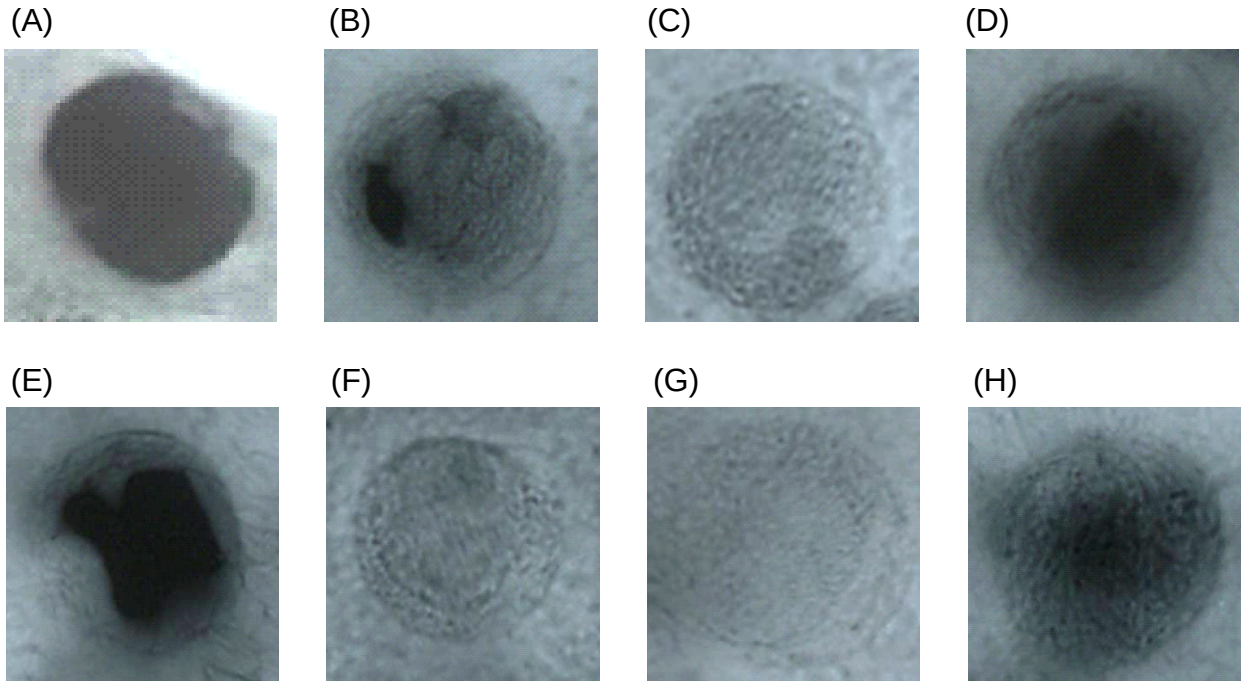

Figure 3-1. Radiographic images of bone defect of monkey skulls 12 weeks after application with phosphate-buffered saline solution (A), gelatin hydrogels incorporating BMP-2 with various water contents (B-G) and insoluble bone matrix incorporating BMP-2 (H). The water content of hydrogels used was 93.8 wt% (B), 97.8 wt% (C and E-G), or 99.7 wt% (D). The BMP-2 doses were 0 μg/site (E), 5 μg/site (B-D and H), 50 μg/site (F), and 200 μg/site (G).

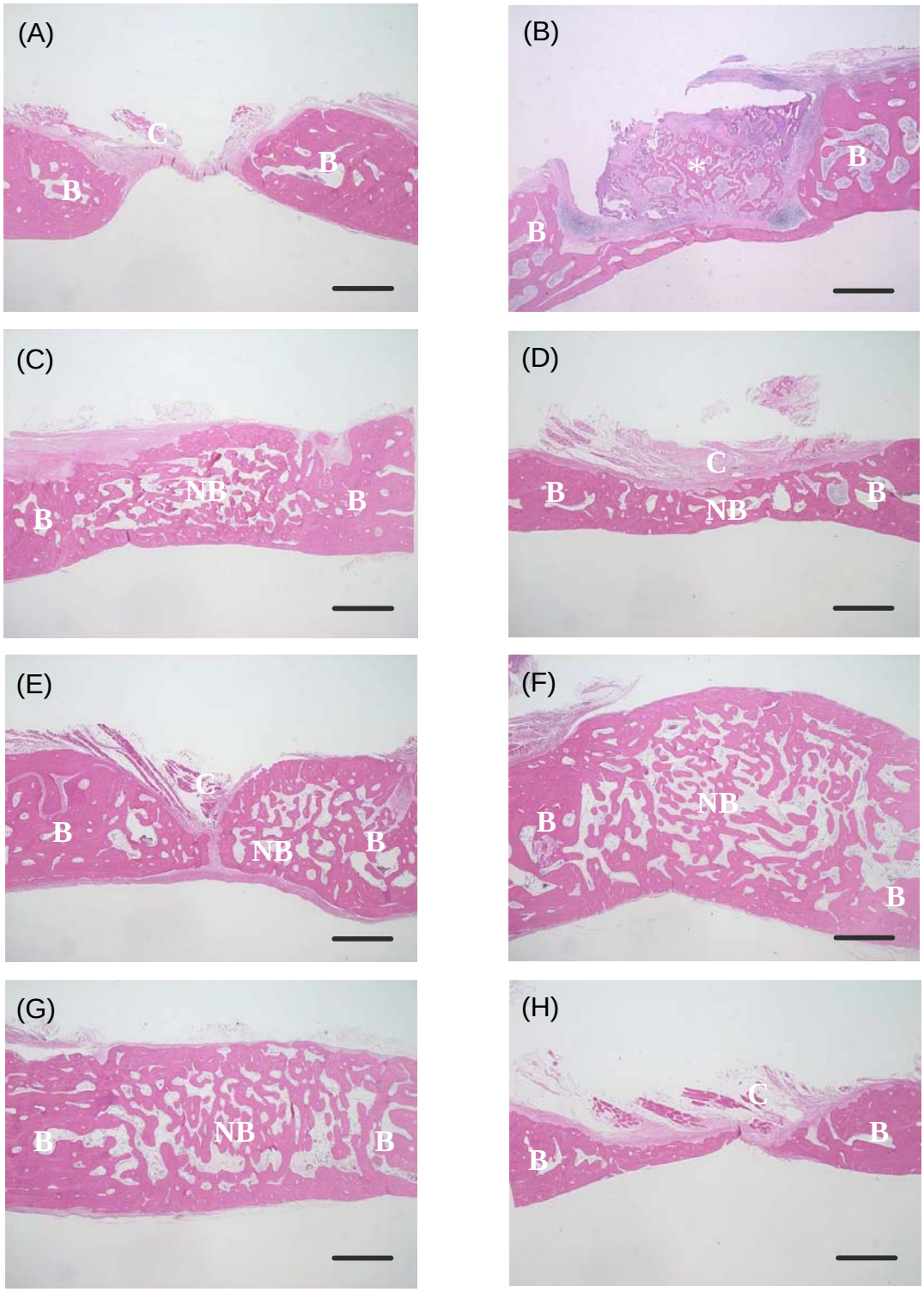

Figure 3-2. Histological cross-sections of bone defect of monkey skulls 12 weeks after application with PBS solution (A), gelatin hydrogels incorporating BMP-2 with various water contents (B-G) and IBM incorporating BMP-2 (H). The water content of the hydrogels was 93.8 (B), 97.8 (C and E-G) or 99.7 wt% (D). The BMP-2 doses were 0 (E), 5 (B–D, and H), 50 (F), and 200 μg/site (G). B; bone, C; connective tissue, and NB; new bone. An astarisk indicates the gelatin hydrogel incorporating BMP-2 remaining in the defect. The bar length is 1 mm.

Histological evaluation of BMP-2-induced bone regeneration

Figure 3-2 shows the histological sections of monkey skull defects 12 weeks after application of different gelatin hydrogels and the IBM incorporating BMP-2. When the skull defect was applied with the empty gelatin hydrogel with a water content of 97.8 wt%, insignificant bone regeneration was observed and soft connective tissues were infiltrated into the defect (Figure 3-2E). On the contrary, new bone regeneration was found in the skull defect applied with the BMP-2-incorporated gelatin hydrogel with a water content of 97.8 wt% (Figures 3-2C, 2F, and 2G), while the defect was completely closed by bone tissue newly formed. BMP-2-incorporated gelatin hydrogels with water contents of 93.8 and 99.7 wt% at a low (5 μg/site) BMP-2 dose did not induce bone regeneration. The gelatin hydrogel with a water content of 93.8 wt% did not degrade and remained at the skull defect 12 weeks after application.

Evaluation of mineral deposition at ulna defects of monkey and rabbit

Table 3-3 summarizes the bone mineral density at the skull defect of monkeys 12 weeks after application of different gelatin hydrogels and the IBM incorporating BMP-2. It is apparent that the BMP-2-incorporated gelatin hydrogel with a water content of 97.8 wt% enhanced the BMD of skull defect to a significantly higher extent than PBS application, although the BMD value was lower than that of the intact bone. The BMD value depended on the types of hydrogels and was significantly higher for the hydrogel with a water content of 97.8 wt% than for that with 99.7 wt%. On the other hand, no significant enhancement of BMD was detected for BMP-2-incorporated gelatin hydrogels with water contents of 93.8 and 99.7 wt% and the BMP-2-incorporating IBM. The BMP-2-free empty hydrogel did not contribute to any increase in the BMD of the skull defect.

Table 3-3. Bone mineral density at monkey skull defects 12 weeks after application.

Application	Hydrogel water content (wt%)	BMD (mg/cm^2)
PBS	–	80.1 ± 7.8
Empty gelatin hydrogel	97.8	128.9 ± 14.8
Gelatin hydrogel incorporating BMP-2	93.8	104.9 ± 6.3
	97.8	188.8 ± 14.6 * †
	99.7	70.0 ± 22.2
IBM	–	99.2 ± 4.8

The BMP-2 dose was 5 μg/site.

The BMD of intact monkey skulls was 216.4 ± 11.4 mg/cm^2.

*$p < 0.05$, significant against the BMD value at the skull bone defect after application of BMP-2-free PBS.

†$p < 0.05$, significant against the BMD value at the skull bone defect after application of gelatin hydrogels incorporating BMP-2 with a water content of 99.7 wt%

Figure 3-3 shows the influence of the BMP-2-dose on the bone regeneration induced by BMP-2-incorporated gelatin hydrogels with a water content of 97.8 wt%. The BMD at the skull defect applied with gelatin hydrogels incorporating BMP-2 became higher with the increasing BMP dose. The gelatin hydrogel incorporating 200 μg of BMP-2 (water content = 97.8 wt%) enhanced the BMD to a significantly higher extent than the BMP-2-free gelatin hydrogel, and the BMD value was similar to that of the intact bone. Free BMP-2 did not enhance the BMD value at the bone defect, and tended to be lower than that applied with the gelatin hydrogel incorporating 200 μg of BMP-2.

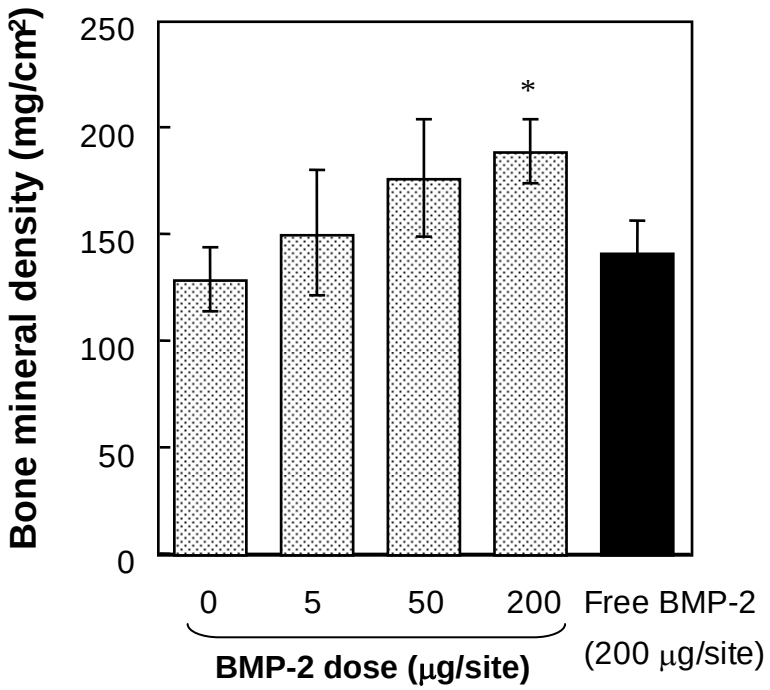

Figure 3-3. Effect of BMP-2 dose on the BMD at bone defect of monkey skulls 12 weeks after application of free BMP-2 (black bar) and gelatin hydrogels incorporating BMP-2 (gray bars). The water content of hydrogel was 97.8 wt%. $^{*}p < 0.05$; significant against the BMD at the skull defect applied with BMP-2-free gelatin hydrogel.

Table 3-4 summarizes the BMD at the skull defect of rabbits 8 weeks after application with different gelatin hydrogels and the IBM incorporating BMP-2. The BMP-2 dose was 5 μg/site for a skull defect. Similarly to the monkey model, the BMD value at the skull defect was significantly increased by application with gelatin hydrogel with a water content of 97.8 wt%. Other applications did not contribute to increase the BMD.

Table 3-4. Bone mineral density at rabbit skull defects 8 weeks after application.

Application	Hydrogel water content (wt%)	BMD (mg/cm^2)
PBS	−	45.9 ± 10.7 *
Free BMP-2	−	65.4 ± 10.5
Empty gelatin hydrogel	97.8	38.0 ± 3.2 *
Gelatin hydrogel incorporating BMP-2	93.8	57.4 ± 11.5 *
	97.8	87.3 ± 6.4
	99.7	62.7 ± 8.0 *
IBM	−	58.3 ± 13.3 *

The BMP-2 dose was 5 μg/site.

The BMD of intact rabbit skulls was 122.9 ± 12.1 mg/cm^2.

*, $p<0.05$, significant against the BMD value at the skull bone defect after application of gelatin hydrogels incorporating BMP-2 with a water content of 97.8 wt%.

DISCUSSION

The present study demonstrates that bone regeneration at the skull defects of non-human primates, monkey induced by gelatin hydrogels incorporating BMP-2 was greatly influenced by the water content of hydrogels and BMP-2 doses. In general, when osteogenic BMP-2 is applied to the bone defect in large animal model, higher doses are normally required for the bone regeneration compared with the case of rodents [16, 17]. It is considered that the difference in the dose among the animal species is attributed to the number of responding cells, the rates of fracture-healing, and the retention time of osteogenic growth factors. If carrier systems for the sustained release of osteogenic growth factors are developed, not only efficient bone formation but also decrease in the dose is expected. We have explored carrier systems composed of gelatin hydrogels with different water contents. The water content of hydrogels could be easily changed only by altering the concentration of gelatin and glutaraldehyde in crosslinking reaction

(Table 3-1). It has been demonstrated that the *in vivo* controlled release profile of BMP-2 was successfully regulated by the water content of hydrogels [10]. The release period of BMP-2 became longer with a decrease in the water content of hydrogels. The profile of BMP-2 release was in good accordance with that of hydrogel degradation, indicating that the BMP-2 release is governed by the degradation of the hydrogel carriers. Furthermore, we have experimentally demonstrated that significantly higher bone formation was induced by the BMP-2-incorporated gelatin hydrogel with a water content of 97.8 wt% than that with the lower or higher water contents both in the muscle of rats and the ulna defect of rabbits [10, 11]. These findings indicate that the release period of BMP-2 is possibly essential to promote the bone induction activity.

In this chapter, a skull defect in monkey of 6 mm in diameter was selected. Radiographic and histological observations revealed no bone regeneration for the control defect applied with PBS and the empty gelatin hydrogel (Figures 3-1A and 1E or Figures 3-2A and 2A). This indicates that the hydrogel itself had no ability for bone. The bone regeneration at the defect applied with BMP-2 solution was also similar to that of defects applied with PBS and the empty gelatin hydrogel, even if the dose of BMP-2 in the free BMP-2 solution was 200 μg (Table 3-3 and Figure 3-3). These results strongly indicate that the size of defect used to assess bone regeneration should be large enough to avoid spontaneous healing. The application of materials without any osteoinduction activity into the skull bone defect results in the formation of fibrous connective tissue rather than bone (Figures 3-1A and 1E).

The activity of gelatin hydrogels incorporating BMP-2 to induce bone regeneration greatly depended on their water content (Tables 3-3 and 3-4 or Figures 3-1 and 3-2). It is likely that the fast-degraded hydrogel could neither prolong the *in vivo* retention of BMP-2 nor protect the defect from the ingrowth of fibrous tissue. When the rate of hydrogel degradation is too slow compared with that of bone regeneration at the skull defect, it is likely that the hydrogel remaining in the defect physically impairs bone

regeneration, even though long-termed release of BMP-2 is achievable. Our previous studies experimentally confirmed that gelatin hydrogels with a slow degradability physically impaired bone regeneration induced by gelatin hydrogels incorporating osteogenic growth factor at both the ulna and skull defect models of rabbits. The osteoinduction activity of the hydrogel with a water content of 97.8 wt% was significantly higher than that with the higher and lower water content [10]. Interestingly, the present dependency of the osteoinduction activity for gelatin hydrogels incorporating BMP-2 is higher correlated to that observed in the previous study. These findings indicate that a balance in the profile between the BMP-2 retention and the bone formation is essential for the bone regeneration induced by gelatin hydrogels incorporating BMP-2.

In clinical application, a collagen sponge, reconstituted from bovine tendon, and collagen based matrix, derived insoluble bone matrix (IBM), have been used as the material for the sustained release of BMPs. A series of preclinical studies suggest that the carriers pharmacologically allowed the proteins to stimulate the activity of local bone induction [18, 19]. It has been recognized that IBM is one of the materials which have been investigated as a promising carrier to reduce the BMP-2 dose [12, 13]. This study also confirmed that the IBM enhanced bone regeneration at the skull defects (Figures 3-1 and 3-2). However, the BMD value was significantly smaller that of the gelatin hydrogel capable for 4-week release of BMP-2. Although there are several reasons to be considered for the increased BMD, the time period of BMP-2 release may be one of keys contributing to the gelatin superiority. Indeed, the time period of BMP-2 was different between gelatin hydrogel and IBM as shown in previous study [12]. On the other hand, chapter 1 indicated that the collagen sponge incorporating BMP-2, having the time profile of BMP-2 release for 2 weeks, showed the enhanced osteoinduction activity at the subcutaneous tissue around the implanted site, but exhibited the lower osteoinduction activity than the gelatin hydrogel [10]. Therefore, optimization of the release profile of BMP-2 by the scaffold design may be important to promote bone

regeneration and reduce the BMP-2 dose.

Many clinical trials using BMPs incorporated scaffolds have been performed against the several cases, such as treatment of fractures, enhancement of spinal fusion, and reconstruction of large bone loss [20-25]. The osteogenetic products composed of BMP-7 (OP-1) and collagen has been commercially available [26]. However, for those applications, high doses of BMPs are generally required. Indeed, the BMP concentration of the commercial available product was 3.5 mg/g [26], and bone regeneration in the clinical trials needs at least more than 1 mg/ml of BMPs [20-25]. The high doses of BMPs can promote the bone regeneration, but eventually cause the systemic side effects [2, 27, 28]. In this chapter, significantly enhanced bone regeneration at monkey skull defects was achieved even at 5 μg/site of BMP-2 dose, as low as that in rabbits (Tables 3-3 and 3-4). This BMP-2 dose is extremely low compared with that of other materials clinically studied. It is also essential to shorten the time period required for bone regeneration in terms of reduction of the physical and spiritual loads of patients. Generally, it takes for more than 6 months after surgery to achieve complete bone repairing clinically [29]. With the gelatin hydrogel incorporating BMP-2, the BMD value recovered at the same level of the intact skulls 12 weeks after surgery which was much shorter than that of IBM incorporating BMP-2 (Figure 3-3). The difference in the time period to complete bone regeneration between the hydrogel system and the IBM of gold standard may be explained in terms of biological harmonization of BMP-2 release and material degradation. By the hydrogel system, BMP-2 of biological activity is retained at the defect for an optimal time period, while the release carrier of hydrogel is degraded to disappear from the defect without any physical impairment for the physiological process of bone regeneration. However, such situation is not always expected for the IBM or other materials. In conclusion, the controlled release technology by the gelatin hydrogel for an appropriate time period enabled a low dose of BMP-2 to induce osteoinduction for non-human primates

REFERENCES

1. J. M. Wozney, and V. Rosen, Bone morphogenetic protein and bone morphogenetic protein gene family in bone formation and repair, *Clin. Orthop. Relat. Res.*, **346**, 26-37 (1998).
2. J. O. Hollinger, H. Uludag, and S. R. Winn, Sustained release emphasizing recombinant human bone morphogenetic protein-2, *Adv. Drug. Deliv. Rev.*, **31**, 303-318 (1998).
3. H. Uludag, D. D'Augusta, R. Palmer, G. Timony, and J. Wozney, Characterization of rhBMP-2 pharmacokinetics implanted with biomaterial carriers in the rat ectopic model, *J. Biomed. Mater. Res.*, **46**, 193-202 (1999).
4. P. J. Boyne, R. E. Marx, M. Nevins, G. Triplett, E. Lazaro, L. C. Lilly, M. Alder, and P. Nummikoski, A feasibility study evaluating rhBMP-2/absorbable collagen sponge for maxillary sinus floor augmentation, *Int. J. Periodont. Rest. Dent.*, **17**, 11-25 (1997).
5. M. Geiger, R. H. Li, and W. Friess, Collagen sponges for bone regeneration with rhBMP-2, *Adv. Drug. Deliv. Rev.*, **55**, 1613-1629 (2003).
6. J. O. Hollinger, J. M. Schmitt, D. C. Buck, R. Shannon, S. P. Joh, H. D. Zegzula, and J. Wozney, Recombinant human bone morphogenetic protein-2 and collagen for bone regeneration, *J. Biomed. Mater. Res. (Appl. Biomater.)*, **43**, 356-364 (1998).
7. M. R. Urist, A. Lietze, and E. Dawson, Beta-tricalcium phosphate delivery system for bone morphogenetic protein, *Clin. Orthop. Relat. Res.*, **187**, 277-280 (1984).
8. H. D. Zegzula, D. C. Buck, J. Brekke, J. M. Wozney, and J. O. Hollinger, Bone formation with use of rhBMP-2 (recombinant human bone morphogenetic protein-2), *J. Bone Joint Surg. Am.*, **79**, 1778-1790 (1997).
9. D. L. Wheeler, D. L. Chamberland, J. M. Schmitt, D. C. Buck, J. H. Brekke, J. O. Hollinger, S. P.

Joh, and K. W. Suh, Radiomorphometry and biomechanical assessment of recombinant human bone morphogenetic protein-2 and polymer in rabbit radius osteotomy model, *J. Biomed. Mater. Res. (Appl. Biomater.)*, **43**, 365-373 (1998).

10. M. Yamamoto, Y. Takahashi, and Y. Tabata, Controlled release by biodegradable hydrogels enhances the ectopic bone formation of bone morphogenetic protein. *Biomaterials*, **24**, 4375-4383 (2003).

11. M. Yamamoto, Y. Takahashi, and Y. Tabata, Enhanced bone regeneration at a segmental bone defect by controlled release of bone morphogenetic protein-2 from a biodegradable hydrogel, *Tissue Eng.*, **12**, 1305-1311 (2006).

12. H. Takita, J. W. Vehof, J. A. Jansen, M. Yamamoto, Y. Tabata, M. Tamura, and Y. Kuboki, Carrier dependent cell differentiation of bone morphogenetic protein-2 induced osteogenesis and chondrogenesis during the early implantation stage in rats, *J. Biomed. Mater. Res.*, **71A**, 181-189 (2004).

13. J. W. Vehof, H. Takita, Y. Kuboki, P. H. Spauwen, and J. A. Jansen, Histological characterization of the early stages of bone morphogenetic protein-induced osteogenesis. *J. Biomed. Mater. Res.*, **61**, 440-449 (2002).

14. Y. Tabata, K. Yamada, H. Liu, S. Miyamoto, N. Hashimoto, and Y. Ikada, Skull bone regeneration in primates in response to basic fibroblast growth factor, *J. Neurosurg.*, **91**, 851-856 (1999).

15. K. Yamada, Y. Tabata, K. Yamamoto, S. Miyamoto, I. Nagata, H. Kikuchi, and Y. Ikada, J. Potential efficacy of basic fibroblast growth factor incorporated in biodegradable hydrogels for skull bone regeneration. *J. Neurosurg.*, **86**, 871-875 (1997).

16. S. T. Yoon, and S. D. Boden, Osteoinductive molecules in orthopaedics: basic science and preclinical studies. *Clin. Orthop. Relat. Res.*, **395**, 33-43 (2002).

17. H. Seeherman, R. Li, and J. Wozney, A review of preclinical program development for evaluating injectable carriers for osteogenic factors, *J. Bone Joint Surg.*, **85-A Suppl 3**, 96-108 (2003).

18. W. Friess, H. Uludag, S. Foskett, R. Biron, and C. Sargeant, Characterization of absorbable collagen sponges as rhBMP-2 carriers, *Int. J. Pharm.*, **187**, 91-99 (1999).

19. H. Uludag, D. D'Augusta, J. Golden, J. Li, G. Timony, R. Riedel, and J. M. Wozney, Implantation of recombinant human bone morphogenetic proteins with biomaterial carriers; a correlation between protein pharmacokinetics and osteoinduction in the rat ectopic model, *J. Biomed. Mater. Res.*, **50**, 227-238 (2000).

20. S. D. Cook, G. C. Baffes, M. W. Wolfe, T. K. Sampath, and D. C. Rueger, The effect of recombinant human osteogenetic protein-1 on healing of large segmental bone defects, *J. Bone Joint Surg.*, **76**, 827-838 (1994).

21. E. H. Groeneveld, J. P. van den Bergh, P. Holzmann, C. M. ten Bruggenkate, D. B. Tuinzing, and E. H. Burger, Histomorphometrical analysis of bone formed in human maxillary sinus floor elevations grafted with OP-1 device, demineralized bone matrix or autogenous bone. Comparison with non-grafted sites in a series of case reports, *Clin. Oral. Implants Res.*, **10**, 499-509 (1999).

22. R. G. Geesink, N. H. Hoefnagels, and S. K. Bulstra, Osteogenetic activity of OP-1 bone morphogenetic protein (BMP-7) in a human fibular defect, *J. Bone Joint Surg.*, **81**, 710-718 (1999).

23. S. D. Boden, T. A. Zdeblick, H. S. Sandhu, and S. E. Heim, The use of rhBMP-2 in interbody fusion cages. Definitive evidence of osteoinduction in humans: a preliminary report, *Spine*, **25**, 376-381 (2000).

24. G. E. Friedlaender, C. R. Perry, J. D. Cole, G. Cierny, G. F. Muschler, G. A. Zych, A. J. LaForte, and S. Yin, Osteogenic protein-1 (bone morphogenetic protein-7) in the tibial nonunions, *J. Bone Joint Surg. Am.*, **83-A Suppl 1**, S151-158 (2001).

25. T. A. Einhorn, Clinical applications of recombinant human BMPs: early experience and future development, *J. Bone Joint Surg. Am.*, **85-A Suppl 3**, 82-88 (2003).

26. M. A. Mont, P. S. Ragland, B. Biggins, G. Friedlaender, T. Patel, S. Cook, G. Etienne, S. Shimmin, R. Kildey, D. C. Rudger, and T. A. Einhorn, Use of bone morphogenetic proteis for musculoskeletal applications. An overview, *J. Bone Joint Surg. Am.*, **86-A Suppl 2**, 41-55 (2004).

27. S. A. Gittens, and H. Uludag, Growth factor delivery for bone tissue engineering, *J. Drug Targ.*, **9**, 407-429 (2001).

28. J. R. Lieberman, A. Daluiski, and T. A. Einhorn, The role of growth factors in the repair of bone. Biology and clinical applications, *J. Bone Joint Surg. Am.*, **84-A**, 1032-1044 (2002).

29. A. Valentin-Opran, J. Wozney, C. Csimma, L. Lilly, and G. E. Riedel, Clinical evaluation of recombinant human bone morphogenetic protein-2, *Clin. Orthop. Relat. Res.*, **395**, 110-120 (2002).

Chapter 4

Ectopic bone formation by controlled release of BMP-2 from biodegradable scaffolds composed of gelatin and ß-TCP

INTRODUCTION

Bone defects which are generated by tumor resection, trauma, and congenital abnormality, have been clinically treated by the implantation of bioceramics or autogenous and allogenous bone grafts. Although autografting is a popular procedure for reconstructive surgery, it has several disadvantages, such as the shortage of donor supply, the persistence of pain, the nerve damage, fracture, and cosmetic disability at the donor site. On the other hand, there are no donor site problems for allografting, while allografting has some clinical risks including disease transmission and immunological reaction [1]. As one trial to overcome the problems, bone tissue engineering has been attracted much attention as a new therapeutic technology which induces bone regeneration by making use of osteoinductive growth factors, osteogenic cells, and scaffolds or their combination [2]. It is no doubt that a combination of osteoinductive growth factors and scaffolds provides an appropriate osteoinductive environment for osteogenic cells.

Osteoinductive growth factors, such as bone morphogenetic protein (BMP), transforming growth factor-ß (TGF-ß), and basic fibroblast growth factor (bFGF), have been investigated to induce bone regeneration in the body [3]. Among them, BMP-2 and BMP-7 (OP-1) have already been applied clinically for bone regeneration at the bone defect, because of their high osteoinduction activity [4, 5]. However, the BMP administrated in the solution form does not always expect the *in vivo* satisfied efficacy in bone regeneration. Therefore, it is necessary to develop a carrier for the controlled release of biologically active BMPs over an extended time period.

Gelatin is a denatured collagen and commercially available as a biodegradable polymer. It has been extensively utilized for pharmaceutical and medical purposes, and its biosafety has been proven

through the long clinical applications [6]. Other advantages of gelatin are the easiness of chemical modification and the commercial availability of samples with different physicochemical properties. We have prepared a biodegradable hydrogel of gelatin for the controlled release of BMP to succeed in inducing bone regeneration [7]. On the other hand, it has been experimentally demonstrated from some researches that the attachment and proliferation of cells on substrates are promoted by the surface coating of gelatin [8-10]. These findings suggest that gelatin is one of the materials compatible to cells.

Since it is preferable that the scaffolds for bone regeneration basically function as the substrate for the attachment and proliferation of osteogenic cells, 3 dimensional biodegradable materials with a porous structure, such as glycolide-lactide copolymer non-woven fabrics, collagen sponges, and calcium phosphate ceramics, have been used [11, 12]. Among them, hydroxyapatite (HAp) and ß-tricalcium phosphate (ß-TCP) of bioactive ceramics have been extensively investigated as the cell scaffold for bone tissue engineering [11-22] because it is well recognized that they are compatible to natural bone tissue. However, since HAp is not practically degraded under the physical condition, it remains inside the bone tissue regenerated. Therefore, as one trial to improve the *in vivo* poor degradability, HAp has been attempted to mix with organic materials of collagen and glycolide-lactide copolymer. The combination was effective in manipulating the degradation and mechanical properties for the HAp scaffolds [23-28]. ß-TCP is advantageous from the viewpoint of material biodegradability, though brittle compared with HAp. On the other hand, some research groups have investigated the osteoinduction of BMP-incorporating composites for different animal models. However, little has been demonstrated on the effect of the bioceramic content on the osteoinduction activity [29-35].

Naturally-occurring bone matrix provides an environment favorable for the *in vivo* osteoinduction in terms of the bone cell scaffold and growth factor delivery vehicle. In this chapter, as a mimic of the natural bone matrix, we have designed a biodegradable cell scaffold of organic-inorganic composite combined with the controlled release nature of BMP. Biodegradable gelatin sponges at different contents of ß-TCP were fabricated. Following incorporation of BMP-2 into the gelatin-ß-TCP scaffolds, their *in vivo* BMP-2 release from the scaffolds was investigated. To obtain fundamental information on *in vivo*

osteoinductivity of gelatin-ß-TCP scaffolds incorporating BMP-2, the *in vivo* osteoinduction activity of gelatin-ß-TCP scaffolds incorporating BMP-2 was assessed at the back subcutis of rats in terms of the ß-TCP content.

EXPERIMENTAL

Materials

A gelatin sample with an isoelectric point (IEP) of 9.0 was prepared through an acidic process of porcine skin collagen type I (Nitta Gelatin Co., Osaka, Japan). ß-TCP granules (2 μm in average diameter) were obtained from Taihei Chemical Industries, Nara, Japan. $Na^{125}I$ (740 MBq/ml in 0.1 N NaOH aqueous solution) was purchased from NEN Research Products, Du Pont, Wilmington, USA. Collagenase was purchased from Sigma Chemical Co., St. Louis, MO, USA. Other chemicals were obtained from Wako Pure Chemical Industries, Osaka, Japan and used without further purification.

Preparation of gelatin scaffolds with or without ß-TCP

Gelatin scaffolds incorporating ß-TCP (gelatin-ß-TCP scaffolds) were prepared by chemical crosslinking of gelatin with glutaraldehyde in the presence of ß-TCP granules at different amounts (Table 4-1). Briefly, 4.29 wt% aqueous solution of gelatin at different contents of ß-TCP (70 ml) was mixed at 5,000 rpm at 37 °C for 3 min by using a homogenizer (ED-12, Nihonseiki Co., Tokyo, Japan). After addition of 2.17 wt% of glutaraldehyde aqueous solution (30 ml), the mixed solution was further mixed for 15 sec by the homogenizer. The resulting solution was cast into a polypropylene dish of 138×138 cm^2 and 5 mm depth, followed by leaving at 4 °C for 12 hr for gelatin crosslinking. Then, the crosslinked gelatin hydrogels with or without ß-TCP were placed into 100 mM of aqueous glycine solution at 37 °C for 1 hr to block the residual aldehyde groups of glutaraldehyde. Following complete washing with double distilled water (DDW), the hydrogels were freeze-dried and cut into cubes of 5×5×5 mm^3.

The resulting scaffolds were sputter-coated with gold/palladium and viewed both on a scanning

electron microscope (SEM, S-2380N, Hitachi, Japan) and a field emission scanning electron microscope with energy dispersive X-ray (EDX) microanalyzer (JSM 6500F, JEOL, Japan). The average pore size and porosity of scaffolds were measured by the methods reported previously (Table 4-1) [36, 37].

Table 4-1. Characterization of gelatin scaffolds incorporating various amounts of ß-TCP prepared

ß-TCP content (wt%)	Pore size (μm)	Porosity (%)	Compression modulus (MPa)
0	184.9 ± 58.2	96.6	0.27 ± 0.01
25	198.2 ± 52.3	96.2	0.52 ± 0.14
50	179.1 ± 27.8	95.9	1.13 ± 0.13
75	185.5 ± 62.4	95.4	2.60 ± 0.32
90	178.2 ± 50.0	95.1	4.97 ± 0.73

In vitro compression resistance of gelatin and gelatin-ß-TCP scaffolds

The *in vitro* compression resistance of gelatin and gelatin-ß-TCP scaffolds in the freeze-dried state was evaluated by measuring their compression moduli at a rate of 1 mm/min (AG-5000B, Shimadzu, Kyoto, Japan). The load-deformation curve was obtained and the compression modulus of scaffolds was calculated from the initial slope of load-deformation curve. Measurement was done five times for each sample to calculate the average value ± the standard deviation of the mean.

Radioiodination of BMP-2

Human recombinant BMP-2 (Yamanouchi Pharmaceutical Co., Japan) was radioiodinated according to the method of Greenwood et al. [38]. Briefly, 4 μl of $Na^{125}I$ solution was added to 40 μl of 1 mg/ml BMP-2 solution containing 5 mM glutamic acid, 2.5 wt% glycine, 0.5 wt% sucrose, and 0.01 wt% Tween 80 (pH 4.5). Then, 0.2 mg/ml of chloramine-T potassium phosphate-buffered solution (0.5 M, pH

7.5) containing 0.5 M sodium chloride (100 µl) was added to the solution mixture. After agitation at room temperature for 2 min, 100 µl of phosphate-buffered saline solution (PBS, pH 7.5) containing 0.4 mg of sodium metabisulfate was added to the reaction solution to stop the radioiodination. The reaction mixture was passed through an anionic-exchange column to remove the uncoupled, free ^{125}I molecules from the ^{125}I-labeled BMP-2.

Preparation of gelatin and gelatin-ß-TCP scaffolds incorporating BMP-2

To prepare gelatin and gelatin-ß-TCP scaffolds incorporating BMP-2, 20 µl of aqueous solution containing BMP-2 (0.25 µg/µl) or ^{125}I-labeled BMP-2 (0.03 µg/µl) was dropped onto the freeze-dried scaffold, followed by leaving it at 4 °C overnight. The resulting scaffold was used as the gelatin and gelatin-ß-TCP scaffolds incorporating BMP-2 without washing. Similarly, 20 µl of BMP-2-free PBS was impregnated into gelatin and gelatin-ß-TCP scaffolds to obtain respective BMP-2-free, empty scaffolds.

In vivo evaluation of BMP-2 release from gelatin and gelatin-ß-TCP scaffolds

Gelatin and gelatin-ß-TCP scaffolds incorporating ^{125}I-labeled BMP-2 were implanted into the back subcutis of 6 week-age female ddY mice (Shimizu Laboratory Supply Inc., Japan) at the central position 15 mm away from their tail root. At different time intervals, the mouse skin including the implanted site of sponge (3×5 cm^2) was excised and the corresponding facia was thoroughly wiped off with a filter paper to absorb ^{125}I-labeled BMP-2. The radioactivity of the gelatin scaffold remained, the skin strip excised, and the filter paper was measured on a gamma counter (ARC-301B, Aloka Co., Ltd., Japan) to assess the time profile of *in vivo* BMP-2 retention. The radioactivity was divided by the original radioactivity of gelatin and gelatin-ß-TCP scaffolds incorporating ^{125}I-labeled BMP-2 to calculate the percent remaining of BMP-2. All the radioactivities were compensated for the natural decay of ^{125}I. Experimental group was composed of 3 mice unless otherwise mentioned.

Histological evaluation of bone tissue ectopically induced by gelatin and gelatin-ß-TCP scaffolds incorporating BMP-2

Gelatin and gelatin-ß-TCP scaffolds incorporating 5.0 μg of BMP-2 were implanted into the back subcutis of Fisher 344 rats (Shimizu Laboratory Supply Inc., Japan). The BMP-2-free, empty scaffold was used as a control. The subcutaneous tissue including gelatin and gelatin-ß-TCP scaffolds with or without BMP-2 incorporation was fixed in 10 wt% neutral-buffered formalin solution 4 weeks after implantation. The tissue samples fixed were conventionally dehydrated in aqueous solutions of ethanol at sequentially increasing concentrations of 70 to 100 vol%, immersed in xylene, and embedded in paraffin. The samples were sectioned at 4 μm thickness and stained by hematoxylin and eosin (HE) to view on an optical microscopy (AX-80, Olympus, Japan).

Biochemical evaluation of BMP-2-induced ectopic bone formation

The samples obtained 2 and 4 weeks after implantation were freeze-dried and grinded. The grinded sample (5 mg) was homogenized in 1 ml of mixed aqueous solution of 0.2 % Nonidet P-40, 10 mM Tris-HCl, and 1 mM $MgCl_2$ (pH 7.5). The homogenate was centrifuged at 12,000 rpm and 4 ^{o}C for 15 min and the alkaline phosphatase (ALP) activity of supernatant obtained was determined by a *p*-nitro phenyl-phosphate method [39].

For the determination of osteocalcin content, the grinded sample (5 mg) was placed for 12 hr in 40 % formic acid aqueous solution (1 ml) for decalcification. During the decalcification process, the non-collagenous proteins of bone matrix were extracted. After desalting of the extracts with a gel filtration using Sephadex^{TM} G-25M column (PD-10, Amersham Pharmacia biotech AB, Sweden), the resulting solution was freeze-dried and subjected to an osteocalcin rat enzyme-linked immunosorbent assay (ELISA) (rat osteocalcin ELISA system, Amersham Biosciences, Tokyo, Japan) [39].

Enzymatic degradation of gelatin and gelatin-ß-TCP scaffolds

Gelatin and gelatin-ß-TCP scaffolds were immersed in Tris buffer (pH 7.4) containing 5 unit/ml

of collagenase at 37 ^{o}C and then washed with distilled water. Appearance of the scaffolds was observed by an optical microscope.

Statistical analysis

All the data were shown as the mean value ± the standard deviation of the mean. The pairwise comparisons of individual group means were conducted based on the one-way ANOVA. Values of $p < 0.05$ were considered statistically significant.

RESULTS

Characterization of gelatin and gelatin-ß-TCP scaffolds

Figure 4-1 shows the electron microscopic structure and EDX image of gelatin and gelatin-ß-TCP scaffolds. Irrespective of the ß-TCP content, the similar intra-structure of sponges was observed. Every scaffold had an interconnected porous structure with the pore size range of 180-200 μm and the porosity around 96 % (Table 4-1). ß-TCP granules were homogeneously localized in the gelatin walls of the scaffolds, while the intensity of the peak for CaKα x-ray depends on the ß-TCP content (Figure 4-1K, 1L, 1M, 1N, 1O). On the other hand, the compression modulus of scaffolds increased with an increase in the content of ß-TCP.

In vivo evaluation of BMP-2 release from gelatin and gelatin-ß-TCP scaffolds incorporating BMP-2

Figure 4-2 shows the *in vivo* decrement patterns of the remaining radioactivity at the implanted site of gelatin and gelatin-ß-TCP scaffolds incorporating ^{125}I-labeled BMP-2. The period of BMP-2 retention was not influenced by the ß-TCP content. Negligibly low radioactivity was detected in the thyroid gland for each experimental group, indicating no release of free radioactive iodine from ^{125}I-labeled BMP-2 (data not shown).

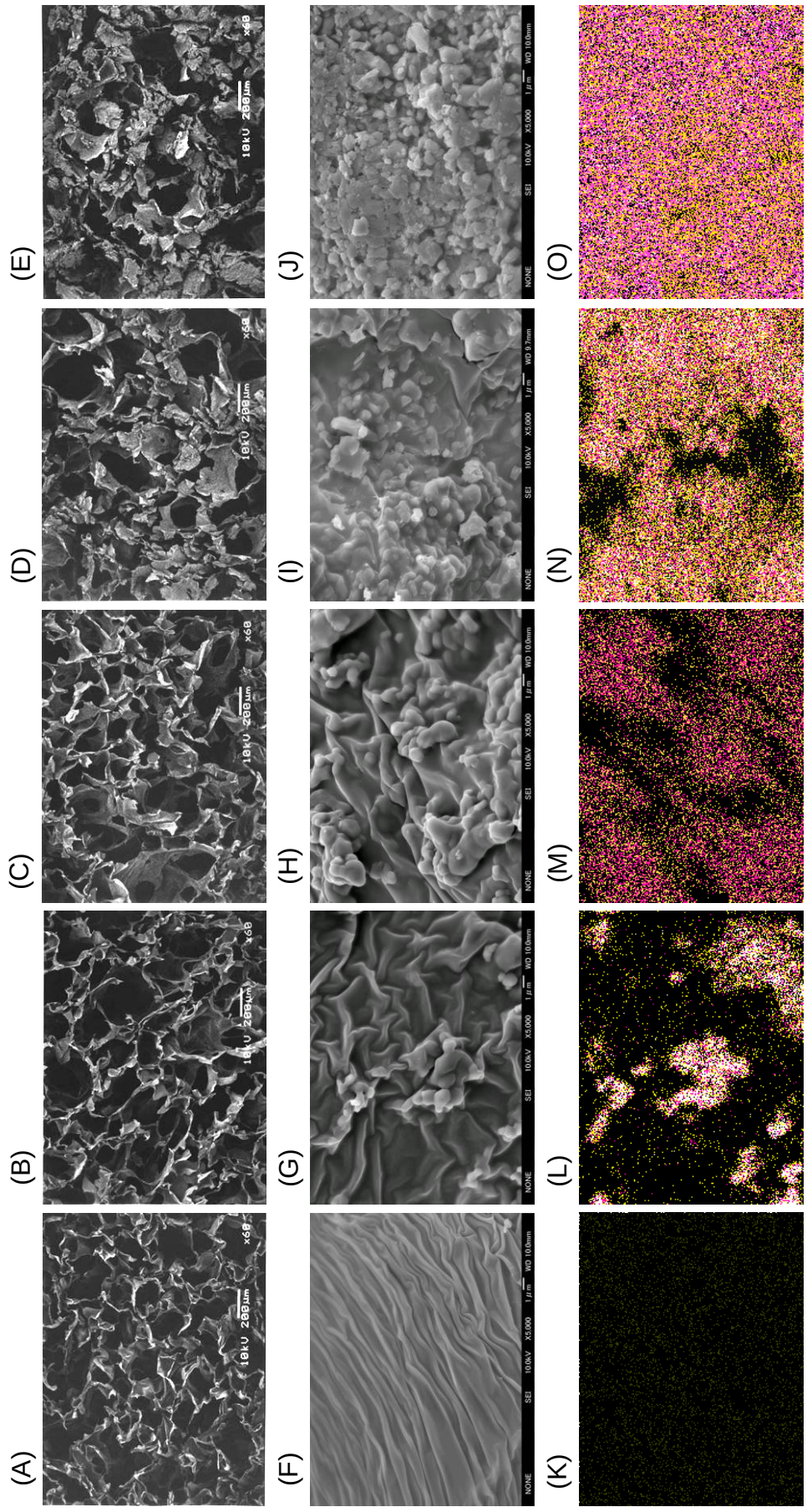

Figure 4-1. Scanning electron micrographs of gelatin scaffolds incorporating 0 (A, F), 25 (B, G), 50 (C, H), 75 (D, I), and 90 wt% of β-TCP (E, J) at the magnification of 60 (A-E) and 5,000 (F-J). EDX images of calcium element for gelatin scaffolds incorporating 0 (K), 25 (L), 50 (M), 75 (N), and 90 wt% of β-TCP (O) at a magnification of 5,000.

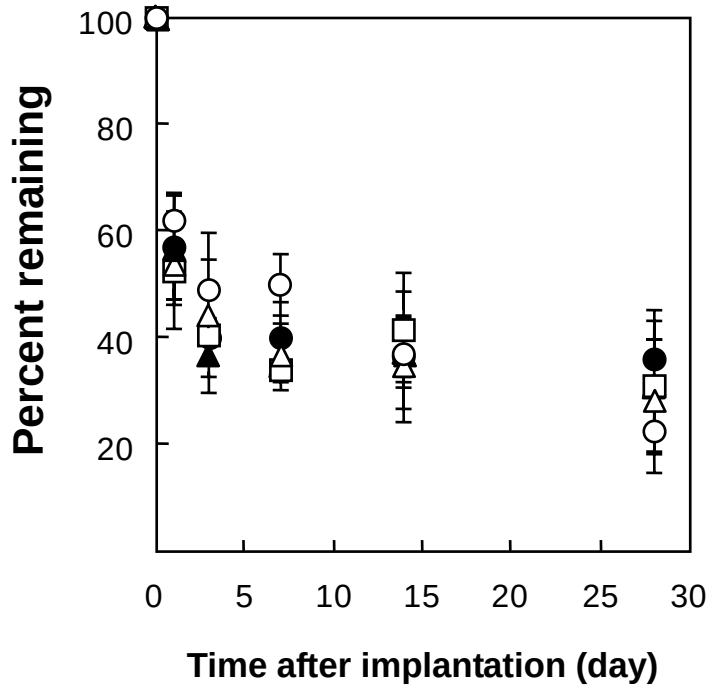

Figure 4-2. *In vivo* time profiles of the radioactivity remaining after the subcutaneous implantation of gelatin-ß-TCP scaffolds incorporating ^{125}I-labeled BMP-2 into the back of mice. The ß-TCP contents of gelatin scaffolds are 0 (○), 25 (△), 50 (□), 75 (●), and 90 wt% (▲).

Ectopic bone formation induced by gelatin and gelatin-β–TCP scaffolds incorporating BMP-2

Figure 4-3 shows the histological section of subcutaneous tissue 4 weeks after implantation of gelatin and gelatin-ß-TCP scaffolds incorporating BMP-2. Every BMP-2-incorporated scaffold induced bone formation homogeneously throughout the scaffolds, although the extent of bone formation was higher in the scaffolds with the lower contents of ß-TCP.

Irrespective of the ß-TCP incorporation, the gelatin and gelatin-ß-TCP scaffolds incorporating BMP-2 enhanced the ALP activity to a significantly higher extent than that of the BMP-2-free scaffolds (Figure 4-4A). The highest ALP activity was observed for the gelatin sponge without ß-TCP. The similar ß-TCP content dependency was observed for the osteocalcin content of subcutaneous tissues around the implanted site of sponges incorporating BMP-2. The BMP-2-incorporated gelatin sponge without ß-TCP exhibited the highest osteocalcin content 4 weeks after the implantation, while the osteocalcin

content decreased with the increasing content of ß-TCP (Figure 4-4B). Incorporation of BMP-2 enabled gelatin scaffolds to enhance the induction activity of bone formation, irrespective of the ß-TCP incorporation.

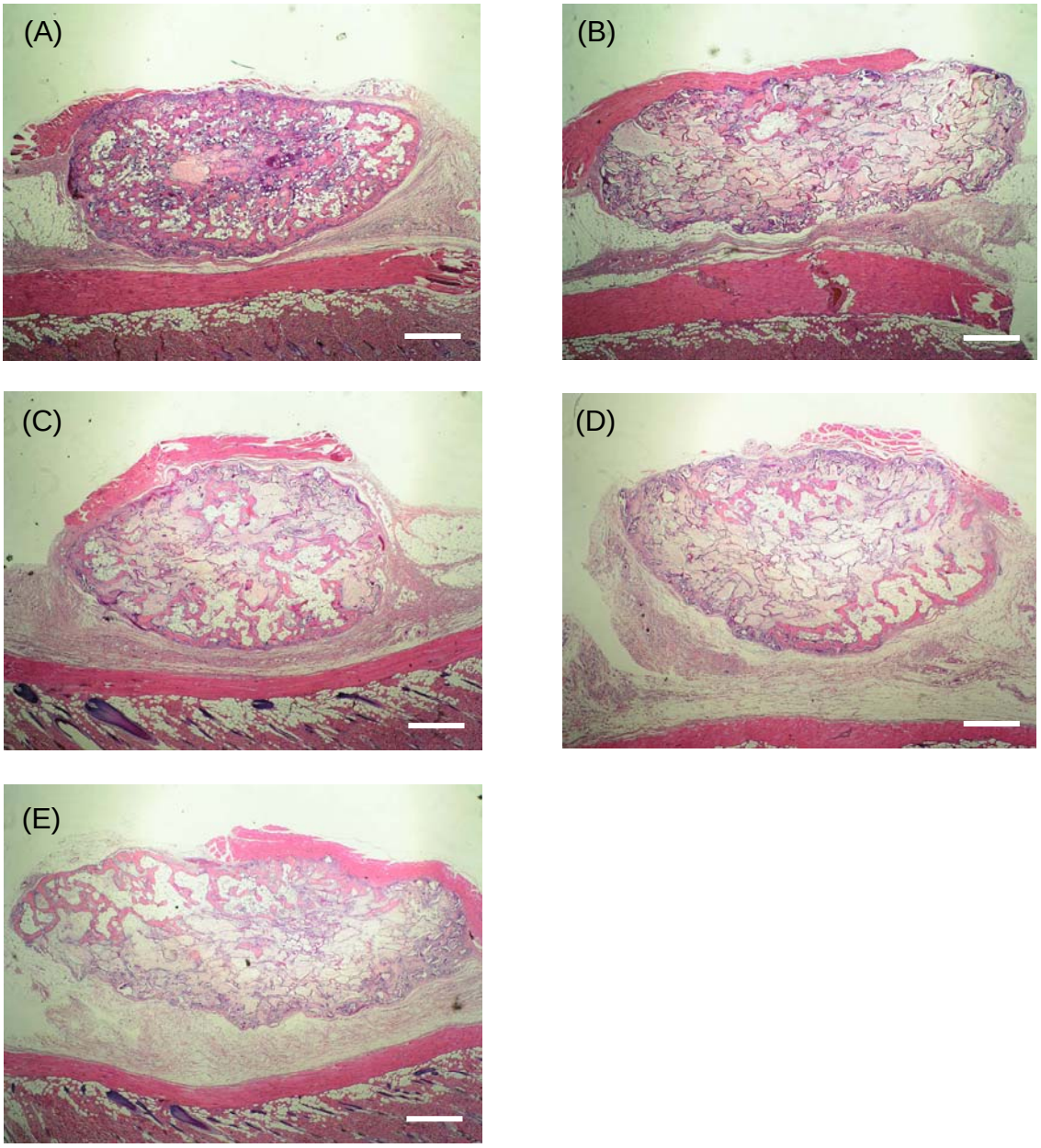

Figure 4-3. Histological cross-sections of subcutaneous tissue around the implanted site of gelatin-ß-TCP scaffolds incorporating BMP-2 4 weeks after implantation into the back subcutis of rats. The ß-TCP contents of gelatin scaffolds are 0 (A), 25 (B), 50 (C), 75 (D), and 90 wt% (E). Bars correspond to 1 mm.

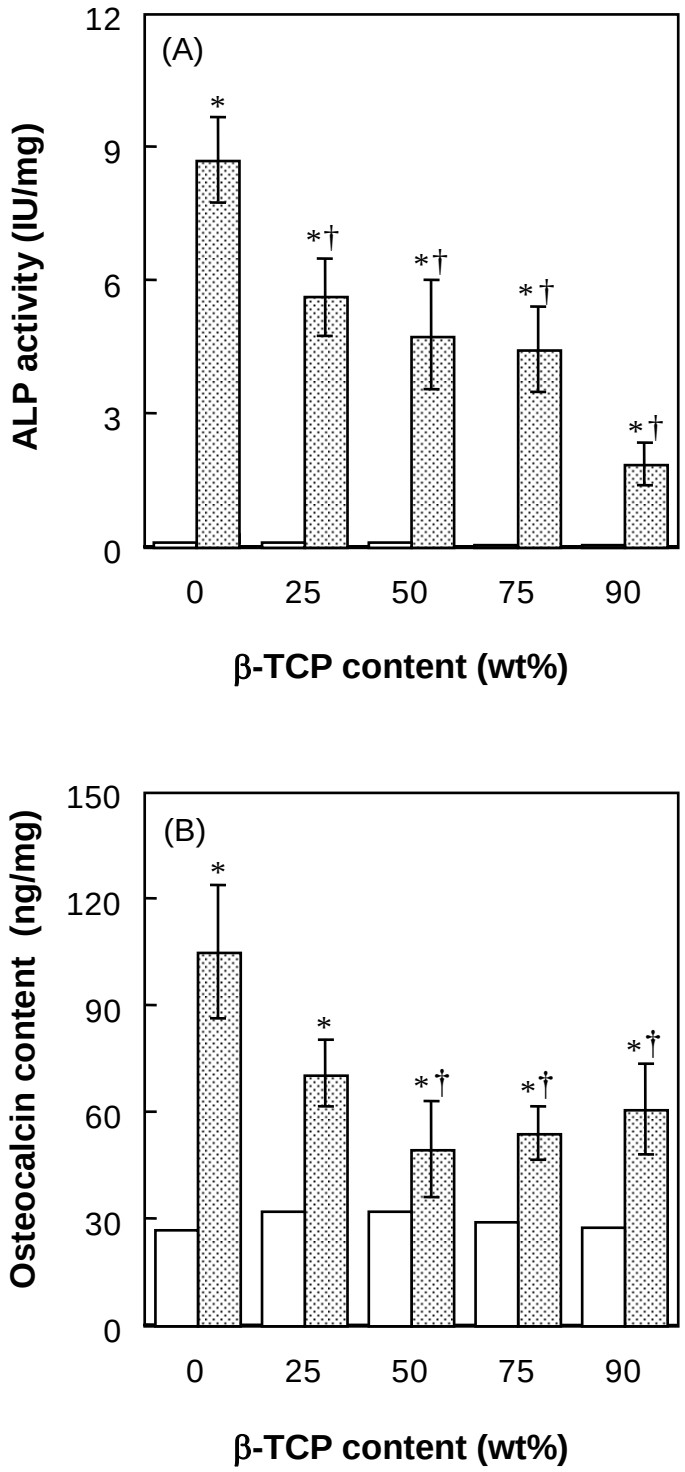

Figure 4-4. ALP activity (A) and osteocalcin contents (B) of tissues around the implanted site of gelatin-β-TCP scaffolds incorporating BMP-2 2 and 4 weeks after implantation, respectively. The BMP-2 doses are 0 (□) and 5 μg (▨). $^{*}p < 0.05$; significant against the ALP activity and the osteocalcin contents of tissues around the implanted site of empty gelatin-β-TCP scaffolds at the corresponding β-TCP amount.

DISCUSSION

This chapter demonstrates that the *in vivo* osteoinductive activity of gelatin-ß-TCP scaffolds incorporating BMP-2 was greatly influenced by the ß-TCP content. In our previous studies, the hydrogel of gelatin in different shapes, such as disks, sheets, and microspheres, could be fabricated to function as the release carrier of various growth factors [40]. Although it is known that gelatin is one of the substrate materials for cell adhesion and proliferation, the hydrogel dose not always function as a good scaffold of migration, proliferation, and differentiation of cells, because of no porous structure necessary for cell infiltration. Therefore, in this chapter, a hydrogel with a porous sponge structure was fabricated by a homogenization process of aqueous gelatin solution. This homogenization process has been reported to prepare a synthetic dermal substitute of collagen [41]. The pore size was adjusted at 180-200 μm since the pore size suitable for cell infiltration and ingrowth of host bone tissue is reported to be in the range of 100-350 μm [42, 43]. As a result, the gelatin sponge obtained functions not only as the release carrier for growth factor, but also as the scaffold of cell attachment and proliferation. For the scaffold preparation, ß-TCP which has been extensively explored as one bioactive substrate was combined. Since spontaneous gelation of gelatin solution homogeneously dispersing various amounts of ß-TCP takes place immediately after leaving them at 4 ^{o}C, no sedimentation of ß-TCP granules was observed in this study. Homogeneous incorporation of ß-TCP enabled the gelatin scaffold to increase the compression modulus without any change in the pore structure. The mechanical resistance of scaffolds against compression in a dry state increased with the increased ß-TCP content (Table 4-1). The scaffold of sponge shape has been used for cell scaffold from the viewpoint of good nutrients and oxygen supply to cells and superior cell infiltration. However, generally a porous structure weakens the mechanical strength of scaffold. Therefore, often the compression modulus of sponge scaffold is not strong enough for cell scaffold application. In experimental and clinical cases, porous HAp and ß-TCP have been widely used because of their inherent osteoconductivity [13-22]. However, there are some disadvantages to be improved, such as poor biodegradability and brittle nature. In addition, it is difficult to freely change the shape of bioceramics

upon applying to the body site of different shapes during the operation. This study clearly indicates that combination of bioceramics with gelatin is one of the effective strategies to overcome the material problems. The gelatin-β-TCP scaffold can be readily cut by a scalpel for the shape change.

When incorporated into gelatin and gelatin-ß-TCP scaffolds and implanted subcutaneously, BMP-2 was retained in the sponges *in vivo* for more than one month and long-termed BMP-2 release was achieved (Figure 4-2). No dependence of *in vivo* BMP-2 release profile on the ß-TCP content was observed. This can be explained in terms of the sponge property for growth factor release. Chapter 1 demonstrates that a biodegradable hydrogel of the same gelatin enabled BMP-2 to release at the implanted site for extended time periods and the BMP-2 release was governed by the degradation of carrier hydrogel [7]. On the other hand, ß-TCP has been investigated as a carrier material for BMP-2 release [44] to show the *in vivo* release profile similar to that of the gelatin sponge without β-TCP incorporation (data not shown). It is highly conceivable that the BMP-2 adsorbed on the surface of ß-TCP can be released through the detachment accompanied with the pore surface erosion, since ß-TCP is biodegradable [45]. Taken together, we can say with fair certainty that BMP-2 is released from the gelatin-ß-TCP scaffold based on the *in vivo* degradation of both gelatin and ß-TCP, although the contribution percentage to the binding site of BMP-2 for release between the gelatin and ß-TCP is not clear yet.

The histological study clearly reveals that gelatin and gelatin-ß-TCP scaffolds incorporating BMP-2 induced bone formation homogeneously throughout the scaffolds (Figure 4-3). For the scaffold of hydrogel type, it was difficult to allow cells to infiltrate into the interior of gelatin hydrogels, and consequently osteogenic differentiation induced by the gelatin hydrogel incorporating BMP-2 was observed only around the hydrogel [46], which is quite different from the case of gelatin sponge reported here. As Wozney et al report [47], the ectopic placement of implants incorporating BMP permits clear differentiation of osteoblast cells throughout osteoinduction for bone tissue formation. It has been considered that BMP activates a set of cellular events including chemotaxis of uncommitted mesenchymal cells and possibly other target cells into the implanted site as well as their differentiation into mineral-depositing osteoblasts. It is likely that the mesenchymal cells recruited into gelatin-ß-TCP scaffolds are stimulated by BMP-2

released from the scaffold enough to allow them to differentiate into bone-forming cells like osteoblasts, resulting in efficient induction of bone formation thereat. The extent of bone formed was greater for the gelatin scaffold incorporating BMP-2 than that of gelatin-ß-TCP scaffold incorporating BMP-2. This suggests that the ß-TCP presence is not always necessary for bone formation, but the BMP-2 release plays a major role in facilitating osteoinduction activity of gelatin-ß-TCP scaffold incorporating BMP-2. In addition, it is possible that the bone formation inside the sponge is basically caused by the pore structure.

The ALP activity and osteocalcin content of subcutaneous tissues around the implanted site of gelatin and gelatin-β-TCP scaffolds incorporating BMP-2 were the highest for the gelatin scaffold without ß-TCP incorporation (Figures 4-4A and 4B). Since osteoinductive materials allow mesenchymal cells around the implanted site to infiltrate into their pores and to differentiate into osteogenic cells therein [11, 12, 44], it is conceivable that the osteoinduction activity of the BMP-2-incorporated sponges is influenced both by the *in vivo* deformation resistance of the scaffolds and the *in vivo* profile of BMP-2 release. The difference in the scaffold deformation can be explained from the viewpoint of the mechanical stability of scaffolds rather than the material degradation. When the compression modulus of gelatin-ß-TCP scaffolds was measured in a freeze-dry state, it became higher with the increased amount of ß-TCP incorporated. On the other hand, the morphological change of gelatin sponges with or without ß-TCP incorporation was evaluated before and after their immersion in collagenase solution (Figure 4-5). Although the compression modulus of scaffolds freeze-dried increased with the increased ß-TCP content (Table 4-1), in a wet state the gelatin-ß-TCP scaffold collapsed easier than the gelatin sponge without ß-TCP incorporation. It is apparent in Figure 4-1 that ß-TCP granules are dispersed in the matrix of gelatin. It is conceivable that gelatin serves as a binder material between ß-TCP particles incorporated to keep the structure of gelatin-ß-TCP scaffolds. Thus, the content of gelatin decreases with an increase in that of ß-TCP. As a result, it is likely that the scaffolds with higher ß-TCP contents are collapsed and deformed easily under wet and proteolytic conditions due to faster loss of gelatin mass by degradation. It is possible that this scaffold deformation bring about loss of the intrasponge space necessary for bone ingrowth, resulting in reduced osteoinduction activity inside the scaffold.

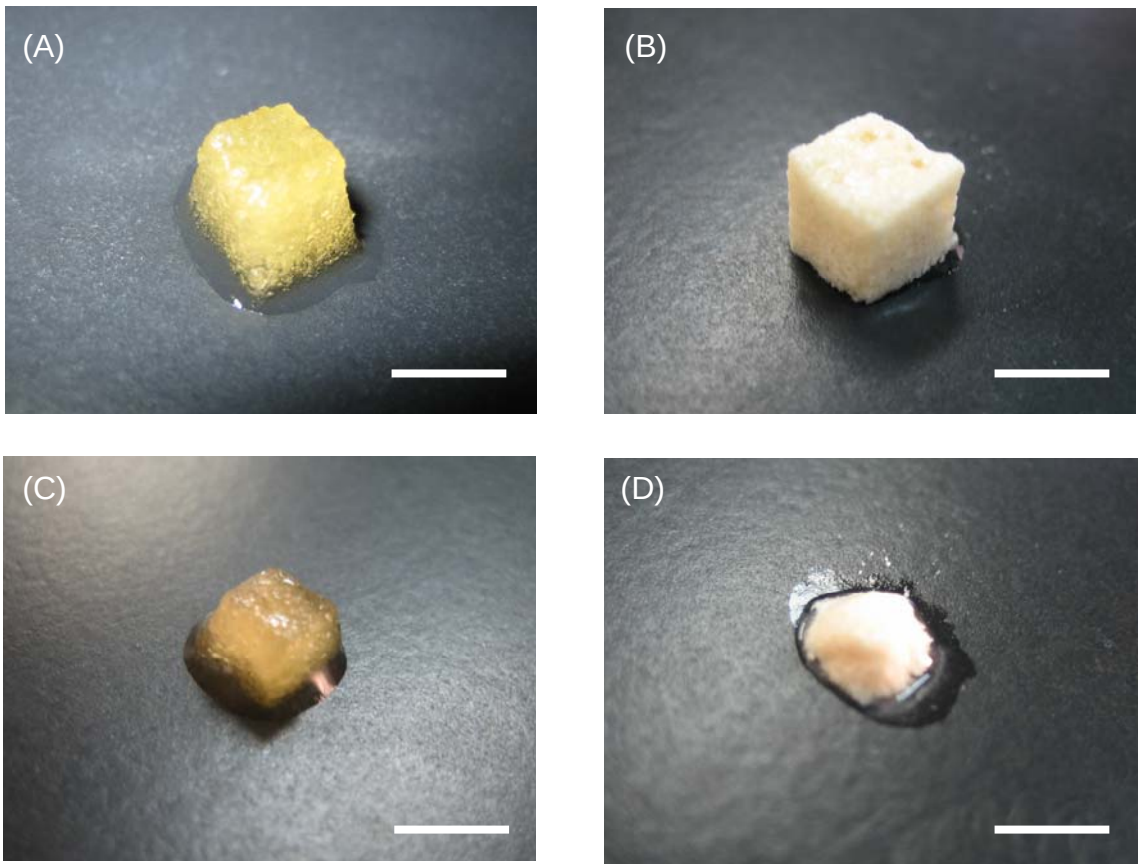

Figure 4-5. Appearance of gelatin-ß-TCP scaffolds before (A, B) and after (C, D) *in vitro* enzymatic degradation. The ß-TCP contents of gelatin scaffolds are 0 (A, C) and 90 wt% (B, D). Bar correspond to 5 mm.

On the other hand, we have demonstrated that the *in vivo* retention of BMP-2 greatly affects the osteoinduction activity of gelatin hydrogels incorporating BMP-2 [7]. In addition, Kaito et al. have demonstrated that even if an interconnected-porous HAp functions as a bioactive and osteoconductive scaffold for bone ingrowth [11, 12], the osteoinductivity of a BMP-2/synthetic biodegradable polymer/HAp composite at an ectopic site is affected by the release profile of BMP-2 from the composite [35]. It is conceivable that the osteoinductivity of BMP-2 released plays a major role in inducing ectopic bone formation much more efficiently than the inherent osteoconductivity of HAp. However, in this study, *in vivo* retention of BMP-2 was not changed by the content of ß-TCP incorporation (Figure 4-2). Taken together, it is likely that the *in vivo* deformation of scaffolds was one factor contributing to the osteoinduction extent of BMP-2-incorporated scaffolds, although the bioactivity remaining for BMP-2

released and the osteoconductivity are not compared quantitatively among different scaffolds.

There have been many reports on the polymer/bioceramics composites, such as collagen/hydroxyapatite, collagen/hydroxyapatite/polylactide, chitosan/gelatin/tricalcium phosphate, collagen/tricalcium phosphate, and gelatin/tricalcium phosphate, for the scaffold of bone tissue engineering. Most of the reports demonstrate the osteoconductivity of the composites from the *in vitro* osteogenic culture and the animal experiment of bone defects [23-28]. On the other hand, some research groups have investigated the osteoinduction of BMP-incorporating composites for different animal models [29-35]. However, little has been investigated about the effect of the bioceramic content on the osteoinduction activity. Various methods have been developed to fabricate polymer/bioceramics composites, such as co-precipitation of hydroxyapatite and collagen in an aqueous collagen solution, hydroxyapatite deposition onto the pore surface of a collagen sponge, and simple mixing hydroxyapatite particles with a polymer solution. Since the characteristics of the composites greatly depend on the fabrication methods, it is difficult to directly compare the present data from the results reported. For example, Kaito et al. fabricated the lactide-co-ethylene glycol copolymer/hydroxyapatite composite incorporating BMP by simple coating of BMP/polymer mixture onto the porous hydroxyapatite block [35]. Asahina et al. implanted hydroxyapatite granules or block with BMP/collagen mixture into a mandible bone defect of monkey [30]. In these studies, the hydroxyapatite scaffold can keep the porous structure for bone formation, while the mixture of BMP and polymer enhances bone formation in the scaffold. On the other hand, Hu et al. reported BMP-incorporated polylactide scaffold containing the precipitate of collagen and hydroxyapatite [32, 33]. It is possible that polylactide functions as a binder material to keep the composite structure. Since the degradation of polylactide is much slower than that of gelatin, it is conceivable that the hydroxyapatite composite with polylactide binder seems to be more stable than that with gelatin binder. The *in vivo* stability of the sponges used in this study depends on the gelatin mass of binder, while the binder mass decreased with an increased in the ß-TCP content. Taken together, it is possible that the pore structure of scaffolds with the higher ß-TCP contents does not maintain due to the faster loss of gelatin mass, resulting in a reduction of the intrasponge space necessary for osteoinduction in

gelatin-ß-TCP scaffolds.

Simple foaming of gelatin solution enabled us to prepare the gelatin scaffold of sponge structure not only to induce *in vivo* infiltration of cells from the surrounding tissues, but also to facilitate *in vitro* cell seeding. We have demonstrated that the attachment, proliferation, and osteogenic differentiation of mesenchymal stem cells (MSC) were influenced by the sponge composition of gelatin and ß-TCP as the cell scaffold [48]. The balance between the cell density of scaffold and the bioactivity of ß-TCP may contribute to the extent of MSC differentiation in the sponge. Indeed the osteoinductive activity without cell seeding decreases with the increased ß-TCP content. However, combination of cell seeding technique and the delivery system of osteoinductive growth factor could mimic naturally-occurring bone matrix system which provides a favorable environment for osteoinduction, resulting in facilitating *in vivo* osteoinduction for bone regeneration.

In conclusion, gelatin scaffolds incorporating various amounts of β-TCP with an average pore size of 180-200 μm were fabricated. The extent of the *in vivo* BMP-2 remaining was similar for gelatin scaffolds with different β-TCP contents, although the osteoinduction of gelatin-β-TCP scaffolds incorporating BMP-2 was affected by the β-TCP content. Since the gelatin-β-TCP scaffold collapsed easier than the gelatin scaffold without β-TCP incorporation under a proteolytic condition, the maintenance of the intrasponge space necessary for the osteoinduction is one factor contributing to the osteoinduction extent of BMP-2-incorporating scaffolds. The present findings will give fundamental information to design the osteoinductive scaffold for bone tissue engineering in terms of bone cell scaffold and growth factor delivery system.

REFERENCES

1. R. Langer, and J. P. Vacanti, Tissue Engineering, *Science*, **260**, 920-926 (1993).
2. H. Petite, V. Viateau, W. Bensaid, A. Meunier, C. de Pollak, M. Bourguignon, K. Oudina, L. Sedel, and G. Guillemin, Tissue-engineered bone regeneration, *Nat. Biotechnol.*, **18**, 959-963 (2000).
3. J. R. Lieberman, A. Daluiski, and T. A. Einhorn, The role of growth factors in the repair of bone. biology and clinical applications, *J. Bone Joint Surg.*, **84-A**, 1032-1044 (2002).
4. A. H. Reddi, Bone morphogenetic proteins: from basic science to clinical applications, *J. Bone Joint Surg.*, **83-A (Suppl. 1, Part 1)**, S1-6 (2001).
5. S. A. Gittens, and H. Uludag, Growth factor delivery for bone tissue engineering, *J. Drug Target.*, **9**, 407-429 (2001).
6. D. Zekorn, Intravascular retention, dispersal, excretion and break-down of gelatin plasma substitutes, *Bibl. Haematol.*, **33**, 131-140 (1969).
7. M. Yamamoto, Y. Takahashi, and Y. Tabata, Controlled release by biodegradable hydrogels enhances the ectopic bone formation of bone morphogenetic protein, *Biomaterials*, **24**, 4375-4383 (2003).
8. L. Bordenave, J. Caix, B. Basse-Cathalinat, C. Baquey, D. Midy, J. C. Baste, and H. Constans, Experimental evaluation of a gelatin-coated polyester graft used as an arterial substitute, *Biomaterials*, **10**, 235-242 (1989).
9. R. Warocquier-Clerout, Y. S. Lee, J. Penhoat, and M. F. Sigot-Luizard, Comparative behaviour of L-929 fibroblastic and human endothelial cells onto crosslinked protein substrates, *Cytotechnology*, **3**, 259-269 (1990).
10. Z. Ma, C. Gao, Y. Gong, J. Ji, and J. Shen, Immobilization of natural macromolecules on poly-L-lactic acid membrane surface in order to improve its cytocompatibility, *J. Biomed. Mater. Res.*, **63**, 838-847 (2002).

11. C. J. Damien, and J. R. Parsons, Bone graft and bone graft substitutes: a review of current technology and applications, *J. Appl. Biomat.*, **2**, 187-208 (1991).

12. T. W. Bauer, and S. T. Simth, Bioactive materials in orthopaedic surgery: overview and regulatory considerations, *Clin. Orthop. Rel. Res.*, **395**, 11-22 (2002).

13. Z. Yang, H. Yuan, W. Tong, P. Zou, W. Chen, and X. Zhang, Osteogenesis in extraskeletally implanted porous calcium phosphate ceramics: variability among different kinds of animals, *Biomaterials*, **17**, 2131-2137 (1996).

14. C. Knabe, F. C. Driessens, J. A. Planell, R. Gildenhaar, G. Berger, D. Reif, R. Fitzner, R. J. Radlanski, and U. Gross, Evaluation of calcium phosphates and experimental calcium phosphate bone cements using osteogenic cultures, *J. Biomed. Mater. Res.*, **52**, 498-508 (2002).

15. H. Yuan, Y. Li, J. D. de Bruijn, K. de Groot, and X. Zhang, Tissue responses of calcium phosphate cement: a study in dogs, *Biomaterials*, **21**, 1283-1290 (2000).

16. M. H. Mankani, S. A. Kuznetsov, B. Fowler, A. Kingman, P. G. Robey, *In vivo* bone formation by human bone marrow stromal cells: effect of carrier particle size and shape, *Biotechnol. Bioeng.*, **72**, 96-107 (2001).

17. E. M. Erbe, J. G. Marx, T. D. Clineff, and L. D. Bellincampi, Potential of an ultraporous beta-tricalcium phosphate synthetic cancellous bone void filler and bone marrow aspirate composite graft, *Eur. Spine J.*, **10 (Suppl 2)**, S141-146 (2001).

18. T. Livingston, P. Ducheyne, and J. Garino, *In vivo* evaluation of a bioactive scaffold for bone tissue engineering, *J. Biomed. Mater. Res.*, **62**, 1-13 (2002).

19. J. S. Boo, Y. Yamada, Y. Okazaki, Y. Hibino, K. Okada, K. Hata, T. Yoshikawa, Y. Sugiura, and M. Ueda, Tissue-engineered bone using mesenchymal stem cells and a biodegradable scaffold, *J. Craniofac. Surg.*, **13**, 231-239 (2002).

20. P. Kasten, R. Luginbuhl, M. van Griensven, T. Barkhausen, C. Krettek, M. Bohner, and U. Bosch, Comparison of human bone marrow stromal cells seeded on calcium-deficient hydroxyapatite, beta-tricalcium phosphate and demineralized bone matrixm, *Biomaterials*, **24**, 2593-2603 (2003).

21. H. Shimaoka, Y. Dohi, H. Ohgushi, M. Ikeuchi, M. Okamoto, A. Kudo, T. Kirita, and K. Yonemasu, Recombinant growth/differentiation factor-5 (GDF-5) stimulates osteogenic differentiation of marrow mesenchymal stem cells in porous hydroxyapatite ceramic, *J. Biomed. Mater. Res.*, **68A**, 168-176 (2004).

22. P. Q. Ruhe, H. C. Kroese-Deutman, J. G. Wolke, P. H. Spauwen, and J. A. Jansen, Bone inductive properties of rhBMP-2 loaded porous calcium phosphate cement implants in cranial defects in rabbits, *Biomaterials*, **25**, 2123-2132 (2004).

23. A. A. Ignatius, M. Ohnmacht, L. E. Claes, J. Kreidler, and F. Palm, A composite polymer/tricalcium phosphate membrane for guided bone regeneration in maxillofacial surgery, *J. Biomed. Mater. Res.*, **58**, 564-569 (2001).

24. C. T. Laurencin, M. A. Attawia, L. Q. Lu, M. D. Borden, H. H. Lu, W. J. Gorum, and J. R. Lieberman, Poly(lactide-co-glycolide)/hydroxyapatite delivery of BMP-2-producing cells: a regional gene therapy approach to bone regeneration, *Biomaterials*, **22**, 1271-1277 (2001).

25. C. Du, F. Z. Cui, X. D. Zhu, and K. de Groot, Three-dimensional nano-HAp/collagen matrix loading with osteogenic cells in organ culture, *J. Biomed. Mater. Res.*, **44**, 407-415 (1999).

26. S. Itoh, M. Kikuchi, Y. Koyama, K. Takakuda, K. Shinomiya, and J. Tanaka, Development of an artificial vertebral body using a novel biomaterial, hydroxyapatite/collagen composite, *Biomaterials*, **23**, 3919-3926 (2002).

27. C. V. Rodrigues, P. Serricella, A. B. Linhares, R. M. Guerdes, R. Borojevic, M. A. Rossi, M. E. Duarte, and M. Farina, Characterization of a bovine collagen-hydroxyapatite composite scaffold for bone tissue engineering, *Biomaterials*, **24**, 4987-4997 (2003).

28. D. Lickorish, J. A. Ramshaw, J. A. Werkmeister, V. Glattauer, and C. R. Howlett, Collagen-hydroxyapatite composite prepared by biomimetic process, *J. Biomed. Mater. Res.*, **68A**, 19-27 (2004).

29. A. Kamegai, N. Shimamura, K. Naitou, K. Nagahara, N. Kanematsu, and M. Mori, Bone formation under the influence of bone morphogenetic protein/self-setting apatite cement composite as a

delivery system, *Biomed. Mater. Eng.*, **4**, 291-307 (1994).

30. I. Asahina, M. Watanabe, N. Sakurai, M. Mori, and S. Enomoto, Repair of bone defect in primate mandible using a bone morphogenetic protein (BMP)-hydroxyapatite-collagen composite, *J. Med. Dent. Sci.*, **44**, 63-70 (1997).

31. T. Tuominen, T. Jamsa, J. Oksanen, J. Tuukkanen, T. J. Gao, T. S. Lindholm, and P. Jalovaara, Composite implant composed of hydroxyapatite and bone morphogenetic protein in the healing of a canine ulnar defect, *Ann. Chir. Gynaecol.*, **90**, 32-36 (2001).

32. Y. Hu, C. Zhang, S. Zhang, Z. Xiong, J. Xu, Development of a porous poly(L-lactic acid)/hydroxyapatite/collagen scaffold as a BMP delivery system and its use in healing canine segmental bone defect, *J. Biomed. Mater. Res.*, **67A**, 591-598 (2003).

33. Y. Y. Hu, C. Zhang, R. Lu, J. Q. Xu, and D. Li, Repair of radius defect with bone-morphogenetic-protein loaded hydroxyapatite/collagen-poly(L-lactic acid) composite, *Chin. J. Traumatol.*, **6**, 67-74 (2003).

34. S. S. Liao, K. Guan, F. Z. Cui, S. S. Shi, and T. S. Sun TS, Lumbar spinal fusion with a mineralized collagen matrix and rhBMP-2 in a rabbit model, *Spine*, **28**, 1954-1960 (2003).

35. T. Kaito, A. Myoui, K. Takaoka, N. Saito, M. Nishikawa, N. Tamai, H. Ohgushi, and H. Yoshikawa, Potentiation of the activity of bone morphogenetic protein-2 in bone regeneration by a PLA-PEG/hydroxyapatite composite, *Biomaterials*, **26**, 73-79 (2005).

36. K. Matsuda, S. Suzuki, N. Isshiki, K. Yoshioka, T. Okada, and Y. Ikada, Influence of glycosaminoglycans on the collagen sponge component of a bilayer artificial skin, *Biomaterials*, **11**, 351-355 (1990).

37. G. Chen, T. Ushida, and T. Tateishi, A biodegradable hybrid sponge nested with collagen microsponges, *J. Biomed. Mater. Res.*, **51**, 273-279 (2000).

38. F. C. Greenwood, W. M. Hunter, and T. C. Gglover, The preparation of ^{131}I-labeled human growth hormone of high specific radioactivity, *Biochem. J.*, **89**, 114-123 (1963).

39. D. Kobayashi, H. Takita, M. Mizuno, Y. Totsuka, and Y. Kuboki, Time-dependent expression of

bone sialoprotein fragments in osteogenesis induced by bone morphogenetic protein, *J. Biochem.*, **119**, 475-481 (1996).

40. Y. Tabata, Tissue regeneration based on growth factor release, *Tissue Eng.*, **9 (Suppl. 1)**, S5-15 (2003).

41. K. Kawai, S. Suzuki, Y. Tabata, Y. Ikada, and Y. Nishimura, Accelerated tissue regeneration through incorporation of basic fibroblast growth factor-impregnated gelatin microspheres into artificial dermis, *Biomaterials*, **21**, 489-499 (2000).

42. J. J. Klawitter, and S. F. Hulbert, Application of porous ceramics for the attachment of load bearing internal orthopedic applications, *J. Biomed. Mater. Res. Sympo.*, **2**, 161-229 (1971).

43. B. P. Robinson, J. O. Hollinger, E. H. Szachowicz, and J. Brekke, Calvarial bone repair with porous D,L-polylactide, *Otolaryngol. Head Neck Surg.*, **112**, 707-713 (1995).

44. M. R. Urist, A. Lietze, and E. Dawson, β-tricalcium phosphate delivery system for bone morphogenetic protei, *Clin. Orthop. Rel. Res.*, **187**, 277-280 (1984).

45. C. P. A. T. Klein, A. A. Driessen, K. de Groot, and A. van den Hooff, Biodegradation behavior of various calcium phosphate materials in bone tissue, *J. Biomed. Mater. Res.*, **17**, 769-784 (1983).

46. M. Yamamoto, K. Kato, and Y. Ikada, Effect of the structure of bone mophogenetic protein carriers on ectopic bone regeneration, *Tissue Eng.*, **2**, 315-326 (1996).

47. J. M. Wozney, and V. Rosen, Bone morphogenetic protein and bone morphogenetic protein gene family in bone formation and repair, *Clin. Orthop. Rel. Res.*, **346**, 26-37 (1998).

48. Y. Takahashi, M. Yamamoto, and Y. Tabata, Osteogenic differentiation of mesenchymal stem cells in biodegradable sponges composed of gelatin and β-tricalcium phosphate, *Biomaterials*, **26**, 3587-3596 (2005).

PART II

OSTEOGENIC DIFFERENTIATION AND BONE REGENERATION OF MSC COMBINED WITH DIFFERENT SCAFFOLDS

Chapter 5

Homogeneous seeding of MSC into non-woven fabric for bone regeneration

INTRODUCTION

The objective of tissue engineering is to induce tissue regeneration for the repairing of damaged or lost tissues and to substitute the biological functions of injured organs by making use of cells with high proliferation and differentiation potential. To prepare cells for tissue engineering applications, it is important to expand *in vitro* cells isolated from a small biopsy of body tissue. The cells are then seeded onto a scaffold to allow further proliferation and differentiation *in vitro* and the cell–scaffold construct is transplanted into the body defect for tissue regeneration and repair.

Mesenchymal stem cells (MSC), which are readily isolated from bone marrow, have attracted much attention for tissue engineering because they are able to proliferate and have the inherent potential to differentiate into the cell lineage of various types, for example, bone, cartilage, muscle, tendon, and other connective tissues. Many research trials have been reported to induce tissue regeneration by use of MSC or their combination with scaffolds and culturing [1-5]. It is important for the formation of MSC–scaffold constructs not only to design an appropriate scaffold but also to develop the appropriate culturing technology, such as the cell-seeding method.

Because the cell-seeding method greatly affects the structural and biological integrity of cell–scaffold constructs, it is essential for successful tissue regeneration to optimize the seeding process. The spatially uniform distribution of cells attached inside the scaffold, and their high density and good cellularity, are required to effectively induce tissue regeneration based on the cell–scaffold construct. It has been demonstrated that the nonuniform distribution of seeded cells and poor cellularity resulted in

inferior preparation of tissue constructs [6-8].

The objective of this chapter was to optimize the conditions for a cell-seeding method involving agitation. Cell attachment to non-woven fabric was evaluated in terms of agitation speed, culture vessel shape, and volume of culture medium. Distribution of cells seeded inside the fabric was investigated and compared with the conventional static seeding method, and cell damage was evaluated.

EXPERIMENTAL

MSC isolation and culture

Mesenchymal stem cells (MSC) were isolated from the bone shaft of femurs of 3-week-old male Fischer 344 rats according to a technique reported by Lennon et al [9]. Briefly, both ends of each rat femur were cut away from the epiphysis, and the marrow was flushed out by expulsion of 1 ml of Dulbecco's modified Eagle's minimum essential medium (DMEM), supplemented with 15 % fetal calf serum and antibiotics (penicillin–streptomycin solution, 50 U/ml), from a syringe through a 21-gauge needle. The cell suspension was collected in two 25-cm^2 flasks (Iwaki Glass, Funabashi, Chiba, Japan), each containing 5 ml of medium. The medium was changed after the initial 3 days of culture and every 3 days thereafter. When the first-passage cells became subconfluent, usually 7–10 days after seeding, the cells were detached from the flasks by treatment for 5 min at 37°C with a solution of 0.25 % trypsin and 0.02 % EDTA in 100 mM phosphate-buffered saline solution (PBS, pH 7.4). Cells were normally subcultured at a density of 2×10^4 cells/cm^2. Second-passage cells at subconfluence were used in all the experiments.

Preparation of non-woven fabrics

Non-woven fabric (3 mm thick; fiber density, 177 g/m^2) prepared from polyethylene terephthalate (PET) fiber, 12 μm in diameter, was kindly supplied by Toray (Shiga, Japan). The porosity was approximately 94 %. The PET non-woven fabric was punched out into 6-mm-diameter disks. The 6-mm disks were prewetted with aqueous ethanol solution (70 vol%) for 30 min to sterilize and enhance their water uptake, and completely rinsed twice with PBS and twice with culture medium for 1 hr each to remove ethanol.

Cell seeding into non-woven fabrics

Two different methods (static and agitation) were used to seed MSC onto PET non-woven fabric, based on a technique reported previously [10]. For the static seeding method, 50 or 200 μl of a cell suspension ($5\times10^5 - 2\times10^8$ cells/ml) was poured onto non-woven fabric in the wells of culture plates (Iwaki Glass) or in 50-ml tubes (Iwaki Glass). For the agitation seeding method, 50 or 200 μl of a cell suspension ($5\times10^5 - 2\times10^8$ cells/ml) and non-woven fabric were placed in the wells of culture plates or in 50-ml tubes on an orbital shaker (Bellco Glass, Vineland, NJ) and agitated at 100–300 rpm for 6 hr. In both methods, the cell-seeded non-woven fabrics were thoroughly washed with PBS to exclude nonadherent cells and subjected to the following analytical assays.

DNA assay

The number of cells attached to non-woven fabric was determined by fluorometric quantification of cell DNA according to the assay reported by Rao and Otto [11]. Briefly, cell-seeded non-woven fabric samples were washed with PBS and stored at 230 °C until assayed. After thawing the samples, they were digested in a buffer solution (pH 7.4) containing proteinase K (0.5 mg/ml) sodium dodecyl sulfate (0.2 mg/ml), and 30 mM sodium citrate–buffered saline solution (SSC) at 55 °C for 12 hr

with occasional mixing. Each enzyme-digested sample (100 μl) was mixed with SSC buffer (400 μl) in a glass tube. After mixing with a dye solution (500 μl; composition: 30 mM SSC, Hoechst 33258 dye [1 μg/ml]), the fluorescence intensity of mixed solution was measured in a fluorescence spectrometer (F-2000; Hitachi, Tokyo, Japan) at excitation and emission wavelengths of 355 and 460 nm, respectively. The calibration curve between the DNA and cell number was prepared by use of cell suspensions with different cell densities. The DNA assay was done three times, independently, for every experimental sample unless otherwise mentioned.

SEM observation of cells attached to non-woven fabrics

Cell-attached non-woven fabric samples, and 6 hr of seeding, were fixed in 10 wt% neutral-buffered formalin solution until ready for embedding. The fixed fabric samples were conventionally dehydrated in sequentially increasing ethanol solutions to 100 vol% ethanol, immersed in xylene, and embedded in paraffin. The samples were sectioned (thickness, 4 μm) and stained with hematoxylin and eosin (HE) to visualize the attachment and distribution of cells inside the fabric. The sample sections were viewed by light microscopy (AX-80; Olympus, Tokyo, Japan) to take their pictures (12 pictures per sample). Every section picture was mechanically divided into three regions (upper, middle, and lower) and the number of cells present in each region was counted.

Histological evaluation of cells attached to non-woven fabrics

The cell-attached non-woven fabrics after 6 hr seeding were fixed in 10 wt% neutral-buffered folmalin solution until ready for embedding. The fixed fabric samples were conventionally dehydrated in sequentially increasing ethanol solutions to 100 vol% ethanol, immersed in xylene, and embedded in paraffin. The samples were sectioned at 4 μm thickness and stained by hematoxylin and eosin (HE) to visualize the attachment and distribution of cells inside the fabric. The sample sections were viewed on a

microscopy (AX-80, Olympus, Tokyo, Japan) to take their pictures (12 pictures/sample). Every section picture was mechanically divided into three regions of upper, middle, and lower, and the number of cells present in each region was counted.

Measurement of LDH activity and medium pH

The extent of cell damage and death during the seeding process was assessed by measuring lactate dehydrogenase (LDH) levels and pH of the medium of samples using a commercial kit (Wako Pure Chemical, Osaka, Japan) and a pH meter (Shindengen Electric Manufacturing, Tokyo, Japan), respectively.

Statistical analysis

All the data were analyzed by Fisher's LSD test for multiple comparison and the statistical significance was accepted at $p < 0.05$. Experimental results were expressed as the means ± the standard deviation of the mean.

RESULTS

Cell attachment to non-woven fabrics

Figure 5-1 shows cell attachment to non-woven fabric after cell seeding by the static or agitation seeding method. The number of cells attached to non-woven fabric by the static seeding method seemed to be low compared with that produced by the agitation seeding method in the larger volume of cell suspension (200 μl), irrespective of the shape of the culture vessel. For the agitation seeding method, more cells were attached to fabric in the tubes than to the wells of culture plates.

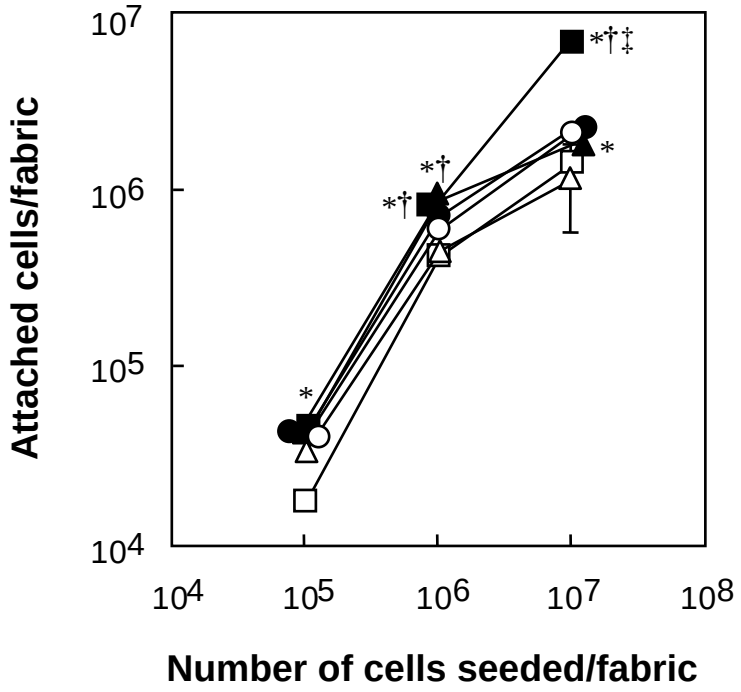

Figure 5-1. Number of cells attached to non-woven fabric as a function of cell number in the seeding solution 6 hr after cell seeding by the static method (open symbols) or by the agitation method (300 rpm) (solid symbols). The matrix was incubated in a culture plate containing medium (50 μl: ○, ●; 200 μl: △, ▲) or in a tube containing 200 μl of medium (□, ■). $^{*}p < 0.05$, significant against cells attached to non-woven fabric after cell seeding by the static method (0 rpm) in the corresponding culture type; $^{\dagger}p < 0.05$, significant against cells attached to non-woven fabric after cell seeding by the agitation method (300 rpm) in a culture plate contained 50 μl of medium; $^{\ddagger}p < 0.05$, significant against cells attached to non-woven fabric after cell seeding by the agitation method (300 rpm) in a culture plate containing 200 μl of medium.

Effect of agitation speed on cell attachment

Figure 5-2 shows the effect of agitation speed on cell attachment to non-woven fabric. The number of cells attached to non-woven fabric increased with an increase in rotating speed for the agitation seeding method in the larger volume of cell suspension (200 μl). No significant difference in the extent of cell attachment was seen with the cell suspension in a volume of 50 μl at the high rotating speed.

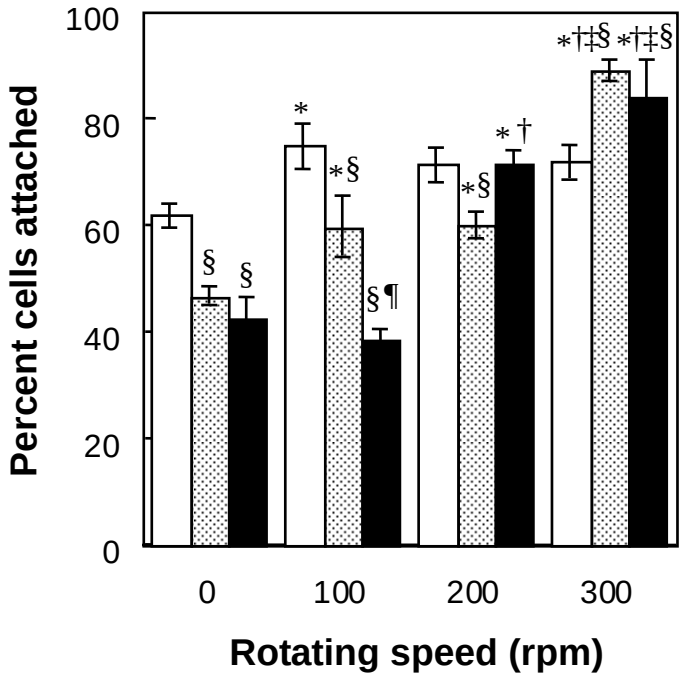

Figure 5-2. Effect of agitation speed on cell attachment to non-woven fabric 6 hr after cell seeding by the static method (0 rpm) or by the agitation method. The number of cells in the seeding solution was 10^6 cells per fabric. Fabric was incubated in a culture plate containing medium (50 μl, □; 200 μl, ⊡) or in a culture tube containing 200 μl of medium (■). $^{*}p < 0.05$, significant against percentage of cells attached at a rotating speed of 0 rpm in the corresponding culture type; $^{\dagger}p < 0.05$, significant against percentage of cells attached at a rotating speed of 100 rpm in the corresponding culture type; $^{\ddagger}p < 0.05$, significant against percentage of cells attached at a rotating speed of 200 rpm in the corresponding culture type; $^{\S}p < 0.05$, significant against percentage of cells attached in a culture plate containing 50 μl medium and rotated at the same speed; $^{\P}p < 0.05$, significant against percentage of cells attached to a culture plate containing 200 μl medium and rotated at the same speed.

SEM of cell attached non-woven fabrics under various cell culture conditions

Figure 5-3 shows scanning electron micrographs of cross-sections of non-woven fabric 6 hr after MSC seeding by the static or agitation seeding method. When middle portions of fabric samples were compared, the cell density was higher for the agitation seeding method than for the static seeding method in the case of tube culture. On the other hand, cells did not distribute to the middle portion of fabric samples in the wells of culture plates. Much higher cell density was observed by culturing cells in tubes rather than in the wells of culture plates.

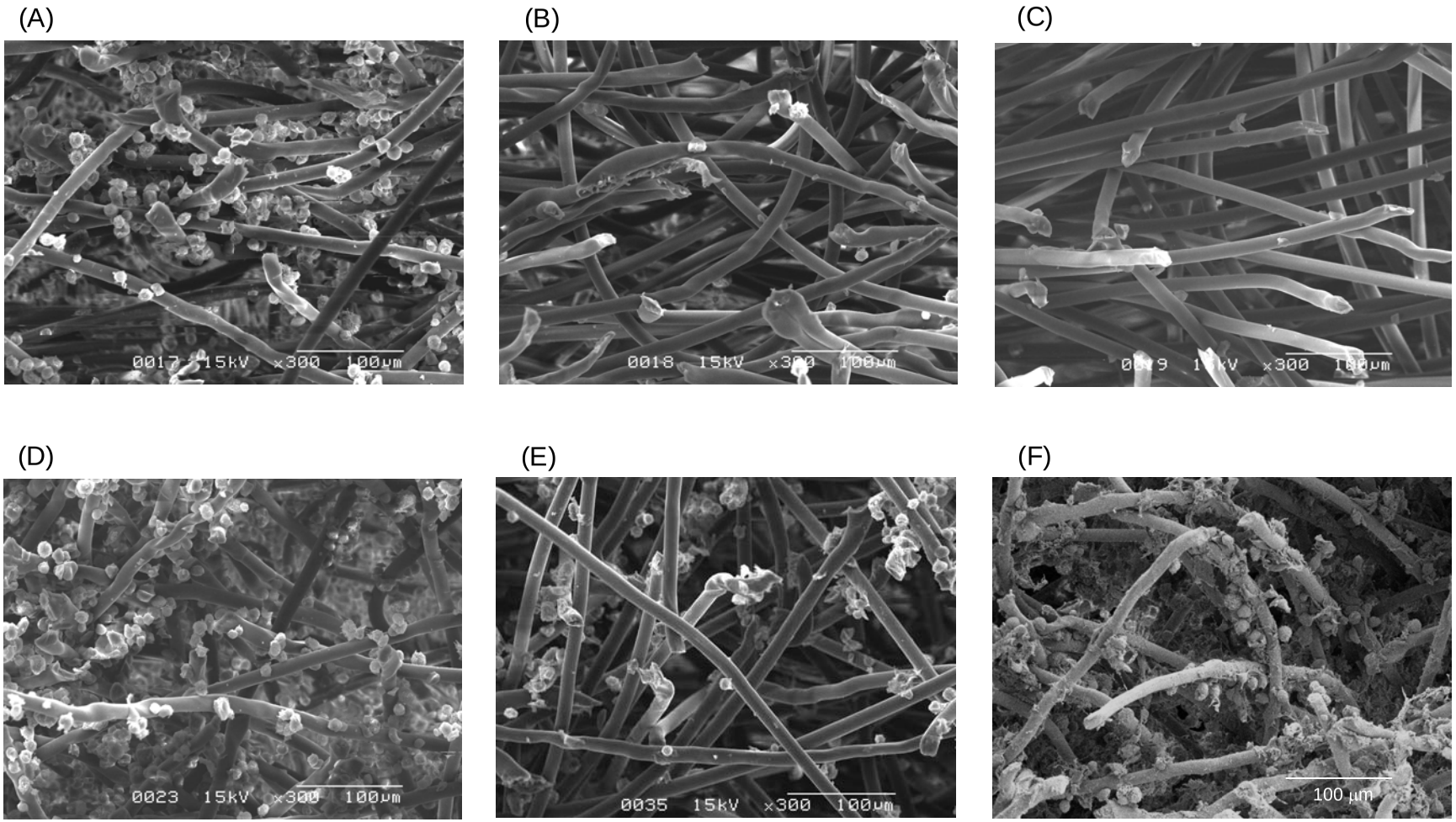

Figure 5-3. Scanning electron micrographs of cells attached to non-woven fabric, taken 6 hr after cell seeding by the static method (A-C) or by the agitation method (300 rpm) (D-F). The number of cells in the seeding solution was 10^7 cells per fabric. Fabric was incubated in a culture plate containing medium (50 μl, A and D; 200 μl, B and E) or in a culture tube containing 200 μl of medium (C and F).

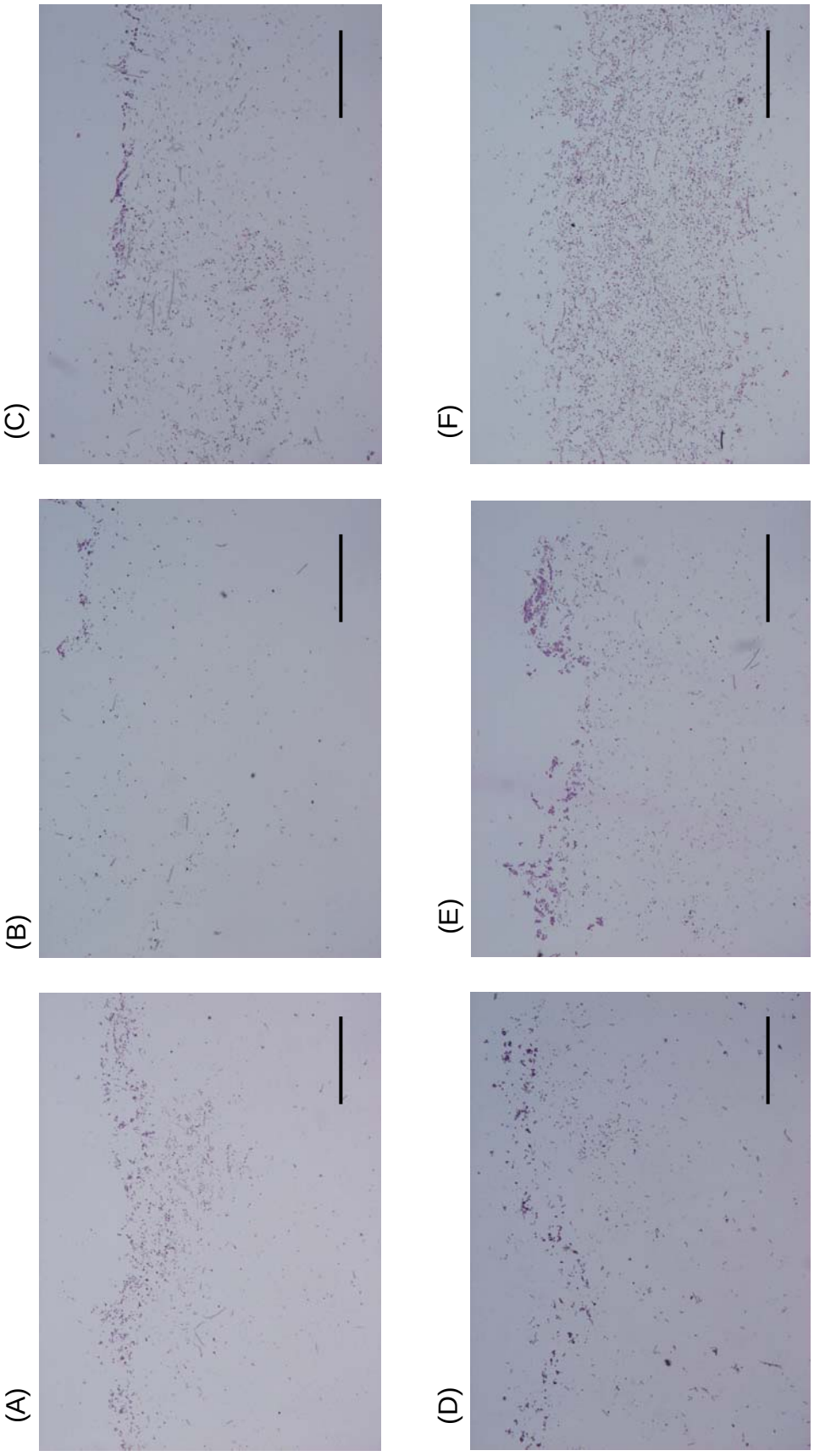

Figure 5-4. Histological sections of cells attached to non-woven fabric, taken 6 hr after cell seeding by the static method (A-C) or by the agitation seeding method (300 rpm) (D-F). Fabric was incubated in a culture plate containing medium (50 µl, A and D; 200 µl, B and E) or in a culture tube containing 200 µl of medium (C and F). The bar length is 1 mm.

Cell distribution to non-woven fabrics

Figure 5-4 shows histological sections of cells attached to non-woven fabric 6 hr after cell seeding by the static or agitation seeding method. Similarly in Figure 5-3, the number of cells adherent to non-woven fabric by the agitation seeding method tended to be high compared with that produced by the static seeding method in the case of tube culture with a larger volume of cell suspension. No significant difference in number of cells attached to non-woven fabric was seen with the small volume (50 μl), irrespective of the seeding method. In the case of agitation seeding, the cells uniformly distributed throughout the non-woven matrix under the culture conditions in culture tubes.

Figure 5-5 shows the distribution of cells attached to non-woven fabric. The number of cells attached by static seeding to non-woven fabric was small compared with that produced by agitation seeding. Irrespective of the seeding method, on culture plates cells distributed mainly onto the upper layer of non-woven fabric; fewer cells were detected in the middle and lower layers of the non-woven fabric. On the other hand, agitation cell-seeding method combined with the use of culture tubes enabled cells to adhere at high density and distribute homogeneously throughout every layer of the fabric.

Metabolism of cells cultured by the static and agitated seeding methods

Figure 5-6A shows the LDH leakage of cells after cell seeding of non-woven fabric by the static or agitation seeding method. LDH leakage increased with incubation time for both cell-seeding methods, but leakage associated with the agitation seeding method was lower than that with the static seeding method. Figure 5-6B shows the pH of culture medium after cell seeding of non-woven fabric by both cell seeding methods. The medium pH of cells cultured by the static seeding method decreased compared with that of the agitation seeding method. Irrespective of the culture vessel type, the decrease in pH value of cells cultured at a suspension volume of 200 μl was significantly larger than that of the other culture

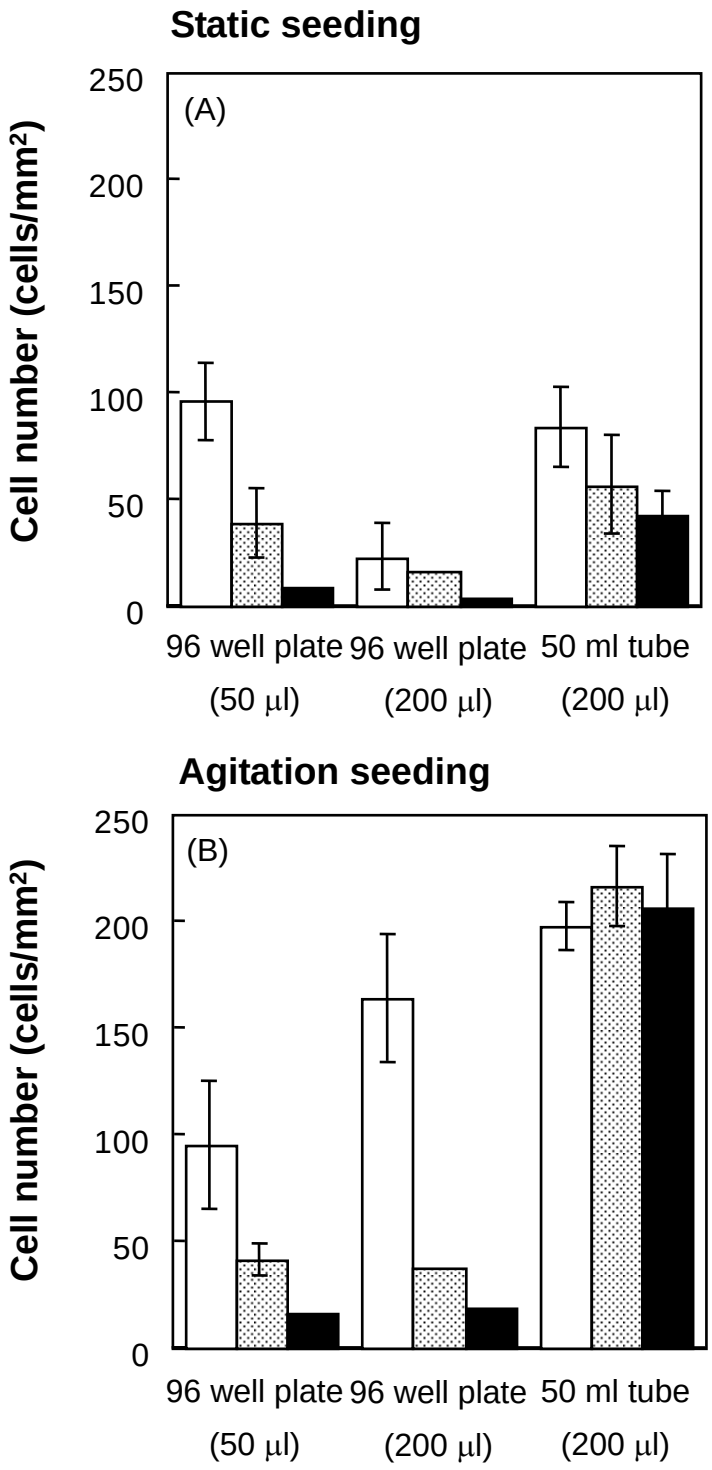

Figure 5-5. Distribution of cells attached to non-woven fabric 6 hr after cell seeding by the static method (A) or by the agitation seeding method (300 rpm) (B). Cells were counted in the upper (□), middle (▨), and lower (■) layers of non-woven fabric.

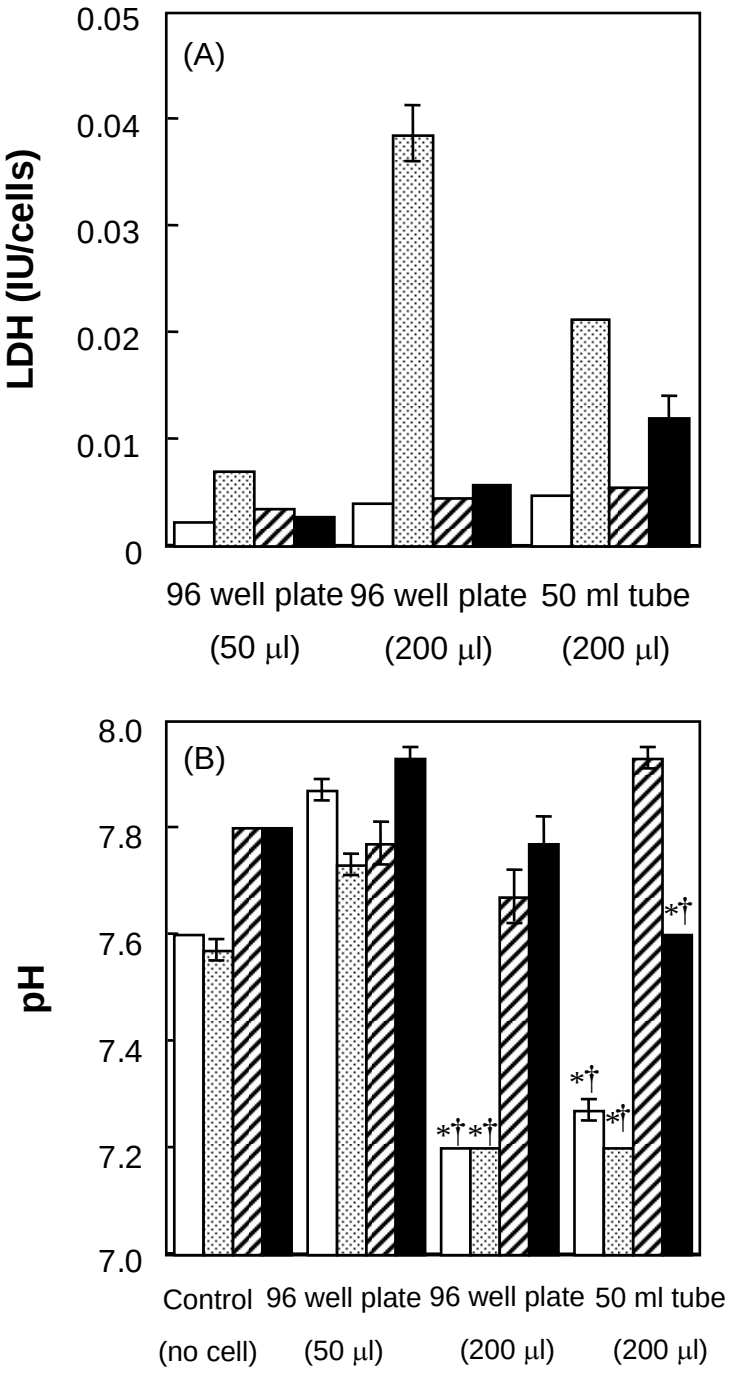

Figure 5-6. LDH leakage of cells (A) and pH of culture medium (B) 6 hr after seeding of non-woven fabric by the static method (□ and ⬚) or by the agitation method (300 rpm) (▨ and ■). The number of cells in the seeding solution was 10^6 cells per fabric. Cell culture was done for 6 hr (□ and ▨) and 24 hr (⬚ and ■). $^{*}p < 0.05$, significant against the pH value of the control group; $^{\dagger}p < 0.05$, significant against the pH value of cells cultured in a suspension volume of 50 μl.

DISCUSSION

From the viewpoint of tissue engineering to enable cells to form a three-dimensional tissue construct, it is important that the cells be attached throughout the scaffold at high density and homogeneously inside the scaffold. Some research has been performed on cell-seeding methods to improve the manner of cell attachment onto scaffolds. Various seeding methods have been tried to investigate cell attachment to various scaffolds: the pouring of cell suspension onto scaffolds [12-14], the injection of cell suspension with a syringe [15], and the seeding of cell suspension to scaffolds in spinner flasks [16-18] and in a perfusion culture system[19, 20]. Kim et al. have reported that the number of cells attached to a scaffold was enhanced with an agitation cell-seeding method, wherein the scaffold is agitated in the cell suspension [21]. There is no doubt that the proposed methods improved cell attachment and growth, but little care was taken concerning cell distribution and cellularity inside the scaffold.

This chapter demonstrates that the agitation cell seeding method enhanced the number of cells attached to a scaffold of non-woven fabric and enabled cells to distribute more homogeneously throughout the scaffold compared with the static cell-seeding method. This enhanced cell attachment depended on the seeding conditions, such as the volume of cell suspension, the rotating speed, and the culture time. These findings were similar to those reported previously [21]. However, it should be noted that the cell distribution is also greatly influenced by the culture conditions and became homogeneous on use of optimal conditions. First, the volume of cell suspension should be larger than that of the scaffold. It is necessary for homogeneous cell distribution that the cell suspension be allowed to agitate around the scaffold. This is why culture tubes are much superior to culture plates in making the cell distribution more homogeneous (Figure 5-5). On the other hand, with culture plates it would be impossible for cells to infiltrate the scaffold from the surrounding medium because the diameter of each culture well was similar to that of the scaffold, and there was no additional room around the scaffold. In the tube cultures, the cell suspension

was always present around the scaffold. As a result, it is likely that the cells readily diffused into the scaffold uniformly. Second, the agitation must be strong enough to keep the cell suspension uniform. If cells sediment during the agitation seeding, homogeneous cell attachment will not be achieved. Uniformity of cell suspension was achieved when the rotating speed was at 250 rpm or higher (data not shown).

LDH leakage as an index of cell damage and death was lower with agitation seeding than with static seeding (Figure 5-6). A decrease in the pH of the culture medium results mainly from the production of wastes, such as lactate, generated by cell metabolism [22]. A lower pH of cells seeded by the static seeding method can be partially explained in terms of waste accumulation. Under static conditions, it is possible that the wastes generated by cells are accumulated in the fabric without being diffused out, because of the lack of motion of the culture medium. This medium stagnation also causes low in-diffusion of fresh medium. Consequently, the reduced metabolic activity would result in increased LDH leakage and decreased medium pH. On the other hand, superior out-diffusion and in-diffusion of culture medium with the agitation method gave attached cells good culture conditions. In conclusion, timely and spatially optimized agitation seeding allows cells to homogeneously distribute into non-woven fabrics for tissue engineering.

REFERENCES

1. T. Yoshikawa, H. Ohgushi, and S. Tamai, Immediate bone forming capability of prefabricated osteogenic hydroxyapatite, *J. Biomed. Mater. Res.*, **32**, 481-492 (1996).
2. S. P. Bruder, N. Jaiswal, N. S. Ricalton, J. D. Mosca, K. H. Kraus, and S. Kadiyala, Mesenchymal stem cells in osteobiology and applied bone regeneration, *Clin. Orthop.*, **355S**, S247-265 (1998).
3. A. S. Goldstein, G. Zhu, G. E. Morris, R. K. Meszenyi, and A. G. Mikos, Effect of osteoblastic culture conditions on the structure of poly(DL-lactic-co-glycolic acid) form scaffolds, *Tissue Eng.*, **5,** 421-434 (1999).
4. H. A. Awad, D. L. Butler, M. T. Harris, R. E. Ibrahim, Y. Wu, R. G. Young, S. Kadiyala, and G. P. Boivin, *In vitro* characterization of mesenchymal stem cell-seeded collagen scaffolds for tendon repair: Effects of initial seeding density on contraction kinetics, *J. Biomed. Mater. Res.*, **51**, 233-240 (2000).
5. A. Bruinink, D. Siragusano, G. Ettel, T. Brandsberg, F. Brandsberg, M. Petitmermet, B. Muller, J. Mayer, and E. Wintermantel, The stiffness of bone marrow cell-knit composites is increased during mechanical load, *Biomaterials*, **22**, 3169-3178 (2001).
6. L. E. Freed, J. C. Marquis, G. Vunjak-Novakovic, J. Emmanual, and R. Langer, Composition of cell-polymer cartilage implants, *Biotechnol. Bioeng.*, **43**, 605-614 (1994).
7. T. Ma, Y. Li, S-T. Yang, D. A. Kniss, Tissue engineering human placenta trophoblast cells in 3-D fibrous matrix: spatial effects on cell proliferation and function, *Biotechnol. Prog.*, **15**, 715-724 (1999).
8. C. T. Holy, M. S. Shoichet, and J. E. Davies, Engineering three-dimensional bone tissue *in vitro* using biodegradable scaffolds: Investigating initial cell-seeding density and culture

period, *J. Biomed. Mater. Res.*, **51**, 376-382 (2000).

9. D. P. Lennon, S. E. Haynesworth, J. E. Dennis, and A. I. Caplan, A chemically defined medium supports *in vitro* proliferation and maintains the osteochondral potential of rat marrow-derived mesenchymal stem cells, *Exp. Cell Res.*, **219**, 211-222 (1995).

10. B. S. Kim, J. Nikolovski, J. Binadio, E. Smiley, and D. J. Mooney, Engineered smooth muscle tissues: regulating cell phenotype with the scaffold, *Exp. Cell Res.*, **251**, 318-328 (1999).

11. J. Rao, and W. R. Otto, Fluorimetric DNA assay for cell growth estimation, *Anal. Biochem.*, **207**, 186-192 (1992).

12. S. L. Ishaug-Riley, G. M. Crane-Kruger, M. J. Yaszemski, and A. G. Mikos, Three-dimensional culture of rat calvarial osteoblasts in porous biodegradable polymers, *Biomaterials*, **19**, 1405-1412 (1998).

13. C. E. Holy, M. S. Shoichet,, and J. E. Davies, Engineering three-dimensional bone tissue *in vitro* using biodegradable scaffolds: Investigating initial cell-seeding density and culture period, *J. Biomed. Mater. Res.*, **51**, 376-382 (2000).

14. H. A. Awad, D. L. Butler, M. T. Harris, R. E. Ibrahim, Y. Wu, R. G. Young, S. Kadiyala, and G. P. Boivin, *In vitro* characterization of mesenchymal stem cell-seeded collagen scaffolds for tendon repair: effects of initial seeding density on contraction kinetics, *J. Biomed. Mater. Res.*, **51**, 233-240 (2000).

15. S. Mizuno, F. Allemann, and J. Glowacki, Effects of medium perfusion on matrix production by bovine chondrocytes in three-dimensional collagen sponges, *J. Biomed. Mater. Res.*, **56**, 368-375 (2001).

16. Y. L. Xiao, J. Riesle, and C. A. Blitterswijk, Static and dynamic fibroblast seeding and cultivation in porous PEO/PBT scaffolds, *J. Materials Sci.*, **10**, 773-777 (1999).

17. K. J. Burg, W. D. Holder, C. R. Jr. Culberson, R. J. Beiler, K. G. Greene, A. B. Loebsack, W. D. Roland, P. Eiselt, D. J. Mooney, and C. R. Halberstadt, Comparative study of seeding methods for three-dimensional polymeric scaffolds, *J. Biomed. Mater. Res.*, **52**, 576 (2000).

18. A. Bruinink, D. Siragusano, G. Ettel, T. Brandsberg, F. Brandsberg, M. Petitmermet, B. Muller, J. Mayer, and E. Wintermantel, The stiffness of bone marrow cell-knit composites is increased during mechanical load, *Biomaterials*, **22**, 3169-3178 (2001).

19. K. P. Walluscheck, G. Steinhoff, and A. Haverich, Endothlial cell seeding of de-endothelialised human arteries: improvement by adhesion molecule induction and flow-seeding technology, *Eur. J. Endovascu. Surg.*, **12**, 46-53 (1996).

20. S. S. Kim, C. A. Sundback, S. Kaihara, M. S. Benvenuto, B. S. Kim, D. J. Mooney, and J. P. Vacanti, Dynamic seeding and *in vitro* culture of hepatocytes in a flow perfusion system, *Tissue Eng.*, **6**, 39-44 (2000).

21. B. S. Kim, A. J. Putnam, T. J. Kulik, and D. J. Mooney, Optimizing seeding and culture methods to engineer smooth muscle tissue on biodegradable polymer matrices. *Biotechnol. Bioeng.*, **57**, 46-54 (1998).

22. R. L. Carrier, M. Papadaki, M. Rupnick, F. J. Schoen, N. Bursac, R. Langer, L. E. Freed, and G. Vunjak-Novakovic, Cardiac tissue engineering: Cell seeding, cultivation parameters, and tissue construct characterization, *Biotechnol. Bioeng.*, **64**, 580-589 (1999).

Chapter 6

Osteogenic differentiation of MSC in non-woven fabrics with different diameters and porosities

INTRODUCTION

Cell scaffolds are important for tissue engineering which is a newly emerging biomedical form to promote the regenerative repairing of damaged or lost tissues and the substitution of organ functions [1-5]. The role of scaffold is to give cells an environment suitable for their proliferation and differentiation to induce tissue regeneration, which may control the size and shape of tissue regenerated. For example, the pore size and porosity of scaffolds have been investigated to demonstrate the material factors which have great influence on the oxygen or nutrient supply to cells for their survival and maintenance of biological activities [6-9]. Therefore, various three-dimensional scaffolds of sponges, knits, and non-woven fabrics have been designed and prepared to achieve the scaffold requirements mentioned above.

For successful tissue regeneration, the cells constituting tissue to be regenerated, such as matured, progenitor, precursor, are necessary. Considering the proliferation activity and differentiation potential of cells, the stem cells are practically promising. Among them, mesenchymal stem cells (MSC) have been widely investigated to use by themselves or combining with the scaffold to realize regenerative medicine because they can be isolated clinically from the bone marrow [10]. It is well known that MSC have the inherent potential to differentiate into the cell lineage of various types [11]. Therefore, many trials have been performed to induce the regeneration of various tissues by combining the MSC with the

scaffolds [12-15]. Ishaug et al. form a mineralized bone-like tissue *in vitro* by culturing rat marrow stromal cells or rat calvarial osteoblasts in the sponge scaffold of lactic acid and glycolic acid copolymer [16]. It is recognized that the proliferation and biological functions of cells are influenced by the cell seeding density or the pore size and porosity of scaffolds [17-21]. The scaffolds of different types have been explored to demonstrate influence of the physicochemical properties on the cell behaviors [22-33]. Among them, influence of the three-dimensional structure of fibrous scaffold on the morphology, proliferation, migration, differentiation, and biological function of cells has been investigated [34]. However, the effect of the fiber diameter of fabric constituting the scaffold on the cell behavior is not examined. The surface morphology of the scaffolds to contact cells is one of the important properties which play a key role in the proliferation and differentiation. In this chapter, the surface morphology was changed by altering the fiber size of non-woven fabrics. The non-woven fabrics of PET fibers were taken for the scaffold because the fabrics of different fibers are practically available. Since the PET fibers are not degraded, the surface morphology is not changed during the cell culture.

The objective of this study is to investigate the attachment, morphology, proliferation, and osteogenic differentiation of MSC in the non-woven fabrics prepared from PET fibers with different diameters. We also examined the effect of fabrics porosity on the proliferation and differentiation of MSC cultured *in vitro*.

EXPERIMENTAL

MSC isolation and culture

Mesenchymal stem cells (MSC) were isolated from the bone shaft of femurs of 3-week-old male Fisher 344 rats according to the technique reported by Lennon et al. [35]. Briefly, both the ends of

rat femurs were cut away from the epiphysis and the bone marrow was flushed out by a syringe (21-gauge needle) with 1 ml of Dulbecco's modified Eagle Minimum Essential medium (DMEM) supplemented with 15 % fetal calf serum (FCS) and 50 U/ml penicillin-streptomycin. The cell suspension (5 ml) was placed into two T-25 flasks (IWAKI Glass Co. Ltd., Chiba, Japan). The medium was changed on the 4th day of culture and every 3 days thereafter. When the cells of the first passage became subconfluent, usually 7-10 days after seeding, the cells were detached from the flask by treatment for 5 min at 37 °C with the solution of 0.25 wt% trypsin and 0.02 wt% Ethylenediaminetetraacetic acid (EDTA) in 100 mM of phosphate-buffered saline solution (PBS, pH 7.4). Cells were normally subcultured at a density of 2×10^4 cells/cm^2. The second-passaged cells at sub-confluence were used for all the experiments.

Preparation of non-woven fabrics

Non-woven fabrics prepared from the polyethylene terephthalate (PET) fiber with different diameters and porosities were kindly supplied from Toray Co., Shiga, Japan (Figure 6-1). The diameter of PET fibers was 2.0, 4.4, 9.0, 12.0, 22.0, and 42.0 μm. From the technical viewpoint of fabric preparation, a small portion of 12 μm PET fibers was incorporated into the fabrics of PET fibers with diameters of 2.0 and 4.4 μm. The fabrics prepared by a melt-blow method were punched out into 6 mm-diameter disks, and then thermally compressed with two glass plates at 150 °C for 30 min to obtain the fabrics of a low porosity shown in Table 6-1. On the other hand, they were homogeneously disentangled with tweezers and their shapes were fixed by thermal compression to prepare the fabrics of a high porosity. The disks were pre-wetted with 70 vol% ethanol aqueous solution for 30 min to sterilize them and enhance their water uptake, and completely rinsed 2 times with PBS and 2 times with the culture medium for 1 hr to remove ethanol.

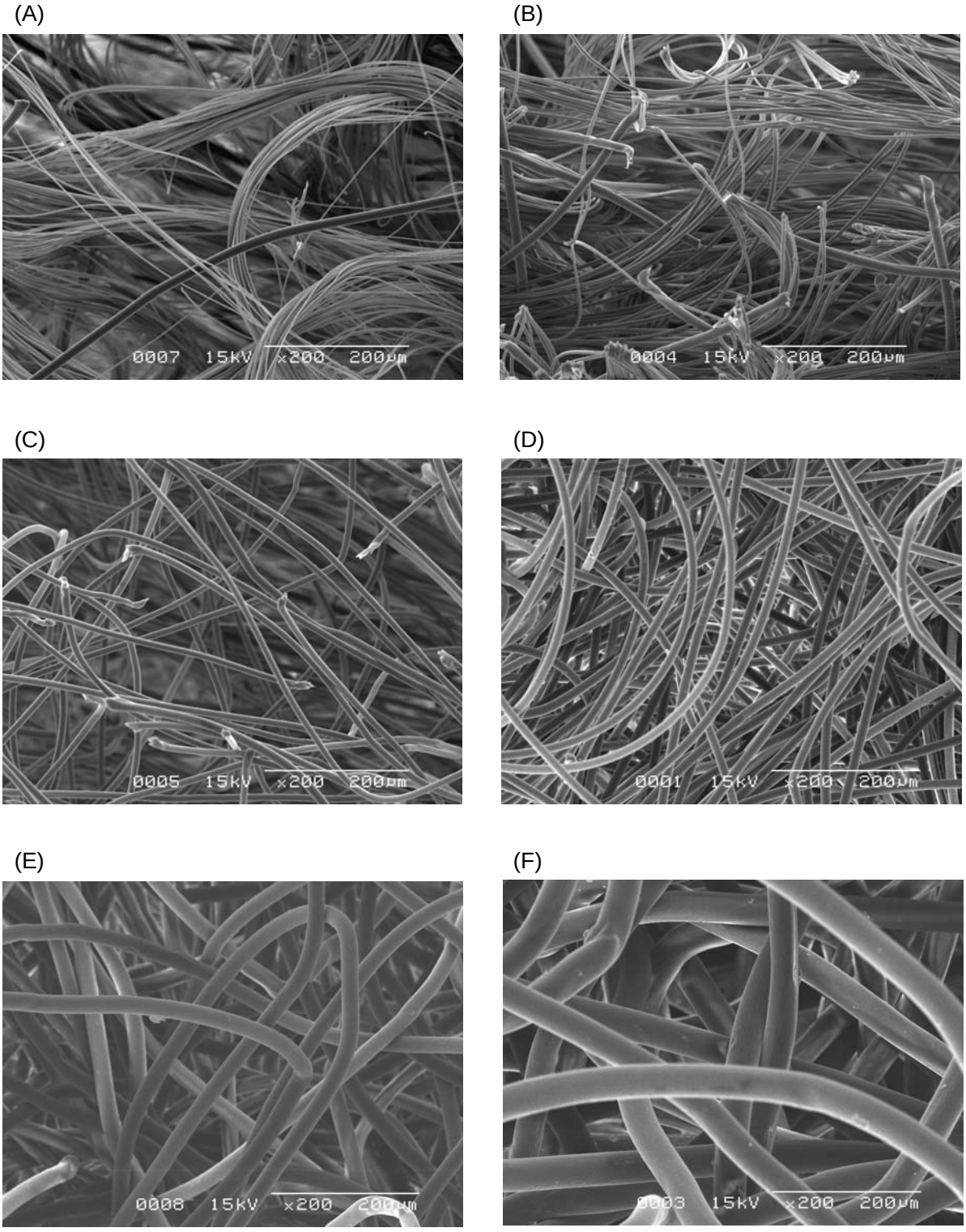

Figure 6-1. Scanning electron micrographs of non-woven fabrics prepared from the PET fiber with diameter of 2.0 (A), 4.4 (B), 9.0 (C), 12.0 (D), 22.0 (E), and 42.0 μm (F).

Table 6-1. Characterization of non-woven fabrics with different porosities prepared from PET fiber with different diameters.

Fiber diameter (μm)	Porosity (%)			Surface area (cm^2)
	Original type	Low porosity type	High porosity type	
2.0	94.0	92.9	97.0	67.3
4.4	96.0	93.4	97.0	26.6
9.0	95.1	92.9	96.8	26.9
12.0	93.6	92.9	96.9	12.1
22.0	94.1	93.0	96.7	7.9
42.0	94.1	93.0	96.7	6.4

Cell seeding into non-woven fabrics and culture of cell seeded fabrics

MSC were seeded into the PET non-woven fabrics with an agitated seeding method because the method is reported to seed cells homogeneously in porous three-dimensional cell scaffolds [36, 37]. For the agitated seeding method, 500 μl of cell suspension (2×10^6 – 2×10^7 cells/ml) and non-woven fabrics with different fiber diameters and porosities were placed in 5-ml tubes with 12 mm diameter (IWAKI Glass Co. Ltd., Chiba, Japan) on an orbital shaker (Bellco Glass, Inc.) and agitated at 300 rpm for 6 hr. The homogeneously MSC-seeded non-woven fabrics were thoroughly washed with PBS to exclude non-adherent cells. The cell-seeded non-woven fabrics were transferred to 12 well tissue culture plates (IWAKI Glass Co. Ltd., Chiba, Japan). Each fabric was maintained in DMEM supplemented with 15 % FCS for 4 weeks at 37 °C in a 95 % air and 5 % CO_2 atomspheric pressure. For bone differentiation, each fabric was maintained in DMEM supplemented with 15 % FCS, 10 nM dexamethasone, 50 μg/ml ascorbic acid, and 10 mM β-glycerophosphate. A DMEM supplemented with 15 % FCS were used as the normal medium for control culture.

SEM observation of cell-seeded non-woven fabrics

The non-woven fabrics with cells attached were fixed with 2.5 wt% glutaraldehyde solution in PBS. After rinsing and dehydration in sequentially increasing ethanol solutions to 100 vol% ethanol, the dehydrated samples were immersed in *t*-butanol, and finally dried in a critical point dryer (ES-2030, Hitachi, Japan). After sputter coating with gold/palladium, the samples were examined using a scanning electron microscope (SEM, S2380N, Hitachi, Japan).

DNA assay

The number of cells attached to the non-woven fabric was determined by the fluorometric quantification of cell DNA according to the assay reported by Rao et al. [38]. Briefly, the cell-seeded non-woven fabrics were washed with PBS and stored at –30 °C until assayed. After thawing the samples, they were lysed in a buffer solution (pH 7.4) containing 0.2 mg/ml sodium dodecylsulfate (SDS), and 30 mM sodium citrate-buffered saline solution (SSC) at 37 °C for 12 hr with occasional mixing. The cell lysate (100 μl) was mixed with the SSC buffer (400 μl) in a glass tube. After mixing with a dye solution (500 μl; composition : 30 mM SSC, 1 μg/ml Hoechst 33258 dye), the fluorescent intensity of mixed solution was measured in a fluorescence spectrometer (F-2000, HITACHI, Japan) at the excitation and emission wavelengths of 355 and 460 nm, respectively. The calibration curve between the DNA and cell number was prepared by use of cells of known numbers. The DNA assay was done 3 times independently for every experimental sample unless otherwise mentioned.

Biochemical evaluation of cell seeded non-woven fabrics

The cells cultured were lysed in 1 ml of a buffer solution (pH=7.4) containing 0.2 mg/ml SDS, and 30 mM SSC at 37 °C for 12 hr with mixing. The cell lysate was centrifuged at 12,000 rpm and 4 °C

for 15 min and the ALP activity of supernatant obtained was determined by a *p*-nitrophenylphosphate method [39].

To determine the osteocalcin content of cells, the cells cultured were treated with 1 ml of 40 % formic acid for 12 hr to decalcify. After the decalcification process, the cell extraction was applied to the gel filtration of Sephadex^{TM} G-25 column (PD-10, Amersham Pharmacia biotech AB, Sweden). The resulting solution was freeze-dried and subjected to an osteocalcin rat enzyme-linked immunosorbent assay (ELISA) (rat osteocalcin ELISA system, Amersham Biosciences, Tokyo, Japan)

Statistical analysis

All the data were analyzed by Fisher's LSD test for multiple comparison and the statistical significance was accepted at $p < 0.05$. Experimental results were expressed as the means ± the standard deviation of the mean.

RESULTS

Cell attachment to the non-woven fabrics prepared from the PET fibers of various diameters

Figure 6-2 shows the scanning electron micrographs of MSC attached to the non-woven fabrics prepared from different PET fibers 6 hr after cell seeding. Cells attached to all the types of non-woven fabrics, while they uniformly distributed throughout the non-woven fabrics. For the non-woven fabric of fibers with 2.0 μm diameter, the shape of MSC attached was spherical. However, the morphology of cells attached became flatter with an increase in the diameter of fabric fibers and cell clustering was observed at the cross-point between the fibers. The porosity of non-woven fabrics had no influence on the morphology of cells.

(A)

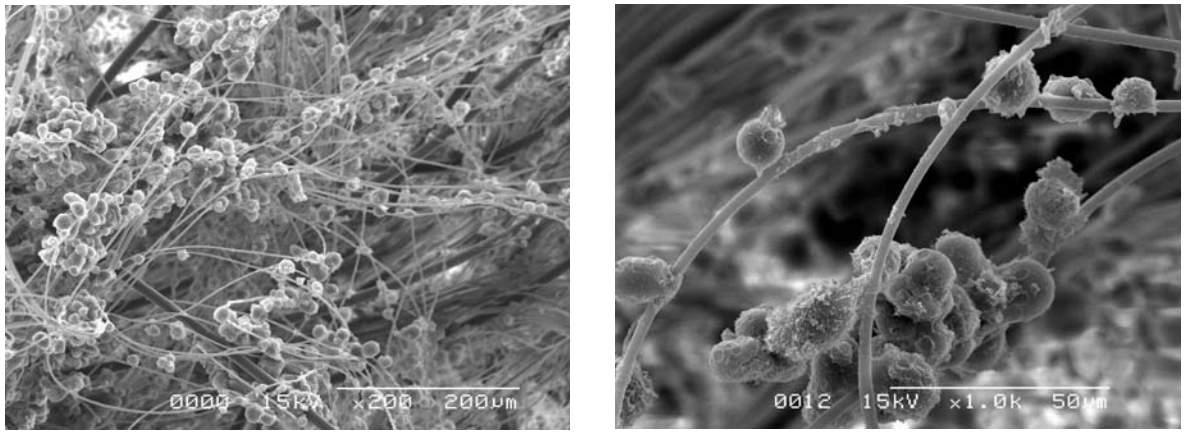

(B)

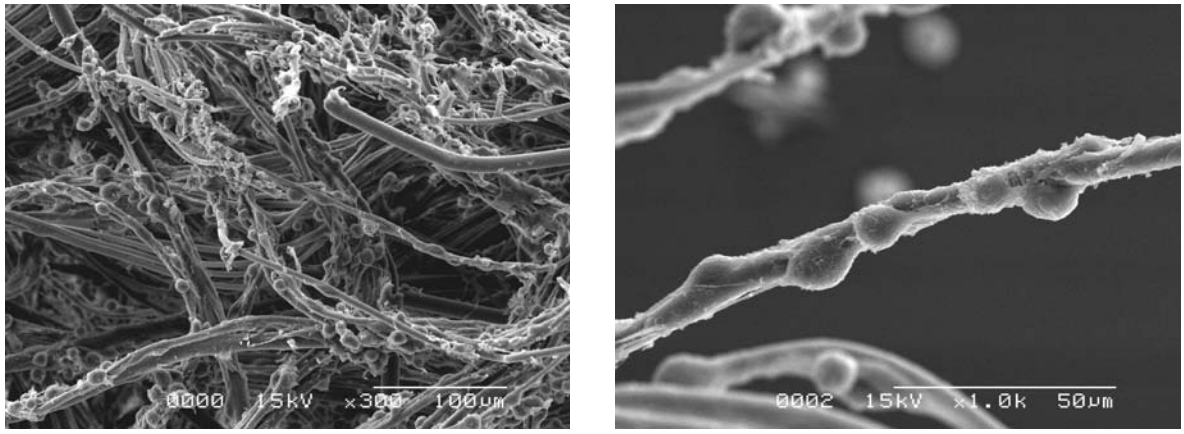

(C)

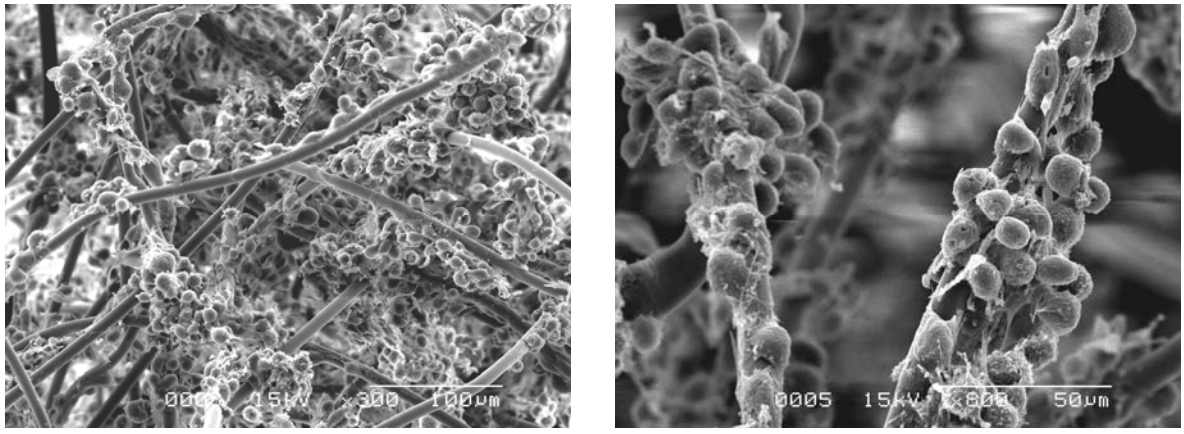

Figure 6-2. Scanning electron micrographs of MSC attached to the non-woven fabrics prepared from the PET fiber with diameter of 2.0 (A), 4.4 (B), 9.0 (C), 12.0 (D), 22.0 (E), and 42.0 μm (F) 6 hr after cell seeding with agitated seeding method. The number of cells applied is 10^7 cells/fabric.

(D)

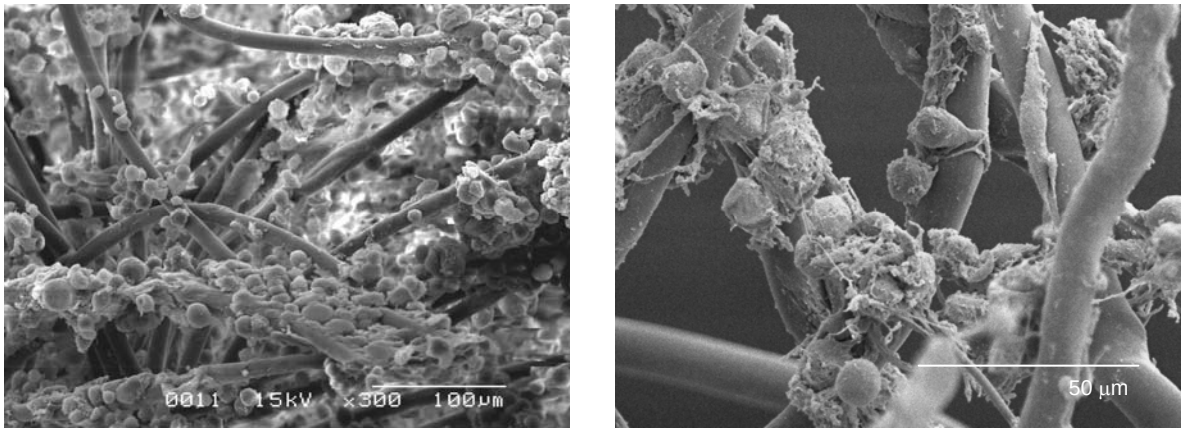

(E)

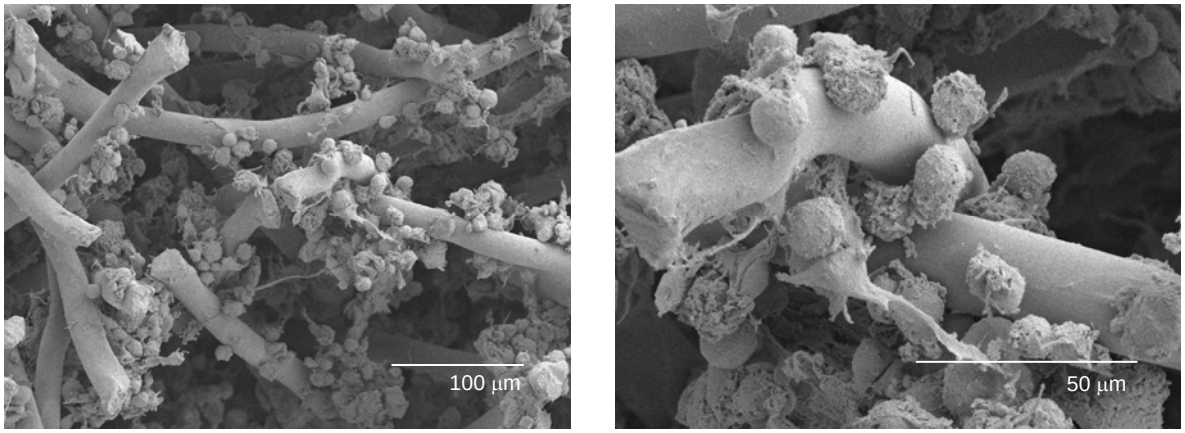

(F)

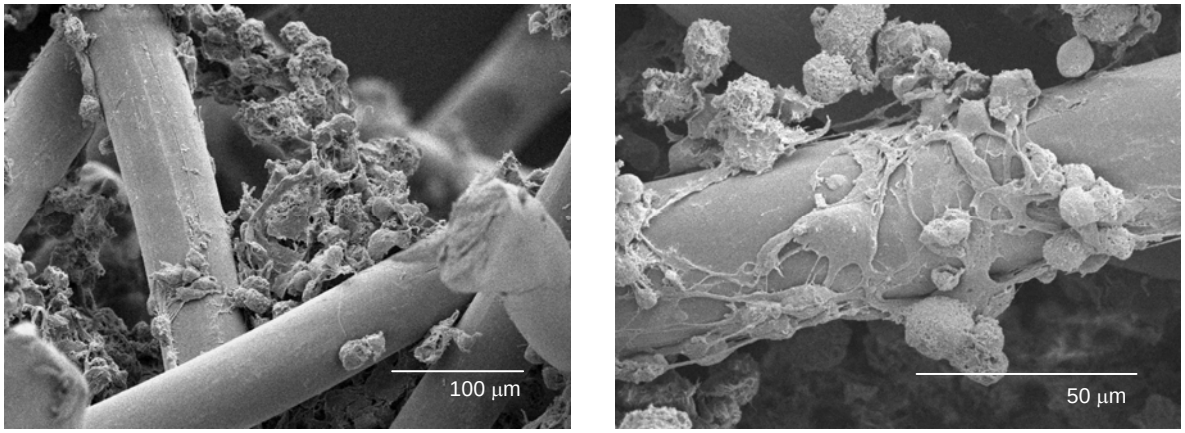

Figure 6-2. (Continued).

Figure 6-3 shows the number of cells attached to the non-woven fabrics with various fiber diameters and porosities. A larger number of cells attached to the non-woven fabrics of larger diameter fibers, irrespective of the porosity of non-woven fabrics. No difference in the effect of fabrics porosity on the cell attachment was observed. The number of cells attached to the non-woven fabrics with fiber diameters of 22.0 and 42.0 μm was significantly larger than that of fabrics with thinner fibers.

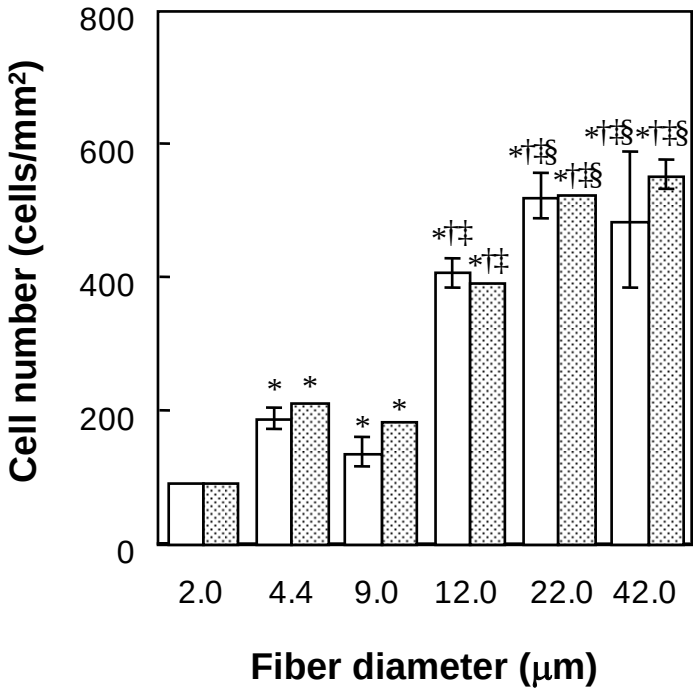

Figure 6-3. The number of cells attached to the non-woven fabrics prepared from the PET fiber with various diameters and 6 hr after cell seeding with agitated seeding method: low (□) and high porosity (▨). The number of cells applied is 10^7 cells/fabric. $^{*}p < 0.05$; significant against the cell attached to the non-woven fabrics with the fiber diameter of 2.0 μm at the corresponding porosity. $^{\dagger}p < 0.05$; significant against the cell attached to the non-woven fabrics with the fiber diameter of 4.4 μm at the corresponding porosity. $^{\ddagger}p < 0.05$; significant against the cell attached to the non-woven fabrics with the fiber diameter of 9.0 μm at the corresponding porosity. $^{\S}p < 0.05$; significant against the cell attached to the non-woven fabrics with the fiber diameter of 12.0 μm at the corresponding porosity. $^{\P}p < 0.05$; significant against the cell attached to the non-woven fabrics with the fiber diameter of 22.0 μm at the corresponding porosity.

Cell proliferation on the non-woven fabrics prepared from the PET fibers with various diameters

Figure 6-4 shows the proliferation profiles of MSC on the non-woven fabrics prepared from PET fibers with various fiber diameters and porosities. MSC proliferated on the fiber of non-woven fabrics although the profile depended on the fiber diameter and fabrics porosity. The cell proliferation tended to level off 21 days after culture, irrespective of the fiber diameter. The initial cell proliferation increased with the increasing fiber diameter and became significant large when the diameter was higher than 12 μm. The non-woven fabrics with high porosity are superior to those with low porosity for cell proliferation.

Bone formation of MSC on the non-woven fabrics prepared from fibers with various diameters

Figure 6-5 shows the ALP activity of MSC on the non-woven fabrics with various diameters and porosities after bone differentiation culture for 4 weeks. Apparently, in any case, the ALP activity of cells cultured in the bone differentiation medium was significantly higher than in the normal medium. Irrespective of the fabric porosity, the ALP activity became maximum for the non-woven fabrics with a fiber diameter of 9.0 μm, while non-woven fabrics with the larger and smaller diameter showed lower ALP activity. When the ALP activity was compared in the porosity of non-woven fabrics, the ALP activity of fabric with lower porosity was significantly higher than that of the higher porosity fabric.

Figure 6-6 shows the osteocalcin content of MSC on the non-woven fabrics with various fiber diameters and porosities after bone differentiation culture for 4 weeks. The non-woven fabrics prepared from the fibers of 9 and 12 μm diameter exhibited high osteocalcin content compared with other non-woven fabrics, irrespective of the fabric porosity. The osteocalcin content for fabrics with the lower porosity was high compared with that of fabrics with the higher porosity. The cells cultured in the normal medium did not contribute to any increase in the osteocalcin content.

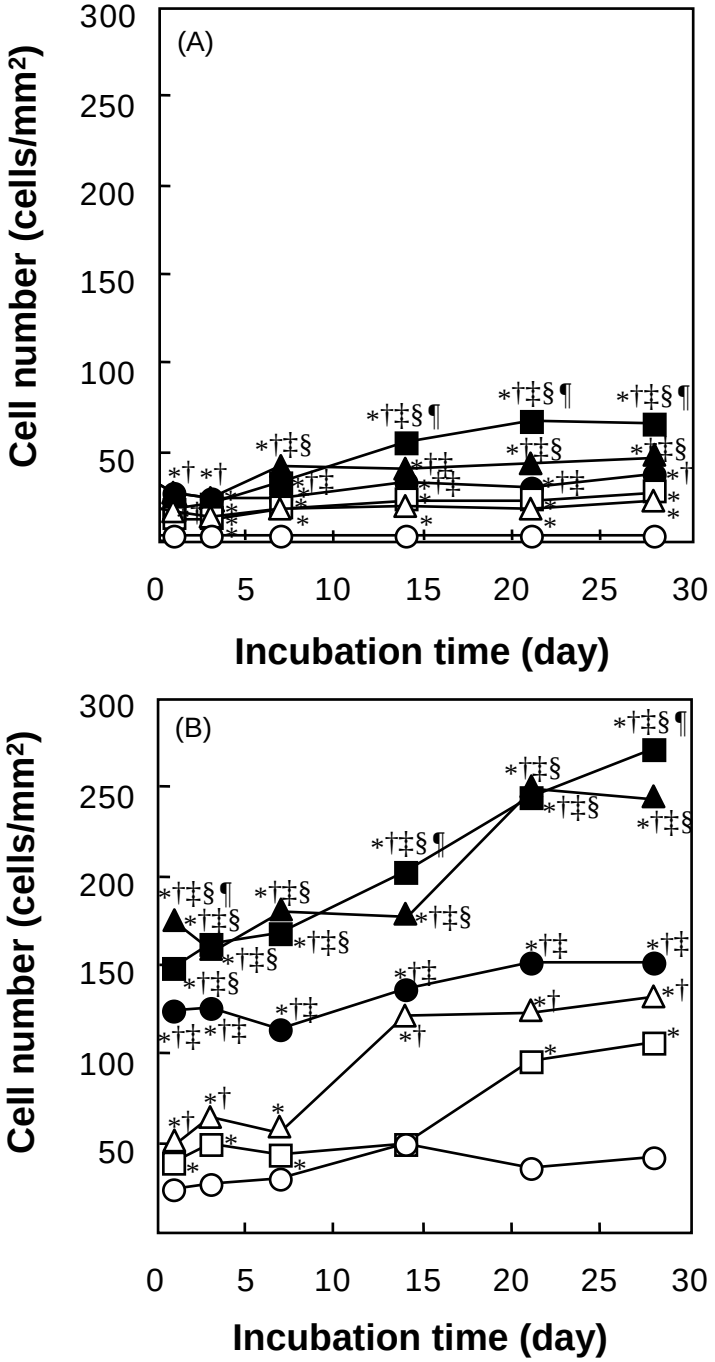

Figure 6-4. Time course of MSC growth in the non-woven fabrics prepared from the PET fiber with various diameters of 2.0 (○), 4.4 (□), 9.0 (△), 12.0 (●), 22.0 (■), and 42.0 μm (▲): low (A) or high porosity (B). *$p < 0.05$; significant against the cell attached to the non-woven fabrics with the fiber diameter of 2.0 μm at the corresponding porosity. †$p < 0.05$; significant against the cell attached to the non-woven fabrics with the fiber diameter of 4.4 μm at the corresponding porosity. ‡$p < 0.05$; significant against the cell attached to the non-woven fabrics with the fiber diameter of 9.0 μm at the corresponding porosity. §$p < 0.05$; significant against the cell attached to the non-woven fabrics with the fiber diameter of 12.0 μm at the corresponding porosity. ¶$p < 0.05$; significant against the cell attached to the non-woven fabrics with the fiber diameter of 22.0 μm at the corresponding porosity.

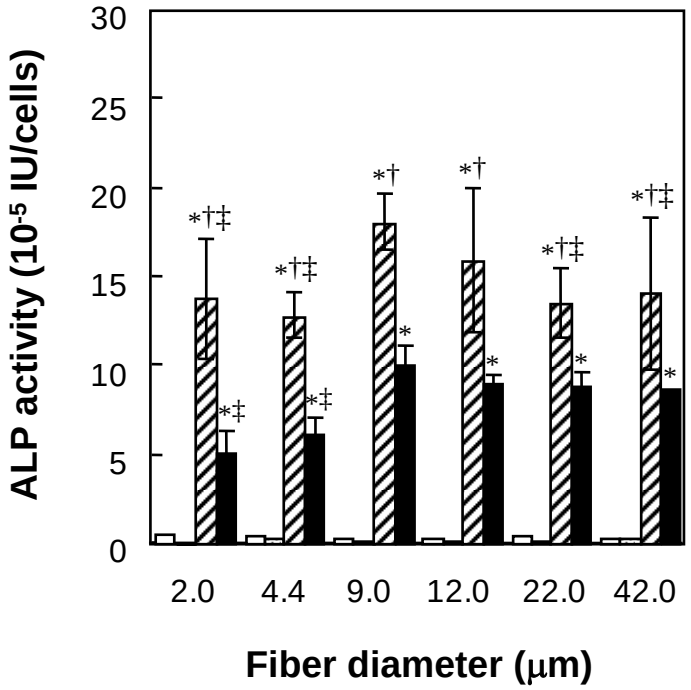

Figure 6-5. ALP activity of MSC cultured in the non-woven fabrics prepared from the PET fiber with various diameters for 4 weeks in the normal (□, ▨) and bone differentiation medium (▨, ■): low (□, ▨) and high porosity (▨, ■). $^{*}p < 0.05$; significant against the ALP activity of MSC cultured on the non-woven fabrics in the normal medium at the corresponding fiber diameter and porosity. $^{\dagger}p < 0.05$; significant against the ALP activity of MSC cultured on the non-woven fabrics with high porosity in the bone differentiation medium. $^{\ddagger}p < 0.05$; significant against the ALP activity of MSC cultured on the non-woven fabrics with the fiber diameter of 9.0 μm at the corresponding porosity and medium.

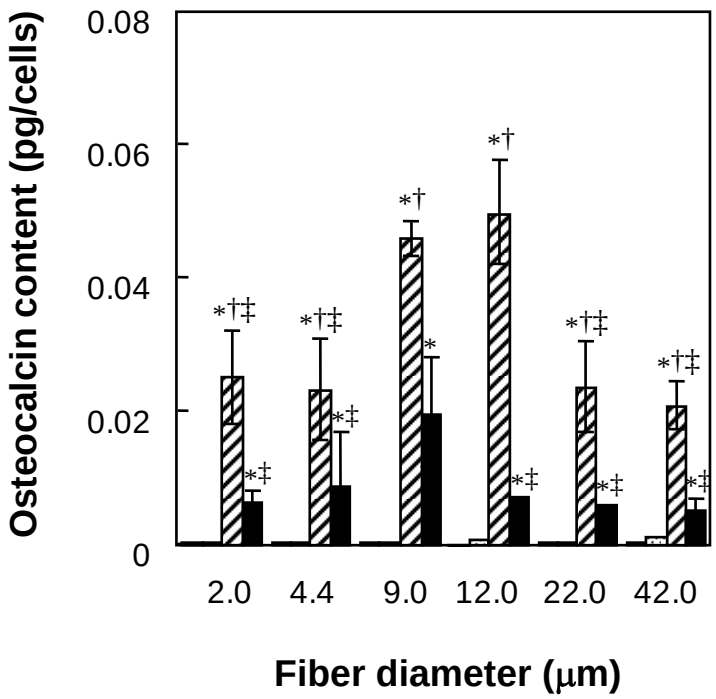

Figure 6-6. Osteocalcin contents of MSC cultured in the non-woven fabrics prepared from the PET fiber with various diameters for 4 weeks in the normal (□, ▨) and bone differentiation medium (▨, ■): low (□, ▨) and high porosity (▨, ■). $^{*}p < 0.05$; significant against the ALP activity of MSC cultured on the non-woven fabrics in the normal medium at the corresponding fiber diameter and porosity. $^{\dagger}p < 0.05$; significant against the ALP activity of MSC cultured on the non-woven fabrics with high porosity in the bone differentiation medium. $^{\ddagger}p < 0.05$; significant against the ALP activity of MSC cultured on the non-woven fabrics with the fiber diameter of 9.0 μm at the corresponding porosity and medium.

DISCUSSION

This chapter demonstrates that the proliferation and differentiation in the PET non-woven fabrics are greatly influenced by the fiber diameter and porosity of fabrics. Based on the concept of *in vivo* tissue engineering, the scaffold material should be bioabsorbed in harmonization with tissue regeneration. However, the biodegradability of scaffold often makes it complicated to evaluate the cell-scaffold interaction. Therefore, the PET non-woven fabric of non-biodegradability was used in this study. Moreover, the porosity of non-woven fabrics could readily be changed by the thermal compression or homogeneous disentanglement. As PET has a glass transition temperature at 80 °C, the shape and thickness of PET non-woven fabrics are easy to change at temperatures higher than the glass transition temperature.

The number of MSC attached to the non-woven fabrics increased with the increasing fiber diameter (Figure 6-3). This tendency can be explained in terms of the surface area for cells to attach. As shown in Figure 6-2, the cells attached in a spherical shape to the non-woven fabrics with a fiber diameter of 2.0 μm. The surface of fiber was too small to allow cells to completely attach to the fiber because the fiber diameter was smaller than the size of cells (about 10 μm). Such unstable attachment will result in decreased number of cells attached. It is likely that this unstable attachment affects the proliferation behavior of cells. For the fabrics of larger diameter fiber, the cells would be able to use the empty surface of fibers to effectively proliferate. Greater proliferation for the non-woven fabrics with high porosity than those that with low porosity can be explained in terms of pore space between the fibers of fabric. The pore space is increased by increasing the porosity of non-woven fabrics. When compared at a same porosity of fabrics, the pore space of non-woven fabrics prepared from larger fibers is larger. It is possible that the larger space enables cells to proliferate better due to the larger space and better supply of oxygen

and nutrients. The narrow space between fibers will suppress the cell proliferation.

Both the ALP activity and osteocalcin content of MSC as bone differentiation markers depended on the porosity of non-woven fabrics and their fiber diameter (Figures 6-5 and 6-6). Higher extent of differentiation may be due to the suppressed cell proliferation. Ma et al. reported the effect of trophoblast differentiation on the non-woven fabrics with different porosities [34]. The differentiation depended on the cell morphology and the cell cycle. The cell morphology, such as cell aggregates, was essential to differentiate and different by the porosity of the non-woven fabrics. The other reports showed that there was a relation between the cell aggregation and the cell function [40, 41]. Goldstein et al. examined the proliferation and differentiation of osteoprogenitor cells seeded as a uniform dispersion or as a single dense cluster in the similar total number of cells [40]. Dense clustered cells demonstrated to significantly diminish their proliferation and collagen synthesis. On the contrary, a significantly higher level of ALP activity and more mineralization were observed, whereas cells proliferated more in the dispersion state. These findings are similar to our results of the cell proliferation and differentiation. In this chapter, the cell morphology and cell cycle may affect the extent of differentiation. Both the ALP activity and osteocalcin content of non-woven fabrics were highest for the non-woven fabrics with the fiber diameters of 9.0-12.0 μm, irrespective of the porosity. These results suggest that the differentiation extent of cells between the non-woven fabrics with different fiber diameters but a same porosity was dependent on the fiber diameter rather than the pore size.

In conclusion, this chapter demonstrated that MSC could attach, proliferate, and differentiate on the PET non-woven fabrics with various diameters and porosities. The fiber diameter and the spatial property affected the morphology, the attached number, the proliferation rate, and bone differentiation of cells. These results will give fundamental information to design the scaffolds suitable to tissue engineering.

REFERENCES

1. I. V. Yannas, J. F. Burke, D. P. Orgill, and E. M. Skrabut, Wound tissue can utilize a polymeric template to synthesize a functional extension of skin, *Science*, **215**, 174-176 (1982).
2. W. G. Rodkey, J. R. Steadman, and S. T. Li, A clinical study of collagen meniscus implants to restore the injured meniscus, *Clin. Orthop*., **367S**, S281-292 (1999).
3. D. W. Hutmacher, A. Kirsch, K. L. Ackermann, and M. B. Hurzeler, A tissue engineered cell-occlusive device for hard tissue regeneration--a preliminary report, *Int. J. Periodontics Restorative Dent.*, **21**, 49-59 (2001).
4. T. Shin'oka, Y. Imai, and Y. Ikada, Transplantation of a tissue-engineered pulmonary artery, *N. Engl. J. Med.*, **344**, 532-533 (2001).
5. M. Ochi, Y. Uchio, K. Kawasaki, S. Wakitani, and J. Iwasa., Transplantation of cartilage-like tissue made by tissue engineering in the treatment of cartilage defects of the knee, *J. Bone Joint Surg. Br.*, **84**, 571-578 (2002).
6. D. J. Mooney, D. F. Baldwin, N. P. Suh, J. P. Vacanti, and R. Langer, Novel approach to fabricate porous sponges of poly(D, L-lactic-co-glycolic acid) without the use of organic solvents, *Biomaterials*, **17**, 1417-1722 (1996).
7. C. S. Ranucci, A. Kumar, S. P. Batra, and P. V. Moghe, Control of hepatocyte function on collagen foams: sizing matrix pores toward selective induction of 2-D and 3-D cellular morphogenesis, *Biomaterials*, **21**, 783-793 (2000).
8. H. Schoof, J. Apel, I. Heschel, and G. Rau, Control of pore structure and size in freeze-dried collagen sponges, *J. Biomed. Mater. Res.*, **58**, 352-357 (2001).
9. I. K. Kwon, K. D. Park, S. W. Choi, S. H. Lee, E. B. Lee, J. S. Na, S. H. Kim, and Y. H. Kim,

Fibroblast culture on surface-modified poly(glycolide-co-epsilon-caprolactone) scaffold for soft tissue regeneration, *J. Biomater. Sci. Polym. Ed.*, **12**, 1147-1160 (2001).

10. D. P. Lennon, S. E. Haynesworth, D. M. Arm, M. A. Baber, and A. I. Caplan, Dilution of human mesenchymal stem cells with dermal fibroblasts and the effects on *in vitro* and *in vivo* osteochondrogenesis, *Dev. Dyn.*, **219**, 50-62 (2000).

11. A. E. Grigoriadis, J. N. Heersche, and J. E. Aubin, Differentiation of muscle, fat, cartilage, and bone from progenitor cells present in a bone-derived clonal cell population: effect of dexamethasone, *J. Cell Biology*, **106**, 2139-2151 (1988).

12. H. Ohgushi, V. M. Goldberg, and A. I. Caplan, Repair of bone defects with marrow cells and porous ceramic. Experiments in rats, *Acta. Orthop. Scand.*, **60**, 334-339 (1989).

13. B. Johnstone, T. M. Hering, A. I. Caplan, V. M. Goldberg, and J. U. Yoo, *In vitro* chondrogenesis of bone marrow-derived mesenchymal progenitor cells, *Exp. Cell Res.*, **238**, 265-272 (1998).

14. S. P. Bruder, A. A. Kurth, M. Shea, W. C. Hayes, N. Jaiswal, and S. Kadiyala, Bone regeneration by implantation of purified, culture-expanded human mesenchymal stem cells, *J. Orthop. Res.*, **16**, 155-162 (1998).

15. H. Petite, V. Viateau, W. Bensaid, A. Meunier, C. de Pollak, M. Bourguignon, K. Oudina, L. Sedel, and G. Guillemin, Tissue-engineered bone regeneration, *Nat. Biotechnol.*, **18**, 959-963 (2000).

16. S. L. Ishaug, G. M. Crane, M. J. Miller, A. W. Yasko, M. J. Yaszemski, and A. G. Mikos, Bone formation by three-dimensional stromal osteoblast culture in biodegradable polymer scaffolds, *J. Biomed. Mater. Res.*, **36**, 17-28 (1997).

17. C. E. Holy, M. S. Shoichet, and J. E. Davies, Engineering three-dimensional bone tissue *in vitro*

using biodegradable scaffolds: investigating initial cell-seeding density and culture period, *J. Biomed. Mater. Res*., **51**, 376-382 (2000).

18. A. Panossian, S. Ashiku, C. H. Kirchhoff, M. A. Randolph, and M. J. Yaremchuk, Effects of cell concentration and growth period on articular and ear chondrocyte transplants for tissue engineering, *Plast. Reconstr. Surg*., **108**, 392-402 (2001).

19. B. Trussell, J. Ward, M. Cox, M. Tucci, H. Benghuzzi, and J. Hughes, Investigating initial cell-seeding density and culture period of fibroblast growing on biodegradable tricalcium phosphate lysine disks, *Biomed. Sci. Instrum*., **38**, 101-106 (2002).

20. Y. Kuboki, Q. Jin, and H. Takita, Geometry of carriers controlling phenotypic expression in BMP-induced osteogenesis and chondrogenesis, *J. Bone Joint Surg. Am*., **83-A Suppl 1**, S105-115 (2001).

21. I. K. Kwon, K. D. Park, S. W. Choi, S. H. Lee, E. B. Lee, J. S. Na, S. H. Kim, and Y. H. Kim, Fibroblast culture on surface-modified poly(glycolide-co-epsilon-caprolactone) scaffold for soft tissue regeneration, *J. Biomater. Sci. Polym. Ed*., **12**, 1147-1160 (2001).

22. L. G. Cima, J. P. Vacanti, C. Vacanti, D. Ingber, D. Mooney, and C. Vacanti, Tissue engineering by cell transplantation using degradable polymer substrates, *J. Biomech. Eng*., **113**, 143-151 (1991).

23. S. P. Hoerstrup, G. Zund, M. Lachat, A. Schoeberlein, G. Uhlschmid, P. Vogt, and M. Turina, Tissue engineering: a new approach in cardiovascular surgery-seeding of human fibroblasts on resorbable mesh, *Swiss Surg*., **S2**, 23-25 (1998).

24. R. Sodian, J. S. Sperling, D. P. Martin, U. Stock, J. E. Mayer, and J. P. Vacanti, Tissue engineering of a trileaflet heart valve-early *in vitro* experiences with a combined polymer, *Tissue Eng*., **5**, 489-494 (1999).

25. J. Mayer, E. Karamuk, T. Akaike, and E. Wintermantel, Matrices for tissue engineering-scaffold structure for a bioartificial liver support system, *J. Control. Rel*., **64**, 81-90 (2000).

26. J. W. Vehof, A. E. Ruijter, P. H. Spauwen, and J. A. Jansen, Influence of rhBMP-2 on rat bone marrow stromal cells cultured on titanium fiber mesh, *Tissue Eng*., **7**, 373-383 (2001).

27. K. Kojima, L. J. Bonassar, A. K. Roy, C. A. Vacanti, and J. Cortiella, Autologous tissue-engineered trachea with sheep nasal chondrocytes, *J. Thorac. Cordiovasc. Surg*., **123**, 1177-1184 (2002).

28. T. Ozawa, D. A. Mickle, R. D. Weisel, N. Koyama, S. Ozawa, and R. K. Li, Optimal biomaterial for creation of autologous cardiac grafts, *Circulation*, **106**, 176-182 (2002).

29. M. S. Widmer, P. K. Gipta, L. Lu, R. K. Meszlenyl. G. R. Evans, K. Brandt, T. Savel, A. Gurlek, C. W. Jr. Patrick, and A. G. Mikos, Manufacture of porous biodegradable polymer conduits by an extrusion process for guided tissue regeneration, *Biomaterials*, **19**, 1945-1955 (1998).

30. L. D. Harris, B. S. Kim, and D. J. Mooney, Open pore biodegradable matrices formed with gas foaming, *J. Biomed. Mater. Res*., **42**, 396-402 (1998).

31. L. D. Harris, B. S. Kim, and D. J. Mooney, Open pore biodegradable matrices formed with gas foaming, *J. Biomed. Mater. Res*., **42**, 396-402 (1998).

32. A. Park, B. Wu, and L. G. Griffith, Integration of surface modification and 3D fabrication techniques to prepare patterned poly(L-lactide) substrates allowing regionally selective cell adhesion, *J. Biomater. Sci. Polym. Ed.*, **9**, 89-110 (1998).

33. J. Gao, J. E. Dennis, L. A. Solchaga, A. S. Awadallah, V. M. Goldberg, and A. I. Caplan, Tissue-engineered fabrication of an osteochondral composite graft using rat bone marrow-derived mesenchymal stem cells, *Tissue Eng*., **7**, 363-371 (2001).

34. B. Chevallay, N. Abdul-Malak, and D. Herbage, Mouse fibroblasts in long-term culture within

collagen three-dimensional scaffolds: influence of crosslinking with diphenylphosphorylazide on matrix reorganization, growth, and biosynthetic and proteolytic activities, *J. Biomed. Mater. Res*., **49**, 448-459 (2000).

35. T. Ma, Y. Li, S. T. Yang, and D. A. Kniss, Effects of pore size in 3-D fibrous matrix on human trophoblast tissue development, *Biotechnol. Bioeng*. **70**, 606-618 (2000).

36. D. P. Lennon, S. E. Haynesworth, R. G. Young, J. E. Dennis, and A. I. Caplan, A chemically defined medium supports *in vitro* proliferation and maintains the osteochondral potential of rat marrow-derived mesenchymal stem cells, *Exper. Cell Res.*, **219**, 211-222 (1995).

37. B. S. Kim,J. Nikolovski, J. Bonadio, E. Smiley, and D.J. Mooney, Engineered smooth muscle tissues: regulating cell phenotype with the scaffold, *Exper. Cell Res.*, **251**, 318-328 (1999).

38. Y. Takahashi and Y. Tabata, Homogeneous seeding of mesenchymal stem cells into nonwoven fabric for tissue engineering, *Tissue Eng.*, **9**, 931-938 (2003).

39. J. Rao and W. R. Otto, Fluorimetric DNA assay for cell growth estimation, *Anal. Biochem.*, **207**, 186-192 (1992).

40. D. Kobayashi, H. Takita, M. Mizuno, Y. Totsuka, and Y. Kuboki, Time-dependent expression of bone sialoprotein fragments in osteogenesis induced by bone morphogenetic protein, *J. Biochem.*, **119**, 475-481 (1996).

41. A. S. Goldstein, Effect of seeding osteoprogenitor cells as dense clusters on cell growth and differentiation, *Tissue Eng.*, **7**, 817-827 (2001).

42. S. P. Baldwin and W. M. Saltzman, Aggregation enhances catecholamine secretion in cultured cells, *Tissue Eng*., **7**, 179-190 (2001).

Chapter 7

Osteogenic differentiation of MSC in biodegradable scaffolds composed of gelatin and ß-TCP

INTRODUCTION

Large bone defects which are associated with reconstruction surgery of trauma, cancer, and total hip arthoplasties, have been clinically treated by bioceramics or autogenous and allogenous bone grafts. Although the autograft is always adapted to the surrounding host tissue for bone regeneration, it has some clinical problems to be resolved, such as the limited donor supply, the risk of infection, hemorrhage, and inadequate resorption rate during healing [1]. On the other hand, the allograft has some clinical disadvantages of histo-incompatibility and disease transfer. As one trial to overcome the problems, bone tissue engineering has been attracted much attention and the basic idea is to regenerate the bone tissue by use of scaffold suitable for migration, proliferation, and differentiation of bone cells [2].

Gelatin is a denatured collagen and commercially available as a biodegradable polymer. It has been extensively utilized for pharmaceutical and medical purposes, and its biosafety has been proven through long clinical applications [3]. Other advantages of gelatin include the usability of materials with different charges and the easiness of chemical modification. We have prepared biodegradable hydrogels from different types of gelatin for the controlled release of various growth factors and succeeded in tissue regeneration by the growth factor release [4]. On the other hand, some researches have demonstrated that the surface coating of substrates with gelatin enhances the attachment and proliferation of cells thereon [5-7]. These findings suggest that gelatin is one of the materials suitable to the substrate of cells.

Bioactive calcium phosphates, such as hydroxyapatite (HAp) and β-tricalcium phosphate (β-TCP), have been intensively investigated as the cell scaffold for bone tissue engineering [8-17] because it is well recognized that they are compatible to natural bone tissue and osteoconductive. However, the

HAp is not practically degraded under the physical condition and remains inside the bone tissue regenerated. Therefore, as one trial to control the *in vivo* degradability, the HAp is combined with organic materials, such as collagen and glycolide-lactide copolymer. It has been reported that the combination improves the degradation and mechanical properties for scaffolds [18-23]. Especially, the combined collagen and HAp has been extensively utilized for bone tissue engineering since the structure is similar to that of nature bone tissue. On the other hand, β-TCP is advantageous from the viewpoint of biodegradability, but brittle compared with HAp. Combination with organic materials has also been trial to overcome the drawback of material properties [22, 23].

It is undoubtedly necessary for successful tissue regeneration to make use of cells constituting tissue to be regenerated, such as mature, progenitor, precursor, and stem cells. Considering the proliferation and differentiation potential of cells, stem cells are practically promising. Among them, mesenchymal stem cells (MSC) have been extensively investigated for the application of regenerative medicine because they can be clinically isolated from the bone marrow [24]. It is well recognized that MSC have an inherent potential to differentiate into the cell lineage of various types [25]. Many trials with MSC have been performed to induce *in vitro* or *in vivo* tissue regeneration by their combination with the scaffolds [2, 26-28]. The scaffold often affects the proliferation and differentiation of MSC.

The objective of this chapter is to evaluate the characticities of gelatin scaffolds incorporating β-TCP (gelatin-β-TCP scaffolds) as the scaffold of MSC from the viewpoint of their mechanical property and osteoinductivity improvement by the β-TCP incorporation. We also examine the effect of culture methods on the proliferation and differentiation of MSC.

EXPERIMENTAL

Materials

A gelatin sample with an isoelectric point (IEP) of 9.0 was isolated from the porcine skin with acidic process (Nitta Gelatin Co., Osaka, Japan) and are here called basic gelatin, because of their electrical

feature. ß-TCP granules (average diameter: 2.89 μm, surface area: 3.22 m^2/g, density: 2.640, Ca/P=1.50, purity: 99.6 %) were obtained from Taihei Chemical Industries, Nara, Japan. Other chemicals were obtained from Wako Pure Chemical Industries, Osaka, Japan and used without further purification.

Preparation of gelatin scaffolds with or without ß-TCP

Gelatin scaffolds incorporating ß-TCP (gelatin-ß-TCP scaffolds) were prepared by chemical crosslinking of gelatin with glutaraldehyde in the presence of ß-TCP granules at different amounts (Table 7-1). Briefly, 4.29 wt% aqueous solution of gelatin at different contents of ß-TCP (70 ml) was mixed at 5,000 rpm at 37 °C for 3 min by using a homogenizer (ED-12, Nihonseiki Co., Tokyo, Japan). After addition of 2.17 wt% of glutaraldehyde aqueous solution (30 ml), the mixed solution was further mixed for 15 sec by the homogenizer. The resulting solution was cast into a polypropylene dish of 138×138 cm^2 and 5 mm depth, followed by leaving at 4 °C for 12 hr for gelatin crosslinking. Then, the crosslinked gelatin hydrogels with or without ß-TCP were placed into 100 mM of aqueous glycine solution at 37 °C for 1 hr to block the residual aldehyde groups of glutaraldehyde. Following complete washing with double distilled water (DDW), the hydrogels were freeze-dried and cut into cubes of 5×5×5 mm^3. The average pore size and porosity of scaffold were measured by the methods reported previously (Table 7-1) [29, 30].

Mechanical test

The compression modulus of gelatin-β-TCP scaffolds was measured by a mechanical apparatus (AG-5000B, Shimadzu, Kyoto, Japan) at a rate of 1 mm/min. The load-deformation curve was obtained and the compression modulus of freeze-dried sample was calculated from the initial slope of load-deformation curve. Measurement was done five times for each sample to calculate the average value ± the standard deviation of the mean.

Table 7-1. Characterization of gelatin scaffolds incorporating various amounts of ß-TCP prepared.

ß-TCP content (wt%)	Pore size (μm)	Porosity (%)	Compression modulus (MPa)
0	184.9 ± 58.2	96.6	0.27 ± 0.01
25	198.2 ± 52.3	96.2	0.52 ± 0.14
50	179.1 ± 27.8	95.9	1.13 ± 0.13
75	185.5 ± 62.4	95.4	2.60 ± 0.32
90	178.2 ± 50.0	95.1	4.97 ± 0.73

MSC isolation and culture

Mesenchymal stem cells (MSC) were isolated from the bone shaft of femurs of 3-week-old male Fisher 344 rats according to the technique reported by Lennon et al. [31]. Briefly, both the ends of rat femurs were cut away from the epiphysis and the bone marrow was flushed out by a syringe (21-gauge needle) with 1 ml of Dulbecco's modified Eagle Minimal Essential medium (DMEM) supplemented with 15 % fetal calf serum (FCS) and 50 U/ml penicillin-streptomycin. The cell suspension (5 ml) was placed into two T-25 flasks (IWAKI Glass Co. Ltd., Chiba, Japan). The medium was changed on the 4th day of culture and every 3 days thereafter. When the cells proliferated became subconfluent, usually for 7-10 days, the cells were detached by treatment for 5 min at 37 °C with 100 mM of phosphate-buffered saline solution (PBS, pH 7.4) containing 0.25 wt% of trypsin and 0.02 wt% of Ethylenediaminetetraacetic acid (EDTA). The cells were subcultured at a density of 2×10^4 cells/cm^2 and cells of the second-passage at sub-confluence were used for all the experiments.

Cell seeding into gelatin-β-TCP scaffolds

MSC were seeded into the gelatin-β-TCP scaffolds by an agitated seeding method because it is

demonstrated that the method was effective in seeding cells homogeneously throughout 3-dimensional porous scaffolds [32, 33]. Briefly, 500 μl of cell suspension (2×10^6 cells/ml) and the scaffold were placed in 5-ml tubes with 12 mm of inner diameter (2236-012, IWAKI Glass Co. Ltd., Chiba, Japan) and agitated on an orbital shaker (ORBITAL SHAKER, Bellco Glass, Inc.) at 300 rpm for 6 hr. The scaffolds homogeneously seeded with MSC were thoroughly washed with PBS to exclude non-adherent cells. The cell-seeded scaffolds were used for cell culture by a static or stirring method.

Cell culture of cell-seeded gelatin-β-TCP scaffolds

The cell-seeded gelatin-β-TCP scaffolds were cultured in a tissue culture plate (static culture method), or spinner flask (stirring culture method). For the static culture, the cell-seeded scaffolds were placed into 12 well multi-well tissue culture plates (3815-012, IWAKI Glass Co. Ltd., Chiba, Japan). The scaffold was incubated in DMEM supplemented with 15 % FCS, 10 nM dexamethasone, 50 μg/ml ascorbic acid, and 10 mM β-glycerophosphate (osteogenic differentiation medium) at 37 °C in a 5 % CO_2-95 % air atomsphere. For the stirring culture, six of the cell-seeded scaffolds were spired by one needle and immobilized in the spinner flasks (1965-00100, Bellco Glass, Inc.). The spinner flask was filled with 150 ml of osteogenic differentiation medium and the stirring rate was 50 rpm. For both the methods, cell culture was performed with the medium change of every 3 days. Change in the volume of gelatin scaffolds with or without β-TCP incorporation was determined by measuring the dimension of scaffolds on a micrometer (500-444, Mitutoyo, Kanagawa, Japan) during cell culture. The number of scaffolds used for each experimental group was 3 and measurement was performed 3 times independently.

SEM observation of cell-seeded gelatin-β-TCP scaffolds

The gelatin scaffolds seeded with cells were fixed with 2.5 wt% glutaraldehyde solution in PBS. After PBS rinsing and the subsequent dehydration with ethanol aqueous solutions at DDW/ethanol ratios of 70/30, 50/50, 30/70, 20/80, 10/90, and 0/100, the dehydrated samples were immersed in *t*-butanol and dried on a critical point dryer (ES-2030, Hitachi, Japan). After sputter coating with gold/palladium, the samples

were viewed on a scanning electron microscope (SEM, S2380N, Hitachi, Japan).

DNA assay

The number of MSC attached to the gelatin-β-TCP scaffolds was determined by the fluorometric quantification of cellular DNA according to the method reported by Rao et al. [34]. Briefly, the cell-seeded scaffolds were washed with PBS and stored at –30 °C until assay. After thawing, the samples were lysed in 30 mM sodium citrate-buffered saline solution (SSC) (pH 7.4) containing 0.2 mg/ml sodium dodecylsulfate (SDS) at 37 °C for 12 hr with occasional mixing. The cell lysate (100 μl) was mixed with the SSC buffer (400 μl) in a glass tube. After mixing with a dye solution (500 μl; 30 mM SSC, 1 μg/ml Hoechst 33258 dye), the fluorescent intensity of mixed solution was measured in a fluorescence spectrometer (F-2000, Hitachi, Japan) at the excitation and emission wavelengths of 355 and 460 nm, respectively. The calibration curve between the DNA and cell number was prepared by use of cells of known numbers. The DNA assay was done 3 times independently for every experimental sample unless otherwise mentioned.

Biochemical and histological evaluations of cell seeded gelatin-β-TCP scaffolds

The cell lysates prepared by the similar procedure described above, were centrifuged at 12,000 rpm and 4 °C for 15 min and the ALP activity of supernatant obtained was determined by a *p*-nitrophenylphosphate method [35].

To determine the osteocalcin content of cells, the cells cultured were mixed in 1 ml of 40 % formic acid for 12 hr to decalcify by using a mixer (MIX-101, IWAKI Glass Co. Ltd., Chiba, Japan). After decalcified samples were centrifuged at 10,000 rpm, the supernatant contained the cell extraction was applied to the gel filtration of Sephadex^{TM} G-25 column (PD-10, Amersham Pharmacia biotech AB, Sweden). The resulting solution was freeze-dried and subjected to an osteocalcin rat enzyme-linked immunosorbent assay (ELISA) (rat osteocalcin ELISA system, Amersham Biosciences, Tokyo, Japan).

The gelatin-β-TCP scaffolds were fixed in 10 wt% neutral-buffered formalin solution and

similarly dehydrated, immersed in xylene, and embedded in paraffin. The samples were sectioned at 4 μm thickness and stained by hematoxylin and eosin (HE) to histologically view on a optical microscopy (AX-80, Olympus, Japan).

Statistical analysis

All the data were analyzed by Fisher's LSD test for multiple comparison and the statistical significance was accepted at $p < 0.05$. Experimental results were expressed as the means ± the standard deviation of the mean.

RESULTS

Characterization of gelatin-β-TCP scaffolds

Figure 7-1 shows the scanning electron micrographs of gelatin scaffolds with or without β-TCP incorporation. Irrespective of the β-TCP amount, the similar intra-structure of scaffolds was observed, while β-TCP granules were homogeneously localized in the gelatin walls of the scaffolds. Every scaffold had an interconnected porous structure with the pore size range of 180-200 μm and the porosity around 96 %. The compression modulus of scaffolds increased with an increase in the amount of β-TCP incorporated (Table 7-1).

Attachment and proliferation of MSC in gelatin-β-TCP scaffolds

Figure 7-2 shows the scanning electron micrographs of gelatin scaffolds incorporating different amounts of β-TCP 6 hr after MSC seeding. The cells attached to all the types of scaffolds at a similar number, while they were uniformly distributed throughout the scaffolds. The morphology of cells attached depended on the scaffold type. The cells attached showed flatter morphology with an increase in the β-TCP amount. For the gelatin scaffold without β-TCP, the shape of MSC attached was spherical.

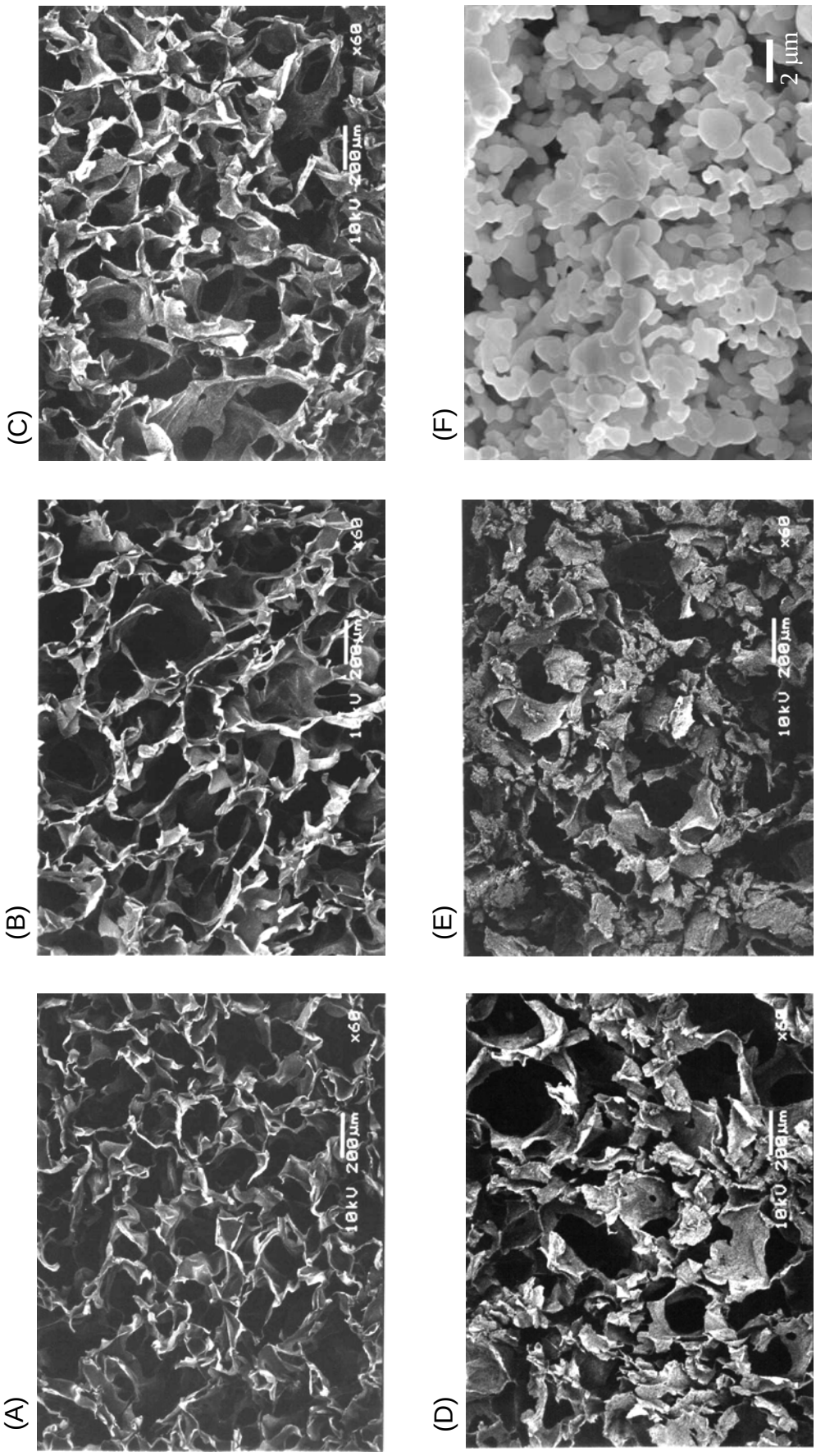

Figure 7-1. Scanning electron micrographs of gelatin scaffolds incorporating 0 (A), 25 (B), 50 (C), 75 (D), and 90 wt% (E) of β-TCP, and β-TCP granules (F)

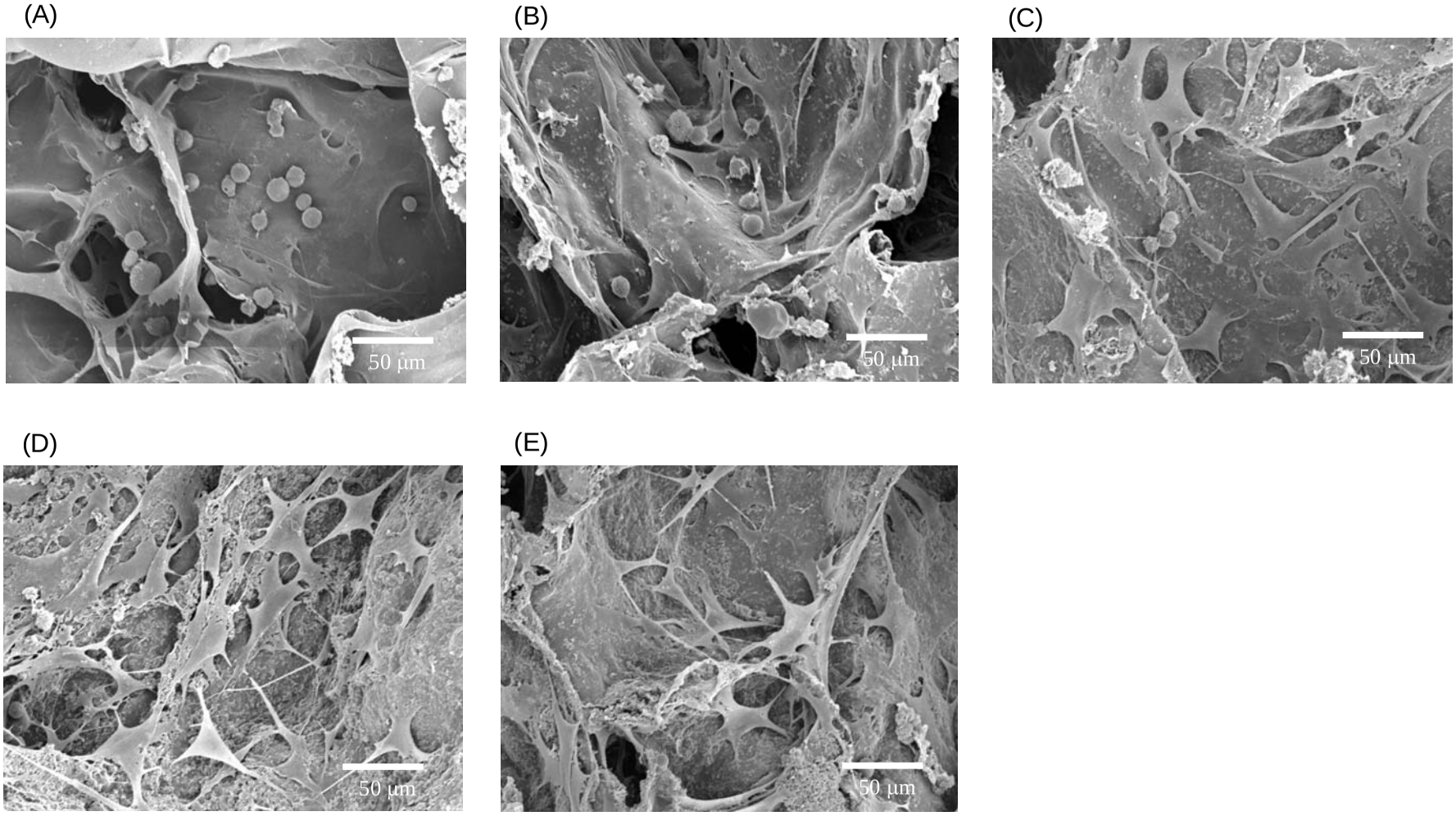

Figure 7-2. Scanning electron micrographs of MSC attached to gelatin scaffolds incorporating 0 (A), 25 (B), 50 (C), 75 (D), and 90 wt% (E) of β-TCP 6 hr after cell seeding by the agitated method. The number of cells applied is 5×10^6 cells/scaffolds

Figure 7-3 shows the proliferation profiles of MSC in the gelatin-β-TCP scaffolds by the static or stirring culture method. MSC proliferated in every scaffold, although the profile depended on the β-TCP amount and culture method. For the static culture, the rate of MSC proliferation increased with the increased β-TCP amount and became significant large when the β-TCP amount was 75 or 90 wt%. On the other hands, MSC proliferation for the initial 1 week was fast by the stirring method compared with that by the static method, although it tended to level off thereafter. The initial proliferation rate was significantly large for the scaffold incorporating 75 or 90 wt% of β-TCP.

Volume change of gelatin-β-TCP scaffolds during culture

Figure 7-4 shows the volume change of gelatin-β-TCP scaffolds during the static and stirring cultures. The scaffold volume changed with culture, although the time profile depended on the β-TCP amount and culture method. For both the culture methods, volume of every scaffold decreased for the initial 1 week. The decreased extent of volume increased with a decrease in the β-TCP amount and the volume decrease was significantly large when the β-TCP amount of scaffolds was lower than 75 wt%. The gelatin scaffold incorporating 90 wt% of β-TCP maintained about 95 % of their initial volume even after 4 weeks culture. No difference in the time profile of scaffolds volume change between the static and stirring methods was observed.

Cell density of MSC cultured in gelatin-β-TCP scaffolds

Figure 7-5 shows the time course of MSC density cultured in gelatin-β-TCP scaffolds by the static and stirring methods. The cell density increased with culture time although the time profile depended on the β-TCP amounts and culture method. For the static culture, when compared at a same culture time, the cell density increased with decreased β-TCP amount and became significant for the gelatin sponges incorporating 75 and 90 wt% of β-TCP. For the stirring culture, cell density in every scaffold increased for the initial 1 week after culture and became significant for the gelatin scaffold incorporating 75 and 90 wt% of β-TCP 3 and 4 weeks after culture.

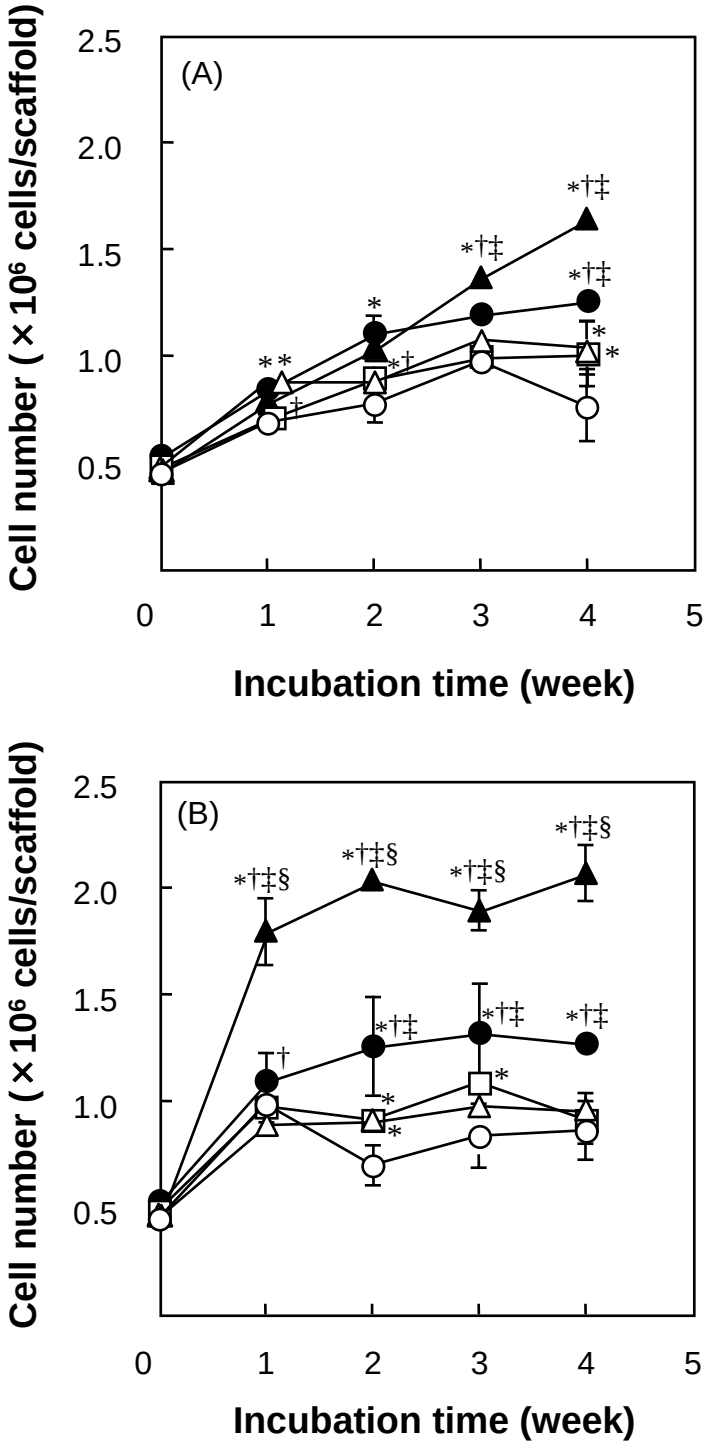

Figure 7-3. Time course of MSC proliferation in the gelatin scaffolds incorporating 0 (○), 25 (△), 50 (□), 75 (●), 90 wt% (▲) of β-TCP by the static (A) or stirring culture method (B). $^{*}p < 0.05$; significant against the cell attached to the gelatin scaffold incorporating 0 wt% of β-TCP. $^{\dagger}p < 0.05$; significant against the cell attached to the gelatin scaffolds combined with 25 wt% of β-TCP. $^{\ddagger}p < 0.05$; significant against the cell attached to the gelatin scaffolds combined with 50 wt% of β-TCP. $^{\S}p < 0.05$; significant against the cell attached to the gelatin scaffolds combined with 75 wt% of β-TCP.

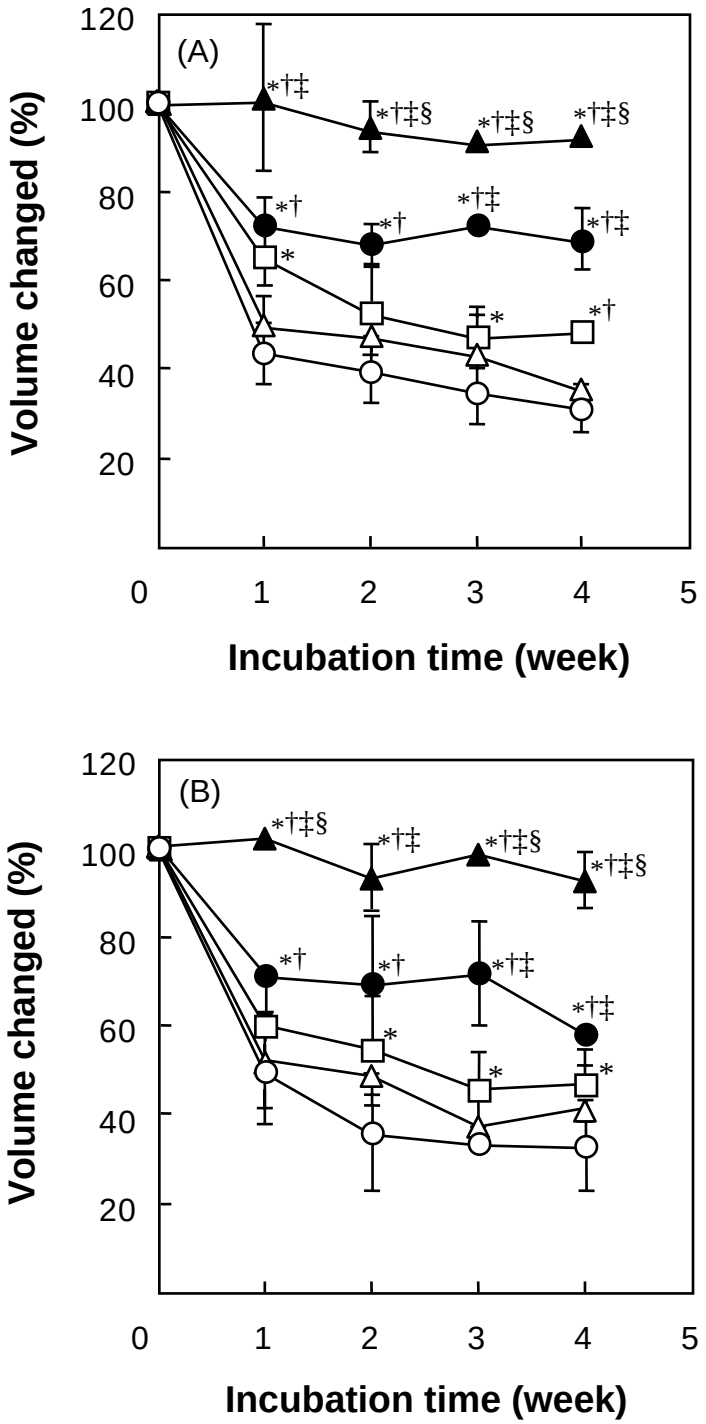

Figure 7-4. Time course of the volume change of gelatin scaffolds incorporating 0 (○), 25 (△), 50 (□), 75 (●), 90 wt% (▲) of β-TCP during the culture with MSC by the static (A) or stirring culture method (B). $^{*}p < 0.05$; significant against the cell attached to the gelatin scaffold incorporating 0 wt% of β-TCP. $^{\dagger}p < 0.05$; significant against the cell attached to the gelatin scaffolds combined with 25 wt% of β-TCP. $^{\ddagger}p < 0.05$; significant against the cell attached to the gelatin scaffolds combined with 50 wt% of β-TCP. $^{\S}p < 0.05$; significant against the cell attached to the gelatin scaffolds combined with 75 wt% of β-TCP.

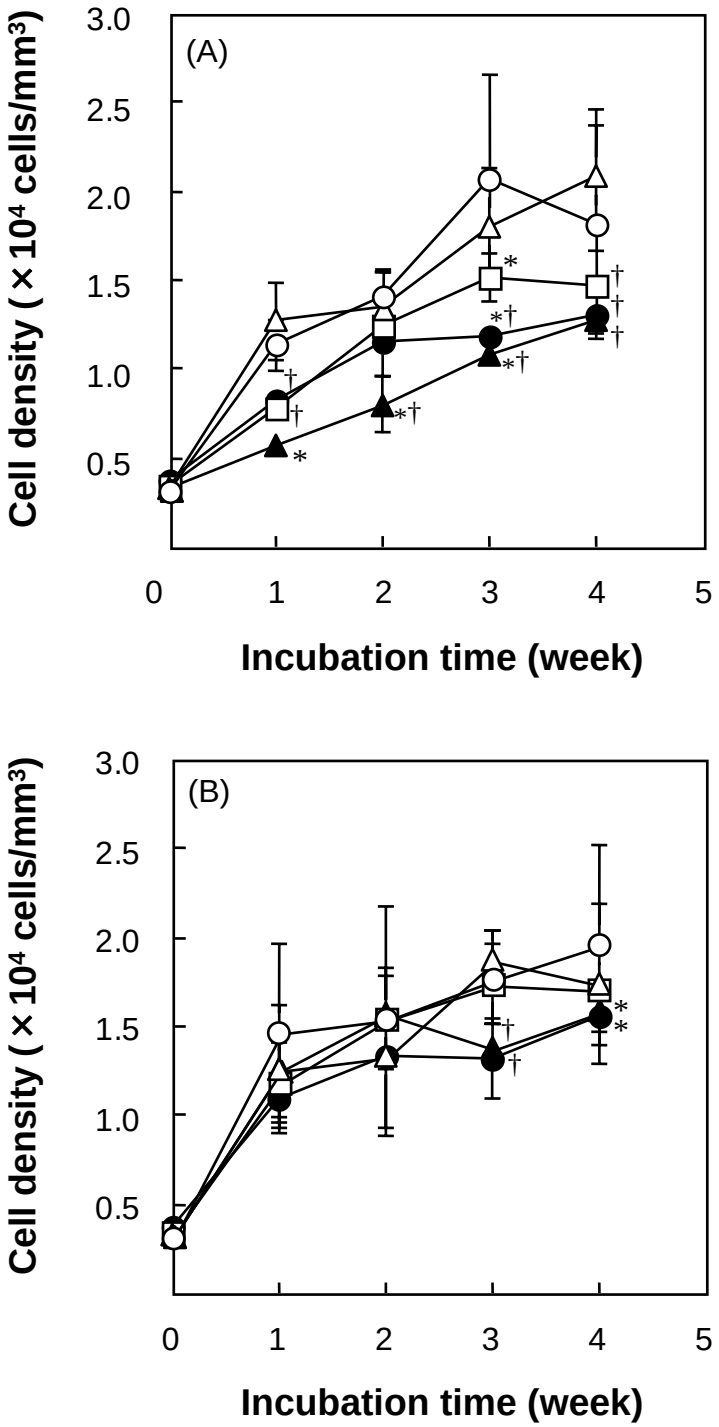

Figure 7-5. Time course of the volume change of gelatin scaffolds incorporating 0 (○), 25 (△), 50 (□), 75 (●), 90 wt% (▲) of β-TCP during the culture with MSC by the static (A) or stirring culture method (B). $^{*}p < 0.05$; significant against the cell attached to the gelatin scaffold incorporating 0 wt% of β-TCP. $^{\dagger}p < 0.05$; significant against the cell attached to the gelatin scaffolds combined with 25 wt% of β-TCP. $^{\ddagger}p < 0.05$; significant against the cell attached to the gelatin scaffolds combined with 50 wt% of β-TCP. $^{\S}p < 0.05$; significant against the cell attached to the gelatin scaffolds combined with 75 wt% of β-TCP.

Osteogenic differentiation of MSC cultured in gelatin-β-TCP scaffolds

Figure 7-6 (A) shows the ALP activity of MSC cultured in gelatin-β-TCP scaffolds 2 weeks after the static and stirring methods. When MSC were cultured by the stirring method, the ALP activity of cells was significantly large compared with that of the static method and became maximum for the scaffold incorporating 50 wt% of β-TCP, while the scaffolds with the larger and smaller amounts of β-TCP showed lower ALP activity. On the contrary, for the static culture, no effect of the β-TCP amount on the ALP activity was observed.

Figure 7-6 (B) shows the osteocalcin content of MSC cultured in gelatin scaffold incorporating β-TCP 4 weeks after the static and stirring methods. The gelatin scaffold incorporating 50 wt% of β-TCP exhibited high osteocalcin content compared with other scaffolds, irrespective of the culture method. The osteocalcin content of MSC cultured in the scaffolds incorporating 25-75 wt% of β-TCP cultured by the stirring method was high compared with that by the static method.

Histological observation of gelatin-β-TCP scaffolds after the static or stirring culture

Figure 7-7 shows the histological cross-sections of gelatin scaffolds containing 50 wt% of β-TCP 4 weeks after the static or stirring culture. As shown in the full cross-section of sponges (Figures 7-7 (A) and (C)), bone formation was observed in the peripheral part of scaffold, irrespective of the culture method. MSC were homogeneously distributed and proliferated in the inner portion of scaffold, although new bone was not formed. Significant bone formation was observed at the peripheral portion of gelatin scaffold cultured by the stirring method compared that of the static method.

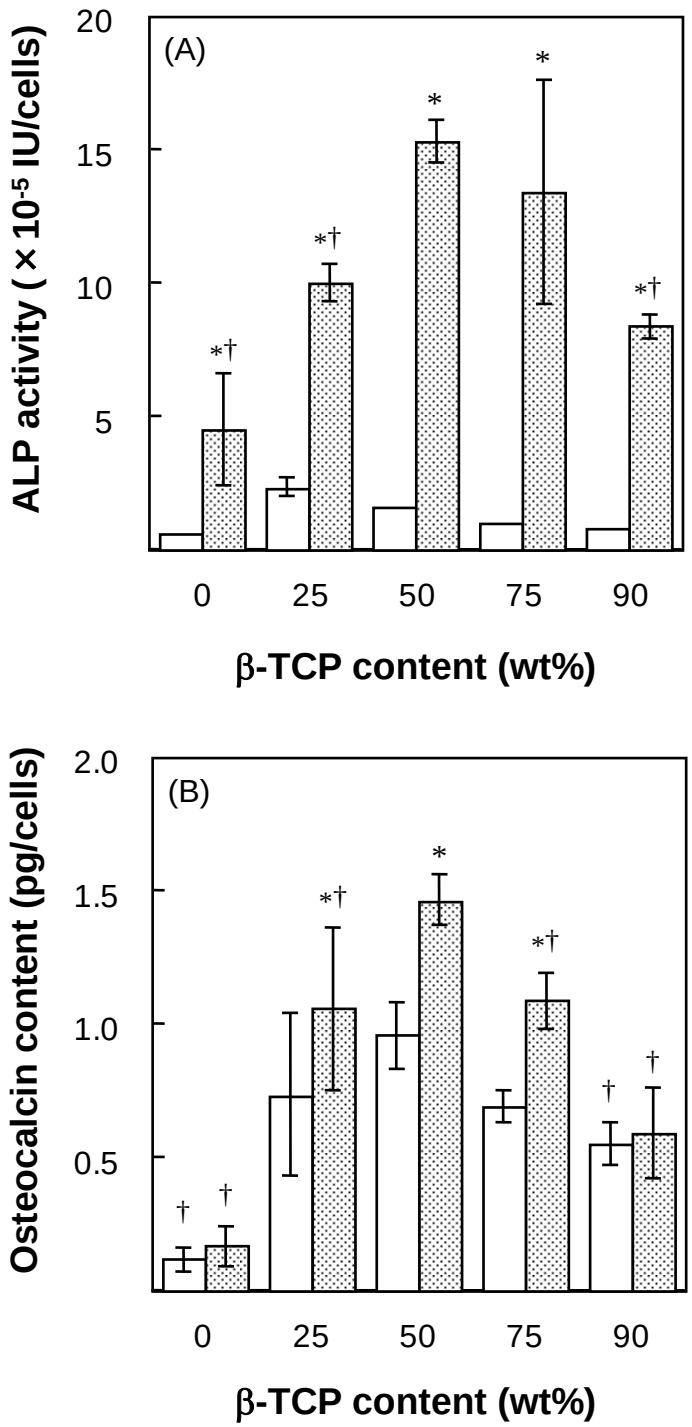

Figure 7-6. ALP activity (A) and osteocalcin content (B) of MSC in gelatin scaffolds incorporating various amounts of β-TCP 2 and 4 weeks after the culture in the osteogenic differentiation medium by the static (□) or stirring method (▨). $^{*}p < 0.05$; significant against the ALP activity or osteocalcin content of MSC cultured by the static method at the corresponding β-TCP content. $^{\dagger}p < 0.05$; significant against the ALP activity or osteocalcin content of MSC in the gelatin scaffold incorporating 50 wt% of β-TCP at the corresponding culture method.

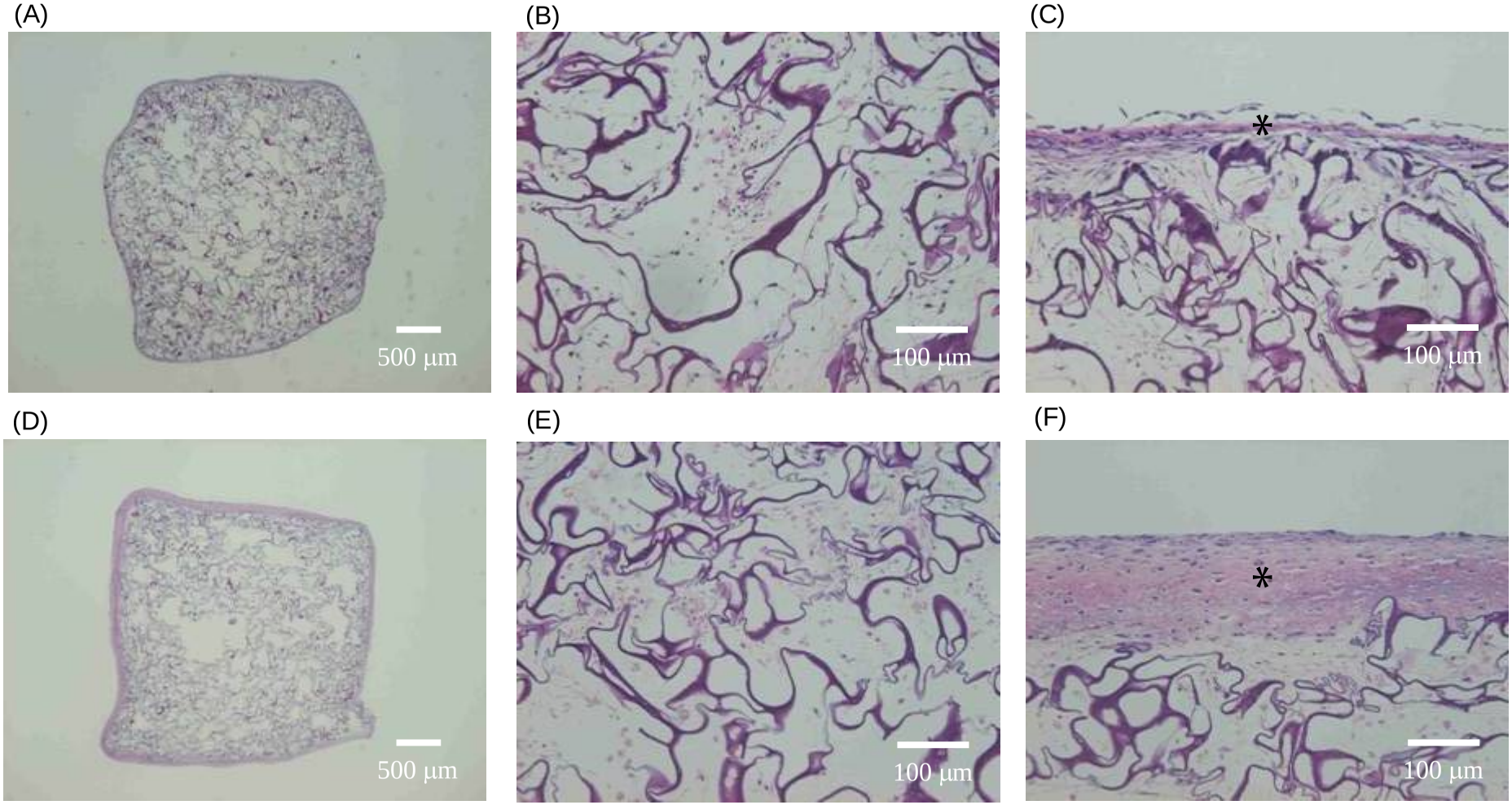

Figure 7-7. Histological cross-sections of MSC attached to gelatin scaffolds incorporating 50 wt% of β-TCP 4 weeks after the culture in the osteogenic medium by the static (A-C) and stirring method (D-F). The scale bar measures 500 μm in full cross section (A and D) and 100 μm in higher magnification views of center in scaffold (B and E) and periphery in scaffold (C and F). Arrows indicate the residual gelatin scaffold incorporating β-TCP. Asterisks indicate the bone newly formed.

DISCUSSION

This chapter demonstrates that the proliferation and differentiation of MSC in the gelatin-β-TCP scaffolds are greatly influenced by the β-TCP amount and culture method. In our previous studies, gelatin has been formulated into the hydrogel of disk, sheet, and microsphere shapes for the release carrier of growth factors [36-38]. They do not have any pore structures necessary for migration, proliferation, and differentiation of cells. It has been recognized that gelatin functions as a substrates for cell adhesion and proliferation [39]. Therefore, the sponge formulation with a pore structure was tried to prepare from gelatin by homogenization of the aqueous solution. This homogenization process has been reported to prepare a synthetic dermal substitute of collagen [40]. The pore size was adjusted at 180-200 μm since the pore size range is suitable for infiltlation of fibroblastic cells into sponge scaffolds, although it can be regulated by the homogenization conditions [41, 42]. As a result, the gelatin sponge obtained functions as a cell scaffold, in addition of the release carrier for the growth factor. For the scaffold preparation, β-TCP which has been extensively explored as one osteogenic substrate was combined. β-TCP incorporation enabled the gelatin scaffold to increase the compression modulus without any change in the pore structure. The compression modulus of scaffolds increased with the increased β-TCP amount (Table 7-1). The scaffold of sponge shape has been used for cell scaffold from the viewpoint of superior property of cell infiltlation. However, the compression modulus is not strong enough for every application to cell scaffold. In clinical cases, porous HAp and β-TCP are often used because of their inherent osteogenic property [8-17]. However, the bioceramics have some disadvantages, such as poor biodegradability and brittle nature. It is also difficult to change the shape of materials during the operation to apply them to different sites. Combination of bioceramics with gelatin is one of the effective strategies to overcome the disadvantages. Incorporation of biodegradable β-TCP granules gave an osteogenic property as well as enhanced resistance to compression to the gelatin sponge without harming the cell compatibility and degradability.

When MSC were cultured in the gelatin-β-TCP scaffolds, the number of MSC proliferated in

the scaffolds increased with an increase in the amount of β-TCP (Figure 7-3). This can be explained in terms of pore space in the scaffolds. As shown in Figure 7-4, the scaffolds deformed with culture time period, although their initial porosity was similar among the scaffolds with different amounts of β-TCP. The deformed extent became smaller for the gelatin scaffold with higher amount of β-TCP incorporated. It is highly conceivable that cells are proliferated in the scaffold with the smaller extent of deformation since there is enough space in the scaffold for cell proliferation. The morphology of cells attached to the sponges also depended on the β-TCP amount and the cell shape became flatter with an increase in the β-TCP amount (Figure 7-2). Incorporation of β-TCP would enhance the compatibility of MSC. This enhanced compatibility may also contribute to enhancement of cells proliferation. MSC proliferated fast for the initial 1 week by the stirring culture compared with the static culture. The number of cells became higher in the scaffolds incorporating 75 and 90 wt% of β-TCP with the stirring culture. This result is due to the improvement of nutrient supply to MSC, in addition of the larger pore space necessary for cell proliferation. The number of cells proliferated by the stirring culture leveled off for the initial 1 week, irrespective of the β-TCP amounts, which is similar to the time profile of sponge deformation (Figure 7-4). This indicates that cell proliferation by the stirring culture was governed by the pore space of scaffolds. On the contrary, in the static culture, MSC gradually proliferated in the scaffold and did not reach to the confluent number even 4 weeks after culture, although the extent of scaffold deformation was similar for both the culture methods. The difference between the two culture methods is the efficiency of oxygen and nutrients supply to cells because the culture medium is circulated in the stirring culture. Taken together, it is likely that cell proliferation in the scaffold was influenced by the oxygen and nutrient supply more strongly. It is reported that the stirring and perfusion cultures enhance mass transfer in the culture medium, and positively function cell proliferation in addition to hydrodynamic or mechanical stimulation to cells [43, 44]. Mechanical strain and fluid shear stress stimulated cells to product prostaglandins, alkaline phosphatase and collagen type I, while they increased the osteoblast proliferation and mineralization [45]. It is conceivable that these phenomena reported may cause enhanced MSC proliferation.

The ALP activity and osteocalcin content of MSC as osteogenic differentiation markers were the highest for the gelatin sponge incorporating 50 wt% of β-TCP 2 and 4 weeks after the stirring culture (Figure 7-6). The osteogenic differentiation of MSC was affected by both the culture method and gelatin/β-TCP composition of scaffolds. The difference in the osteogenic differentiation between the static and stirring culture methods may be explained from the viewpoint of hydrodynamic or mechanical stimulation as described above. Various properties of sponges which may affect the cell proliferation, change with the gelatin/β-TCP composition of the scaffolds. Firstly, the cell density became higher with the decreased β-TCP amount. Goldstein et al. reported that dense cluster cells derived from the bone marrow showed to significantly enhance the differentiation activity compared with dispersed cells [46]. It is possible that the higher cell density promotes the osteogenic differentiation of MSC. We prepared gelatin scaffolds incorporating other ceramics granules with the same size, such as HA, α-TCP, and alumina, at different mixing ratios of gelatin and β-TCP. When MSC were cultured in the scaffolds, the gelatin scaffold incorporating β-TCP exhibited the highest ALP activity among them, although the cell density of all the scaffolds was same (unpublished data). This finding suggests that β-TCP itself functions to enhance the osteogenic differentiation of MSC. Therefore, it is likely that the extent of MSC differentiation became higher with the increased amounts of β-TCP. On the other hand, the cell compatibility to the sponge surface became better with an increase in the β-TCP amount (Figure 7-2). This phenomenon suggests that the β-TCP presence had a biological influence on MSC. Taken together, it is possible that the balance between the cell density of scaffold and the β-TCP action to cells contributes to the extent of MSC differentiation in the scaffold, resulting in the strongest osteogenic differentiation for the gelatin scaffold incorporating 50 wt% of β-TCP.

Simple foaming of gelatin solution permitted the gelatin scaffold of sponge structure not only to facilitate *in vitro* cell seeding and the *in vivo* infiltration of cells from the surroundings, but also to function as the release carrier for growth factor. The release profile of BMP-2 could be readily changed by altering the crosslinking extent in sponge preparation, while it greatly contributes to the BMP-2-induced bone formation [47]. This sponge system is also applicable to the controlled release of other growth factors,

while different combinations of cells and growth factors are being planned in future.

In conclusion, gelatin-β-TCP scaffolds with an average pore size of 180-200 μm were fabricated. MSC attached, proliferated, and differentiated in the sponges, although the morphology and number of MSC attached or the osteogenic differentiation of MSC depended on the β-TCP composition of scaffolds and the culture method. These results will give fundamental information to design the scaffolds suitable to bone tissue engineering.

REFERENCES

1. R. Langer, and J. P. Vacanti, Tissue Engineering, *Science*, **60**, 920-926 (1993).
2. H. Petite, V. Viateau, W. Bensaid, A. Meunier, C. de Pollak, M. Bourguignon, K. Oudina, L. Sedel, and G. Guillemin, Tissue-engineered bone regeneration, *Nat. Biotechnol.*, **18**, 959-963 (2000).
3. D. Zekorn, Intravascular retention, dispersal, excretion and break-down of gelatin plasma substitutes, *Bibl. Haematol.*, **33**, 131-140 (1969).
4. Y. Tabata, Tissue regeneration based on growth factor release, *Tissue Eng.*, **9**, S5-15 (2003).
5. L. Bordenave, J. Caix, B. Basse-Cathalinat, C. Baquey, D. Midy, J. C. Baste, and H. Constans, Experimental evaluation of a gelatin-coated polyester graft used as an arterial substitute, *Biomaterials*, **10**, 235-242 (1989).
6. R. Warocquier-Clerout, Y. S. Lee, J. Penhoat, and M. F. Sigot-Luizard, Comparative behaviour of L-929 fibroblastic and human endothelial cells onto crosslinked protein substrates, *Cytotechnology*, **3**, 259-269 (1990).
7. Z. Ma, C. Gao, Y. Gong, J. Ji, and J. Shen, Immobilization of natural macromolecules on poly-L-lactic acid membrane surface in order to improve its cytocompatibility, *J. Biomed. Mater. Res.*, **63**, 838-847 (2002).
8. Z. Yang, H. Yuan, W. Tong, P. Zou, W. Chen, and X. Zhang, Osteogenesis in extraskeletally implanted porous calcium phosphate ceramics: variability among different kinds of animals, *Biomaterials*, **17**, 2131-2137 (1996).
9. C. Knabe, F. C. Driessens, J. A. Planell, R. Gildenhaar, G. Berger, D. Reif, R. Fitzner, R. J. Radlanski, and U. Gross, Evaluation of calcium phosphates and experimental calcium phosphate bone cements using osteogenic cultures, *J. Biomed. Mater. Res.*, **52**, 498-508 (2000).
10. H. Yuan, Y. Li, J. D. de Bruijn, K. de Groot, and X. Zhang, Tissue responses of calcium phosphate cement: a study in dogs, *Biomaterials*, **21**, 1283-1290 (2000).

11. M. H. Mankani, S. A. Kuznetsov, B. Fowler, A. Kingman, and P. G. Robey, *In vivo* bone formation by human bone marrow stromal cells: effect of carrier particle size and shape, *Biotechnol. Bioeng.*, **72**, 96-107 (2001).

12. E. M. Erbe, J. G. Marx, T. D. Clineff, and L. D. Bellincampi, Potential of an ultraporous beta-tricalcium phosphate synthetic cancellous bone void filler and bone marrow aspirate composite graft, *Eur. Spine J.*, **10**, S141-146 (2001).

13. T. Livingston, P. Ducheyne, and J. Garino, *In vivo* evaluation of a bioactive scaffold for bone tissue engineering, *J. Biomed. Mater. Res.*, **62**, 1-13 (2002).

14. J. S. Boo, Y. Yamada, Y. Okazaki, Y. Hibino, K. Okada, K. Hata, T. Yoshikawa, Y. Sugiura, and M. Ueda, Tissue-engineered bone using mesenchymal stem cells and a biodegradable scaffold, *J. Craniofac. Surg.*, **13**, 231-239 (2002).

15. P. Kasten, R. Luginbuhl, M. van Griensven, T. Barkhausen, C. Krettek, M. Bohner, and U. Bosch, Comparison of human bone marrow stromal cells seeded on calcium-deficient hydroxyapatite, beta-tricalcium phosphate and demineralized bone matrix, *Biomaterials*, **24**, 2593-2603 (2003).

16. H. Shimaoka, Y. Dohi, H. Ohgushi, M. Ikeuchi, M. Okamoto, A. Kudo, T. Kirita, and K. Yonemasu, Recombinant growth/differentiation factor-5 (GDF-5) stimulates osteogenic differentiation of marrow mesenchymal stem cells in porous hydroxyapatite ceramic, *J. Biomed. Mater. Res.*, **68A**, 168-176 (2004).

17. P. Q. Ruhe, H. C. Kroese-Deutman, J. G. Wolke, P. H. Spauwen, and J. A. Jansen, Bone inductive properties of rhBMP-2 loaded porous calcium phosphate cement implants in cranial defects in rabbits, *Biomaterials*, **25**, 2123-2132 (2004).

18. A. A. Ignatius, M. Ohnmacht, L. E. Claes, J. Kreidler, and F. Palm, A composite polymer/tricalcium phosphate membrane for guided bone regeneration in maxillofacial surgery, *J. Biomed. Mater. Res.*, **58**, 564-569 (2001).

19. C. T. Laurencin, M. A. Attawia, L. Q. Lu, M. D. Borden, H. H. Lu, W. J. Gorum, and J. R. Lieberman, Poly(lactide-co-glycolide)/hydroxyapatite delivery of BMP-2-producing cells: a

regional gene therapy approach to bone regeneration, *Biomaterials*, **22**, 1271-1277 (2001).

20. C. Du, F. Z. Cui, X. D. Zhu, and K. de Groot, Three-dimensional nano-HAp/collagen matrix loading with osteogenic cells in organ culture, *J. Biomed. Mater. Res.*, **44**, 407-415 (1999).

21. S. Itoh, M. Kikuchi, Y. Koyama, K. Takakuda, K. Shinomiya, and J. Tanaka, Development of an artificial vertebral body using a novel biomaterial, hydroxyapatite/collagen composite, *Biomaterials*, **23**, 3919-3926 (2002).

22. C. V. Rodrigues, P. Serricella, A. B. Linhares, R. M. Guerdes, R. Borojevic, M. A. Rossi, M. E. Duarte, and M. Farina, Characterization of a bovine collagen-hydroxyapatite composite scaffold for bone tissue engineering, *Biomaterials*, **24**, 4987-4997 (2003).

23. D. Lickorish, J. A. Ramshaw, J. A. Werkmeister, V. Glattaue, and C. R. Howlett, Collagen-hydroxyapatite composite prepared by biomimetic process, *J. Biomed. Mater. Res.*, **68A**, 19-27 (2004).

24. D. P. Lennon, S. E. Haynesworth, D. M. Arm, M. A. Baber, and A. I. Caplan, Dilution of human mesenchymal stem cells with dermal fibroblasts and the effects on *in vitro* and *in vivo* osteochondrogenesis, *Dev. Dyn.*, **219**, 50-62 (2000).

25. A. E. Grigoriadis, J. N. Heersche, and J. E. Aubin, Differentiation of muscle, fat, cartilage, and bone from progenitor cells present in a bone-derived clonal cell population: effect of dexamethasone, *J. Cell Biol.*, **106**, 2139-2151 (1988).

26. H. Ohgushi, V. M. Goldberg, and A. I. Caplan, Repair of bone defects with marrow cells and porous ceramic. Experiments in rats, *Acta Orthop. Scand.*, **60**, 334-339 (1989).

27. B. Johnstone, T. M. Hering, A. I. Caplan, V. M. Goldberg, and J. U. Yoo, *In vitro* chondrogenesis of bone marrow-derived mesenchymal progenitor cells, *Exp. Cell Res.*, **238**, 265-272 (1998).

28. S. P. Bruder, A. A. Kurth, M. Shea, W. C. Hayes, N. Jaiswal, and S. Kadiyala, Bone regeneration by implantation of purified, culture-expanded human mesenchymal stem cells, *J. Orthop. Res.*, **16**, 155-162 (1998).

29. K. Matsuda, S. Suzuki, N. Isshiki, K. Yoshioka, T. Okada, and Y. Ikada, Influence of

glycosaminoglycans on the collagen sponge component of a bilayer artificial skin, *Biomaterials*, **11**, 351-355 (1990).

30. G. Chen, T. Ushida, and T. Tateishi, A biodegradable hybrid sponge nested with collagen microsponges, *J. Biomed. Mater. Res.*, **51**, 273-279 (2000).

31. D. P. Lennon, S. E. Haynesworth, R. G. Young, J. E. Dennis, and A. I. Caplan, A chemically defined medium supports *in vitro* proliferation and maintains the osteochondral potential of rat marrow-derived mesenchymal stem cells, *Exp. Cell Res.*, **219**, 211-222 (1995).

32. B. S. Kim, J. Nikolovski, J. Bonadio, E. Smiley, and D. J. Mooney, Engineered smooth muscle tissues: regulating cell phenotype with the scaffold, *Exp. Cell Res.*, **251**, 318-328 (1999).

33. Y. Takahashi and Y. Tabata, Homogeneous seeding of mesenchymal stem cells into nonwoven fabric for tissue engineering, *Tissue Eng.*, **9**, 931-938 (2003).

34. J. Rao and W. R. Otto, Fluorimetric DNA assay for cell growth estimation, *Anal. Biochem.*, **207**, 186-192 (1992).

35. D. Kobayashi, H. Takita, M. Mizuno, Y. Totsuka, and Y. Kuboki, Time-dependent expression of bone sialoprotein fragments in osteogenesis induced by bone morphogenetic protein, *J. Biochem.*, **119**, 475-481 (1996).

36. Y. Tabata, S. Hijikata, and Y. Ikada, Enhanced vascularization and tissue granuration by basic fibroblast growth factor impregnated in gelatin hydrogels, *J. Control. Rel.*, **31**, 189-199 (1994).

37. A. Iwakura, Y. Tabata, T. Koyama, K. Doi, K. Nishimura, K. Kataoka, M. Fujita, and M. Komeda, Gelatin sheet incorporating basic fibroblast growth factor enhances sternal healing after harvesting bilateral internal thoracic arteries, *J. Thorac. Cardiovasc. Surg.*, **126**, 1113-1120 (2003).

38. K. Kawai, S. Suzuki, Y. Tabata, Y. Ikada, and Y. Nishimura, Accelerated tissue regeneration through incorporation of basic fibroblast growth factor-impregnated gelatin microspheres into artificial dermis, *Biomaterials*, **21**, 489-499 (2000).

39. A. J. Kuijpers, P. B. van Wachem, M. J. van Luyn, J. A. Plantinga, G. H. Engbers, J. Krijgsveld, S.

A. Zaat, J. Dankert, and J. Feijen, *In vivo* compatibility and degradation of crosslinked gelatin gels incorporated in knitted Dacron, *J. Biomed. Mater. Res.*, **51**, 136-145 (2000).

40. S. Suzuki, K. Matsuda, N. Isshiki, Y. Tamada, K. Yoshioka, and Y. Ikada, Clinical evaluation of a new bilayer "artificial skin" composed of collagen sponge and silicone layer, *Br. J. Plast. Surg.*, **43**, 47-54 (1990).

41. J. J. Klawitter and S. F. Hulbert, Application of porous ceramics for the attachment of load bearing internal orthopedic applications, *J. Biomed. Mater. Res. Sympo.*, **2**, 161-229 (1971).

42. B. P. Robinson, J. O. Hollinger, E. H. Szachowicz, and J. Brekke, Calvarial bone repair with porous D,L-polylactide, *Otolaryngol. Head Neck Surg.*, **112**, 707-713 (1995).

43. J. Glowacki, S. Mizuno, J. S. Greenberger, Perfusion enhances functions of bone marrow stromal cells in three-dimensional culture, *Cell Transplant.*, **7**, 319-326 (1998).

44. L. Meinel, V. Karageorgiou, R. Fajardo, B. Snyder, V. Shinde-Patil, L. Zichner, D. Kaplan, R. Langer, and G. Vunjak-Novakovic, Bone tissue engineering using human mesenchymal stem cells: effects of scaffold material and medium flow, *Ann. Biomed. Eng.*, **32**, 112-122 (2004).

45. V. I. Sikavitsas, J. S. Temenoff, and A. G. Mikos, Biomaterials and bone mechanotransduction, *Biomaterials*, **22**, 2581-2593 (2001).

46. A. S. Goldstein, Effect of seeding osteoprogenitor cells as dense clusters on cell growth and differentiation, *Tissue Eng.*, **7**, 817-827 (2001).

47. M. Yamamoto, Y. Takahashi, and Y. Tabata, Controlled release by biodegradable hydrogels enhances the ectopic bone formation of bone morphogenetic protein, *Biomaterials*, **24**, 4375-4383 (2003).

Chapter 8

Bone regeneration at an X-ray irradiated ulna defect of rabbits by biodegradable scaffolds of gelatin and ß-TCP enabling bone morphogenetic protein-2 release plus autologous bone marrow

INTRODUCTION

After a large bone is surgically resected for tumor, X-ray irradiation for the surrounding tissue is often performed to prevent the recurrence and metastases of tumor. This tissue irradiation is effective for the surgical treatment of cancer. Although this irradiation treatment brings about good, it is reported that X-ray irradiation eventually induces osteoradionecrosis, such as the suppression of neovascularization, cell proliferation, collagen synthesis, and alkaline phosphatase activity [1, 2]. Consequently, bone healing at the site of tumor resection is often impaired. From the clinical viewpoint, such an impaired healing is a serious problem to be resolved [3]. Therefore, it is practically necessary to develop a technology to induce bone regeneration even under unhealthy conditions X-ray irradiated.

Bone tissue engineering has been attracted much attention as a new therapeutic technology to induce the tissue regeneration at the large bone defect, while it may substitute for the conventional autograft or allograft treatment [4, 5]. Bone regeneration has been achieved by making use of osteoinductive growth factors, osteogenic cells, and the scaffolds or their combination. It has been demonstrated that a combination of the scaffold with cells or an osteoinductive growth factor provides an appropriate environment for osteoinductivity [6, 7].

As scaffolds for bone regeneration, bioactive calcium phosphates, such as hydroxyapatite (HAp)

and ß-tricalcium phosphate (ß-TCP), have been intensively investigated because it is well recognized that they are compatible to the natural bone tissue and osteoconductive [8, 9]. However, bioactive calcium phosphate itself is of brittle nature and low biodegradability. As one trial to tackle these problems, we have prepared biodegradable scaffolds from gelatin and ß-TCP (gelatin-ß-TCP scaffolds), and investigated their feasibility in the scaffold for bone regeneration *in vitro*. The attachment, proliferation, and osteogenic differentiation of mesenchymal stem cells (MSC) were observed although the extent was influenced by the composition of gelatin and ß-TCP in scaffold [11]. Among osteoinductive growth factors, bone morphogenetic protein (BMP) has been applied to induce bone regeneration at the critical defect as large as impossible to naturally repair [12-14]. However, BMP administrated in the solution form does not always expect the therapeutic efficacy in bone regeneration because of the *in vivo* short half-life. The gelatin-ß-TCP scaffolds could release BMP-2 in a controlled fashion, and the controlled release of BMP-2 induced *in vivo* bone regeneration at a bone defect [15] and ectopic bone formation [10]. These findings indicate that the gelatin-ß-TCP scaffolds can function not only as a cell scaffold for MSC, but also as the release carrier of BMP-2. However, to evaluate the osteogenic activity of the scaffold, normal animals were used in healthy conditions. From the clinical viewpoint, it is necessary to experimentally confirm whether or not the gelatin-β-TCP scaffold can function well to induce bone regeneration even in an unhealthy condition.

The objective of this study is to evaluate the feasibility of the gelatin-ß-TCP scaffold as the scaffold to enhance bone regeneration at a segmental ulna defect of rabbits X-ray irradiated. The gelatin-ß-TCP scaffold incorporating BMP-2 for the controlled release with or without the combination of autologous bone marrow was implanted into the ulna defect and the bone regeneration activity at the defect was assessed in terms of the histological and computed tomographic examinations.

EXPERIMENTAL

Materials

A gelatin sample with an isoelectric point (IEP) of 9.0, isolated from the porcine skin with an acidic process, was kindly supplied from Nitta Gelatin Co., Osaka, Japan. ß-Tricalcium phosphate (ß-TCP) granules (the average diameter = 2.89 μm, the surface area = 3.22 m^2/g, the density = 2.640 g/cm^3, the Ca/P=1.50, the purity = 99.6 %) were obtained from Taihei Chemical Industries, Nara, Japan. Other chemicals were purchased from Wako Pure Chemical Industries, Osaka, Japan and used without further purification.

Scaffolds

Gelatin scaffolds incorporating ß-TCP (gelatin-ß-TCP scaffolds) were prepared by chemical crosslinking of gelatin with glutaraldehyde in the presence of ß-TCP according to the previous study [10]. When mesenchymal stem cells (MSC) were cultured in the gelatin-ß-TCP scaffolds with an average pore size of 180-200 μm, both the ALP activity and osteocalcin content became maximum for the scaffold with a ß-TCP amount of 50 wt% [11]. Based on the data, the gelatin scaffold incorporating 50 wt% of β-TCP was used in this study. Briefly, 4.29 wt% aqueous solution of gelatin containing the same amount of ß-TCP granules (70 ml) was mixed at 5,000 rpm at 37 °C for 3 min by using a homogenizer (ED-12, Nihonseiki Co., Tokyo, Japan). After addition of 2.17 wt% of glutaraldehyde aqueous solution (30 ml), the mixed solution was further mixed for 15 sec by the homogenizer. The resulting solution was cast into a polypropylene dish of 138×138 cm^2 and 5 mm depth, followed by leaving at 4 °C for 12 hr for gelatin crosslinking. Then, the crosslinked gelatin hydrogels with ß-TCP granules homogeneously dispersed were placed into 100 mM of aqueous glycine solution at 37 °C for 1 hr to block the residual aldehyde

groups of glutaraldehyde. Following complete washing with double distilled water (DDW), the hydrogels were freeze-dried and cut into a square disk shape (20×5×5 mm^3). When measured by the methods reported previously [16, 17], the average pore size and porosity of scaffolds were 180 μm and 95.9 %, respectively.

Preparation of gelatin-β-TCP scaffolds incorporating BMP-2 with or without bone marrow combination

To prepare gelatin-β-TCP scaffolds incorporating BMP-2, 170 μl of phosphate-buffered saline solution (PBS, pH 7.5) containing 17 μg of BMP-2 was dropped onto one freeze-dried scaffold, followed by leaving it at 4 °C overnight to allow to swell the scaffold by the solution. The resulting scaffold was used without washing as the gelatin-β-TCP scaffold incorporating BMP-2. Similarly, 170 μl of BMP-2-free PBS was impregnated into one gelatin-β-TCP scaffold to obtain the BMP-2-free, empty gelatin-β-TCP scaffold.

To combine the gelatin-β-TCP scaffold incorporating BMP-2 prepared with autologous bone marrow of rabbits, skeletally mature New Zealand white rabbits (20-week age, male, 3.5 kg, Shimizu Laboratory, Supply Inc., Japan) were used. A 2 cm-length supermedial incision of the rabbits which will be used to prepare a segmental bone defect for bone evaluation was made, and the tissue overlying the diaphysis of the tibia was dissected under anesthetization with xylazine (5 mg/kg) and ketamine (25 mg/kg). A hole of approximately 2 mm in a diameter was made by an electric drill at supermedial port of tibia, and the bone marrow was aspirated with a syringe with an 18-gauge needle. Then, the bone marrow aspirate (500 μl) was carefully inoculated into the gelatin-ß-TCP scaffold incorporating BMP-2 as homogeneously as possible, followed by leaving it for 1 hr to obtain the gelatin-β-TCP scaffold incorporating BMP-2 combined with autologous bone marrow.

Surgical procedure to evaluate bone regeneration at the ulna defect of rabbits with or without X-ray irradiation

In vivo bone regeneration experiment was performed by use of a segmental ulna defect model of rabbits according to the surgical procedure previously reported [18] under the Institutional Guidelines of Kyoto University on Animal Experimentation. The right forelimb of rabbits was X-ray irradiated and the contralateral left one was not irradiated. Briefly, X-ray irradiation was carried out to the right ulna, radius, and the surrounding soft tissues using an X-ray source (MI-201, Shimadzu, Kyoto, Japan) at 250 kVP and 16 mA with a 0.5-mm Cu filter at a dose of 5 Gy/fraction over an 8-week period (the total dose = 40 Gy) under the same anesthetization conditions described above. Following the rabbits irradiated were carefully observed for one month after the last irradiation in terms of skin ulcerization and health conditions, a 4 cm-length supermedial incision was made and the tissue overlying the radius diaphysis was dissected under anesthetization. A segmental defect (20 mm length) was prepared in the radius with a surgical oscillating saw supplemented by copious sterile saline water irrigation. The experimental samples applied to the ulna defects of rabbits with and without X-ray irradiation were the gelatin-ß-TCP scaffold incorporating 17 μg of BMP-2 (BMP), the gelatin-ß-TCP scaffold incorporating 17 μg of BMP-2 with 500 μl of autologous bone marrow harvested from the tibia (BMP-BM), and the BMP-2-free, empty gelatin-ß-TCP scaffold (control) as shown in Table 8-1. Fixation of the ostectomized bone was not necessary due to the fibro-osseous union between the ulna and radius located distal and proximal to the surgical site. The soft tissue was approximated with interrupted 4-0 Vicryl^{TM} (Ethicon Inc., Somerville, NJ) and the skin was closed with 3-0 silk sutures. At 6 weeks postoperatively, all the animals were killed by the overdose administration of anesthetic agents. The radius-ulna complex containing the defect was taken out, fixed in 10 wt% neutral phosphate-buffered formalin solution to assess bone regeneration.

Table 8-1. Overall experimental design for *in vivo* evaluation of the bone regeneration at the rabbit ulna with or without X-ray irradiation.

Experimental group	Application	BMP dose (μg/site)	Number of animals	
			Radiation	Non-radiation
Control	Empty gelatin-β-TCP scaffold	0	3	3
BMP	Gelatin-β-TCP scaffold incorporating BMP-2	17	3	3
BMP-BM	Gelatin-β-TCP scaffold incorporating BMP-2 plus autologous bone marrow	17	3	3

Assessment of bone regeneration

Bone regeneration at the ulna defect was assessed by micro computed tomography (μCT), peripheral quantitative computed tomography (pQCT), and histological examinations. The three-dimensinal images of bone regeneration were visualized by μCT (SMX-100T, Shimadzu, Kyoto, Japan) at 32 kVP and 35 μA with a resolution of 58.7 μm.

The total bone mineral content (BMC) of each bone defect was measured by using pQCT (XCT Research SA+, Stratec Medizintechnik, GmbH, Birkenfeld, Germany) scanning at 80×80×460 μm voxel sizes. This instrument was calibrated with a phantom of known mineral content according to the manufacture's instruction.

Bone specimens were placed into 10 % neutral phosphate-buffered formalin solution, decalcified with 10 % formic acid, and processed for the paraffin embedding. The histological sections of 3 μm in thickness were prepared and stained with hematoxylin and eosin to view by a light microscopy (AX-80T, Olympus, Tokyo, Japan).

Statistical Analysis

All the data were statistically analyzed using Fisher's least significant difference test for multiple comparisons and statistical significance was accepted to be less than 0.05. The experimental results were expressed as the mean ± the standard deviation of the mean.

RESULTS

μCT measurement of rabbit ulna defects

Figure 8-1 shows the μCT images of rabbit ulna defects with or without X-ray irradiation 6 weeks after different applications of gelatin-ß-TCP scaffolds. Irrespective of X-ray irradiation, bone regeneration at the defect was detected for the BMP-BM group, and the osseous bridging from the proximal to the distal host tissue was also detected (Figures 8-1I - 1L). The BMP group induced bone regeneration throughout the whole area of ulna defect in the non-irradiation case and the ossess bridging was observed (Figures 8-1E and 1F), while the bone regeneration was suppressed by X-ray irradiation (Figures 8-1G and 1H). On the contrary, no bone regeneration was observed at the bone defect both X-ray irradiated and non-irradiated for the control group (Figures 8-1A - 1D).

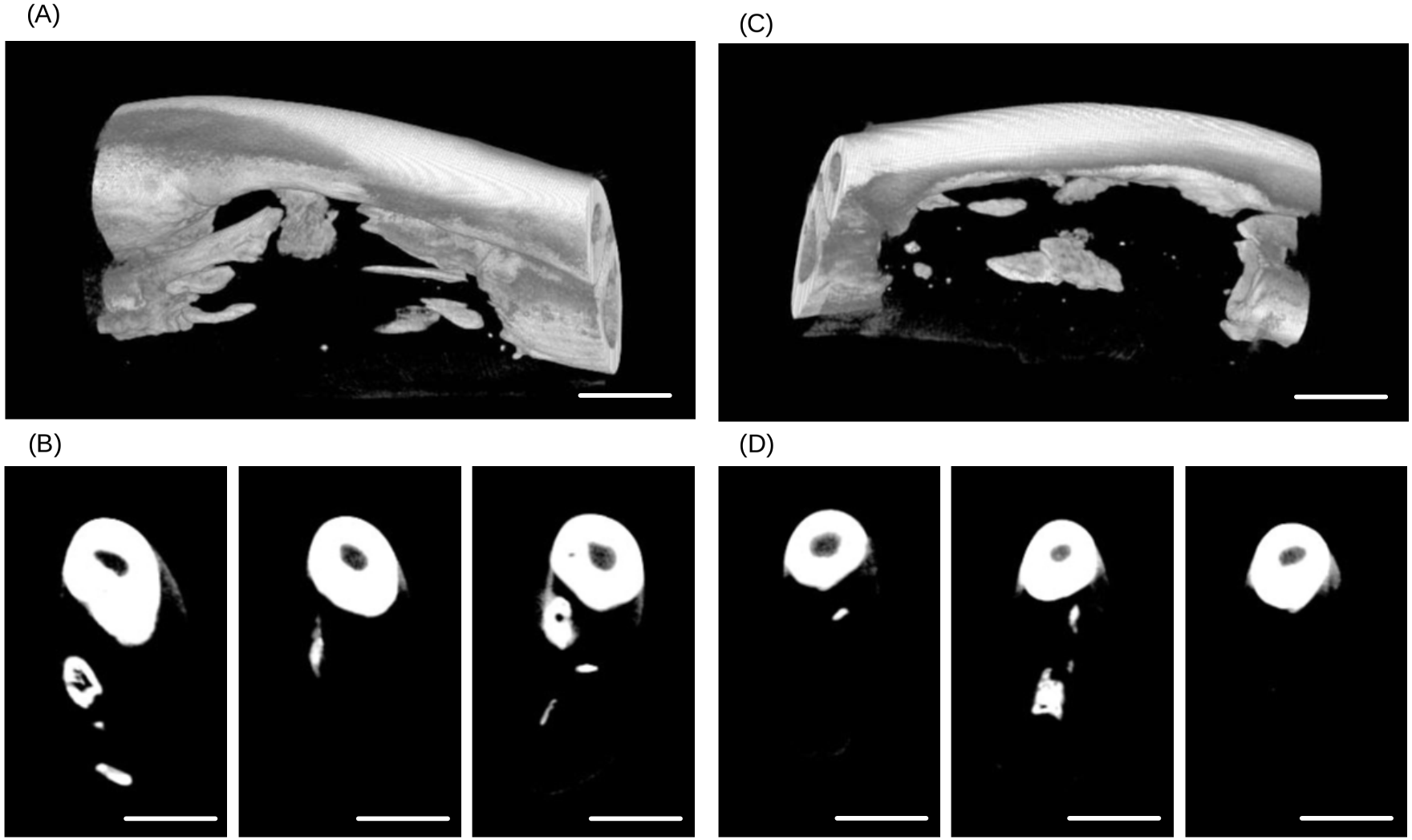

Figure 8-1. μCT images of longitudinal (A, C, E, G, I, and K) and cross-sections (B, D, F, H, J, and L) of rabbit ulna defects with (C, D, G, H, K, and L) and without X-ray irradiation (A, B, E, F, I, and J) 6 weeks after application of empty gelatin-ß-TCP scaffolds (control) (A-D), gelatin-ß-TCP scaffolds incorporating BMP-2 (BMP) (E-H), and gelatin-ß-TCP scaffolds incorporating BMP-2 plus bone marrow (BMP-BM) (I-L). The 3 cross-sectional images from left to right indicate the section at distal, center, and proximal positions in ulna defects. Every bar corresponds to 1 mm length.

Figure 8-1. (Continued).

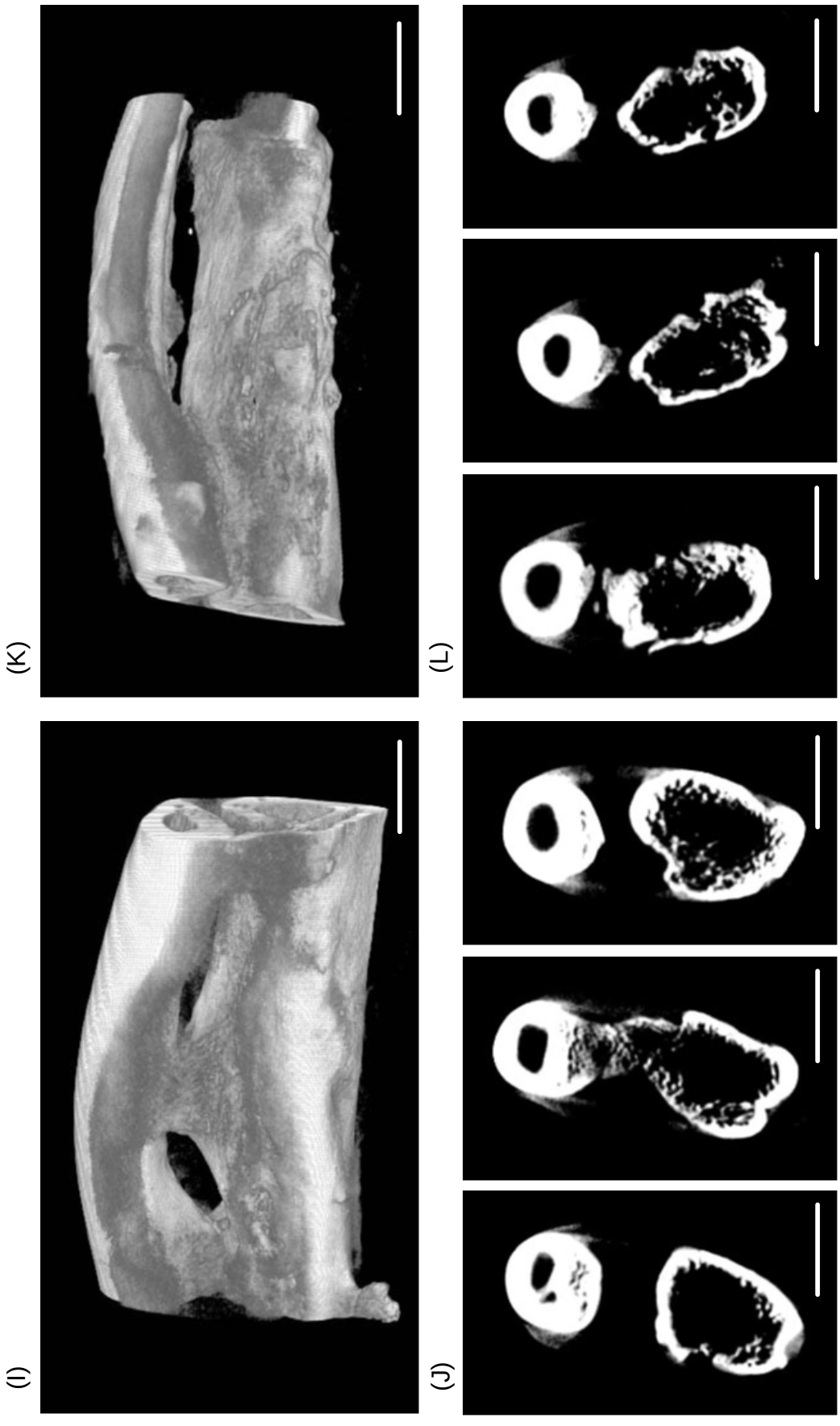

Figure 8-1. (Continued).

Histological evaluation

Figure 8-2 shows the histological sections of rabbit ulna defects 6 weeks after different applications of gelatin-ß-TCP scaffolds. The BMP-BM group exhibited new bone regeneration at the ulna defect and osseous bridging between the proximal and distal host bone tissue, irrespective of X-ray irradiation treatment (Figures 8-2E and 2F). Especially, regeneration of cortex-like bone was found at the peripheral area of the ulna bone for the BMP-BM group. New bone regeneration was found throughout the whole area of ulna defect without X-ray irradiation for the BMP group (Figure 8-2C), while the ulna defect following X-ray irradiation was occupied by both the regenerated bone and infiltrated soft connective tissues, and osseous bridging between the proximal and distal host bone tissue was not observed (Figure 8-2D). On the contrary, when the ulna defect was applied with the empty gelatin-ß-TCP scaffold (control group), insignificant bone regeneration was observed, and soft connective tissues were infiltrated into the defect, irrespective of X-ray irradiation treatment (Figures 8-2A and 2B). The gelatin-ß-TCP scaffolds did not degrade and remained at the ulna defect in control group 6 weeks after application.

Mineral deposition at the ulna defect of rabbits

Figure 8-3 shows the total bone mineral contents (BMC) at the ulna defect of rabbits with or without X-ray irradiation 6 weeks after different applications of gelatin-ß-TCP scaffolds. The BMC values in both the control and BMP groups at the ulna defect with X-ray irradiation were significantly lower than those of the non-irradiated normal animal. The BMP enhanced the BMC values to a significantly higher extent than the control group, irrespective of X-ray irradiation. The BMC values at the ulna defect without X-ray irradiation for the BMP group was the same level as those of the BMP-BM group, whereas the BMC values at the ulna defect X-ray irradiated was significantly lower than those of BMP-BM group and the intact bone. The BMP-BM enhanced the BMC values similar to that of the intact bone, irrespective of X-ray irradiation.

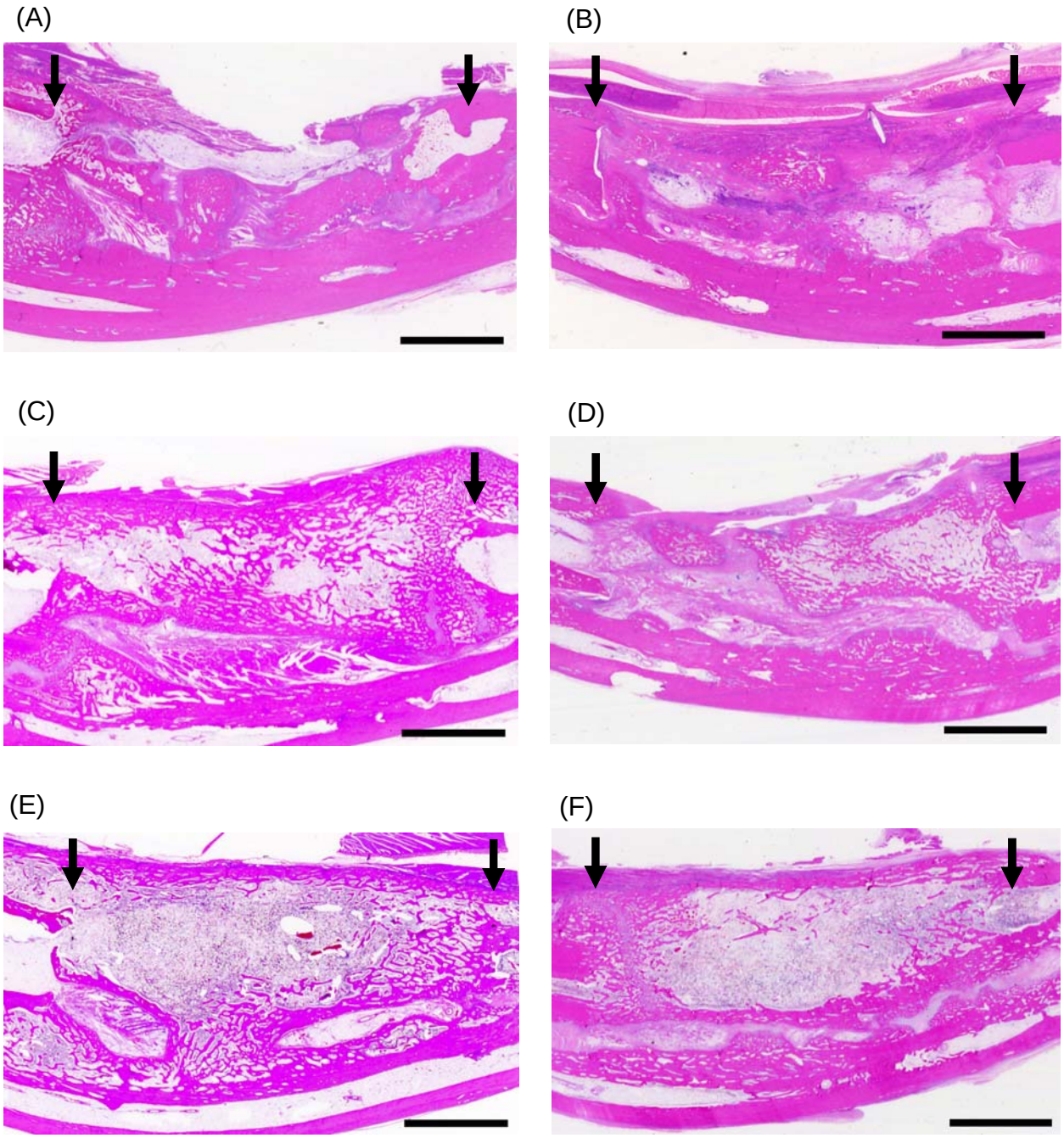

Figure 8-2. Histological sections of rabbit ulna defects with (B, D, and F) and without X-ray irradiation (A, C, and E) 6 weeks after application of empty gelatin-ß-TCP scaffolds (control) (A and B), gelatin-ß-TCP scaffolds incorporating BMP-2 (BMP) (C and D), and gelatin-ß-TCP scaffolds incorporating BMP-2 plus bone marrow (BMP-BM) (E and F). Triangle indicates the interface between the defect and the host bone. Every bar corresponds to 1 mm length.

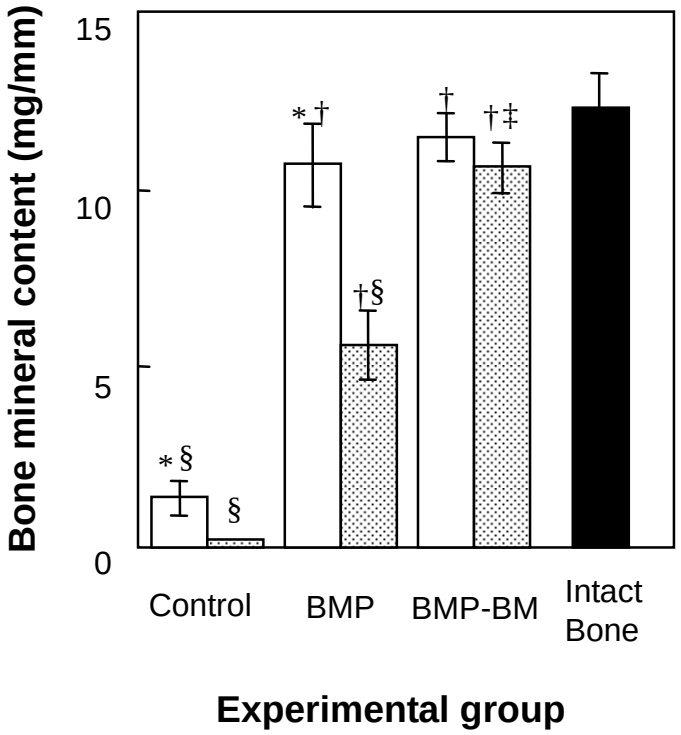

Figure 8-3. Bone mineral content (BMC) at rabbit ulna defects with (▨) and without X-ray irradiation (□) 6 weeks after application of empty gelatin-ß-TCP scaffolds (control), gelatin-ß-TCP scaffolds incorporating BMP-2 (BMP), and gelatin-ß-TCP scaffolds incorporating BMP-2 plus bone marrow (BMP-BM). (■) indicates the BMC of the intact bone. $^{*}p < 0.05$; significant against the BMC at the ulna defects with radiation treatment. $^{\dagger}p < 0.05$; significant against the BMC in control group at the corresponding radiation treatment. $^{\ddagger}p < 0.05$; significant against the BMC in BMP group at the corresponding radiation treatment. $^{\S}p < 0.05$; significant against the BMC of the intact bone.

DISCUSSION

After the surgical resection of tumor, the X-ray irradiation around the tissue is normally performed to prevent the tumor recurrence and metastases. On the other hand, the natural potential to heal bone tissue is much damaged by the irradiation, while the dead of key cells for wound healing and the inhibition of neovascularization are observed [19]. From the viewpoint of wound healing, the X-ray irradiation may not be always recommended. Consequently, the bone healing is delayed or suppressed and the union of materials implanted to the host tissue is not expected. The technology of bone tissue engineering will positively improve these therapeutic issues. The present study assessed the promising potential of gelatin-ß-TCP scaffolds in inducing bone regeneration at a segmental ulna defect of rabbits X-ray irradiated.

In the clinical situation, it is practically important to select the timing and total dose of X-ray irradiation because the irradiation conditions required depend on the types of tumor. The dose of radiation high enough to suppress the recurrence of tumor should be selected. In addition, the divided radiation is commonly used not only to achieve high tumor killing activity [20], but also to minimize the radio damages of skin and the surrounding tissues. At the total dose of 20 Gy, natural bone regeneration was observed to the same extent as that of non-irradiated tissue defect (data not shown). However, X-ray irradiation at the total dose of 40 Gy reduced the natural osteogenic activity of bone tissue although the apparent tissue damages were not observed. The total dose of 40 Gy is clinically used. Taken together, in this study, 8-time devided X-ray irradiation of 5 Gy (total dose of 40 Gy) was selected as the irradiation condition.

In this study, the gelatin-ß-TCP scaffold was used as the scaffold for bone regeneration. It has been demonstrated that the gelatin-ß-TCP scaffold functioned not only as the release carrier of BMP-2, but also the cell scaffold for cell seeding, proliferation, and osteogenic differentiation. From the viewpoint of

the release carrier, the optimization of BMP-2 release profile is important to efficiently induce bone regeneration. The time period of BMP-2 release depended on that of scaffold degradation which can be readily changed by the water content of scaffold by altering the concentration of gelatin and gultaldehyde used for scaffold preparation. Our previous study indicates that the gelatin-ß-TCP scaffold with a water content of 97.8 % exhibited the highest activity of BMP-2-induced osteogenesis [10]. On the other hand, from the viewpoint of cell scaffold, the amount of ß-TCP in the scaffolds was key to govern the scaffold ability for bone regeneration. It has been demonstrated that the amount of ß-TCP incorporated into the scaffold affected the extent of osteogenic differentiation, and the strongest osteogenic differentiation was observed for the gelatin scaffold incorporating 50 wt% of ß-TCP [11]. In addition, incorporation of ß-TCP enabled the gelatin scaffold to increase the compression modulus without any change of pore structure. Taken together, the gelatin scaffold incorporating 50 wt% of ß-TCP with a water content of 97.8 % was used for bone regeneration in this study.

A rabbit ulna defect of 20-mm length was selected as a critical-sized defect according to the method previously reported [18]. It was found that such an ulna bone resection did not impair the survival function of experimental animals. It was experimentally confirmed that no bone regeneration was observed both at the ulna defect without any applications and after the application of free BMP-2 solution (17 μg/site), irrespective of X-ray irradiation (data not shown). The μCT and histological results clearly indicated no bone regeneration for the empty gelatin-ß-TCP scaffold (control group) (Figures 8-1A-1D or Figures 8-2A and 2B), which is similar to the case performed previously with the β-TCP-free gelatin hydrogel [18]. This finding indicates that the gelatin-ß-TCP scaffold itself had no ability for bone regeneration although it contains ß-TCP granules which have been reported as an osteoinductive substance upon implanting into the bone defect.

The activity of the gelatin-ß-TCP scaffold incorporating BMP-2 (BMP group) to induce bone

regeneration was suppressed by X-ray irradiation (Figures 8-1E-1H or Figures 8-2C and 2D). From the histological examination, the ulna defect was partially occupied by the soft connective tissue. This phenomenon can be explained in terms of cellularity and vascularity of the bone tissue X-ray irradiated. Firstly, X-ray irradiation decreases the number of osteogenic cells. Dudziak et al. have reported that the exposure of ionizing radiation to the bone tissue decreased the proliferation of osteoblast-like cells in a dose-dependent manner [21]. Secondly, the osteogenic activity of cells was suppressed by X-ray irradiation. The differentiation activity of osteoblasts is often damaged by X-ray irradiation therapy [22]. In addition, it has been demonstrated that the progenitor stem cells present in the irradiated area was so damaged that could not respond to a BMP signal [23]. Thirdly, X-ray irradiation suppresses angiogenesis. When vascular endotherial growth factor (VEGF) of angiogenesis in the bone tissue was inactivated by X-ray irradiation, the morphogenesis and the remodeling process during the endochondral ossification were both inhibited, resulting in the impaired bone regeneration [24].

Significant bone regeneration at the ulna defect X-ray irradiated for the BMP-BM group (Figures 8-1F and 2F) strongly demonstrates that the presence of bone marrow contributed to bone regeneration at the irradiated area even when the BMP-2 release system was applied. It is reported that the calcium phosphate scaffold combined with bone marrow significantly improved bone regeneration after X-ray irradiation, whereas the scaffold without bone marrow did not induce bone regeneration [25]. It is likely that the autologous bone marrow incorporated efficiently proliferated and differentiated to osteogenic cells in the gelatin-ß-TCP scaffolds, resulting in enhanced bone regeneration. In addition, the cellular events were also promoted by the BMP-2 released. Taken these results into consideration, combination of cells with high osteogenetic potentials with BMP-2 is essential for bone regeneration at the defect X-ray irradiated where the key cells and growth factor are both biologically damaged or lost.

For bone regeneration, it is important to recover the bone tissue from the functional and

structural viewpoints. Among the bone functions, the mechanical property is considered to be one of the key factors in the clinical case. It is well recognized that the bone mineral density (BMD) and bone mineral content (BMC) are strongly related to the mechanical property of bone [26]. The BMP-BM enhanced the BMC values at the bone defect as high as that of the intact bone, irrespective of X-ray irradiation (Figure 8-3). In addition, the cross-sectional μCT images revealed that the regeneration of cortical-like bone could be detected throughout the ulna defect (Figures 8-1J and 1L). These findings suggest that both the structural and functional regeneration could be achieved by gelatin-ß-TCP scaffolds incorporating BMP-2 combined with autologous bone marrow even in the unhealthy condition. In conclusion, considering that both gelatin and ß-TCP are clinically usable, the gelatin-ß-TCP scaffold is a practical promising scaffold to induce bone regeneration.

REFERENCES

1. I. Meyer, Infectious diseases of the jaws, *J. Oral Surg.*, **28**, 17-26 (1970).

2. R. E. Marx, Osteoradionecrosis: a new concept of its pathophysiology, *Oral Maxillofac. Surg.*, **41**, 283-288 (1983).

3. A. Valentin-Opran, J. Wozney, C. Csimma, L. Lilly, and G. E. Riedel, Clinical evaluation of recombinant human bone morphogenetic protein-2, *Clin. Orthop. Relat. Res.*, **395**, 110-120 (2002).

4. S. P. Bruder and B. S. Fox, Tissue Engineering of Bone, *Clin. Orthop. Rel. Res.*, **367S**, S68-83 (1999).

5. A, J. Salgado, O. P. Coutinho, and R. L. Reis, Bone Tissue Engineering: State of the Art and Future Trends, *Macromol. Biosci.*, **4**, 743-765 (2004).

6. H. Petite, V. Viateau, W. Bensaid, A. Meunier, C. de Pollak, M. Bourguignon, K. Oudina, L. Sedel, and G. Guillemin, Tissue-engineered bone regeneration, *Nat. Biotechnol.*, **18**, 959-963 (2000).

7. B. D. Boyan, C. H. Lormann, J. Romero, and Z. Schwartz, Bone and cartilage tissue engineering, *Clin. Plast. Surg*. **26**, 629-645 (1999).

8. H. Ohgushi and A. I. Caplan, Stem cell technology and bioceramics: from cell to gene engineering, *J. Biomed. Mater. Res.*, **48**, 913-927 (1999).

9. A. El-Ghannam, Bone reconstruction: from bioceramics to tissue engineering, *Expert Rev. Med. Devices*, **2**, 87-101 (2005).

10 Y. Takahashi, M. Yamamoto, and Y. Tabata, Enhanced osteoinduction by controlled release of bone morphogenetic protein-2 from biodegradable sponge composed of gelatin and β-tricalcium

phosphate, *Biomaterials*, **26**, 4856-4865 (2005).

11 Y. Takahashi, M. Yamamoto, and Y. Tabata, Osteogenic differentiation of mesenchymal stem cells in biodegradable sponges composed of gelatin and β-tricalcium phosphate, *Biomaterials*, **26**, 3587-3596 (2005).

12 J. M. Wozney and V. Rosen, Bone morphogenetic protein and bone morphogenetic protein family in bone formation and repair, *Clin. Orthop.*, **346**, 26-37 (1998).

13. R. G. T. Geesink, N. H. M. Hoefnagels, S. K. Bulstra, Osteogenic activity of OP-1 morphogenetic protein (BMP-7) in a human fibular defect, *J. Bone Joint Surg. Br.*, **81-B**, 710-718 (1999).

14. J. R. Lieberman, A. Daluski, and T. A. Einhorn, The role of growth factors in the repair of bone: biology and clinical applications, *J. Bone Joint Surg. Am.*, **84-A**, 1032-1044 (2002).

15 M. Yamamoto, Y. Takahashi, and Y. Tabata, Controlled release by biodegradable hydrogels enhances the ectopic bone formation of bone morphogenetic protein, *Biomaterials*, **24**, 4375-4383 (2003).

16. K. Matsuda, S. Suzuki, N. Isshiki, K. Yoshioka, T. Okada, and Y. Ikada, Influence of glycosaminoglycans on the collagen sponge component of a bilayer artificial skin, *Biomaterials*, **11**, 351-355 (1990).

17. G. Chen, T. Ushida, and T. Tateishi, A biodegradable hybrid sponge nested with collagen microsponges, *J. Biomed. Mater. Res.*, **51**, 273-279 (2000).

18. M. Yamamoto, Y. Takahashi, and Y. Tabata, Enhanced bone regeneration at a segmental bone defect by controlled release of bone morphogenetic protein-2 from a biodegradable hydrogel, *Tissue Eng.*, **12**, 1305-11 (2006).

19. J. W. Doyle, Y-Q Li, A. Salloum, T. J. FitzGerald, and R. L. Walton, The effects of radiation on neovascularization in a rat model, *Plast. Reconst. Surg.*, **98**, 129-135 (1996).

20. E. J. Hall and D. J. Brenner, The dose-rate effect revisited: radiobiological considerations of importance in radiotherapy, *Int. J. Radioat. Oncol. Biol. Phys.*, **21**, 1403-1414 (1991).

21. M. E. Dudziak, P. B. Saadeh, B. J. Mehrara, D. S. Steinbrech, J. A. Greenwald, G. K. Gittes, and M. T. Longaker, The effects of ionizing radiation on osteoblast-like cells *in vitro*. *Plast. Reconstr. Surg.*, **106**, 1049-1061 (2000).

22. S. Matsumura, A. Jikko, H. Hiranuma, A. Deguchi, and H. Fuchihata, Effect of X-ray irradiation on proliferation and differentiation of osteoblast, *Calcif. Tissue Int.*, **59**, 307-308 (1996).

23. M. Arnold, P. Stas, J. Kummermehr, S. Schultz-Hector, and K-R. Trott, Radiation-induced impairment of bone healing in the rat femur: effects of radiation dose, sequence and interval between surgery and irradiation, *Radiot, Oncol.*, **48**, 259-265 (1998).

24. H. P. Gerber, T. H. Vu, A. M. Ryan, J. Kowalski, Z. Werb, and N. Ferrara, VEGF couples hypertrophic cartilage remodeling, ossification and angiogenesis during endochondral bone formation, *Nat. Med.*, **5**, 623-628 (1999).

25. O. Malard, J. Guicheux, J-M. Bouler, O. Gauthier, C. B. de Montreuil, E. Aguado, P. Pilet, R. LeGeros, and G. Daculsi, Calcium phosphate scaffold and bone marrow for bone reconstruction in irradiated area: a dog study, *Bone*, **36**, 323-330 (2005).

26. R. H. Li, M. L. Bouxsein, C. A. Blake, D. D'Augusta, H. Kim. X. J. Li, J. M. Wozney, and H. J. Seeherman, rhBMP-2 injected in a calcium phosphate paste (α-BSM) accelerates healing in the rabbit ulnar osteotomy model, *J. Orthop. Res.*, **21**, 997-1004 (2003).

SUMMARY

Chapter 1.

The objective of this chapter is to develop a carrier for the controlled release of BMP-2 suitable for enhancement of the bone regeneration activity. Hydrogels with different water contents were prepared through glutaraldehyde crosslinking of gelatin with an isoelectric point of 9.0 under varied reaction conditions. Following subcutaneous implantation of the gelatin hydrogels incorporating ^{125}I-labeled BMP-2 into the back of mice, the *in vivo* retention period of BMP-2 prolonged with a decrease in the water content of hydrogels used, although every time period was much longer than that of BMP-2 solution injection. Ectopic bone formation studies demonstrated that ALP activity and osteocalcin content around the implanted site of BMP-2-incorporated gelatin hydrogels were significantly high compared with those around the injected site of BMP-2 solution. The values became maximum for the gelatin hydrogel incorporating BMP-2 with a middle period of BMP-2 retention, while bone formation was histologically observed around the hydrogel incorporating BMP-2. The ALP activity was significantly higher than that of the collagen sponge incorporating BMP-2. We concluded that the controlled release technology of BMP-2 for a certain time period was essential to induce the potential activity for bone formation.

Chapter 2.

The objective of this chapter is to investigate feasibility of a biodegradable hydrogel of gelatin as the controlled release carrier of BMP-2 suitable for enhancement of bone regeneration at a segmental bone defect. Hydrogels with three different water contents were prepared through glutaraldehyde crosslinking of gelatin with an isoelectric point of 9.0 under varied reaction conditions.

A segmental critical-sized defect (20 mm) was created at the ulnar bone of New Zealand white rabbits skeletally matured and gelatin hydrogels incorporating BMP-2 (17 μg/hydrogel) were implanted into the defects. When bone regeneration was evaluated by soft X-ray observation and BMD measurement, the gelatin hydrogels incorporating BMP-2 exhibited significantly high osteoinduction activity compared with free BMP-2, although the activity depended on the water content of hydrogels. Significantly higher BMD enhancement was observed for the gelatin hydrogel with a water content of 97.8 wt% than that with the lower or higher water content. We concluded that the biodegradable gelatin hydrogel is a promising controlled release carrier of BMP-2 for bone regeneration at the segmental bone defect.

Chapter 3.

The objective of this study is to investigate feasibility of a biodegradable gelatin hydrogel as the controlled release carrier of BMP-2 to enhance bone regeneration at a skull defect of non-human primates. Hydrogels with three different water contents were prepared through glutaraldehyde crosslinking of gelatin with an isoelectric point of 9.0 under varied reaction conditions. A critical-sized defect (6 mm in diameter) was prepared at the skull bone of cynomolgus monkeys skeletally matured while gelatin hydrogels incorporating various doses of BMP-2 were applied into the defects. When the bone regeneration was evaluated by soft X-ray and BMD examinations, the gelatin hydrogel incorporating BMP-2 exhibited significantly high osteoinduction activity compared with an IBM incorporating BMP-2 which is one of the best osteoinduction systems, although the activity depended on the water content of hydrogels. The highest BMD enhancement was observed for the gelatin hydrogel with a water content of 97.8 wt% among all types of hydrogels. Moreover, the gelatin hydrogel enabled BMP-2 to induce the bone regeneration induction in non-human primates even at low doses. It is concluded that the controlled release of BMP-2 for a certain time period was essential to induce the

osteoinductive potential of BMP-2.

Chapter 4.

Biodegradable gelatin sponges at different contents of ß-TCP were fabricated to allow BMP-2 to incorporate into them. The *in vivo* osteoinduction activity of the scaffolds incorporating BMP-2 was investigated, while their *in vivo* profile of BMP-2 release was evaluated. The sponges prepared had an interconnected pore structure with an average pore size of 200 μm, irrespective of the ß-TCP content. The *in vivo* release test revealed that BMP-2 was released *in vivo* at a similar time profile, irrespective of the ß-TCP content. The *in vivo* time period of BMP-2 retention was longer than 28 days. When the osteoinduction activity of gelatin or gelatin-ß-TCP scaffolds incorporating BMP-2 was studied following the implantation into the back subcutis of rats in terms of histological and biochemical examinations, homogeneous bone formation was histologically observed throughout the sponges, although the extent of bone formation was higher in the sponges with the lower contents of ß-TCP. On the other hand, the level of alkaline phosphatase activity and osteocalcin content at the implanted sites of sponges decreased with an increase in the content of ß-TCP. The gelatin scaffold exhibited significantly higher osteoinduction activity than that of any gelatin-ß-TCP scaffold, although every scaffold with or without ß-TCP showed a similar *in vivo* profile of BMP-2 release. In addition, the *in vitro* collagenase digestion experiments revealed that the gelatin-ß-TCP scaffold collapsed easier than the gelatin scaffold without ß-TCP incorporation. These results suggest that the maintenance of the intrasponge space necessary for the osteoinduction is one factor contributing to the osteoinduction extent of BMP-2-incorporating scaffolds.

Chapter 5.

MSC were isolated from the bone marrow of rats and seeded into a non-woven fabric of PET by the agitated and static methods. The MSC attachment was investigated in terms of the number of cells attached to the fabric, their distribution inside the fabric, and the cell damage. The number of MSC attached was larger for the agitated seeding method than for the static seeding method. The higher the rotating speed in the agitated seeding, the larger the number of cells attached. When the cell suspension was seeded to the fabric at the culture medium volume of 50 and 200 μl in the well of culture plate or the culture tube, the best cell attachment was observed for the tube culture group at the larger volume. The cells were attached more homogeneously throughout the fabric at a larger number than the case of other culture groups. It is possible that the agitating of cell suspension allows cells to infiltrate uniformly into the inside of fabric, resulting in homogeneous distribution of cells in the fabrics. A biochemical study revealed that neither the agitated nor static seeding methods gave cells any damages, irrespective of the medium volume and the type of culture vessel. We conclude that the agitated seeding is a promising method to formulate a homogeneous construct of fabric and MSC.

Chapter 6.

The proliferation and osteogenic differentiation of MSC were investigated in three-dimensional non-woven fabrics prepared from PET fiber with different diameters. When seeded into the fabrics of cell scaffold, more MSC attached in the fabric of thicker PET fibers than that of thinner ones, irrespective of the fabric porosity. The morphology of cells attached became more spread with an increase in the fiber diameter of fabrics. The rate of MSC proliferation depended on the PET fiber diameter and porosity of fabrics: the bigger the fiber diameter of fabrics with higher porosity, the higher their proliferation rate. When the ALP activity and osteocalcin content of MSC cultured in

different types of fabrics were measured to evaluate the ostegenic differentiation, they became maximum for the non-woven fabrics with a fiber diameter of 9.0 μm, although the values of low-porous fabrics were significantly high compared with those of high porous fabrics. We concluded that the attachment, proliferation, and bone differentiation of MSC were influenced by the fiber diameter and porosity of non-woven fabrics as the scaffold.

Chapter. 7.

Biodegradable gelatin scaffolds incorporating various amounts of ß-TCP (gelatin-ß-TCP) were fabricated and the *in vitro* osteogenic differentiation of MSC isolated from rat bone marrow in the scaffolds was investigated. The gelatin-ß-TCP scaffolds have an interconnected pore structure with the average size of 180-200 μm, irrespective of the ß-TCP amount. The stiffness of the scaffolds became higher with an increase in the amount of ß-TCP. When seeded into the scaffolds by an agitated method, MSC were homogeneously distributed throughout the scaffold. The morphology of cells attached got more spread with the increased ß-TCP amount. The rate of MSC proliferation depended on the ß-TCP amount and culture method: the higher the ß-TCP amount in the stirring culture, the higher the proliferation rate. The deformed extent of gelatin-ß-TCP scaffolds was suppressed with the increased amount of ß-TCP. When measured to evaluate the osteogenic differentiation of MSC, the ALP activity and osteocalcin content became maximum for the scaffold with a ß-TCP amount of 50 wt%, Although both the values were significantly high in the stirring culture compared with those in the static culture. We concluded that the attachment, proliferation, and osteogenic differentiation of MSC were influenced by scaffold composition of gelatin and ß-TCP as the cell scaffold.

Chapter 8.

The objective of this study is to evaluate the feasibility of gelatin scaffolds incorporating β-tricalcium phosphate (β-TCP) granules (gelatin-ß-TCP scaffolds) to enhance bone regeneration at a segmental ulna defect of rabbits X-ray irradiated. After X-ray irradiation to the ulna bone, segmental critical-sized defects of 20 mm length were created, and then the gelatin-ß-TCP scaffolds with or without bone morphogenetic protein-2 (BMP-2) and the sponges incorporating BMP-2 plus autologous bone marrow were applied into the defects to evaluate bone regeneration. The gelatin-ß-TCP scaffolds incorporating BMP-2 (BMP) enhanced bone regeneration at the ulna defect to a significantly great extent compared with the BMP-2-free scaffolds (control). However, for the bone X-ray irradiated, the BMP did not achieve bone regeneration as effectively as that without X-ray irradiation. When combined with autologous bone marrow, the BMP exhibited significantly high osteoinductivity, irrespective of X-ray irradiation. The value of bone mineral content (BMC) at the ulna defect was the level similar to that of the intact bone. It is concluded that the combination of bone marrow with gelatin-ß-TCP scaffold enabling BMP-2 release is a promising way to induce bone regeneration at the segmental bone defect following X-ray irradiation.

LIST OF PUBLICATIONS

Chapter 1. Masaya YAMAMOTO, Yoshitake TAKAHASHI, and Yasuhiko TABATA, "Controlled release by biodegradable hydrogels enhances the ectopic bone formation of bone morphogenetic protein", *Biomaterials*, **24**, 4375-4383 (2003).

Chapter 2. Masaya YAMAMOTO, Yoshitake TAKAHASHI, and Yasuhiko TABATA, "Enhanced bone regeneration at a segmental bone defect by controlled release of bone morphogenetic protein-2 from a biodegradable hydrogel", *Tissue Engineering*, **12**, 1305-1311 (2006).

Chapter 3. Yoshitake TAKAHASHI, Masaya YAMAMOTO, Keisuke YAMADA, Osamu KAWAKAMI, and Yasuhiko TABATA, "Skull bone regeneration in non-human primates by controlled release of bone morphogenetic protein-2", *Tissue Engineering*, **13**, 293-300 (2007).

Chapter 4. Yoshitake TAKAHASHI, Masaya YAMAMOTO, and Yasuhiko TABATA, "Enhanced osteoinduction by controlled release of bone morphogenetic protein-2 from biodegradable sponge composed of β-tricalcium phosphate", *Biomaterials*, **26**, 4856-4865 (2005).

Chapter 5. Yoshitake TAKAHASHI, and Yasuhiko TABATA, "Homogeneous seeding of mesenchymal stem cells into non-woven fabric for tissue engineering", *Tissue Engineering*, **9**, 931-938 (2003).

Chapter 6. Yoshitake TAKAHASHI, and Yasuhiko TABATA, "Effect of the fiber diameter and porosity of non-woven PET fabrics on the osteogenic differentiation of mesenchymal stem cells", *J. Biomater. Sci. Polym. Edn.*, **15**, 41-57 (2004).

Chapter 7. Yoshitake TAKAHASHI, Masaya YAMAMOTO, and Yasuhiko TABATA, “Osteogenic differentiation of mesenchymal stem cells in biodegradable sponges composed of gelatin and β-tricalcium phosphate”, *Biomaterials*, **26**, 3587-3596 (2005).

Chapter 8. Yoshitake TAKAHASHI, Masaya YAMAMOTO, Akishige HOKUGO, Satoshi ITASAKA, Masahiro HIRAOKA, and Yasuhiko TABATA, “Bone regeneration at an X-ray irradiated ulna defect of rabbits by biodegradable sponges of gelatin and ß-tricalcium phosphate enabling bone morphogenetic protein-2 release plus autologous bone marrow cells”, in preparation.

ACKNOWLEDGEMENTS

The present research was carried out from 2000 to 2007 under the continuous guidance of Dr. Yasuhiko Tabata, Professor of Institute for Frontier Medical Sciences, Kyoto University.

The author would like to express sincere gratitude to Professor Tabata for his constant guidance, encouragement, valuable discussion, and detailed criticism on the manuscript throughout the present work. The completion of the present research has been an exciting project and one which would not have been possible without his guidance.

The author is also indebted to Dr. Masaya Yamamoto, Assistant Professor of Institute for Frontier Medical Sciences, Kyoto University, for his constant guidance, encouragement, valuable discussion, intimate advice, and detailed criticism on whole experiments as well as the manuscript throughout the present work.

The author is very grateful to Dr. Akishige Hokugo, Research Fellow of Institute for Frontier Medical Sciences, Kyoto University, Dr. Keisuke Yamada, Associate Professor of Graduate School of Medicine, Kyoto University, and Dr. Osamu Kawakami, Graduate School of Medicine, Kyoto University, for their significant advice and helps on the animal experiments. The author wishes to express his sincere appreciation to Dr. Masahiro Hiraoka, Professor of Graduate School of Medicine, Kyoto University, and Dr. Satoshi Itasaka, Instructor of Graduate School of Medicine, Kyoto University, for his instruction of orthovoltage X-ray machine. The author also expresses to his great thanks to Dr. Takayoshi Nakano, Associate Professor of the Department of Materials Science and Engineering, Osaka University, for the technical instruction of μCT and pQCT, respectively.

The author wishes to express his thanks to Dr. Yoshito Ikada, Emeritus Professor of Institute for Medical Sciences, Kyoto University, Mr. Yasuo Negishi, Mr. Takashige Oka, Dr. Masakazu Suzuki,

and Dr. Shojiro Matsuda, Gunze Ltd. who gave him an opportunity to study at Kyoto University. The author also wishes to express his thanks to all members of Medical Laboratory, Research and Development Center, Gunze. Ltd, for their kind help and continuous encouragement.

General acknowledgements are due to Mrs. Miyuki Takasaki and Ms. Kyoko Bamba, Secretaries of Professor Tabata's Laboratory, and other members of Professor Tabata's Laboratory and of Institute for Frontier Medical Sciences, Kyoto University, for their kind help.

Finally, the author would like to express his sincere appreciation to Dr. Yoshiharu Kimura, Professor of the Department of Polymer Science and Engineering, Kyoto Institute of Technology, and Dr. Tetsuji Yamaoka, Director of Biomedical Engineering, National Cardiovascular Center Research Institute, who inspired the author to come in the attractive scientific field of polymer chemistry.

July, 2007

Kyoto

Yoshitake Takahashi